Mice co-expressing human APP$_{Swe/Ind}$ and TGF-β1 as a tool for the identification of Alzheimer's disease therapies

by

Panayiota Papadopoulos

A thesis submitted to the Faculty of Graduate Studies and Research
in partial fulfillment of the requirements of the degree of
Doctor of Philosophy

June 2012
Department of Integrated Program of Neuroscience
Faculty of Medicine
McGill University
Montréal, Québec

Don't be safe, be brilliant.

George Santayana

Table of Contents

Abstract

Elevated brain levels of amyloid-β (Aβ) and transforming growth factor- β1 (TGF-β1) are thought to contribute to the cognitive and cerebrovascular alterations of Alzheimer's disease (AD). Here, we sought to investigate the role of simultaneous increases of Aβ and TGF-β1 on cerebrovascular, neuronal, glial and mnemonic function using a bitransgenic mouse model concurrently overexpressing a mutated form of the human amyloid precursor protein ($APP_{Swe,Ind}$) and a constitutively active form of TGF-β1 (A/T mice). In addition, we attempted to counter these deficits using three different pharmacological agents: the peroxisome proliferator-activated receptor (PPARγ) agonist pioglitazone (20mg/kg/day), the 3-hydroxy-3-methyl-glutaryl-CoA reductase inhibitor simvastatin (40mg/kg/day) and the angiotensin II receptor type 1 antagonist losartan (10 and 25mg/kg/day), all of which with previously demonstrated efficacy in singly APP and TGF mouse models. We found that A/T mice exhibited spatial learning and memory impairments, together with an early progressive decline in cerebrovascular dilatory capacity, preserved contractility, and reduction in constitutive nitric oxide (NO) synthesis. Altered levels of vasodilator-synthesizing enzymes and fibrotic proteins were also apparent with increasing age. A/T mice featured glial and neuronal dysfunctions, as well as neurovascular and neurometabolic coupling deficits to sensory stimulation that were normalized only by pioglitazone. The latter also improved reversal learning in adult, but not in aged A/T mice, despite worsening effects on vasodilatory function. Similar negative effects were observed with simvastatin on dilatory function, and simvastatin additionally failed to improve neurovascular coupling and cognitive deficits. In contrast, losartan at the low, but not at the high dose displayed minor benefits on the learning

capacity of A/T mice and significantly improved spatial memory. Although neurovascular coupling to sensory stimulation was not normalized by either dose, the low and high doses of losartan improved vasodilatory function without normalizing the baseline NO production essential to maintain blood vessel tone. Together, these findinds suggest that A/T mice, which integrate the comorbid factor of AD cerebrovascular dysfunction to the amyloid pathology, may well reflect the complexity that one faces when attempting to rescue function in AD patients. It may also represent an improved model to test new therapeutic strategies.

Résumé

Des taux élevés d'amyloide-β (Aβ) et du 'transforming growth factor-β1' (TGF-β1) dans le cerveau contribuent aux altérations cognitives et cérébrovasculaires de la maladie d'Alzheimer. Dans cette thèse, nous avons tenté de cerner le rôle d'une augmentation simultanée d'Aβ et de TGF-β1 sur les fonctions cérébrovasculaires, neuronales, gliales et mnémoniques chez une souris bitransgénique qui surexprime ces deux peptides (souris A/T). Nous avons aussi tenté de remédier aux anomalies identifiées chez la souris A/T en utilisant trois agents pharmacologiques différents. Ces traitements sont : la pioglitazone (20mg/kg/jour), un agoniste des récepteurs (PPARγ), la simvastatin (40mg/kg/jour), un inhibiteur de la '3-hydroxy-3-methyl-glutaryl-CoA réductase', le losartan (10 et 25mg/kg/jour), un antagoniste du récepteur de type 1 de l'angiotensine II, dont l'efficacité a été démontrée dans des modèles de souris transgéniques qui surproduisent indépendamment l'Aβ ou le TGF-β1. Nous avons trouvé que les souris A/T avaient des déficits d'apprentissage et de mémoire, et qu'elles présentaient un déclin précoce et progressif de la capacité dilatatrice des vaisseaux cérébraux, et une réduction de la synthèse constitutive du monoxyde d'azote (NO), mais que la contractilité était préservée. Des niveaux altérés d'enzymes impliquées dans la synthèse de molécules vasodilatatrices et des protéines médiatrices de la fibrose vasculaire étaient également apparents. Les souris A/T présentaient aussi des dysfonctions gliales et neuronales, ainsi que des déficits de couplages neurovasculaire et neurométabolique, qui étaient contrés uniquement par la pioglitazone. La pioglitazone améliorait aussi la capacité d'apprentissage de type 'reversal learning' chez les souris adultes et non chez les souris âgées, tout en exerçant des effets négatifs sur les fonctions vasodilatatrices. Des effets néfastes sur la capacité

des vaisseaux à se dilater ont aussi été observés avec la simvastatine qui, par contre, n'a pu reproduire les bienfaits cognitifs et sur le couplage neurovasculaire observés avec la pioglitazone. Seul le traitement avec la faible dose de losartan a amélioré de façon modeste les capacités d'apprentissage des souris A/T et a significativement rétabli leur mémoire spatiale. Cependant, l'augmentation de perfusion cérébrale induite par une stimulation sensorielle n'était pas normalisée par le losartan à aucune dose, et le losartan a complètement (dose faible) ou partiellement (dose élevée) rétabli les fonctions dilatatrices sans toutefois améliorer la production constitutive du NO essentiel pour le maintain du tonus vasculaire. L'ensemble de ces résultats suggère que les souris A/T, qui combinent la pathologie de l'Aβ aux dysfonctions cerébrovasculaires induites par le TGF-β1, reflètent la complexité de la maladie humaine et mettent en évidence les défis à relever pour traiter efficacement les patients atteints d'Alzheimer. Les souris A/T pourraient donc représenter un modèle amélioré afin de tester de nouvelles approches thérapeutiques.

List of Abbreviations

Aβ: amyloid-beta
ACA: anterior cerebral artery
ACE: angiotensin converting enzyme
ACh: acetylcholine
AChE: acetylcholinesterase
AD: Alzheimer's disease
ADAS-cog: Alzheimer's disease Assessment Scale
AICD: APP intracellular domain
Ang: angiotensin
APP: amyloid precursor protein
APLP: amyloid precursor-like protein
APOE: apolipoprotein E
ARBs: angiotensin receptor blockers
AT1R: angiotensin II type 1 receptor
AT2R: angiotensin II type 2 receptor
AT4R: angiotensin II type 4 receptor
BA: basilar artery
BACE: β-site APP cleaving enzyme
BBB: blood-brain barrier
BM: basement membrane
CAA: cerebral amyloid angiopathy
CBF: cerebral blood flow
CGRP: calcitonin gene-related peptide
CALCRL: calcitonin receptor-like receptor
cAMP: cyclic adenosine monophosphate
$[cAMP]_i$ intracellular cAMP concentration
CGU: cerebral glucose uptake/utilization
ChAT: choline acetyltransferase
CNS: central nervous system
Co-Smad: common-partner Smad
COX: cyclooxygenase
CSF: cerebrospinal fluid
CTF: C-terminal fragment
CTGF: connective tissue growth factor
DAB: 3,3'-diaminobenzedene
EC: endothelial cell
ECM: extracellular matrix
EETs: epoxyeicosatrienoic acids

Egr-1: early growth response protein 1
eNOS: endothelial nitric oxide synthase
ER: endoplasmic reticulum
ET-1: endothelin-1
ETA: endothelin-A receptor
ETB: endothelin-B receptor
FA: formic acid
fMRI: functional magnetic resonance imaging
[18F]FDG: 2-deoxy-2-[18F]fluoro-D-glucose
GFAP: glial fibrillary acidic protein
GFP: green fluorescent protein
GLUT-1: glucose transporter 1
GPI: glycophosphatidylinositol
HMG-CoA: hydroxymethylglutaryl coenzyme A
HSPG: heparan sulfate proteoglycan
ICA: internal carotid artery
IDE: insulin-degrading enzyme
IEGs: immediate-early genes
IF: intermediate filament
IFN-γ: interferon-gamma
IL-1β: interleukin-1β
iNOS: inducible nitric oxide synthase
I-Smads: inhibitory Smads
KATP: ATP-sensitive K+ channel
KIR: inward rectifier K+ channel
KV: voltage-dependent K+ channel
L-NNA: Nω-nitro-L-arginine
LDF: laser Doppler flowmetry
LRP: low-density lipoprotein receptor-related protein
LTP: long-term potentiation
MCA: middle cerebral artery
MCI: mild cognitive impairment
MMSE: Mini Mental Status Exam
MMP9: matrix metalloproteinase 9
MMSE: Mini-Mental State Examination
NADPH oxidase: nicotinamide adenine dinucleotide phosphate-oxidase
NEP: neprilysin
NFT: neurofibrillary tangle
NGFI-A: nerve growth factor-induced protein A
NGF: nerve growth factor

NMDA: N-methyl-D-aspartate
NO: nitric oxide
NOS: nitric oxide synthase
NSAID: non-steroidal anti-inflammatory drug
$O2\cdot^{-}$: superoxide
$ONOO^{-}$: peroxynitrite
PBS: phosphate-buffered saline
PCA: posterior cerebral artery
PDGFβ: platelet-derived growth factor beta
PET: positron emission tomography
PKA: protein kinase A
PPARγ: peroxisome proliferator-activated receptor gamma
PPREs: peroxisome proliferator response elements
PS: presenilin
RAGE: receptor for advanced glycation end products
RAMP1: receptor activity-modifying protein 1
RAS: renin-angiotensin system
ROS: reactive oxygen species
R-Smad: receptor-regulated Smad
RXR: retinoid X receptor
SARA: Smad anchor for receptor activation
SNP: sodium nitroprusside
SOD1: superoxide dismutase 1 or copper/zinc superoxide dismutase (Cu/ZnSOD)
SOD2: superoxide dismutase 2 or manganese superoxide dismutase (MnSOD)
SMC: smooth muscle cell
SUV: standard uptake value
TGF-β1: transforming growth factor-beta 1
TNF-α: tumor necrosis factor-alpha
TZD: thiazolidinedione
VA: vertebral artery
VEGF: vascular endothelial growth factor
Zif268: zinc finger protein 225
5-HT: 5-hydroxytryptamine or serotonin
τ: tau

Preface to the Introduction

Alzheimer's disease (AD), a neurodegenerative disorder characterized by progressive memory loss and declining cognitive abilities, constitutes a personal and societal misfortune of great proportions. Research in laboratories and clinics has identified many features of this debilitating disease yet, no cure has been established. Important gaps in our knowledge and in discriminating between triggering and aggravating pathogenic factors seem to cast additional doubt on the path forward. The hypothesis that amyloid-β (Aβ) peptide species are the primary causative agents of AD maintains considerable support among researchers. However, a growing body of evidence shows that Aβ peptides are unlikely to be the only feature in AD etiology. This has resulted in the expansion of research strategies, some of which focus on disease-triggering mechanisms and others on lessening the harm induced by secondary pathogenic processes. Indeed, key therapeutic targets may be uncovered by directing our focus towards the brain's vascular system and incorporating knowledge of cerebrovascular disorders into the 'neurocentric' dogma of AD. Neurons are the main executors of cognitive function and intuitively, the main research focus and AD therapeutic target. However, brain function including learning and memory also rely on an intact cerebral circulation, which provides nutrients to an organ with no energy reserves and a high metabolic demand. In this dissertation, the neuronal and vascular approaches will be addressed, and complemented by the effects of therapeutic interventions.

Author Contributions

Chapter 2: I carried out some of the microreactivity experiments on vessels from WT and A/T mice, of the supplemental table 1 and figure 1, which earned me authorship after revisions of the manuscript from the journal. All other experiments were mainly done by the first co-authors.

Chapter 3: In this chapter, I conducted all experiments and analysis of results except for the laser Doppler flowmetry which was done by Ms Priscilla Fernandes. Dr. Pedro Rosa-Neto contributed to the analysis of the PET scans. I did all other treatments, quantification, statistical analysis and figures. I wrote the manuscript with contribution from Dr. Hamel.

Chapter 4: I carried out all experiments except for the laser Doppler flowmetry and immunostaining of Iba-1, which were done by Dr. Xin-Kang Tong. Also, I carried out all treatments, quantification, statistical analysis and figures. I wrote the manuscript with valuable input from Dr. Hamel.

Chapter 5: I conducted all experiments of both doses of losartan, except for laser Doppler flowmetry and thioflavin S staining. I carried out all treatments, quantification, statistical analysis and figures. I wrote the manuscript with contribution from Dr. Hamel.

General Discussion: I initiated the idea to test the combinatory treatment of simvastatin and chitin together in A/T mice. Dr. Xin-Kang Tong did all chitin injections in the ventricles, and the laser Dopple flowmetry. I carried all other experiments, treatments, analysis and figures.

Appendix, Item 1: This was an invited symposium article in which I contributed to the ABT-627 treatments, some microvessel reactivity data and the behaviour test of ABT-

627 (ETA receptor antagonist) along with Dr. Brice Ongali. Dr. Brice Ongali also conducted the treatment and reactivity data of A-192621. I conducted the ABT-627 treatments and wrote the manuscript with Dr. Hamel, which earned me first co-authorship.

Originality of work

1. This study is the first to functionally characterize arterial, hemodynamic, and cognitive integrity of young, adult and old APP/TGF mice (line J20/T64). An earlier study had evaluated the effects of TGF-β1 on amyloidogenesis of the APP/TGF brain vasculature using another APP line, the H6line. Indeed, the relative levels of cerebral transgene expression are greater in the H6 line, but hippocampal $A\beta_{1-x}$ and $A\beta_{1-42}$ plaque load is greater and formed at a younger age in the J20 line making our bitransgenic models slightly different. Our findings show that this model features progressive memory impairment, gliosis, parenchymal Aβ plaques, and combines arterial and hemodynamic dysfunction with the structural pathology (CAA and fibrosis) found in AD. This led us to suggest it as a complete model of AD cerebrovascular and brain dysfunction with which to investigate new therapeutic avenues.

2. Our results were the first to show the interactive effects of chronic Aβ- and TGF-β1-upregulation against pioglitazone, simvastatin and losartan.

3. We uncovered that pioglitazone can benefit neuroinflammation, cerebral perfusion and glucose metabolism of APP/TGF mice without altering levels of soluble or deposited Aβ, a finding of great interest for AD patients devoid of cerebrovascular pathology, as it worsened vasodilatory function in adult vasculature. It may also be of great interest to these patients as they often get diagnosed at a time when Aβ-related neuropathology is well established and irreversible.

4. We were the first to show that pioglitazone and simvastatin may have worsening effects on cerebrovascular dysfunction in APP/TGF mice, a mouse model exhibiting a fuller extent of AD neuropathology, thus better mimicking subjects with AD. Prior

studies in singly APP model had shown cerebrovascular improvement, yet singly APP do not display all aspects of the disease.

5. Our work is the first to show that simvastatin therapy appears to be a weak therapeutic candidate for late AD patients, as APP/TGF mice may represent an advanced stage of AD.

6. Our results provided insights for the divergent results obtained in statin clinical trials and, particularly, their reported efficacy only in early AD, as the neuropathological condition of APP/TGF mice may be beyond the therapeutic window of statin efficacy in AD.

7. Our work is the first to show recovery of circulatory and brain dysfunction in APP/TGF mice using a losartan. Although losartan demonstrated limited benefits in spatial learning and memory in adult A/T mice treated for 3 months, studies with longer treatment duration may offer a better protection.

Acknowledgements

I am deeply indebted to my thesis supervisor, Dr. Edith Hamel for her exceptional mentorship, openness and collaborative spirit which inspired the course of my PhD research project. I received unequivocal scientific molding through her constant feedback and constructive criticism that further developed my research-driven organizational and planning skills. Through her, I saw how endurance, perseverance, and hard work could help in achieving ones personal and professional goals. I also saw how independence, creativity, and novelty in scientific thinking could influence great discoveries. Simply said, Dr. Hamel helped me grow as a scientist and gain confidence as an individual.

I am sincerely thankful to Dr. Xin-Kang Tong, our laboratory manager. He critically directed my use of laboratory equipment and provided an invaluable structure to my PhD experience. His strict work ethic, dedication and passion for science, his boundless creativity and above all, his philanthropic values were an exceptional source of inspiration. I am also very much in debt to Dr. Josephine Nalbantoglu, my academic advisor, for her openness, guidance and support throughout my PhD. Many thanks to my committee members Dr. Clarke and Dr. Ruthazer for their care and scientific guidance. I warmly thank Dr. Pedro Rosa-Neto and Dr. Brice Ongali for their collaborative spirit and scientific discussions.

I extend my gratitude to Dr. Clotilde Lecrux for her friendship, her help and scientific discussions. Thank you to Dr. Nektaria Nicolakakis for her care and help in vessel reactivity. Many thanks to my lab members, our secretary Linda Michel and her colleague Toula Papadopoulos, Ming-Kai Ho, Jean-Paul Acco, the secretarial staff of the IPN department, and the staff of the wonderful animal facility. Also, I am grateful to my

friends for their love and endless support throughout this journey including Wiam Belkaid, Hilda Bigdeli, Ghilda Bigdeli, Eric Gravel, Emma Jakmakjian, Michelle Kouspou, Dina Levi, Maria Manarolis, Marie-Ange Meny, Despina Neophytou, Stella Neophytou, Annie Rahal and Christiana Trifonos, but most of all, I am grateful to my Godparents, my sisters Despina and Nicole, and especially my parents, for always encouraging me to aim for the stars. I was fortunate to have their constant support through the challenges of research, but also through those of life!

General Introduction

History of Alzheimer's disease

In 1907, the Bavarian psychiatrist, Dr. Alois Alzheimer was the first to describe the neuropathogical characteristics of the brain of Augusta D., a patient suffering from progressive dementia. With the use of Bielschowsky silver staining, Dr. Alzheimer identified degenerating neurons with miliary foci of deposits (senile plaques) and bundles of fibrils (neurofibrillary tangles, NFT) scattered all over the cortex, a pathology which was latter labeled "Alzheimer's disease (AD)" by Emil Kraepelin (Alois Alzheimer's colleague) in 1910. Influential studies in the mid-1960s by Robert Terry and Michael Kidd (Terry, 1963, Kidd, 1964) and then, late-1960s by Gary Blessed recognized that many cases of common senile plaque were neuropathologically similar (Blessed et al., 1968) occurring along an age continuum, with relatively rare cases appearing before the age of 60 and the occurrence rising gradually through and beyond.

In 1979, in Chicago, the Alzheimer Association was established by Jerome Stone and other Americans with afflicted family members, increasing public recognition and awareness of the disease. In 1984, the amyloid beta (Aβ)-protein was isolated and partially characterized by George Glenner from AD brains or brains of Down syndrome patients (Glenner and Wong, 1984a, b), followed by the microtubule associated protein, tau (τ), as the main component of the neurofibrillary tangles, two years later (Brion et al., 1985, Grundke-Iqbal et al., 1986b, Kosik et al., 1986, Nukina and Ihara, 1986, Wood et al., 1986, Nixon, 2007) (Figure 1). In 1987, the amyloid protein precursor (APP) was cloned followed by the identification of the disease mutations in 1990 and 1991 (Kang et al., 1987, Levy et al., 1990, Goate et al., 1991). Together, these discoveries led to modern

Alzheimer research. Much progress in our understanding of the mechanisms related to the disorder has been made since then, although the cause still remains elusive. With an estimated 36 million sufferers worldwide, these figures are said to multiply several-folds in the next decades with numbers doubling every 20 years to reach 66 million by 2030, and 115 million by 2050 (WorldAlzheimerReport, 2011). These numbers highlight the urgent need for an intervention that may halt or delay progression from mild cognitive impairment (MCI), a precursor period of isolated memory loss, to probable AD.

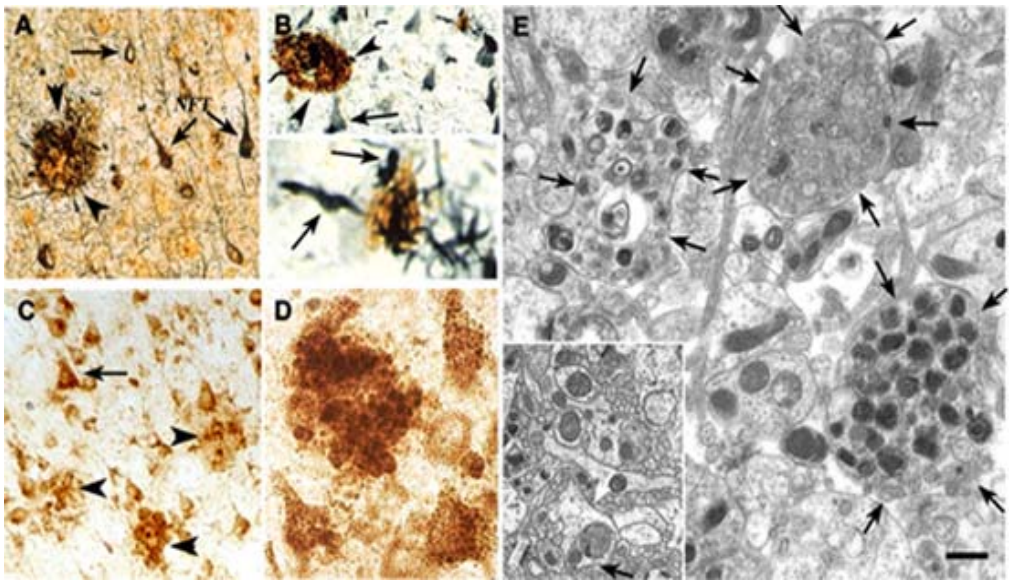

Image from: *Nixon et al., 2007 J Cell Sci.*

Figure 1: Hallmark features of Alzheimer's disease. A, Aβ plaques (arrowheads) and neurofibrillary tangles (arrow) in AD brain by the Bielschowsky silver stain. **B,** Double staining against paired-helical-filament (PHF) tau (arrows) and Aβ (arrowheads) **C, D** Lysosomes of pyramidal neurons (C, arrow) and dystrophic neurites associated with plaques (C, arrowheads; and D) were stained with Cathepsin D antibody. E, Visualization of abnormally enlarged dystrophic neurites (arrows) compared to neurites of normal brain (inset) using electron microscopy, bar = 500nm.

Overview

AD, the most common form of progressive dementia, is mainly associated to Aβ plaques (discussed below) and NFT, peculiar thread-like structures of hyperphosphorylated τ within distorted neurites (Grundke-Iqbal et al., 1986a, Iqbal et al., 1989). Disturbances in axonal transport, decreased levels of neurotrophic factors, neurotransmitters like acetylcholine, and of their respective receptors also define the pathology. Plaque-associated microglia and astrocytes, together with synaptic and neuronal loss are other AD manifestations (Mesulam, 1999, Selkoe, 2001, 2011), synaptic loss being the best correlate of dementia in AD (Coleman et al., 2004). Cerebrovascular and metabolic disturbances have also become critical features of AD (Iadecola, 2004, Zlokovic, 2011). Such manifestations predominate in specific brain areas essential for cognitive functions including the hippocampus followed by association cortices, specifically the entorhinal and frontal cortex, and subcortical structures (Arnold et al., 1991).

Contrary to the rare, early-onset form of AD, the cause of the vast majority of cases of sporadic AD (~95%) is unknown. The major risk factor though is age. In addition, epidemiological studies propose that vascular diseases, including type 2 diabetes, atherosclerosis, hypertension, stroke and hypercholesterolemia confer high probability of developing AD (Kalaria, 2000), with the risk being significantly enhanced when these factors are concomitant (Luchsinger et al., 2005). The fact though that the sporadic AD is phenotypically indistinguishable, both clinically and histopathologically, from familial AD – except for the age of onset – implies that studying genetic AD may be informative about the mechanisms leading to the sporadic form, an approach employed in the present work.

1. Hallmarks of Alzheimer's disease

1.1 Memory deficit

Dementia (of latin origin meaning 'madness', from *de-* 'without' + *ment*, the root of *mens* 'mind') refers to a syndrome of a loss of cognitive ability in a previously unimpaired person, beyond the levels of normal aging. The most common form of dementia among the elderly is AD.

1.1.1 Normal cognitive function

1.1.1.1 Memory systems

Memory is the ability to retain, reactivate, and reconstruct information over periods of time. It is a complex function which draws on a diverse range of modalities to reconstruct a copy of the original past.

Declarative memory is a way our memory represents the world, which is subdivided into two forms: semantic memory and episodic memory. Semantic memory involves memory for factual or 'encyclopedic' knowledge for which specific 'time and place' of the original experience is not remembered (i.e. historical events, mathematical tables, cognitive maps) (Dickerson and Eichenbaum, 2010). Episodic memory involves information about the time and place of an event, as well as detailed information about the event itself, making it a more personal recollection of daily experiences. The ability to talk about a gathering, for instance, that took place in the previous weeks or months, greatly depends on intact episodic memory function. The results of brain imaging, neuropsychological and physiological studies of brain lesions of patients and animals allowed the distinction between these multiple forms of memory and the different brain systems involved (Dickerson and Eichenbaum, 2010). The act of remembering an

episodic memory is orchestrated by a large network of brain areas, including components of the medial temporal lobe (parahippocampal cortical areas and the hippocampus), but also neocortical association areas. The neocortical areas involved in episodic memory mediate many cognitive processing functions such as effortful retrieval (Buckner and Wheeler, 2001, Buckner et al., 2008) and reversal learning or the ability to unlearn a previously learned contingency favouring a switch or an adaptation to the new contingency (Fellows, 2011). Also, dissociated prefrontal regions make functionally separate contributions each processing function (Buckner and Wheeler, 2001).

1.1.2 Cognitive clinical symptoms and diagnosis of AD

AD often becomes symptomatic as minor episodic memory deficits gradually and sporadically impedes ones daily life. Early AD behavioural characteristics vary from loss of thought at midsentence to avoidance of novelty and decreased spontaneity. Concentration and learning impairments, loss of executive functioning, language and visuo-spatial dysfunctions are other clinical manifestations that may be accompanied by irritability, impatience and even depression in the beginning of the disease as patients are still aware of their loss of control (Emilien et al., 2004). Apraxia (inability to control fine and gross motor movement), agnosia (failure to recognize objects or people), motor disturbances, incontinence and agitation have been reported in later stages of the disease, (Cummings, 2004). At end stages, this neurodegenerative disorder leads to death within about eight years from diagnosis, or ranging from one to 20 years (Sadock & Sadock, 2005).

A **clinical diagnosis** can either be "possible" when atypical AD symptoms cannot be categorized under another disease or "probable" when all dementia causes, except AD,

are excluded (Cummings, 2004). MCI is often considered the earliest clinical sign of probable AD. For a complete clinical diagnosis, a patient must present symptoms of memory loss evaluated with specific clinical diagnostic tests mentioned below and another cognitive impairment including language, perception, praxis, calculation and problem solving. A **definitive diagnosis** is confirmed with a pathological examination or a brain autopsy with detected extracellular Aβ plaques and intracellular NFT (McKhann et al., 1984).

1.1.2.1 Clinical Diagnostic tests

1.1.2.1.1 Human tests

The cognitive subscale of the Alzheimer's disease Assessment Scale (ADAS-cog) is widely used for assessment of cognitive function in AD patients as is the Mini Mental Status Exam (MMSE), the most popular cognitive testing instruments used to screen dementia in clinical trials. Briefly these tests measure disturbances of orientation to time and place, immediate recall, short-term verbal memory, calculation, language, and construct ability which are often referred to as the core symptoms of AD. The ADAS score ranges from 0-70, with a higher score from baseline signifying a decline in cognition (Rosen et al., 1984, Skinner et al., 2012). The total number of points on the MMSE is 30, with higher numbers indicating less impairment. A score of 20 to 24 suggests mild dementia, 13 to 20 indicates moderate dementia, and <12, severe dementia (Schreurs, 2010).

1.1.2.1.2 Memory evaluation paradigms in rodents

In preclinical studies, the effects of transgenes or treatments can be investigated on animal learning and memory using a variety of behavioural paradigms. The *Morris*

watermaze (Morris, 1984) is currently the most widely used paradigm for the evaluation of visuo-spatial learning and memory skills in rodents, which corresponds to the highest cognitive level in rodents. Briefly and also described in chapters 2-5, mice learn the location of a hidden platform using visual cues. Their escape latency is used as a surrogate of their learning ability which is reinforced by the undesirable water environment. Spatial memory is established in a subsequent probe trial with the platform removed in which their preference for the platform location is indicative of their memory (Deipolyi et al., 2008). Nevertheless, this task is among the most stressful of cognitive paradigms as rodents are immersed in water (D'Hooge and De Deyn, 2001, Kalueff et al., 2007). *Avoidance tasks* are also extensively used to assess cognitive function in rodents, during which rodents learn to avoid an environment associated to an aversive stimulus (such as foot-shock). In such test, the animals walk freely between the dark/enclosed or the bright/lit compartments of a chamber and learn to associate certain properties of the chamber to a foot shock. The task depends on the innate preference of rodents for dark, enclosed spaces over open areas (Van Dam and De Deyn, 2006). Learning and memory is viewed as the latency to pass the gate in order to avoid the stimulus. However, in this task, declarative memory is not readily discernible from the procedural memory components of the task, unlike in the watermaze task and so less utilized. Dry-land mazes such as the *radial-arm maze* paradigm – during which the rodent must select an arm of the radial maze that contained a food pellet (the reinforcer) during the previous trial – are sometimes preferred over the stressful and physically demanding watermaze task (Harrison et al., 2009). However, food restriction prior to this behavioural experiment limits its value for preclinical evaluation in AD mouse models. Another task used in the

field of AD is the *Barnes maze* which has gained recognition as a dry-land maze with no food deprivation. Like the watermaze, the Barnes maze is based on a delayed match-to-place experiment performed on a circular-shaped platform with escape holes ringed all around (Harrison et al., 2006). In a defined period of time, the rodent initially placed in the center of the platform must find the target escape hole to flee the brightly lit, open surface of the maze using spatial cues. Again, this task depends on the innate preference of rodents for dark, enclosed spaces over open areas. Their escape latency defines their learning ability.

1.1.3 Involvement of immediate early genes in memory formation

The large mnemonic capacity of the brain depends on intrinsic neural networks whose synaptic connectivity and strength are altered according to certain patterns of neuronal activity (Hebb, 1949). Behavioral studies have shown that newly synthesized mRNA and proteins are mandatory for long-term memory but not short-term memory formation (Davis and Squire, 1984) and long-lasting forms of synaptic plasticity such as long-term potentiation (LTP) (Bliss and Collingridge, 1993, Kandel, 2001b, a). Administration of protein synthesis inhibitors effectively blocked long-term memory formation when used just after learning, while they had no effect several hours after training (Squire and Barondes, 1972, Freeman et al., 1995, Nader et al., 2000). LTP is likewise inhibited as mRNA or protein synthesis is blocked immediately after LTP inducing stimulation (Frey et al., 1988). Therefore, gene expression occurring immediately after a stimulus has emerged as a critical element for the maintenance of long-lasting neuronal changes aside from a series of molecular events such as the activation of neurotransmitter and kinase systems and Ca^{2+} influx. These inducible genes transiently and rapidly activated have

been identified and classified as a subset of genes called immediate-early genes (IEGs) (Morgan and Curran, 1991, Lanahan and Worley, 1998).

Of interest to Chapter 3, early growth response protein 1 (Egr-1), also known as Zif268 (zinc finger protein 225), NGFI-A (nerve growth factor-induced protein A), Krox-24, TIS8 or ZENK, is one such immediate early gene, encoding a zinc finger transcription factor (Milbrandt, 1987, O'Donovan et al., 1999). Induction of LTP (Cole et al., 1989) among other learning experiences (Guzowski et al., 2001, Hall et al., 2001) has been associated with an upregulated expression of Zif268/Egr-1 in certain brain areas including the dentate gyrus (Richardson et al., 1992). Inversely, Egr-1 knock-out mice have shown impairment of late-phase LTP and important memory deficits as assessed in the watermaze, taste aversion, and object recognition tasks (Jones et al., 2001) and in a reactivation paradigm (Bozon et al., 2003). These deficits were in line with findings in rats infused with Egr-1 antisense oligonucleotides into the brain (Lee et al., 2004, Lee et al., 2005). Similarly, various mouse models of AD with memory deficits display decreased baseline (Dickey et al., 2003, Tong et al., 2012) or cognitive task-induced (Blanchard et al., 2008) Egr-1 mRNA or protein levels in hippocampus.

1.2 Aβ accumulation

The term amyloid was initially used in 1860 and generally referred to misfolded protein aggregate with starch-like properties (Berchtold and Cotman, 1998). Today, its use denotes a β-pleated sheet structure visualized by histochemical dyes such as Congo red and Thioflavin S (Goedert and Spillantini, 2006). The amyloid protein, a 4-kDa peptide of 36 to 43 amino acids called Aβ, owes its biochemical identity to studies that isolated

the meninges of AD patients (Glenner and Wong, 1984b) and cortex of AD and aged Down syndrome patients (Masters et al., 1985). Sequentially, it is believed that Aβ plaques spontaneously start as [1] nonfibrillar, preamyloid 'diffuse plaques', [2] continuously aggregating into fibrillar, compact deposits known as 'mature plaques', [3] subsequently displaying a dense core of ~8 to 10nm amyloid filaments with a halo of dystrophic neurites hence named 'neuritic plaques'. Noteworthily, Aβ plaques have been documented in cognitively normal elders, albeit diffusely distributed in brain with no abnormal neurites or reactive glial cells, perhaps an explanation to why they are not demented (Selkoe, 2011) .

1.2.1 APP, the amyloid precursor protein

The Aβ peptide is derived from the proteolytic cleavage of the amyloid precursor protein (APP), a large transmembrane glycoprotein, located on chromosome 21, and part of the amyloid precursor-like proteins (APLPs) family (Goldgaber et al., 1987, Kang et al., 1987, Robakis et al., 1987, Tanzi et al., 1987). Alternative APP splicing generates isoforms of different amino acid length: APP695, mainly expressed by neurons and predominantly found in the brain, and APP751 with APP770, produced by all peripheral non-neuronal cells, and brain cells (Ho et al., 1996). The physiological roles of APP are as of yet incompletely defined although it appears that APP is involved in neuronal survival, post-injury repair, axonal transport and synapse formation (Priller et al., 2006, Selkoe, 2011). Soluble Aβ is found in small amounts in the cerebrospinal fluid (CSF, 3-8 nM) and plasma (under 500 pM) of healthy individuals (Haass et al., 1992, Seubert et al., 1992) suggesting that soluble Aβ also has a physiological function (Kamenetz et al., 2003).

1.2.2 APP cleavage by secretases

APP undergoes multiple post-translational modifications such as glycosylation, phosphorylation and tyrosine sulfation together with various types of proteolytic processing before yielding peptide fragments. Its proteolytic cleavage can occur along two pathways: [1] non-amyloidogenic and [2] amyloidogenic pathway (Figure 2). Both extensively remove the extracellular domain to release membrane-anchored carboxy-terminal fragments. Cleavage of the Aβ sequence by the α-secretase initiates the non-amyloidogenic pathway, releasing a large N-terminal sAPPα fragment leaving behind a membrane-bound 83-residue C-terminal fragment, C83 (Figure 2). The latter is further digested by a γ-secretase enzyme multisubunit complex composed of presenilin (PS-1 mainly, or PS-2), APH-1, PEN-2 and nicastrin, liberating a neuroprotective p3 peptide and the amyloid intracellular domain (AICD), also called γ-cleaved C-terminal fragment (γCTF, ~50a.a.) (Esch et al., 1990) known to translocate to the nucleus to regulate transcription of genes involved with synaptic function (Cao and Sudhof, 2001).

Amyloidogenic processing is initiated by the sequential enzymatic actions of β-secretase named β-site APP cleaving enzyme 1 (BACE) (Vassar et al., 1999), generating a soluble sAPPβ product and membrane-bound C99. The latter is subsequently cleaved by γ-secretase within the membrane-spanning domain yielding the Aβ fragment, which may vary between 39 to 43 residues-long (depending on the site of γ-secretase cleavage) and AICD. The amyloidogenic processing has been linked to the lipid raft region of membrane enriched in sphingomylelin, cholesterol, and glycophosphatidylinositol (GPI)–anchored proteins. Instead, the non-amyloidogenic APP cleavage occurs outside a raft (Selkoe, 2001).

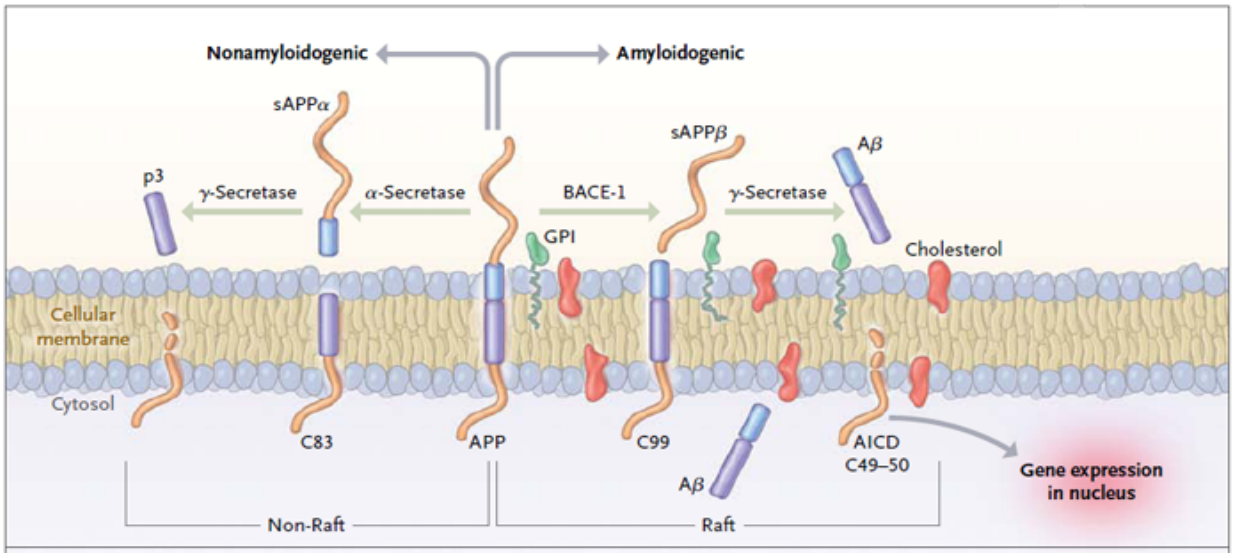

Image from: *Quefurth & Laferla 2010. NEJM*

Figure 2: Schematic representation of the nonamyloidogenic and amyloidogenic APP processing. The non-amyloidogenic pathway is initiated by α-secretase cleavage, which occurs in the middle of the Aβ sequence, and results in the release of several soluble APP fragments. The amyloidogenic pathway releases Aβ peptides through cleavage by β- and γ-secretases.

1.2.3 Mutations in APP and PS underlie familial AD

The APP and PS gene mutations (Chartier-Harlin et al., 1991, Goate et al., 1991, Levy-Lahad et al., 1995, Rogaev et al., 1995, Sherrington et al., 1995) cause autosomal dominant disorders including the rare, early-onset (as early as 30 years old) form of AD representing ~5% of cases (Selkoe, 2011). Over 100 mutations were found in the PS-1 gene on chromosome 14, others in the PS-2 gene on chromosome 1, and ~16 mutations to the APP gene on chromosome 21 (Tanzi and Bertram, 2005). The majority are missense mutations localized near the α-, β-, or γ-secretase cleavage sites. These mutations modify the APP proteolytic processing increasing Aβ production, especially $A\beta_{42}$ (Figure 3) (Van Dam and De Deyn, 2006, Selkoe, 2011). The mutations are named after the nationality or location of the first family in which that specific mutation was demonstrated, and the position of some mutated residues are indicated by three-digit numbers and the single-

letter amino acid code (Figure 3). APP transgenic mice used in this thesis are driven by the platelet-derived growth factor-β (PDGF-β) carry the Indiana (717V→F) and Swedish double mutation (670/671KM→NL) (Figure 3).

Image modified from: *Van Dam & De Deyn 2006. Nature Reviews*

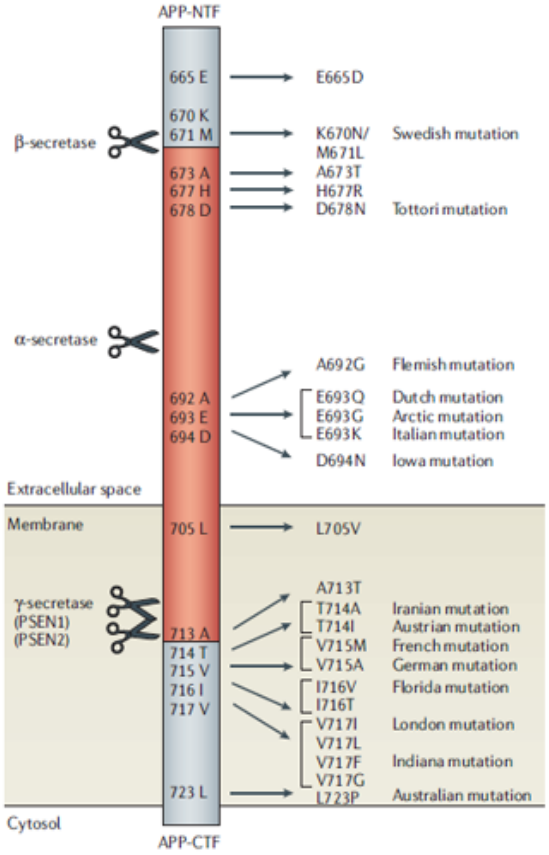

Figure 3: APP mutations associated with early-onset AD. Most mutations are in close vicinity of secretase-cleavage sites, influencing APP processing. The Aβ sequence is indicated in red. A, alanine; Aβ, amyloid-β; APP-NTF, N-terminal fragment of the amyloid precursor protein; APP-CTF, C-terminal fragment of the amyloid precursor protein; D, aspartic acid; E, glutamic acid; F, phenylalanine; G, glycine; H, histidine; I, isoleucine; K, lysine; L, leucine; M, methionine; N, asparagine; P, proline; PSEN, presenilin; Q, glutamine; R, arginine; S, serine; T, threonine; V, valine; Y, tyrosine.

1.2.4 Sporadic AD

In contrast to the hereditary, early onset form of AD, patients with the sporadic form of AD representing ~95% of the cases show symptoms at a later age (after 65 years old). Although age is ubiquitously accepted as a primary risk factor, sporadic AD has been linked to polymorphisms in selected alleles that predispose to the disease, but a

cause has yet to be determined. As such, the most recognized polymorphism is in the gene for the Aβ-binding apolipoprotein E (APOE), located on chromosome 19 where ε4 allele carriers of APOE are more susceptible than the ε2 or ε3 carriers (Poirier et al., 1993, Strittmatter et al., 1993). Of note, many homozygote ε4 carriers remain AD-free (Selkoe, 2001, Tanzi and Bertram, 2005). Sporadic AD may also be explained by a diseased vasculature and impaired brain hemodynamics with amyloidosis as a downstream event (de la Torre, 2004, Zlokovic, 2011). Amyloidosis may be a result of a collective disturbance in production, a disproportional influx (Bell and Zlokovic, 2009) and/or a defective clearance of Aβ (Farris et al., 2007) through a dysfunctional blood-brain-barrier (BBB) or perivascular drainage over and above the alterations due to aging (Bennett et al., 2000). Thus, Aβ accumulation and deposition does not occur through Aβ overproduction like familial AD.

Based on observational studies, diabetes (Luchsinger, 2008) and cardiovascular diseases such as hypercholesterolemia (Solomon and Kivipelto, 2009, Stefani and Liguri, 2009), and hypertension (Launer et al., 1995) have also emerged as potential factors in developing AD in old age with additive effects (Yaffe, 2007). Multiple complex mechanisms link vascular risk factors to cognitive impairment including the degenerative changes in the cerebrovascular vessels that may cause EC and BBB dysfunction (Duron and Hanon, 2008). Consequently, EC may produce an excess of free radicals and induce oxidative stress (see section 1.6.2.2) with increased BBB permeability to proteins leading to Aβ accumulation (Duron and Hanon, 2008). Insulin has also been linked to AD pathology. Specifically, in vitro studies indicate that insulin causes a significant increase in extracellular Aβ levels (Luchsinger, 2008). As such, patients with type 2 diabetes

mellitus or precursor hyperinsulinemia may have insulin-induced increases in Aβ levels. Furthermore, cholesterol is a key regulator of neuronal function that may regulate Aβ plaque deposition in the brain (Solomon and Kivipelto, 2009, Stefani and Liguri, 2009).

1.2.5 Perturbation of Aβ homeostasis

It is believed that AD may ensue when Aβ levels are disturbed. Indeed studies have reported a decreased level and/or activity of Aβ-degrading enzymes : neprilysin (NEP) produced by neurons, and insulin-degrading enzyme (IDE), generated by neuronal, vascular and microglial cells in AD patients (Yasojima et al., 2001, Cook et al., 2003, Morelli et al., 2004). Disturbances of BBB transporters that regulate brain Aβ influx and efflux are also said to be involved. Indeed, studies done on AD patients and mouse models have reported an enhancement of parenchymal amyloid that has been linked to a downregulation of the low-density lipoprotein receptor-related protein (LRP) – which removes Aβ from the brain (Wu et al., 2005) – and an upregulation of the receptor for advanced glycation end products (RAGE) – which brings peripherally-derived Aβ from the blood to the brain (Yan et al., 1996, Deane et al., 2003, Zlokovic, 2005). Lastly, the structural alterations displayed in AD vessels (Perlmutter and Chui, 1990, Vinters et al., 1996, Zarow et al., 1997) could, in part impede perivascular drainage including the removal of Aβ and interstitial fluid out of the brain to cervical lymph nodes.

1.2.6 Detrimental effects of soluble Aβ

Activated glial cells (see 1.3) and distorted neurites within and around Aβ plaques may indicate an attempt by the central nervous system (CNS) to remove this fibrillar material. However, mounting evidence points to soluble Aβ oligomers (dimers, nonamers, dodecamers) as the pathogenic species associated with AD-related abnormalities

including memory deficits, replacing the view that Aβ needed to assemble into fibrils and aggregate for neurotoxic effects. Indeed, soluble and not insoluble Aβ levels distinguished AD patients from high pathologic controls who featured Aβ plaques and met pathological criteria for the disease but had no ante mortem signs of dementia (Lue et al., 1999). Synaptic loss was also not apparent. In line with this human study, in young transgenic AD mouse models, cognitive deficits and loss of synaptic terminals were reported prior to plaque deposition (Hsia et al., 1999, Mucke et al., 2000). Comparison of young transgenic mouse lines featuring either substantial or no Aβ plaque deposition showed similar neuronal and memory deficits. Instead, Aβ*56 was a better determinant of functional deficits (Cheng et al., 2007). Interestingly, transient reduction of Aβ*56 corresponded with memory restoration in aged Tg2576 mice (Lesne et al., 2008). Bitransgenic mice co-overexpressing APP and NEP showed reduced plaque burden, persistent levels of Aβ oligomers, and unchanged spatial memory deficits (Meilandt et al., 2009). Disturbance of ion homeostasis, Ca^{2+}-mediated excitotoxicity and free radical-induced oxidative stress have been observed as a consequence to Aβ oligomer neurotoxicity (Tanzi and Bertram, 2005). Decreased mitochondrial activity, increased caspase activity and massive cell death were also reported in human cortical neuronal cultures treated with Aβ oligomers (Deshpande et al., 2006). Therefore, the identification of soluble Aβ oligomers as diffusible assemblies capable of interfering with synaptic function and integrity warrants an opening for understanding AD memory loss.

1.3 Neurofibrillary tangles

The microtubule-associated protein tau (τ) becomes hyperphosphorylated and accumulates in the somato-dendritic compartment of neurons in several neurodegenerative diseases including AD (Mandell and Banker, 1996, Lee et al., 2001). It aggregates in ~10-nm paired helical insoluble filaments that form lesions called neurofibrillary tangles (NFTs) (Morris et al., 2011).

These τ-induced lesions are thought to contribute to AD pathogenesis as they occur in specific cognitive-related brain areas including the limbic system and the neocortex in a well predictable pattern. Interestingly, the formation of these lesions correlates with the degree of cognitive deficits (Bancher et al., 1993, Giannakopoulos et al., 2003). In addition, the amount of τ found in the CSF increases as the pathology progresses (Hampel et al., 2010). The sequence of tangle development and its association with cognition outlines the Braak and Braak classification scheme, where transentorhinal stages I/II correspond to normal cognition, limbic stages III/IV suggest cognitive impairment and neocortical stages V/VI, dementia (Braak et al., 1999). τ deposits may also be found in the elderly and in multiple unrelated neurodegenerative diseases with no Aβ deposits or neuritic plaques (Morris et al., 2011), Moreover, in a triple transgenic AD mouse model which developed both plaques and NFTs, removal of Aβ resulted in clearance of early τ pathology (Oddo et al., 2003) placing NFT formation downstream of amyloidosis.

1.4 Activated glia

1.4.1 Reactive astrocytes

Being as abundant as neurons (Hilgetag and Barbas, 2009), astrocytes are primordial in ionic and neurotransmitter homeostasis in the extracellular space for neuronal and synaptic function. They are also instrumental in the regulation of cerebral blood flow and perfusion as they receive inputs from multiple synapses while making contact with the local vasculature (Iadecola and Nedergaard, 2007, Carmignoto and Gomez-Gonzalo, 2010). More specifically, glutamatergic synapses are known to regulate astrocytic signaling through activation of metabotropic glutamate and purinergic receptors on astrocytes for localized actions on vessels. Tightly connected amongst them through gap junctions, astrocytes use two waves of signal propagation: evoked intracellular Ca^{2+} or ATP signaling that spreads to neighbouring cells via the gap junctions (Haydon and Carmignoto, 2006). Glial fibrillary acidic protein (GFAP) is an intermediate filament (IF) protein expressed by astrocytes, which is upregulated upon astrocytic activation, hence used as a marker for astrocytic activation. Like microglia, astrocytes are plaque-associated glial cells surrounding, internalizing and degrading Aβ deposits, as shown ex vivo with transplanted astrocytes isolated from enhanced green fluorescent protein expressing adult and neonatal mice into the hippocampi of APPSwe/PS1dE9 transgenic and WT mice. (Wyss-Coray et al., 2003, Pihlaja et al., 2008). Astrocytes also secrete cytokines, chemokines and other inflammatory agents with accelerating potential towards disease progression (Wyss-Coray, 2006).

1.4.2 Reactive microglia

Mesodermal in origin, microglial cells are resident immunological cells responsible for normal tissue maintenance and monitoring of the extracellular microenvironment. Microglial cells are highly ramified with very dynamic processes even during nonpathological conditions. They are considered to be the brain's tissue macrophages and the primary immune effectors of the CNS, and they are known to play a role in amyloid degradation. Indeed, amyloid-associated microglia employ a macropinocytic or receptor-mediated phatocytotic mechanism in the AD brain for the internalization of soluble and fibrillar Aβ, respectively (Stalder et al., 1999, Mandrekar et al., 2009). These soluble peptides are then trafficked into late endolysosomal compartments for the final stages of degradation. To this regard, the most successful of the amyloid clearing interventions – immunization – has been indirectly associated to microglial activation (Hardy and Selkoe, 2002, Barger, 2005). Recent evidence has also highlighted the importance of stimulating the infiltration of blood-derived monocytes and macrophages over resident cells in restricting plaque growth (Yong and Rivest, 2009), in light of their reduced or ineffective Aβ phagocytic aptitude (Fiala et al., 2005). Indeed, inhibition of microglial recruitment from the periphery in APP/PS1 transgenic mice resulted in increased plaque burden (Simard et al., 2006) indicating that additional factors are necessary for effective phagocytic activity in vivo. In reality, as microglia reach Aβ, new cells continue to be added over time, increasing in volume; particularly, peripheral immune cells supplement the process (Bolmont et al., 2008). Studies with respect to the contribution of microglia in Aβ clearance are paralleled by those focusing on the potential negative inflammatory

effects induced by microglia with release of cytokines and other inflammatory mediators (Town et al., 2005).

1.5 Hypometabolism

The BBB consists of a physical barrier between the circulating blood and the CNS. In AD, BBB alterations consist of a reduction in the endothelial glucose transporter 1 (GLUT-1) and glucose transporter activity in the hippocampus and cerebral cortex (Kalaria and Harik, 1989, Simpson et al., 1994, Farkas and Luiten, 2001).

Even more, studies in AD patients (Fukuyama et al., 1994, Mosconi et al., 2004, Langbaum et al., 2009) and AD mouse models (Niwa et al., 2002) have established a link between a decline in GLUT-1 and early decreases in basal cerebral glucose utilization (CGU). Indeed, brain glucose hypometabolism in patients with clinically identified and autopsy-confirmed AD patients is characterized by a progressive reduction in fluorodeoxyglucose positron emission tomography (FDG-PET) predominantly in the temporoparietal brain area (Mielke et al., 1996, Hoffman et al., 2000, Jagust et al., 2007). MCI patients who have an increased risk of AD neuropathology and subsequent conversion to probable AD also feature the same decline (Arnaiz et al., 2001, Drzezga et al., 2005) suggesting that measures of temporoparietal cerebral metabolism may aid in predicting the evolution to AD for patients with MCI.

In vivo experiments in healthy rat brain showed that glucose preferentially fuels astrocytes during neuronal activity even though neurons have greater metabolic needs (Chuquet et al., 2010). Astrocytes then supply neurons with glycolytic products, particularly lactate, for use in oxidative metabolism (Pellerin and Magistretti, 2003).

Hence, the FDG-PET results may predominantly reflect the declining glucose metabolic activity in astrocytes and, to a lesser extent, the declining oxidative metabolism in neurons. This may be due to the declining neuronal function and resulting lowered metabolic demand, and/or to impaired hemodynamics and GLUT-1 losses in damaged brain vessels.

1. 6 Cerebrovascular pathology in Alzheimer's disease

1.6.1 Cerebral circulation

The brain is one of the most perfused organs in the body. Although it comprises ~2% of the total body mass, it receives up to 20% of the cardiac output, consuming ~20% and ~25% of the body's oxygen and glucose (Zlokovic, 2011). Its arterial blood supply depends on two pairs of large arteries: [1] the right and left *internal carotid artery* (ICA), and [2] the right and left *vertebral arteries* (VA) which join distally to form the *basilar artery* (BA) (Figure 4A) (Harrison et al., 2002). Proximally, the basilar artery joins the two internal carotid arteries and other communicating arteries to form a ring at the base of the brain known as the *circle of Willis*, named after Sir Thomas Willis, an English doctor of the 17th century. The circle of Willis gives rise to three pairs of main arteries, the *anterior* (ACA), *middle* (MCA), and *posterior cerebral* (PCA) *arteries* (Figure 4A), of which the former or the latter were used for vascular function analysis throughout my studies, as described in subsequent chapters (also see 1.5.1.1.1).

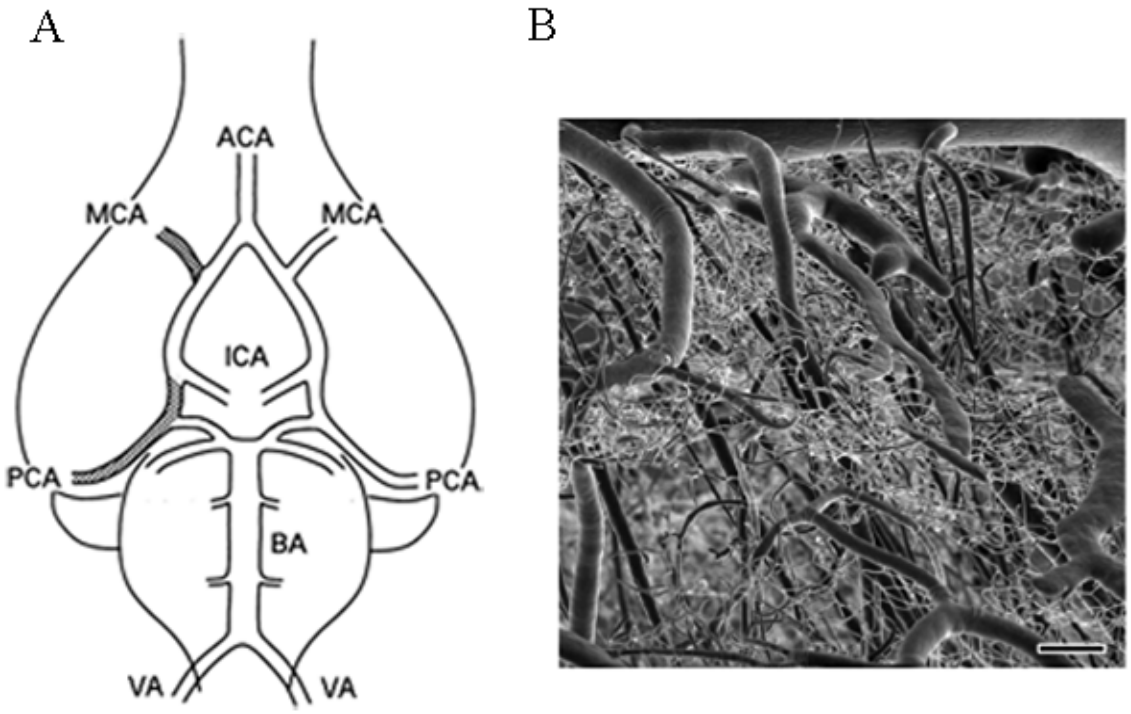

Image A from: *Harrison et al., 2002 Cerebral Cortex*
Image B modified from: *Kitagawa et al., 1998 JCBFM*.

Figure 4: Diagram of the vasculature of the circle of Willis in mouse. A, The middle cerebral artery (MCA) is shown in crosshatch and the posterior cerebral artery (PCA), in dots. **B,** Vasculature perfusing temporal cortex of chinchilla. Upper panels, bar = 500μm and lower panels, bar = 100μm.

The pial arteries and arterioles branching from the circle of Willis are intracranial vessels that run along the surface of the brain within the pia-arachnoid membranes (leptomeninges). Cerebrospinal fluid surrounds these pial vessels that progressively penetrate the brain parenchyma to form the microcirculation which supplies oxygenated blood and nutrients to brain cells (Figure 4B, 5) (Kitagawa et al., 1998, Iadecola, 2004). The penetrating arteries become parenchymal arterioles and capillaries which are almost completely surrounded by astrocytic end-feet (Figure 5) (Iadecola, 2004, Zlokovic, 2011).

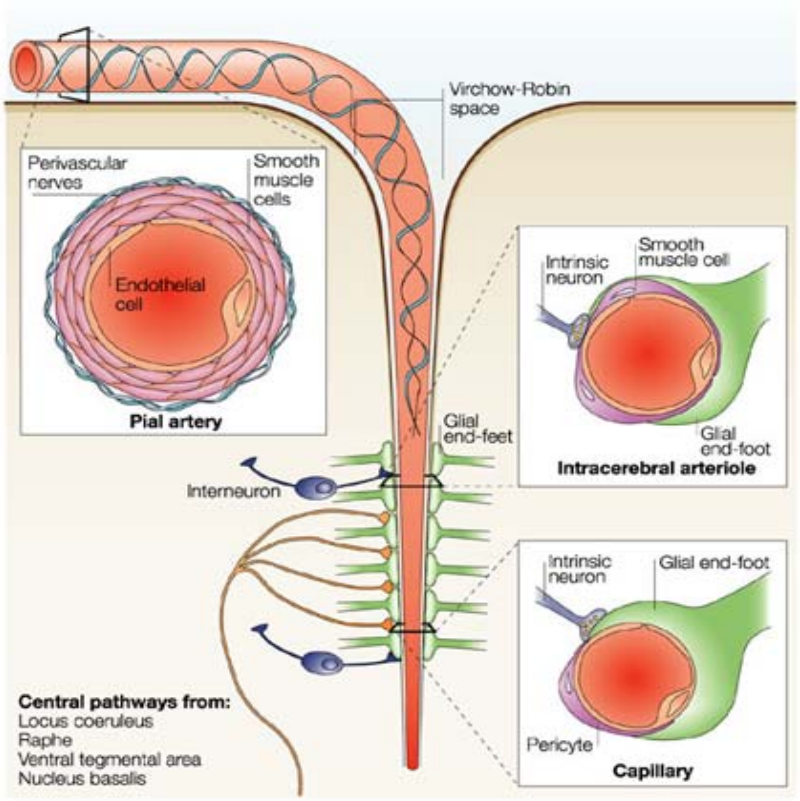

Image from: *Iadecola 2004 Nature Rev Neuroscience*

Figure 5: Intracerebral circulation. Penetrating arteries become arterioles and capillaries which feed the brain with intracerebral circulation.

1.6.1.1 A cerebral vessel and its layers

The wall of cerebral arteries and arterioles consist of three concentric layers: [1] the innermost layer or the *tunic intima*, which consists of a single layer of endothelial cells (ECs); [2] the *tunica media*, which contains mostly smooth muscle cells (SMC) with some elastin and collagen fibers; and [3] the *tunica adventitia*, the outermost layer which mainly comprises collagen fibers, fibroblasts, and associated cells such as perivascular nerves (in large and small pial arteries) and pericytes and astrocytic end-feet (in parenchymal arterioles and capillaries). There are important structural and functional

differences between pial arteries and smaller parenchymal arterioles (Figure 5). Structurally, pial vessels have several layers of circumferentially oriented smooth muscle cells and so possess greater basal tone, than parenchymal arterioles which only have one layer (and none in capillaries). The architecture of cerebral arteries forms an impressively secure network, in part through the Circle of Willis, such that occlusion of one artery may not significantly affect cerebral blood flow (CBF) (Nishimura et al., 2007). In contrast, occlusion of a single arteriole may result in significant reductions in flow and damage to the surrounding local tissue (or infarction) since arterioles are long and largely unbranched, which may explain, in part, the great susceptibility to injury of the deep structures of the brain (Nishimura et al., 2007). Despite their differences, all vessels in the brain possess specialized ECs sealed by tight junctions. This unique morphological and functional barrier between blood and brain, also known as the blood–brain barrier (BBB), meticulously regulates the exchange of nutrients, solutes, and water.

1.6.1.1.1 Endothelial cell and cerebrovascular reactivity

ECs control vascular function by responding to various hormones, neurotransmitters and vasoactive factors. Resting vessel tone is established by EC tonic production of a potent vasodilator: nitric oxide (NO). Tonically, these vasodilatory effects are counterbalanced by the effects of vasoconstrictors including endothelin-1 (ET-1) (Kolb-Bachofen et al., 2006). Inhibition of the NO-synthesizing enzyme, endothelial nitric oxide synthase (eNOS), constricts blood vessels due to the unopposed tonic action of the counteracting vasoconstrictors.

In experiments of vascular reactivity, endothelial function is assessed upon agonist incubation, such as acetylcholine (ACh)-induced dilatation. As ACh binds to M5

muscarinic receptors (Hamel, 2004), ACh leads to receptor-mediated synthesis and diffusion of NO to adjacent SMC, activating soluble guanylate cyclase. This in turn increases cGMP levels, decreases intracellular Ca^{2+} concentrations and relaxes the SMC. A damaged endothelium causes disrupted production of the abovementioned factors. Interestingly, unlike ACh-dilatation, many vasodilators like calcitonin gene-related peptide (CGRP) may also act directly on the SMC (Figure 6, right) with the opening of smooth muscle K^+ channels (Hong et al., 1996, Vedernikov et al., 2002) or because its G-protein-coupled receptor called calcitonin receptor-like receptor (CALCRL) is also located on smooth muscle in pial vessels (Moreno et al., 1999) and in periphery (Brain and Grant, 2004) (Figure 6, left).

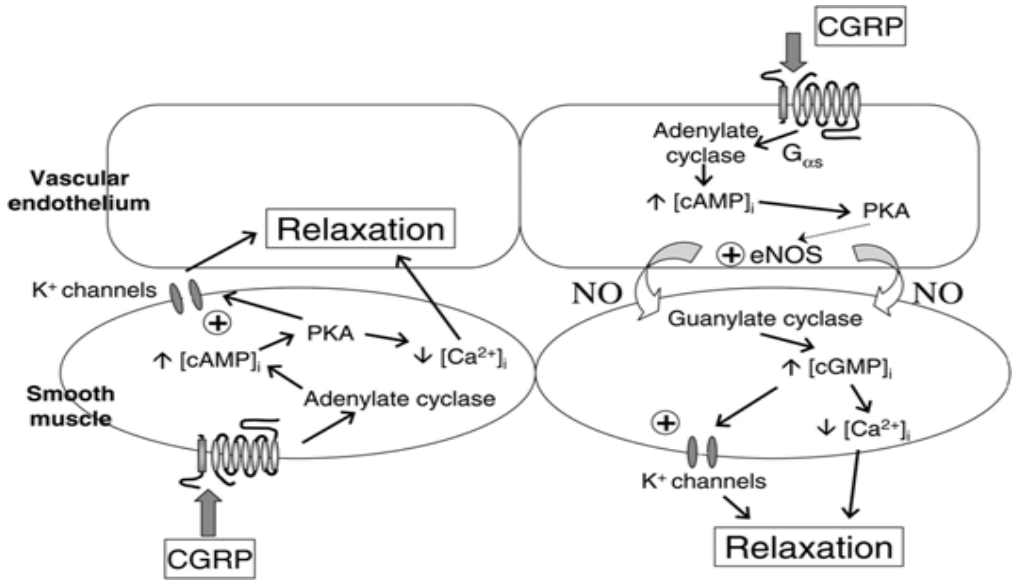

Image from: *Brain 2004 Physiological Reviews*

Figure 6: Signaling pathways of vasodilation to CGRP. Right: endothelium-dependent vasodilatation to CGRP. CGRP, a potent vasodilator mediates its effects by activating a heteromeric receptor composed of a G-protein coupled receptor called calcitonin receptor-like receptor (CALCRL) linked to single transmembrane domain receptor activity-modifying protein 1 (RAMP1). Like many other vasodilators including ACh, binding to its receptor induces receptor-mediated NO synthesis and diffusion via the soluble guanylate cyclase for muscle relaxation. Interestingly, CALCRLs are not only located on ECs but also on SMCs. *Left*: endothelium-

independent vasodilatation to CGRP. Activation of CGRP receptors on SMCs is coupled to production of cyclic adenosine monophosphate (cAMP) by adenylate cyclase. The increase in intracellular cAMP concentration ($[cAMP]_i$) in turn stimulates protein kinase A (PKA). K^+ channels then open activating Ca^{2+} sequestration mechanisms to cause SMC dilatation.

1.6.1.2 The neurovascular unit

Upon neuronal activation, evoked CBF relies on the synchronized actions of neurons, astrocytes and vascular cells that compose the neurogliovascular unit (Iadecola, 2004, Hamel, 2006). Indeed, signals generated by a network of activated neurons are transduced into vasomotor responses and changes in local CBF through interplay between the neuronal, astroglial and vascular components of the neurovascular unit. This intimate relationship between neural activity and CBF is known as neurovascular coupling or functional hyperemia, which underlies the signals used in modern neuroimaging techniques including positron emission tomography (PET) and functional magnetic resonance imaging (fMRI). This coupling response is altered in many pathological states, such as hypertension and AD (Girouard and Iadecola, 2006).

A commonly used paradigm in functional studies is the evoked CBF of rodent barrel cortex upon whisker stimulation. It is also widely used in AD studies as the somatosensory cortex has been reported to be an area of reduced functional hyperemia in APP mice (Niwa et al., 2000). The most often used method in mice experiments involves real-time measurements of the hemodynamic changes using a laser Doppler flowmetry (LDF) probe placed above the barrel cortex opposite to the stimulated whiskers (Lecrux and Hamel, 2011) (Figure 7). With this model, a ~15-25% increase in CBF is usually observed (Koehler et al., 2009, Lecrux and Hamel, 2011). It therefore represents a robust

model for the investigation of possible cortical neurovascular coupling alterations in pathology.

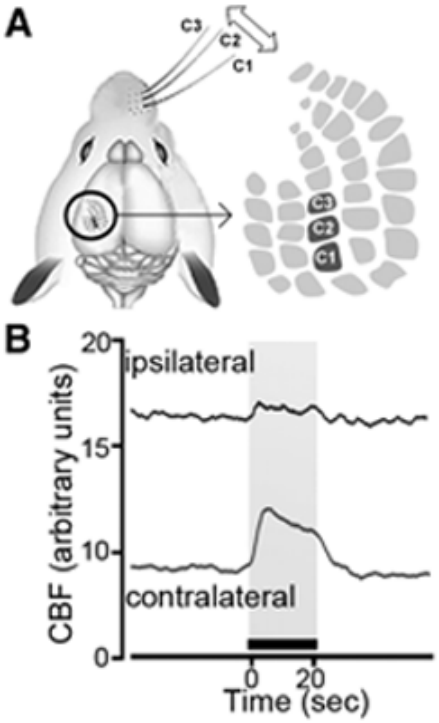

Image modified from: *Lecrux et al., 2011 J. Neurosc.*

Figure 7: Evoked CBF in somatosensory cortex upon whisker stimulation. A, Schematic representation of stimulated whiskers C1, C2 and C3 on the right snout of a rat and corresponding barrels in the somatosensory cortex. For evoked CBF measurements, all whiskers are usually stimulated. **B,** Representative cortical CBF recordings in the ipsilateral and contralateral cortices before, during and after whisker stimulation (20 sec, as depicted by black bar). Upon whiskers stimulation, CBF is significantly increased in the contralateral cortex.

1.6.2 Features of cerebrovascular pathology

1.6.2.1 Hypoperfusion

An early and important contributing factor to AD pathogenesis is chronic cerebral hypoperfusion, which is thought to precede neurodegeneration and cognitive deficits (Farkas and Luiten, 2001, de la Torre, 2004, Iadecola, 2004). Indeed, in AD patients, CBF is decreased both at rest (Bateman et al., 2006, Vicenzini et al., 2007) and during functional hyperemia (Hock et al., 1997, Rosengarten et al., 2006) by 10 to 30% in the temporoparietal, frontal, posterior cingulate cortex, and/or hippocampus compared to age-matched elderly (Farkas and Luiten, 2001). Interestingly, dementia severity occurs

proportionally to this gradual decline (Farkas and Luiten, 2001). The Rotterdam (Ruitenberg et al., 2005) and Honolulu-Asia Aging (Freitag et al., 2006) studies with respectively lower middle cerebral artery BF velocity or midlife hypertension are examples demonstrating a link between chronic hypoperfusion and dementia. In rodents, vessel occlusion in rats (Farkas et al., 2007, Barros et al., 2009) and vessel stenosis in mice (Miki et al., 2009) have induced impairments in memory tasks. Nevertheless, the hypoperfusion in AD has not earned a causal role in dementia. Instead, it is widely recognized as an aggravating factor as highlighted by the worsening of memory deficits induced by hypoxia in APP mice (Sun et al., 2006).

1.6.2.2 Aβ-induced cerebrovascular oxidative stress

Soluble Aβ induces vascular dysfunction through a pro-oxidant pathway involving NADPH oxidase (Niwa et al., 2000, Shimohama et al., 2000, Abramov et al., 2004), a multiunit membrane-bound enzyme generating superoxide ($O_2\cdot^-$) through the transfer of electrons from NADPH to molecular oxygen. The interaction of the superoxide with nitric oxide (NO) decreases NO bioavailability and produces reactive intermediates that oxidize macromolecules and impair their function, such as the peroxynitrite radical ($ONOO^-$), thus further aggravating oxidative stress and resulting in both compromised resting and stimulus-evoked cerebrovascular responses evident throughout the AD brain (Butterfield et al., 2001). APP mice overexpressing soluble Aβ reproduce these deficits (Butterfield et al., 2001, Park et al., 2005, Tong et al., 2005) which in turn are abolished by pharmacologically scavenging $O_2^{\cdot-}$ (Tong et al., 2005), by coexpressing APP with the $O_2^{\cdot-}$ scavenger, superoxide dismutase (SOD), or by inhibition of NADPH oxidase, using APP mice lacking the catalytic subunit of the enzyme (Iadecola et al., 1999, Park et al.,

2005). Vascular dysfunction was substantially restored after acute depletion of soluble Aβ via administration of γ secretase inhibition (Han et al., 2008). Results in older APP mice implicated not only the soluble but also the insoluble vascular Aβ in causing significant impairments in vasomotor functions (Han et al., 2008), described below (2.4.4).

1.6.2.3 Cerebral amyloid angiopathy, CAA

Insoluble Aβ deposition within vessel walls, known as cerebral amyloid angiopathy (CAA) is the most commonly referred element of the AD cerebrovascular pathology created by the binding of Aβ to an upregulated basement membrane (see 2.4.5) (Herzig et al., 2006). CAA is another consequence of faulty clearance or increased production of Aβ across the BBB. It mainly disrupts the integrity of leptomeningeal and cortical small and medium-sized arteries and arterioles where there is an ongoing substitution of the vascular SMC layer (Christie et al., 2001). As arteries stiffen, Aβ is deposited in interstitial fluid drainage pathways further impeding the drainage of soluble Aβ from the brain altering homeostasis and the neuronal environment (Weller et al., 2008). Failure of perivascular drainage has two major consequences: [1] intracerebral hemorrhage associated with rupture of Aβ-loaded arteries; and [2] exacerbation of neurodegenerative and cognitive processes resulting in cognitive decline and dementia proportionally to the severity of CAA (Attems et al., 2007, Weller et al., 2008).

1.6.2.4 Basement membrane (BM) thickening

BM thickening of the cerebrovasculature serves as a nidus for plaque formation, playing a significant role in the formation of CAA (Herzig et al., 2006). AD-associated vascular

BM alterations are defined by both thickening and vacuolization with abnormally enlarged and rounded pericytes. Moreover, immunocytochemistry results have demonstrated the involvement of primordially three intrinsic BM components, namely collagen type IV, laminin, and heparan sulfate proteoglycan (HSPG) disrupting the endothelial surface in hindered brain areas of AD (Perlmutter and Chui, 1990, Zarow et al., 1997) in consequence of either a decreased turnover or upregulated synthesis of these matrix proteins (Kalaria and Pax, 1995) by endothelial cells, pericytes and astroglial cells. These perivascular fibrotic alterations are beyond those related to the burden of age (Mancardi et al., 1980) mediated by unknown molecular mediators although, evidence points to the contribution of the pro-fibrotic cytokine, transforming growth factor-beta 1 (TGF-β1).

1.6.2.5 Transforming growth factor-beta 1 (TGF-β1)

TGF-β is a secreted cytokine that exists in at least three distinct isoforms called TGF-β1, -β2, and -β3. In brain, TGF-β2, TGF-β3, and TGF-β receptors are widely distributed (Unsicker et al., 1991). Apart from their isoform-specific effects (Bottinger et al., 1997), all isoforms are critical in embryonic development and tissue homeostasis during adult life (Itoh et al., 2000). Latent TGF-β acts as a sensor to perturbations in the extracellular matrix (ECM). TGF-β1 is expressed mostly in response to aging and/or disturbances (Finch et al., 1993, Nichols, 1999, Bye et al., 2001) including mechanical injury (Lin et al., 2005) and ischemic stroke (Krupinski et al., 1996), consequently activating the latent peptide prompting fibrosis and wound repair (Ignotz and Massague, 1986, Annes et al., 2003) as a compensatory measure (Leask and Abraham, 2004). The predominant isoform underlying deregulations in TGF-β signaling is TGF-β1 which acts through endocrine

signaling, while TGF-β2 and TGF-β3 use local autocrine and paracrine modes of cellular communication (Bottinger et al., 1997).

The SMAD pathway is the canonical signaling pathway that TGF-β family members signal through. In this pathway, TGF-β dimers bind to a type II serine/threonine kinase receptors which recruits and phosphorylates two type I receptors. The type I kinase activates receptor-regulated Smads (R-Smads) 2 and/or 3, which associate with the common-partner Smad (Co-Smad) 4. Smad anchor for receptor activation (SARA) recruits Smad2 from the cytosol to the type I receptor. The heteromeric Smad complex then translocates to the nucleus where it interacts with coactivators to regulate expression of target genes (Figure 8), including the profibrotic connective tissue growth factor (CTGF). TGF-β1 ends its own activation by inducing inhibitory Smads (I-Smads) that bind to the type I kinase, thus competing with R-Smads. Cytokines such as TNF-α and IFN-γ may also terminate the profibrotic response.

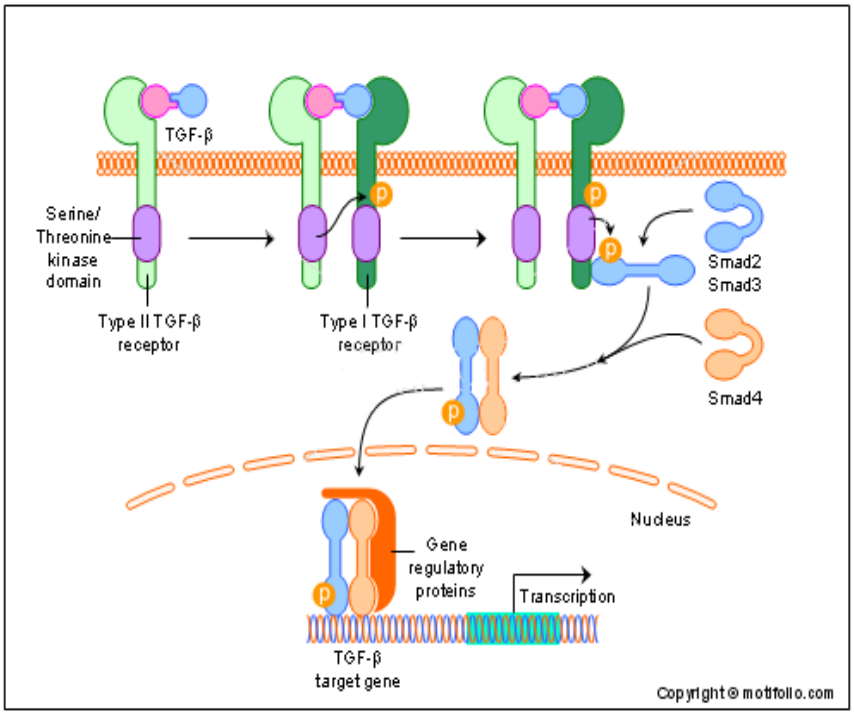

Image modified from: *http://www.motifolio.com/5111158.html*

Figure 8: Smad-dependent signaling cascade activated by TGF-β. Activation of type I/II receptors by TGF-β results in the formation of the heteromeric Smad complexes that accumulate in the nucleus for regulation of target genes

Interestingly, TGF-β1 is chronically elevated in numerous neurodegenerative diseases (Buckwalter and Wyss-Coray, 2004), including AD. In fact, studies have shown elevated levels of TGF-β1 in the serum (Malaguarnera et al., 2006), cerebrospinal fluid (Wyss-Coray et al., 1997, Tarkowski et al., 2002), amyloid plaques (van der Wal et al., 1993), and in brain vessels in AD patients (Grammas and Ovase, 2002). TGF-β1 gene polymorphisms have also been considered as a possible risk factor for developing AD (Luedecking et al., 2000). Indeed, whereas TGF-β1 has been shown to have beneficial effects (Boche et al., 2003, Tesseur and Wyss-Coray, 2006, Caraci et al., 2008), it also exerts harmful ones including reduced neurogenesis (Buckwalter et al., 2006), enhanced vascular fibrosis (Wyss-Coray et al., 2000) and hypoperfusion (Gaertner et al., 2005),

similar to the vascular alterations seen in AD. Indeed, transgenic TGF mice recapitulate well the cerebrovascular pathology of AD (see 2.2.2) (Wyss-Coray et al., 2000).

2. Animal models of AD

From nematodes (*Caenorhabditis elegans*) to fruit flies, rodents, rabbits and primates, animal models have been an invaluable tool in dissecting the pathogenic features and underlying mechanisms of AD. Although the genetic, familial early onset form of AD accounts for only ~5% of AD cases, models expressing pathogenic mutations of human genes have become crucial in unravelling disease processes, and contributing to drug discovery and development.

2.1 Aβ infusion models

Administration of Aβ in rodents (Jhoo et al., 2004) has been used to reproduce the clinical outcomes of AD pathology including learning and memory impairments. Infusions are Aβ-species specific and mainly made in the cerebral ventricles, nucleus basalis of Meynert (nbM) or hippocampus. Rats with intracerebroventricular infusion of Aβ exhibit Aβ accumulation, gliosis, impaired LTP in the CA1 field of the hippocampus, as well as learning and memory deficits (Nitta et al., 1994, Nitta et al., 1997, Itoh et al., 1999). Although this approach may be informative about the Aβ species mediating the pathology, infusion models have produced inconsistent results, possibly related to methodological differences across studies such as the site of infusion, the type of injected peptide, its concentration, and the length of Aβ exposure (chronic versus acute) (Dodart and May, 2005).

2.2 Transgenic mouse models

AD-related mutations (see 2.3.3) led to the creation of transgenic mice harbouring mutated or wild-type human APP and/or PS genes, which feature key aspects of AD neuropathology, including cognitive impairment and cerebrovascular dysfunction. A first attempt to generate transgenic models was based on overexpression of the entire sequence of the human APP gene (Yamaguchi et al., 1991, Buxbaum et al., 1993, Lamb et al., 1993). Although the APP transgene was successfully expressed, these models did not evidence plaque deposition or any AD-related neuropathological changes. It was later understood that besides its overexpression, APP must also be mutated for the production of high-enough levels of Aβ species, which later led to the generation of new animal models combining APP overexpression with human AD mutations (Hsiao et al., 1995, Moechars et al., 1999). These models today serve as useful tools in the study and understanding of the induced AD alterations, and in the evaluation of treatment efficacy. Of course, these models do not fully emulate the human pathology, and so challenges still remain in establishing the equivalence of the resulting phenotypes with what is truly seen in AD.

For instance, models overexpressing the human APP lack neuronal loss or neurodegeneration, while expressing synaptic dysfunction. In addition, although some models – including the APP mouse model – feature τ hyperphosphorylation, they do not develop the human AD-related tangle pathology (Janus and Westaway, 2001, Dodart and May, 2005, McGowan et al., 2006). This could be due to the inability of mouse τ to assemble into fibrils, unlike the human τ. Thus, transgenic-based research has mainly focused on the Aβ pathology, except for the triple transgenic mouse model by the group

of LaFerla also harboring the τ gene mutations related to frontotemporal dementia (Oddo et al., 2003). This model overexpresses the mutated PS1, APP and τ, and develops NFTs (Oddo et al., 2003). Another differing point between transgenic APP models and human AD is the degree of the cholinergic deficit observed, which is almost 3 times more extensive in humans than in mice (~80% vs. ~30% respectively) (Aucoin et al., 2005). This may be explained by the fact that in humans, the nbM, which degenerates in AD, is the only source of cholinergic input to the cortex. In contrast, in rodents, intrinsic cortical cholinergic interneurons, which are absent from primates, supply up to 30% of this input (Johnston et al., 1981, Mesulam, 2004), and so could compensate for the loss of basal forebrain afferents.

In anyway, the natural occurrence of the pathology is not always reproducible. Firstly, the required insertion of the human mutated APP into the small mouse genome since the rodent peptide Aβ is less prone to aggregate into oligomers and fibrils (Farris et al., 2007) can potentially instigate unknown alterations in physiology, learning and memory in transgenic animals. Secondly, protein overexpression in rodents is widespread whereas a peptide or isoform in the pathology may be overexpressed in a specific cell type or subcellular compartment of a specific brain region. For instance, the APP mice of the J20 line overexpress an alternatively spliced minigene encoding all three mutated human APP isoforms, i.e. APP751, 770, 695 (Games et al., 1995; Mucke et al, 2000), whereas neurons in the brain express APP695 in abundance. The artificial upregulation of transgenes from birth to death surely does not mirror the reality of the pathology. Nevertheless, despite these limitations, transgenic mice are important tools in deciphering various aspects of AD pathology, and in testing therapy in an *in vivo* setting.

The most widely used animal models of the APP-based hypothesis are the following: [1] the PDAPP line, the first AD mouse model harbouring the Indiana mutation (V717F) under the control of a PDGF promoter, which leads to a tenfold elevation of hAPP and proportional Aβ levels in the brain; [2] the Tg2576 mouse line carrying the Swedish double mutation (K670N/M671L) on the 695 hAPP controlled by the hamster PrP promoter; [3] APP23Tg mice with the 751 isoform of hAPP harbouring the double Swedish mutation but, under the control of the Thy-1.2 promoter with the transgene is overexpressed sevenfold; [4] the TgCRND8 mouse, carrying both the Swedish and Indiana mutations, and the 695 hAPP isoform under the control of hamster PrP promoter. It is one of the earliest-onset AD models developing plaque as early as 3 months of age (Chishti et al., 2001); [5] the J9 and J20 lines expressing both the Swedish and Indiana mutations. Unlike TgCRND8, these mice have mutations on the hAPP 770 isoform under the control of the promoter PDGF (described in 3.1); [6] APP Dutch mutation, rather than amyloid deposition, causes a hereditary form of cerebral haemorrhage with insertion of the E693Q mutation under the Thy-1.2 promoter (Herzig et al., 2004). For more on these models, see (Balducci and Forloni, 2011). Below is a description of the two mouse models namely singly transgenic mice overexpressing Aβ (APP mice) and TGF-β1 (TGF mice), which were used to generate the bitransgenic mouse model (Chapter 1) used in this work.

2.2.1 Aβ-overexpressing mice (APP) (J20 line)

APP mice used in this thesis overexpress a mutant form of the human APP and progressively develop AD neuropathology and cognitive dysfunction. More specifically, they overexpressed the Swedish (670/671KM→NL) and Indiana (717V→F) mutations

driven by the neuronal platelet-derived growth factor beta (PDGFβ) promoter on a C57BL/6J background (line J20) (Mucke et al., 2000). The Indiana mutation heightens the Aβ1-42 levels, while the Swedish double mutation mainly increases Aβ1-40 levels. By 2-4 months of age, APP mice display high levels of soluble Aβ, and by 5-6 months, Aβ senile plaques in the cortex/hippocampus, neuritic plaques, CAA, cholinergic denervation, synaptic loss, and severe spatial memory impairments in the Morris watermaze that worsens with age (Mucke et al., 2000, Palop et al., 2003, Aucoin et al., 2005). They also feature activated glia, decreased synaptophysin immunoreactivity, and a cerebrovascular pathology characterized by reduced hemodynamic responses and decreased vasodilatory capacity ascribed to Aβ-induced oxidative stress (Tong et al., 2005, Nicolakakis et al., 2008). These cerebrovascular dysfunctions are clearly detected at 4 months of age, when oxidative stress-related NADPH oxidase-derived $O_2^{\cdot -}$ radicals significantly hinders vasodilatory function. The cerebrovascular deficits are countered by antioxidant therapy both in vitro and in vivo (Tong et al., 2005, Nicolakakis et al., 2008). Functionally, APP mice display cerebrovascular dysfunctions with progressive impairments in endothelium-dependent and -independent dilatations. By the age of 12 months, vascular Aβ accumulation, namely CAA is noticeable, reminiscent of that seen in AD patients (Tong et al., 2005, Tong et al., 2009). These mice are widely used to understand the role of amyloidosis on memory loss and the overall cerebrovascular and neuronal AD pathology (Mucke et al., 2000, Niwa et al., 2000, Park et al., 2005).

2.2.2 TGF-β1-overexpressing mice (TGF)

Transgenic mice that overexpress a constitutively active form of TGF-β1 driven by the glial fibrillary acidic protein (GFAP) promoter (line T64) (Wyss-Coray et al., 1995)

mimic several aspects of the cerebrovascular pathology seen in AD, such as reduced cerebral perfusion (Gaertner et al., 2005). It is also marked by a decreased glucose metabolism (Galea et al., 2006). Moreover, TGF-β1 overexpression induces cerebral vasculature remodeling (i.e. vessel fibrosis) delineated by augmented extracellular matrix (ECM) protein deposition in the vascular basement membrane (Wyss-Coray et al., 2000), as reported in AD brain vessels (Kalaria and Pax, 1995, Tong et al., 2005). Functionally, TGF mice display cerebrovascular dysfunctions unresponsive to antioxidants (unlike APP mice) with progressive impairments in endothelium-dependent and -independent dilatations, as well as a selective reduction in endothelin-1 (ET-1) contractile response in elderly animals (Tong et al., 2005, Hamel et al., 2008, Nicolakakis et al., 2011). These dysfunctions have been associated with reduced synthesis of vasoactive molecules in the blood vessels, altered ETA receptor signalling and upregulation of vascular ETB receptor levels (Tong et al., 2005, Tong and Hamel, 2007). Glial activation is also prominent in TGF mice (Lacombe et al., 2004). Unlike APP mice, TGF mice do not exhibit Aβ plaques in the parenchyma nor in the blood vessels. Cholinergic deficits (Nicolakakis et al., 2011) and memory impairments (Papadopoulos et al., 2010, Nicolakakis et al., 2011) are also absent in TGF mice marking the limitations of this model to recapitulate the full AD pathology.

Collectively, these genetically engineered mice mimic specific complementary facets of AD cerebrovascular pathology, which led to the creation of the APP/TGF mouse model by the group of Wyss-Coray with the H6 line APP mice and the T64 TGF mice in effort to further decipher their interactive implications related to Aβ deposition (Wyss-Coray et al., 1997). These mice though were never tested functionally in terms of

vascular and memory deficits. Hence, the first experimental chapter of my thesis will be aimed at fully characterizing these deficits in APP/TGF mice generated from the crossing of J20 APP mice with T64 TGF mice, since they are the only available model that combines the cognitive and TGF-β1-related cerebrovascular pathology seen in AD patients.

3. Therapies

The gap in understanding AD pathology has significantly compromised the progression of effective drug discoveries leaving the number of investigated therapeutic avenues unsuccessful.

3.1 Current treatments and alternative approaches

Five drugs are presently FDA approved for the treatment of AD and prescribed to mild-to-moderate cases of AD, despite minimal symptomatic relief during a limited timeline (Courtney et al., 2004). Four of these drugs (tacrine or Cognex®, donepezil or Aricept®, rivastigmine or Exelon®, galantomine or Reminyl®) are acetylcholinesterase inhibitors designed to enhance the availability of brain acetylcholine (ACh) at cholinergic synapses by deactivating acetylcholinesterase, the enzyme responsible for the degradation of this neurotransmitter, thus facilitating neural transmission. Of note, the first one is no longer in use due to liver-toxicity side-effects (Watkins et al., 1994). The rational for the development of cholinomimetics is based on the well documented role of the cholinergic system in learning and memory (Deutsch et al., 1966, Deutsch, 1971, Bartus et al., 1985), as well as the progressive degeneration of brain cholinergic neurons in AD patients

(Whitehouse et al., 1981). The fifth (Namenda®, memantine HCl) is an NMDA receptor antagonist which can be prescribed to moderate-to-severe AD patients alone or together with a cholinesterase inhibitor (Reisberg et al., 2003). This therapy is based on evidence for an overactive glutamate system in AD, where glutamate receptors are excessively activated resulting in neuronal Ca^{2+} overload and excitotoxic death. Memantine, which occupies the same NMDA channel site as Mg^{2+}, blocks the tonic pathological activation of NMDA receptors while allowing physiological activation (Molinuevo et al., 2005).

Alternative approaches have also been considered including the use of anti-inflammatory agents such as non-steroidal anti-inflammatory drugs (McGeer and McGeer, 2004, Cote et al., 2012), selective COX-2 inhibitors (Trepanier and Milgram, 2010) and anti-amyloid drugs including β-amyloid aggregate inhibitors, γ-secretase modulators and anti-Aβ immunization. These strategies are under development on the basis of eliminating the production and aggregation of the Aβ peptide to counter cognitive impairment at a time when it is still reversible, as demonstrated in rats (Klyubin et al., 2005). The main target though is soluble Aβ rather than Aβ plaques as furthered by the disappointing findings of the amyloid peptide vaccine (AN1792), which resulted in Aβ plaque clearance, but failed in stopping the progression to severe dementia (Holmes et al., 2008).

Finally, an attractive therapeutic effort for AD is the control of the predominant risk factors such as diabetes, hypercholesterolemia or hypertension. Hence, medications currently used to control these diseases and, particularly those with pleiotropic effects including the anti-diabetic drug pioglitazone, a peroxisome proliferator-activated receptor gamma (PPARγ) agonist; the anticholesterol agent simvastastin, a cholesterol-lowering

statin, and the antihypertensive drug losartan, an angiotensin II receptor type 1 (AT1R) antagonist have been considered as promising therapeutic avenues.

3.2 Pioglitazone

The peroxisome proliferator-activated receptors (PPARs) are a family of three (α, γ, β/δ) ligand-activated nuclear transcription factors encoded by different genes, which regulate peripheral glucose metabolism. Each member controls expression of a specific set of genes encouraging fat storage and insulin sensitivity upon dietary intake. Synthetic PPARγ ligands, a family of thiazolidinediones including pioglitazone (Actos®, Takeda pharmaceuticals) and rosiglitazone, are currently prescribed as oral anti-diabetic mediators to patients with type 2 diabetes based on their ability to decrease insulin resistance. Like other nuclear hormone receptors, PPARs form a heterodimer with the retinoid X receptor (RXR) for 9-*cis* retinoic acid and bind specific response elements within promoters. Upon ligand activation, the PPAR:RXR complex initiates or represses transcription of target genes (Figure 9).

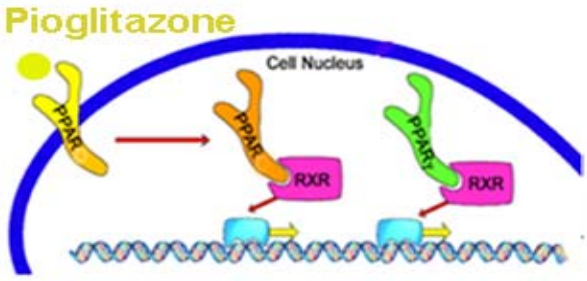

Image modified from: http://en.wikipedia.org/wiki/File:PPAR-diagram.png

Figure 9: Pioglitazone activation. Upon binding of the agonist, PPARs heterodimerize with the common retinoid X receptor (RXR) and recruit coregulators and chromatin

modifying enzymes to specific DNA sequences, named peroxisome proliferator response elements (PPREs), in the promoters of target genes.

PPARs were recently found in brain cell types including vascular endothelial cells (Bishop-Bailey and Hla, 1999), astrocytes (Dello Russo et al., 2003) and neurons (Izawa et al., 2009). Studies have shown that their activation is involved in normal vascular and brain function, and are therapeutic under pathological conditions, including AD (Pedersen et al., 2006, Nicolakakis and Hamel, 2010).

Encouraging preliminary results from clinical trials on cognition were released before the start of my PhD studies with a 6-month rosiglitazone treatment in mild to moderate AD patients (Watson et al., 2005, Risner et al., 2006). Since though, rosiglitazone has been associated with increased risk for cardiovascular side effects (Nissen and Wolski, 2010), although pioglitazone seems to have a better cardiovascular safety profile (Lincoff et al., 2007, Ciudin et al., 2012). In addition, the use of pioglitazone in our laboratory (Nicolakakis et al., 2008, Nicolakakis et al., 2011) provided promising results.

What originally sparked interest in selecting pioglitazone as a therapeutic target for AD was its ability to cross the BBB (Maeshiba et al., 1997). This choice was additionally based on its proven efficacy to regulate genes in oxidative, inflammatory and remodeling pathways (Kersten et al., 2000), as well as reverse cerebrovascular dysfunction in humans (Martens et al., 2005) and in animal models of hypertension and diabetes (Diep et al., 2002, Bagi et al., 2004). Evidence also demonstrates that PPARγ agonists inhibit vascular remodeling following injury (Phillips et al., 2003). Upregulation of extracellular matrix turnover of molecules such as CTGF, vascular endothelial growth

factor (VEGF) and collagen IV together with altered neurometabolic coupling in diseased animals including AD models were reported to be normalized by PPARγ agonists (Fu et al., 2001). Another well documented property ascribed to PPARγ is their ability to silence inflammatory gene expression. Anti-inflammatory effects of pioglitazone were corroborated in various mouse models of AD. COX-2 and inducible nitric oxide synthase (iNOS) expression were attenuated in the cortex and hippocampus of 10-month-old APPV717I mice upon acute 7-day pioglitazone treatment (Heneka et al., 2005). Also, astrocytic activation was significantly reduced in cortex of APP (Nicolakakis et al., 2008, Escribano et al., 2010, Toledo and Inestrosa, 2010) and TGF (Lacombe et al., 2004, Nicolakakis et al., 2011) mice treated with pioglitazone. In our laboratory, we have also found that pioglitazone overcomes cerebrovascular dysfunction, lessened neurometabolic coupling, and cerebral oxidative stress in aged APP (Nicolakakis et al., 2008) and TGF (Nicolakakis et al., 2011) mice. Collectively, the above-mentioned studies advocate the use of these agonists in treating AD as they provide significant symptomatic benefits. This potential will be assessed in Chapter 2 of my thesis where I will test the therapeutic efficacy of pioglitazone in adult and aged APP/TGF mice on several AD landmarks.

3.3 Simvastatin

Statins, the most potent hypocholesterolemic drugs, are competitive inhibitors of hydroxymethylglutaryl coenzyme A (HMG-CoA) reductase, the rate-limiting enzyme of the mevalonate pathway, an intermediary product in cholesterol synthesis (Figure 10).

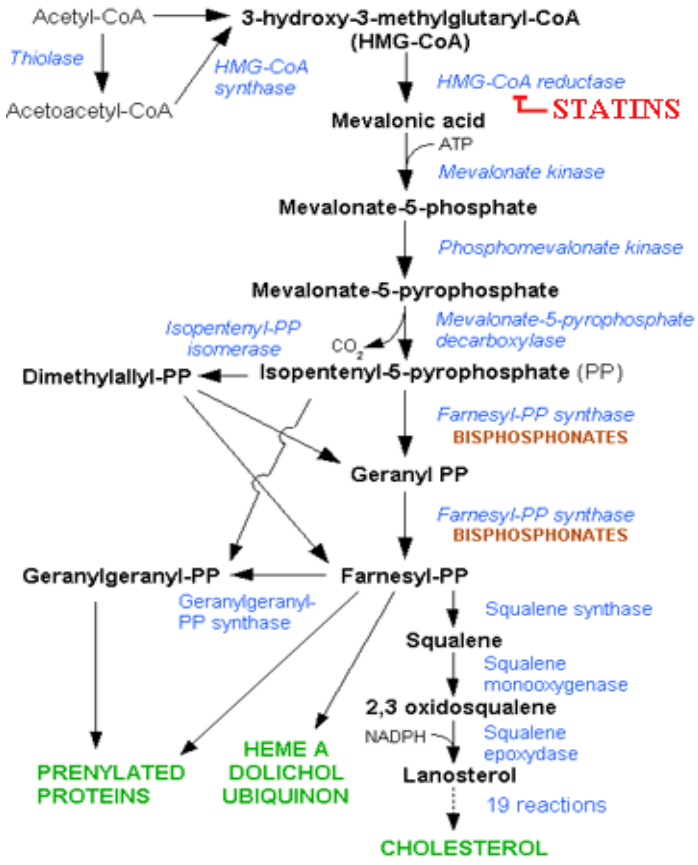

Image modified from: *http://psychology.wikia.com/wiki/Statins*

Figure 10: Statins mechanism of action. Statins act competitively by inhibiting HMG-CoA reductase, the rate-limiting enzyme of the mevalonate pathway, and in turn the cascade that leads to cholesterol synthesis together with other compounds.

Recent evidence suggests that statins have therapeutic potential in AD. Many epidemiological studies have linked statins to a reduced incidence of AD in statin-prescribed patients (Jick et al., 2000, Wolozin et al., 2000, Haag et al., 2009). Other studies have associated statin use to a delayed cognitive decline in mild to moderate AD (Sparks et al., 2005) and in normocholesterolemic AD patients (Simons et al., 2002), Working memory improvements in adults at risk for AD have also been reported (Carlsson et al., 2008). These benefits have been mainly ascribed to the pleiotropic

effects of statins and not to their cholesterol lowering effects (Jick et al., 2000, Cimino et al., 2007). Indeed, it is their benefits on neuropathological AD hallmarks including amyloid burden (Friedhoff et al., 2001, Simons et al., 2002), neuroinflammation, and cerebral hypoperfusion (Cordle and Landreth, 2005, Cimino et al., 2007) that led to believe that statins may be useful in remedying the pathophysiology of AD.

Additionally, in support of these reported benefits in man, studies in AD mouse models showed that statins normalized several AD hallmarks (Li et al., 2006, Tong et al., 2009, Kurata et al., 2011, Tong et al., 2012). More specifically, brain-penetrant simvastatin (Saheki et al., 1994), our choice of statin, has shown favorable outcome on cerebral vasomotor function, brain glucose metabolism and neurovascular coupling in a mouse model of AD (Tong et al., 2009, Tong et al., 2012). Benefits were also seen in reduced brain oxidative stress and inflammation (Tong et al., 2009, Tong et al., 2012), but with minor or no reductions in soluble Aβ levels (Tong et al., 2009, Tong et al., 2012), the latter in agreement with some but not all previous studies (Chauhan et al., 2004, Li et al., 2006). Spatial memory was also normalized by simvastatin in different APP mouse models depending on the dose used and the age of treatment onset (Li et al., 2006, Tong et al., 2012). Indeed, aged Tg2576 mice (Li et al., 2006) substantially benefited from a higher dose (50mg/kg/day vs 40mg/kg/day in our study) of simvastatin treatment, a finding that was not reproduced by our group in aged APP mice treated with 40mg/kg/day for 6 months (Tong et al., 2012). Yet, studies in AD patients have generated mixed results (Arvanitakis et al., 2008, Butterfield et al., 2011, Sano et al., 2011), and it was argued that statins may exert benefits only if administered early in the disease process (Sano et al., 2011, Shepardson et al., 2011b, a, Sparks, 2011). Simvastatin thus

merits additional investigation as these associations are still highly debatable (Arvanitakis and Knopman, 2010, Feldman et al., 2010, Sano et al., 2011). In this respect, the third experimental chapter of my thesis will evaluate the potential benefit of simvastatin in the newly developed APP/TGF mice that recapitulate the cerebrovascular and cognitive deficits of AD.

3.4 Losartan

The renin-angiotensin system (RAS) has been implicated in the pathogenesis of hypertension, atherosclerosis and heart failure (Probstfield and O'Brien, 2010) and, more recently, in AD (Kehoe et al., 2009). However, little is known about the related mechanisms underlying memory. The brain RAS consists of the conversion of the precursor angiotensinogen by renin (acting upon its amino terminal) into decapeptide angiotensin I (AngI), a substrate for angiotensin converting enzyme (ACE), a zinc metalloprotease, which hydrolyzes the carboxy terminal of AngI to form the octapeptide angiotensin II (AngII), which effects are mediated through the AngII type 1 (AT1R) and type 2 (AT2R) receptors. AngII not only regulates blood pressure and fluid balance, but also mediates its pathophysiological effects including vasoconstriction, oxidative stress and inflammation through AT1R, predominantely found in blood vessels, liver, kidneys, heart and brain. AT2R are located in the same tissues, but have physiologically contrasting actions including vasodilatation, neuronal differentiation and axonal regeneration (Hunyady and Catt, 2006). AngII may also convert to downstream active metabolites, notably Angiotensin IV (AngIV) that binds the AT4 receptor (Hunyady and Catt, 2006, Wright and Harding, 2008) (Figure 11).

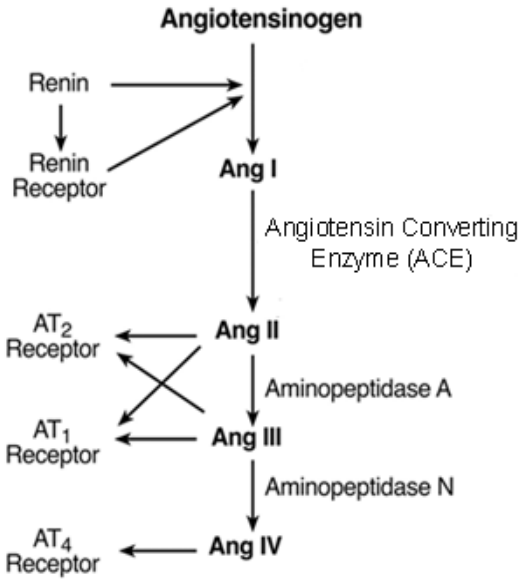

Image modified from: *Hunyady L , Catt K J 2006 Molecular Endocrinology*

Figure 11: RAS.
The key players of the signaling cascade for Ang II generation are shown.

The use of antihypertensive therapy that selectively prevents the actions of AngII on the AT1R, but spares those of AT2R, has been correlated with a lower decrease in mean MMSE and a lower cognitive decline during a 3 year follow-up among AD subjects (Duron et al., 2009). Two small studies in which AD patients were treated with ACE inhibitors for six or 12 months showed cognitive improvements that require replication in larger longitudinal investigations (Ohrui et al., 2004, Hajjar et al., 2008). However, two clinical studies highlighted the importance of selectively blocking the AT1R as opposed to working upstream from this receptor, with ACE inhibitors. Indeed, compared to ACE inhibitor lisinopril, telmisartan significantly improved episodic memory and visuospatial abilities in elderly subjects, in parallel to blood pressure lowering (Fogari et al., 2006). Aged subjects taking angiotensin receptor blockers (ARBs) – including losartan – compared to those taking ACE inhibitors had greater reduction in incidence of AD (Li et

al., 2010b). Even more, those who switched from an ACE inhibitor to an ARB were at significantly lower risk of incident dementia than those who did not switch, further strengthening the therapeutic value of the ARBs (Li et al., 2010b). Noteworthily, these were normotensive subjects, so blood pressure changes may not accounted for these beneficial effects.

In AD mouse models, a range of AT1R antagonist showed efficacy in improving cognition independently or not of amyloidosis (Wang et al., 2007, Mogi et al., 2008, Takeda et al., 2009, Tsukuda et al., 2009). These studies were conducted on $A\beta_{1-40}$ infused mice or singly Tg2576 transgenic AD mice that recapitulate the Aβ-induced pathology of AD. With regards to AD-related processes, positive effects on CBF have been reported with olmesartan in young APP23 mice (Takeda et al., 2009, Maxwell and Hogan, 2010). Hence, the positive effects reported for ARBs and, particularly, AT1R antagonists deserve to be substantiated further in a model that more adequately recapitulates the AD pathological features than the Aβ-injected mice or the classic APP mice. In this respect, the last experimental chapter of my thesis will address the potential benefit of losartan in APP/TGF mice with a combined Aβ- and TGF-β1 pathology.

Rationale, Hypothesis, Specific aims

Rationale

Several studies have been devoted at identifying a treatment for AD, and animal models have been invaluable in dissecting the pathogenic mechanisms. The characterization of transgenic mouse model of amyloidosis integrating the comorbid factor of cerebrovascular pathology with the concurrent overexpressions of Aβ and TGF-β1 may best recapitulate the complexity of the human disease and may thus be useful to test strategies aimed at rescuing disrupted neuronal, glial, and vascular networks.

Hypotheses

AD transgenic mice concomitantly overexpressing Aβ and TGF-β1 display cerebrovascular, neuronal, glial and cognitive deficits, which may be amenable to therapeutic interventions that bear promise in AD patients.

Specific aims

1. Characterize the cognitive and cerebrovascular outcome of combined Aβ and TGF-β1 pathologies in bitransgenic mice overexpressing a mutated form of the human amyloid precursor protein ($APP_{Swe,Ind}$, line 20) and a constitutively active form of transforming growth factor β1 (TGF, line T64), herein referred to as A/T mice.
2. Test the efficacy of pioglitazone (20mg/kg/day) to reverse AD-related memory and cerebrovascular deficits in adult (6 months treatment, 12-15 months old at endpoint) and aged (3 months treatment, 18-21 months old at endpoint) A/T mice.

3. Assess the benefits of simvastatin (40mg/kg/day) on cognitive and cerebrovascular deficits in young (6 months treatments, 9 months old at endpoint) A/T mice.
4. Evaluate the capacity of the AT1R antagonist losartan (10 and 25mg/kg/day) in preventing cognitive and cerebrovascular impairments in young (3 months treatments, 6 months old at endpoint) A/T mice.

Preface to Chapter 2

In AD, Aβ and TGF-β1 may be upregulated in parallel or may drive one another, such that at a certain time point, the AD brain experiences the interactive effects of Aβ and TGF-β1. We sought to investigate the consequences of APP and TGF-β1 concomitant overexpression, and functionally characterize arterial, hemodynamic, and cognitive integrity of young, adult and old APP/TGF mice.

We investigated in chapter 2, the interactive effects of APP and TGF-β1 overexpression in young, adult and old A/T mice on spatial memory, evoked CGU and CBF, cerebrovascular reactivity. A/T mice featured progressive cerebrovascular dysfunction insensitive to antioxidant treatment as antioxidant approaches were ineffective *in vitro*, and no change was detected in levels of the endogenous superoxide scavenger, SOD2, in vessels at any age. Instead, deficits were accompanied by a cerebrovascular pathology that combined the cerebrovascular amyloid angiopathy (CAA) seen in APP mice with the vascular fibrosis characteristic of the TGF model. In addition, A/T mice displayed progressive astrocytic activation, Aβ pathology and impairment in evoked cerebral blood flow and glucose uptake along with a spatial memory decline, thus bringing together cerebrovascular, glial and cognitive aspects of AD pathophysiology. We therefore concluded that A/T mice represent an interesting model with which to test the efficacy of compounds such as pioglitazone, simvastatin and losartan previously shown to counteract both Aβ and TGF-β1-induced dysfunction.

Chapter 2

Transgenic mice overexpressing APP and TGF-β1 feature cognitive and vascular hallmarks of Alzheimer's disease

Brice ONGALI[†], Nektaria NICOLAKAKIS[†], Clotilde LECRUX, Tahar ABOULKASSIM, Pedro ROSA-NETO, Panayiota PAPADOPOULOS, Xin-Kang TONG and Edith HAMEL

[†]These authors contributed equally.

Abstract

High brain levels of amyloid-beta (Aβ) and transforming growth factor-β1 (TGF-β1) have been implicated in the cerebrovascular and cognitive alterations of Alzheimer's disease (AD). We sought to investigate the impact of combined increases in Aβ and TGF-β1 on cerebrovascular, neuronal and mnemonic function using transgenic mice overproducing these peptides (A/T mice). In particular, we measured cerebrovascular reactivity, evoked cerebral blood flow and glucose uptake during brain activation, cholinergic status and spatial memory, along with cerebrovascular fibrosis, amyloidosis and astrogliosis, and their evolution with age. An assessment of perfusion and metabolic responses was considered timely, given ongoing efforts for their validation as AD biomarkers. Relative to wild-type littermates, A/T mice displayed an early progressive decline in cerebrovascular dilatory ability, preserved vasocontractility, and reduction in constitutive nitric oxide synthesis that establishes resting vessel tone. Altered levels of vasodilator-synthesizing enzymes and fibrotic proteins, resistance to antioxidant treatment and unchanged levels of the antioxidant enzyme, superoxide dismutase-2, accompanied these impairments. A/T mice featured deficient neurovascular and neurometabolic coupling upon whisker stimulation, cholinergic denervation, cerebral and cerebrovascular Aβ deposition, astrocyte activation, and impaired Morris water maze performance, which gained severity with age. The combined Aβ and TGF-β1-driven pathology recapitulates salient cerebrovascular, neuronal and cognitive AD landmarks, and yields a versatile model towards highly anticipated diagnostic and therapeutic tools for patients featuring Aβ and TGF-β1 increments.

Introduction

Alzheimer's disease (AD) features neuronal and synaptic dysfunction, abnormal cerebral protein deposits, activated glia and progressive cognitive decline (de la Torre, 2004, Zlokovic, 2005, Kalaria et al., 2008). AD patients also exhibit structural cerebrovascular alterations (Mancardi et al., 1980, Perlmutter and Chui, 1990), and early deficits in resting and evoked cerebral glucose uptake (CGU) and cerebral blood flow (CBF) responses, which can undermine optimal brain function, and aggravate an ongoing pathogenic process (Iadecola, 2004, Sun et al., 2006, Langbaum et al., 2009). These changes have been linked to increased levels and deposition of amyloid-beta (Aβ) in brain parenchyma (senile plaques) and blood vessel walls (cerebral amyloid angiopathy, CAA) (Vinters et al., 1996, Roher et al., 2003), and to upregulation of the profibrotic transforming growth factor-β1 (TGF-β1), perhaps a key molecular mediator of the AD cerebrovascular pathology (Wyss-Coray et al., 1997, Wyss-Coray et al., 2000, Grammas and Ovase, 2002, Tarkowski et al., 2002, Tong et al., 2005).

Transgenic mice overproducing Aβ and TGF-β1 (A/T mice) were originally developed to study the possible modulatory role of TGF-β1 on amyloid deposition (Wyss-Coray et al., 1997, Wyss-Coray et al., 2001). These early studies reported decreased plaque burden and accelerated vascular Aβ accumulation in young and adult A/T animals (Wyss-Coray et al., 1997, Wyss-Coray et al., 2001). More recently, reduced parenchymal and vascular Aβ deposition was demonstrated when TGF-β signaling was genetically blocked in old transgenic AD mice (Town et al., 2008). Though contradictory, these studies collectively suggest that TGF-β1 may regulate amyloid pathology in the AD brain, an idea supported by the correlation between TGF-β1 mRNA levels and CAA

scores in patients (Wyss-Coray et al., 1997). Although the amyloid pathology has been partially characterized in A/T animals, data is completely lacking on their cognitive and cholinergic status, functional cerebrovascular integrity, and evoked perfusion and metabolic responses to neuronal activation. Such results would aid in the validation of A/T mice for the study of AD. It is therefore all the more surprising that this information is unavailable given the known detrimental cerebrovascular effects of Aβ and TGF-β1 (Iadecola et al., 1999, Gaertner et al., 2005, Park et al., 2005, Tong et al., 2005), and the current interest in activity-driven brain hemodynamics and metabolism as clinical predictors or markers for AD therapeutic efficacy.

We sought to characterize the progression of cerebrovascular and cognitive markers with age in A/T mice. Particularly, we studied arterial reactivity and responsiveness to antioxidants *in vitro*, and investigated vascular proteins related to vasomotor function, oxidative stress and fibrosis. Additionally, we examined glial activation, amyloidosis, and indicators of neuronal/cognitive integrity, i.e., the cholinergic innervation, the neuronally-driven cerebral blood flow (CBF) and glucose uptake (CGU) responses during whisker stimulation, and performance in the Morris water maze. Our novel findings highlight A/T mice as a most suitable model in which to explore therapeutic strategies against cerebrovascular and neuronal alterations of AD pathophysiology.

Materials and Methods

A/T transgenic mice. All experiments were in compliance with the Animal Ethics Committee of the Montreal Neurological Institute and the guidelines of the Canadian Council on Animal Care. A/T animals were generated from the crossing of mice

overexpressing mutated human amyloid precursor protein (APPSwe,Ind) driven by the platelet-derived growth factor β promoter (APP mice, line J20) (Mucke et al., 2000) and mice overexpressing constitutively active TGF-β1 under the control of the glial fibrillary acidic protein (GFAP) promoter (TGF mice, line T64) (Wyss-Coray et al., 1995) on a C57BL/6J background. Approximately equal numbers of female and male heterozygous transgenic A/T mice and age-matched wild-type (WT) littermates were used at 6-8 (young), ~12 (adult) and ~18 (old) months of age. Singly transgenic APP or TGF mice of the same ages, either littermates of the A/T mice or from different cohorts, were used for comparisons with A/T mice in some experiments, and similarly prepared. Transgenes were detected with touchdown PCR on tail-extracted DNA (Tong et al., 2005). Mice were housed under a 12h light-dark cycle, in a room with controlled temperature (23°C) and humidity (50%), with food and tap water available *ad libitum*.

Vascular and brain tissue collection. Mice were killed by cervical dislocation. Middle cerebral arteries (MCAs) were immediately tested in reactivity studies, while vessels of the circle of Willis and their branches, along with cortex and hippocampus were collected, snap-frozen and stored (-80°C) for subsequent Western blot and ELISA studies. Separate mouse cohorts were perfused intracardially (4% paraformaldehyde (PFA) in 0.1M phosphate-buffered saline, pH=7.4) under deep anaesthesia (65mg/kg sodium pentobarbital, intraperitoneally, i.p.), and brains post-fixed overnight. Some hemibrains were cryoprotected, frozen in isopentane and stored (-80°C) until cutting into 25μm-thick free-floating coronal sections on a freezing microtome. Others were embedded in paraffin and cut 5μm-thick for use in immuno/histochemistry.

Vascular reactivity. Isolated, pressurized and sub-maximally preconstricted (serotonin, 2×10^{-7}M) MCA segments were tested for dilatation to acetylcholine (ACh; 10^{-10} to 10^{-5}M) or calcitonin gene-related peptide (CGRP; 10^{-10} to 10^{-6}M) using on-line videomicroscopy (Tong et al., 2005). Constriction to endothelin-1 (ET-1; 10^{-10} to 10^{-6}M) or diameter decrease during nitric oxide (NO) synthase (NOS) inhibition with N^{ω}-nitro-L-arginine (L-NNA; 10^{-5}M; 35min) were tested on vessels at basal tone. In some vessels, dilatation to ACh was tested before and after incubation (30-60min) with the free radical scavenger superoxide dismutase (SOD; 120U/mL; Sigma, ON, Canada) or an inhibitor of NADPH oxidase (apocynin; 1mM; Sigma), the main enzymatic source of superoxide ($O_2^{\cdot -}$) in brain vessels of APP mice (Park et al., 2005). Percent changes in vessel diameter from basal or preconstricted tone were plotted as a function of agonist concentration or time course of NOS inhibition. The maximal response (EAmax) and the concentration eliciting half of the EAmax (EC_{50} value or pD_2=-[log EC_{50}]) generated by GraphPad Prism software (4, San Diego, CA, USA) were used to evaluate agonist efficacy and potency, respectively.

Western blot. Vessels were sonicated in Laemmli buffer for protein extraction, as described (Tong et al., 2005). Proteins (12-15µg) were separated by SDS-PAGE and transferred to nitrocellulose membranes, which were incubated (1h) in TBST blocking buffer (50mM Tris.HCl, pH=7.5, 150mM NaCl, 0.1% Tween 20) containing 5% skim milk, then incubated overnight with either rabbit anti-SOD2 (1:2000; Stressgen, MI, USA), -connective tissue growth factor (CTGF; 1:300; Abcam, MA, USA), -vascular endothelial growth factor (VEGF; 1:500; Santa Cruz Biotechnology, CA, USA), -matrix metalloproteinase 9 (MMP9; 1:1000; Millipore, MA, USA) or mouse anti-endothelial

NOS (eNOS; 1:500; BD Transduction Laboratories, CA, USA), -cyclooxygenase-2 (COX-2; 1:200; Santa Cruz Biotechnology), or -β-actin (1:10000; Sigma). Membranes were further incubated (2h) with horseradish peroxidase-conjugated secondary antibodies (1:2000; Jackson ImmunoResearch, PA, USA), and proteins visualized with Enhanced ChemiLuminescence (ECL Plus kit; Amersham, ON, Canada) using phosphorImager (Scanner STORM 860; GE Healthcare, NJ, USA), followed by densitometric quantification with ImageQuant (5.0, Molecular Dynamics, CA, USA).

ELISA measurement of Aβ. Levels of soluble and insoluble $A\beta_{1-40}$ and $A\beta_{1-42}$ were measured in hemicortices using an ELISA-based assay (BioSource International, CA, USA), as previously described in full (Nicolakakis et al., 2008), and results expressed as nanomoles per gram of protein in the supernatant or formic acid (FA)-soluble fraction.

Histochemistry and immunohistochemistry. Dewaxed thin sections (5µm) were stained with 1% Sirius red (~30min) to reveal total collagen in the pia and intracortical microvessels (MVs) or were pretreated with 1% H_2O_2 (10min) and incubated overnight at room temperature with goat anti-collagen I (1:300; Millipore), -choline acetyltransferase (ChAT; 1:250; Millipore) or mouse anti-Aβ (6E10 targeting total Aβ; 1:3000; Covance, CA, USA) followed by species-specific biotinylated IgG, the avidin-biotin complex, and the reaction visualized with 0.05% 3,3'-diaminobenzidine-nickel (DAB-Ni; Vector Laboratories, CA, USA). ChAT immunostaining was tested only in adult and old A/T mice when cholinergic innervation is preserved in TGF mice (Nicolakakis et al., 2011), but significantly reduced in singly transgenic APP mice (Aucoin et al., 2005, Nicolakakis et al., 2008). Free-floating thick sections were stained with 1% Thioflavine S (8min) to reveal mature, dense core amyloid plaques or incubated with rabbit anti-GFAP (1:1000;

DAKO, ON, Canada), followed by donkey anti-rabbit cyanin 2 (Cy2)-conjugated secondary antibody (1:400; Jackson ImmunoResearch) for the detection of activated astrocytes. Sections were observed under light microscopy or epifluorescence (Leitz Aristoplan microscope, Leica, NY, USA), and digital pictures acquired (Coolpix 4500; Nikon, Tokyo, Japan). Double immunodetection of activated astrocytes and Aβ plaques was performed with simultaneous incubation of rabbit anti-GFAP and mouse 6E10, followed by donkey anti-rabbit Cy2- and anti-mouse Cy3-conjugated secondary antibodies.

Staining quantification. Digital images (2-3 sections/mouse, 3-5 mice/group) taken under the same conditions were analyzed with MetaMorph (6.1r3, Universal Imaging, PA, USA). Collagen I and Sirius red staining intensities of the pia and intracortical MVs (4-13 vessels/mouse) were quantified in magnified images and expressed as an optical density (OD) ratio against the intensity of the adjacent parenchyma. The areas of interest (somatosensory/cingulate cortex, hippocampus) containing Thioflavine S- and GFAP-positive elements were manually outlined in low-power images, while high-power microscope images of layers II to IV of the somatosensory cortex were used for quantification of ChAT-immunoreactive fibres (cell bodies were excluded). The number and/or area occupied by Thioflavine S-positive plaques, GFAP-positive astrocytes and ChAT-positive cholinergic fibres was quantified and expressed as number or surface area occupied in the delineated areas of interest.

Morris watermaze. The ability of mice to learn and remember the location of a hidden platform located in a predefined (target) quadrant using visuospatial cues was tested for five consecutive days in a circular pool filled with water (25°C, clouded with powdered

skim milk), as previously described (Nicolakakis et al., 2008). At least 2 hrs after the last hidden platform trial on day 5, mice were submitted to a 60s probe trial (platform removed), followed by a cue trial (30s) testing visual acuity and motivation, which required escape to a visible platform in at least one of two trials. Mice that failed to reach the visible platform were excluded from the analysis. Daily escape latencies to the hidden platform, as well as percent time spent and distance traveled in the target quadrant during the probe trial, along with swim speed, were measured with the 2020 Plus tracking system and Water 2020 software (Ganz FC62D video camera; HVS Image, UK). Animals were dried under a heating lamp after each trial, and all experiments were started at the same time every day.

Laser Doppler flowmetry (LDF). In all age groups, LDF measurements of evoked CBF (Transonic Systems Inc., NY, USA) in response to sensory stimulation were carried out one week following the Morris water maze in anesthetised mice (ketamine, 80mg/kg i.p.; Wyeth, QC, Canada) fixed in a stereotaxic frame (Nicolakakis et al., 2008). CBF was recorded prior to, during and after whisker stimulation (20s at 8-10Hz), with 4-5 recordings acquired every 30 to 40s and averaged per mouse. Cortical CBF change was expressed as percent increase relative to baseline. The entire procedure was performed blind to the identity of the mouse.

[^{18}F]fluoro-2-deoxy-D-glucose ([^{18}F]FDG)-PET. Eighteen month-old A/T mice and WT littermates were fasted overnight and scanned for cerebral uptake of [^{18}F]FDG induced by whisker stimulation (8-10Hz, electric toothbrush, 45min) under isoflurane sedation (1-2% in medical air) in a **CTI Concorde** R4 microPET scanner (Siemens Preclinical Solutions, TN, USA), as previously described (Nicolakakis et al., 2008). Animals were kept warm

with a heating lamp, while cardiac and respiration rate were maintained stable through online monitoring (Biopac Inc., USA). Glycemia levels were measured before and after scans, and were similar in both WT and A/T groups (not shown). Functional metabolic images were reconstructed using a maximum a posteriori probability algorithm (MAP), and coregistered to respective high-resolution WT or A/T mouse structural MRI templates. MR images were acquired in separate groups of mice (WT, n=5 and A/T, n=4) with a 7 T Bruker Pharmascan system (Bruker Biospin, Ettlingen, Germany) using a 28mm inner-diameter quadrature volume resonator, and a 3D True FISP sequence with the following parameters: matrix size=128×128×64, field of view (FOV)=1.8cm×1.8cm×0.9cm, spatial resolution=140μm×140μm×140μm, excitation flip angle=30º, repetition time (TR)=5.2ms, echo time (TE)=2.6ms, number of excitations (NEX)=4, number of phase cycles=4, total scan time=35min. The images were reconstructed using a maximum intensity algorithm and the population averages generated using the approach described elsewhere (Lau et al., 2008). Regions of interest (ROIs) were drawn on the somatosensory cortices and the magnitude of activation expressed as the ratio of [^{18}F]FDG standard uptake value (SUV) in the activated contralateral relative to the ipsilateral cortex (Kornblum et al., 2000). Final images represent the SUV obtained by correcting individually for animal body weight and injected radioactivity dose.

Statistical analysis. Data are Mean ± SEM, and were compared by Student's *t* test or one-way analysis of variance (ANOVA) followed by Newman-Keuls post-hoc tests. Morris water maze latency curves were analyzed by two-way ANOVA followed by

Bonferroni post-hoc test, with day and genotype as factors. All statistical analyses were performed with GraphPad and $p<0.05$ was considered significant.

Results

A/T mice develop an early, progressive decline of cerebral arterial function

Isolated MCAs from young and adult A/T mice displayed ~50% loss of their ability to dilate to ACh and CGRP relative to vessels of age-matched WT littermates (Fig. 1, Suppl. Table 1). By 18 months of age, A/T mice further exhibited significantly impaired maximal diameter decrease during NOS inhibition with L-NNA, indicating a decline in constitutive endothelial nitric oxide (NO) release that is crucial for establishing resting vessel tone. There was no contractile deficit to ET-1 in A/T arteries at any age (Fig. 1, Suppl. Table 1). The progressive deficits in arterial responsiveness could not be attributed to desensitization of cerebrovascular receptors, as agonist potencies (pD_2 values) were comparable between WT and A/T mice at all ages (Suppl. Table 1). Cerebrovascular impairments of similar magnitude have been consistently measured in singly transgenic APP and TGF mice (Suppl. Fig. 1, Suppl. Table 1). Noteworthy was the lack of a synergistic Aβ and TGF-β1 effect in A/T arteries, as evidenced in the qualitative comparison with reactivity data from APP and TGF arteries. This was particularly well illustrated in A/T mice by: 1) their preserved contractile response to ET-1, in contrast to the deficit in TGF arteries, 2) milder CGRP deficit relative to that in aged TGF animals, and 3) later decline in L-NNA response versus its early onset in the singly transgenic lines.

A/T mice display arterial dysfunction not related to oxidative stress

We sought to elucidate the mechanism of cerebrovascular impairment in aged A/T mice by treating arteries with SOD or apocynin, which respectively scavenges $O_2^{\cdot -}$ and abrogates its production. Antioxidants have been shown to normalize cerebrovascular responses of APP (Iadecola et al., 1999, Tong et al., 2005, Nicolakakis et al., 2008, Tong et al., 2009), but not TGF mice (Nicolakakis et al., 2011), and we wished to determine whether free radicals accounted for the cerebrovascular dysfunction in the A/T model. These *in vitro* antioxidant approaches were ineffective as they were unable to restore ACh-mediated dilatations (Fig. 2A). Furthermore, no significant change was detected in A/T vessels at any age in the levels of the antioxidant enzyme SOD2, which is induced by $O_2^{\cdot -}$ and can be used as an indicator of enhanced oxidative stress (Fig. 2B). Instead, pial vessels from A/T mice exhibited changes in enzymes synthesizing vasodilators, i.e. reduced levels of COX-2 beginning as a trend in young, and becoming significant in adult and old mice, as well as significant upregulation of eNOS in young mice. A/T arteries also featured robust increases in levels of growth factors (VEGF, CTGF) involved in vascular fibrosis, starting in young and persisting in old mice. Arteries also exhibited late upregulation of MMP9, an enzyme involved in the breakdown of the extracellular matrix during vascular remodeling (Fig. 2B). Furthermore, A/T mice featured significant collagen accumulation in penetrating MVs and in the surface pial membrane, resulting in its greater thickness (Fig. 2C). Sirius red staining intensity was markedly augmented in the pia (81%) and MVs (39%) compared to the adjacent parenchyma of 18 month-old A/T mice, with substantially smaller increments in WT animals in these respective vascular beds (pia: 29%, MVs: 21%). Analogous collagen I increases were seen in the pia

(74%) and MVs (42%) of A/T mice (Fig. 2C), which likely accounted for the increased rigidity of their vessels perceived during dissection, handling, and cannulation. In contrast, collagen I immunostaining was very weak in WT mice, being increased by 14% in the pia but barely detectable in MVs (1%) relative to the parenchyma (Fig. 2C), confirming our previous report of collagen I upregulation in the context of vascular pathology (Tong et al., 2005). Collectively, these data argue against oxidative stress as the main pathogenic mechanism of vascular dysfunction, and point to disturbances in enzymes and proteins underlying vascular structure and signaling. We cannot rule out that chronic *in vivo* antioxidant treatment might be effective. However, based on the recent failure of this approach in TGF mice featuring similar cerebrovascular fibrosis, vascular protein alterations, and *in vitro* resistance to antioxidants (Nicolakakis et al., 2011), we are inclined to consider alternate mechanisms of vascular dysfunction in A/T mice, ones most likely shared with the TGF model.

A/T mice exhibit AD-like neuropathological changes

A/T mice exhibited an increase in levels of soluble and insoluble $A\beta_{1\text{-}40}$ and $A\beta_{1\text{-}42}$ between 6-8 and 12 months, with further increases in levels of $A\beta_{1\text{-}40}$, but not of $A\beta_{1\text{-}42}$ at 18 months of age, as measured in the cortex by ELISA (Fig. 3A). They also displayed age-dependent Aβ plaque deposition in the cortex and hippocampus, shown by a gradual increase in the number and surface area (plaque load) occupied by Thioflavine S-positive dense core plaques from young to adult animals (Fig. 3B). Between 12 and 18 months, plaque number reached a plateau in the hippocampus, or slightly decreased in the cortex, while plaque load continued to expand or stayed the same in the respective areas, indicating an increase in the size of certain plaques during this period. Together with the

significant increments in soluble and insoluble $A\beta_{1-40}$ from 12 to 18 months, this finding suggests that existing Aβ plaques may have acted as seeds for additional $A\beta_{1-40}$ deposition. In comparative experiments, we found a trend for diminished plaque load in young A/T relative to APP mice, which became significant in adult and aged animals (Suppl. Fig. 2). This would support the argued modulatory effect of TGF-β1 on amyloid deposition, and suggest a clearance phenomenon, as previously observed in young and old A/T mice (Wyss-Coray et al., 1997, Wyss-Coray et al., 2001). Its occurrence later in our model may reflect the higher Aβ levels of the J20 APP line (Mucke et al., 2000) used to generate A/T mice, instead of the previously-used J9 (Wyss-Coray et al., 1997, Wyss-Coray et al., 2001). Finally, inspection of Aβ immunoreactivity in thin sections from 18 month-old A/T mice revealed parenchymal Aβ senile plaques and widespread CAA in pial, intracortical and hippocampal brain vessels (Fig. 3C), confirming previous reports in young and adult A/T animals (Wyss-Coray et al., 1997, Wyss-Coray et al., 2001).

In addition, A/T mice displayed an inflammatory response characterized by activated GFAP-positive astrocytes. The GFAP-positive area in the cortex increased from young to old A/T mice, with a smaller age-dependent activation in WT animals. Activated astrocytes in A/T mice distributed in clusters as well as diffusely throughout the cortex (Fig. 4A), and surrounded Aβ plaques and amyloid-laden vessels (Fig. 4B). Interestingly, this pattern was reminiscent of both the cluster-like activation of APP mice (Nicolakakis et al., 2008) and diffuse, perivascular astrocytosis of TGF mice (Wyss-Coray et al., 1995, Wyss-Coray et al., 1997, Nicolakakis et al., 2011).

Neuronal and cognitive impairments in A/T mice

Adult and aged A/T mice featured a ~22-23% reduction ($p<0.05$ for both ages) in the number of cortical cholinergic fibres (Fig. 5A). Further, [^{18}F]FDG-PET scans following whisker stimulation revealed a significant impairment of glucose uptake in the activated somatosensory cortex of aged A/T animals (activation ratio A/T: 0.99±0.01 vs. WT: 1.06±0.02, $p<0.05$) (Fig. 5B) that may have derived from the observed alterations in vascular, astroglial and neuronal compartments (Papadopoulos et al., 2010). Moreover, there was a gradual loss of the neuronally-driven hemodynamic response to sensory stimulation, which was significant in adult (-31%, $p<0.001$) and progressively more severe in aged animals (-41%, $p<0.001$) (Fig. 5C). The extent of the deficit compared well to that seen in APP mice, although it was more progressive (Suppl. Table 2). Finally, A/T mice showed increased latencies to locate the hidden platform in the Morris water maze at 6-8 months of age, whereas performance in the probe trial was lower but not significantly different from that of control mice, indicating a learning deficit but no clear memory impairment at this age. A significant deficit in probe trial performance emerged in 12 month-old and continued in 18 month-old A/T animals (Fig. 6), which was not due to differences in swim speed, visual acuity, locomotor defects or lack of motivation, as demonstrated by successful escape onto the visible platform. Comparatively, APP mice showed deficits in both the learning and memory components of the test at all ages, as shown at 6 months, whereas TGF mice performed as well as WT mice in this task up to 18 months of age (Suppl. Fig. 3).

Discussion

Since the original development of transgenic mice overproducing both Aβ and TGF-β1 (Wyss-Coray et al., 1997, Wyss-Coray et al., 2001), this is the first characterization of their cerebrovascular, neuronal and mnemonic integrity. More importantly, our study provides novel functional data on activity-induced changes in cerebral glucose uptake and cerebrovascular status that are in line with current research initiatives to develop markers for early diagnosis and treatment efficacy. As a result, the A/T model may be used to better assess interactions between Aβ and TGF-β1 in AD, and to develop therapeutic strategies that can rescue both cerebrovascular and mnemonic hallmarks of AD pathophysiology.

AD-like cerebrovascular pathology in A/T mice and therapeutic implications

An appealing characteristic of A/T mice is the development of a functional and structural cerebrovascular pathology, simultaneously triggered by soluble Aβ, TGF-β1, CAA and basement membrane thickening, as seen in human AD (Mancardi et al., 1980, Perlmutter and Chui, 1990, Pellerin et al., 2007, Park et al., 2008). The interaction between vascular fibrosis and CAA is of interest, as matrix proteins such as collagen and perlecan accumulating in AD basement membranes (Pellerin et al., 2007), have the ability to bind Aβ and enhance its fibrillogenesis (Roher et al., 1993). CAA may thus result from the enhanced capacity of thickened vessels to amass Aβ. This would agree with the ability of TGF-β1 to prompt vascular Aβ deposition when overexpressed in the brain of young APP mice (2 to 3 months), as CAA was not seen in singly transgenic APP animals of equivalent age (Wyss-Coray et al., 1997). It is also in line with the reported correlation between TGF-β1 mRNA levels and CAA scores in AD brains (Wyss-Coray et al., 1997).

CAA may additionally result from vascular wall alterations that hinder vessel pulsations believed to drive Aβ clearance along the perivascular drainage route within arterial and arteriolar basement membranes (Kalaria and Pax, 1995). Such a scenario is supported by the perivascular accumulation of Aβ seen here in concentric circles around some A/T brain vessels (Fig. 3C). A/T mice thus offer the opportunity to test whether strategies that can reverse or attenuate excessive matrix protein accumulation and vascular stiffness will diminish CAA. Used in conjunction with Aβ immunotherapy, these could help counter the transient increase in CAA and risk of cerebral microhaemorrhages reported with vaccination in AD models (Castillo et al., 1997) and human trials (Weller et al., 2008). In addition, attenuating CAA could improve the function of astrocytes, key intermediaries in neurovascular coupling (Wilcock et al., 2009a). CAA can induce loss of the water channel aquaporin 4 and of various potassium channel subtypes in astrocytic end-feet (Boche et al., 2008) that, combined with the progressive astrocyte activation measured here, could have contributed to the age-related impairment of perfusion responses. Normalizing CAA could thus ameliorate glial function and perfusion.

Therapies against the deleterious vasoactive properties of soluble Aβ would be most useful (Haydon and Carmignoto, 2006). Indeed, the peptide potently deregulates vascular function, even in young APP mice devoid of CAA, by activating vascular NADPH oxidase and $O_2^{\cdot -}$ synthesis, which results in the sequestration of vasodilators and free radical damage to vascular enzymes and receptors (Iadecola et al., 1999, Park et al., 2005, Tong et al., 2005, Tong et al., 2009). These dysfunctions are promptly reversed by antioxidants *in vitro* and *in vivo*, even in arteries from aged APP mice (Tong et al., 2005, Nicolakakis et al., 2008, Wilcock et al., 2009b). A caveat to pure antioxidant therapy is

warranted by its inefficacy when applied to fibrotic TGF arteries (Tong et al., 2005), and here, to A/T arteries. Both the $O_2^{\cdot -}$ scavenger SOD, and NADPH oxidase inhibitor, apocynin, were unable to restore ACh-mediated dilatations. Though chronic *in vivo* antioxidant treatment would be ultimately conclusive, it was ineffective in TGF mice (Nicolakakis et al., 2011), suggesting that a combined approach with compounds targeting structural alterations or vasodilatory signaling pathways should be favoured.

The relevance of the A/T model for the study of altered brain hemodynamics in AD is strengthened not only by reports of TGF-β1 upregulation in the brain and vasculature of AD patients (Wyss-Coray et al., 1997, Wyss-Coray et al., 2000, Grammas and Ovase, 2002, Tarkowski et al., 2002, Han et al., 2008), but also in elderly individuals who have suffered a stroke (Hamel et al., 2008), and in subjects with hypertension and diabetes (Luterman et al., 2000), conditions that acutely or chronically limit CBF, and increase the risk for developing AD (Krupinski et al., 1996, Iadecola, 2004), especially if they co-occur in the same individual (Peterson, 2005). In at-risk patients, TGF-β1 could conceivably regulate Aβ production directly. This is suggested by the presence of a TGF-β1-responsive element in the APP promoter, and TGF-β1-stimulated release of endogenous $A\beta_{1\text{-}40/42}$ peptides by cultured human astrocytes (Kalaria, 2000). Alternatively, TGF-β1 production may be triggered by Aβ (Luchsinger et al., 2005), or both peptides may be upregulated concomitantly in neurons, glia and vascular cells by acute ischemic events or chronic cerebrovascular insufficiency (Lesne et al., 2003, Cheng et al., 2009). In A/T mice, Aβ and TGF-β1 are overproduced from birth and throughout the lifespan and it seems that their interaction is responsible for the progressive hemodynamic deficit of A/T animals. This deficit appears later than in APP or TGF mice,

surpasses that of TGF animals but reaches that of APP mice (Suppl. Table 2). In all, this emphasizes the usefulness of the A/T model as a platform for pursuing strategies aimed at counteracting impaired brain hemodynamics that could promote or result from Aβ and TGF-β1 elevations.

Contribution of Aβ versus TGF-β1 to the neuronal and cognitive status of A/T mice

The cholinergic, metabolic and cognitive deficits of A/T mice reflect mainly an Aβ-driven process, as they are not exhibited by singly transgenic TGF mice (Nicolakakis et al., 2008), and the deficit severity matches that of APP mice (Bennett et al., 2000, Aucoin et al., 2005, Nicolakakis et al., 2008). Namely, the loss of cortical ChAT-positive fibres, a landmark of AD (Dhandapani and Brann, 2003) reproduced in APP mouse models (Geula and Mesulam, 1989, Wong et al., 1999, Jaffar et al., 2001, Aucoin et al., 2005), but not in TGF mice (Nicolakakis et al., 2008), has been attributed to the cholinotoxic effects of soluble Aβ (Klingner et al., 2003). It seems unrelated to Aβ deposition since no relationship could be established between the presence and location of Aβ plaques and denervation severity (Aucoin et al., 2005). However, despite the increase in soluble Aβ oligomers from adult to old A/T mice, the cholinergic denervation did not gain in severity with aging. This stabilization could result from a TGF-β1 protective effect on neurons. In support of such a role is the delayed probe trial deficit in 12 month-old A/T mice relative to its earlier onset in 6 month-old APP animals, known for their early synaptic and cognitive dysfunction (Hsia et al., 1999, Auld et al., 2002). TGF-β1-mediated neuroprotection has been suggested during ischemic and Aβ injuries (Palop et al., 2003, Luchsinger et al., 2005, Cheng et al., 2009) through the regulation of pro- and anti-apoptotic proteins or factors that counter the effects of Aβ, such as collagen VI (Palop et

al., 2003, Luchsinger et al., 2005, Caraci et al., 2008). However, evidence for a TGF-β1 neurodegenerative action has also been presented (Tesseur et al., 2006, Town et al., 2008). Further, neuronal malfunction was apparent in A/T mice, in the form of impaired stimulus-evoked CGU and eventual spatial memory decline. Moreover, given the detrimental cerebrovascular effects of TGF-β1 (Gaertner et al., 2005, Tong et al., 2005, Tong and Hamel, 2007, Salins et al., 2008, Nicolakakis et al., 2011), alternative neuroprotective approaches should be considered. For example, therapies aimed at the cellular and molecular underpinnings of the impaired metabolic response may hold promise. These include key glycolytic enzymes or neuronal (GLUT3) and vascular/astrocytic (GLUT1) glucose transporters that are reduced in AD (Simpson et al., 1994).

Conclusion

The present study highlighted the progressive circulatory and neuronal deficits resulting from Aβ and TGF-β1 co-overproduction. As both elements coexist and interact in the AD brain, and altered brain hemodynamics are receiving renewed attention in AD pathogenesis, the current study provides new data on a unique mouse model with which to test strategies aimed at rescuing disrupted neuronal, glial and vascular networks.

Acknowledgements Supported by grants from the Canadian Institutes of Health Research (CIHR, MOP-84275, EH) and the Alzheimer Society of Canada (EH), a CIHR studentship (NN), and fellowships (BO) from les Fonds de la Recherche en Santé du Québec and Jeanne Timmins Costello, as well as a Heart and Stroke foundation of Canada/Canadian Stroke Network Fellowship (CL). We thank Dr. L. Mucke (Gladstone Inst. of Neurological Disease and Dept. Neurology, UCSF, CA, USA) and the J. David

Gladstone Institutes for the $hAPP_{Swe,Ind}$ and TGF-β1 transgenic mouse breeders, Ms. P. Fernandes for the laser Doppler flowmetry experiments, Mr. A. Aliaga for performing the PET scans, and Mr. J. Cakiroglu and Dr. B. Bedell (Small Animal Imaging Laboratory, SAIL, Montreal Neurological Institute) for the MRI templates.

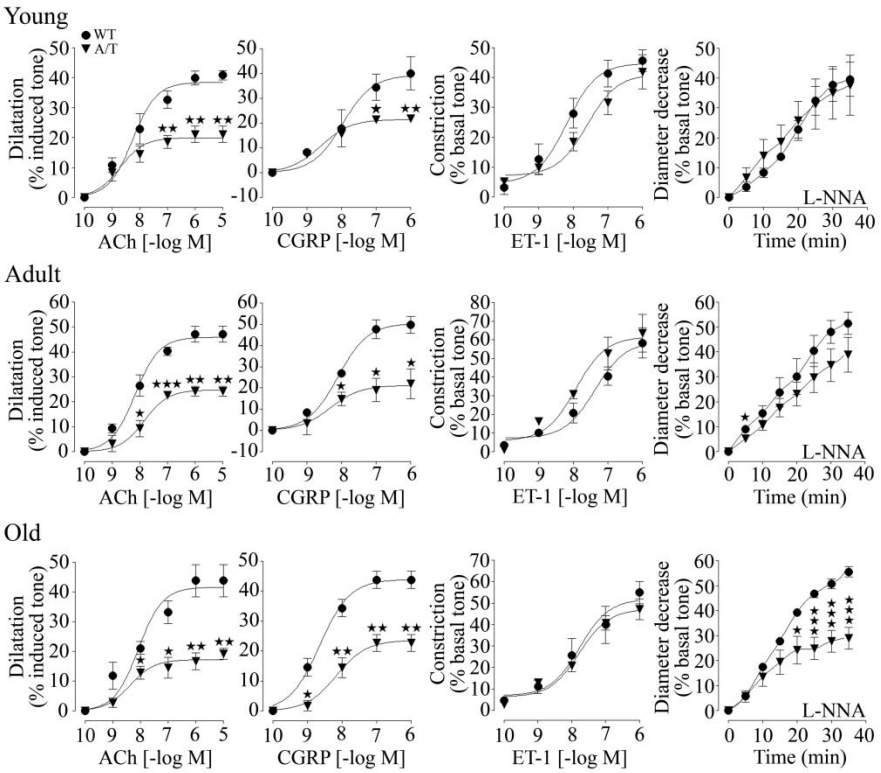

Figure 1. Age-related impairment in cerebrovascular reactivity in young (6-8 months), adult (~12 months) and old (~18 months) A/T mice (inverted triangle) relative to age-matched wild-type (WT) littermates (circle). Early dilatory deficits to ACh and CGRP in young and adult A/T mice were accompanied by a late decline in constitutive NO synthesis in old A/T animals, as seen with L-NNA-mediated inhibition of NOS (10^{-5}M). Constriction to ET-1 was preserved at all ages. Error bars represent SEM. Number of animals are indicated in Suppl. Table 1. Comparison to WT using Student's *t* test. ★p<0.05, ★★p<0.01, ★★★p<0.001.

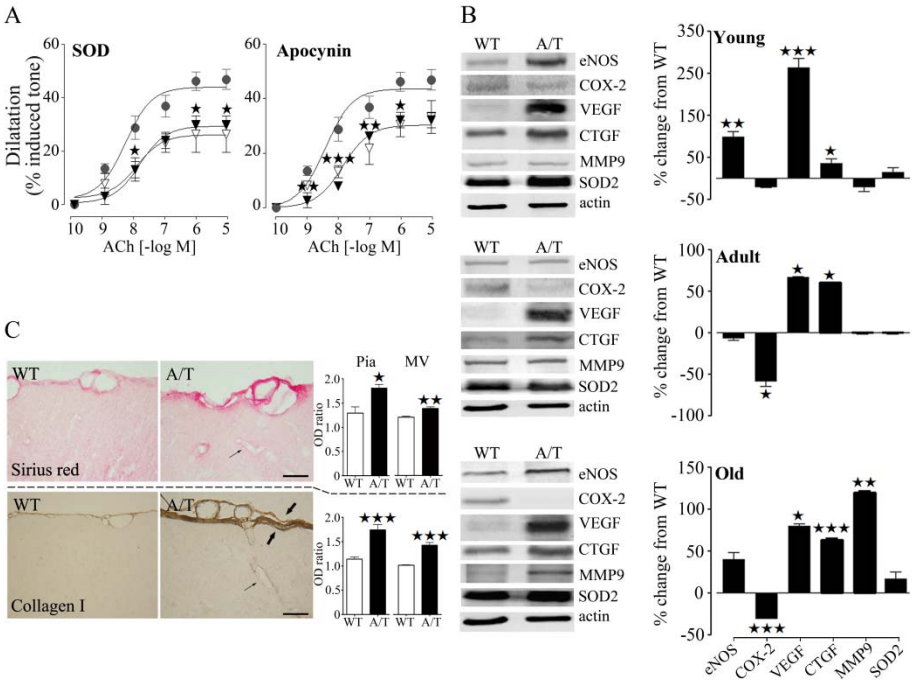

Figure 2. A/T mouse vessels were characterized by resistance to antioxidants, alterations in vascular signaling molecules and cerebrovascular fibrosis. ***A,*** The impaired ACh-mediated dilatation of aged A/T (inverted black triangle) relative to wild-type (WT) mice (circle) was not improved in A/T arteries after *in vitro* incubation (inverted white triangle) with the $O_2^{\cdot -}$ scavenger SOD or a blocker of its synthesis, apocynin (n=3-4 mice/group). ***B,*** Disturbed levels of vasodilator synthesizing enzymes, eNOS and COX-2, and of markers related to vascular remodeling, VEGF, CTGF, MMP9, but not of the oxidative stress marker SOD2, as measured by Western blot in pial vessels of A/T relative to WT mice. Actin was used to normalize loading variation (n=3-6 mice/group). ***C,*** Collagen accumulation in the pia (thick arrows) and intraparenchymal microvessels (MVs, thin arrows) of 18 month-old A/T relative to WT mice, measured as an optical density (OD) ratio of the vessel intensity to that of adjacent parenchyma in Sirius red-stained (top panels) and collagen I-immunoreactive (bottom panels) 5μm-thick paraffin sections (n=3-9 mice/group). Scale bar, 20 μm. Error bars represent SEM. ★p<0.05, ★★p<0.01, ★★★p<0.001 when compared with WT using Student's *t* test or one-way ANOVA followed by Newman-Keuls post-hoc test.

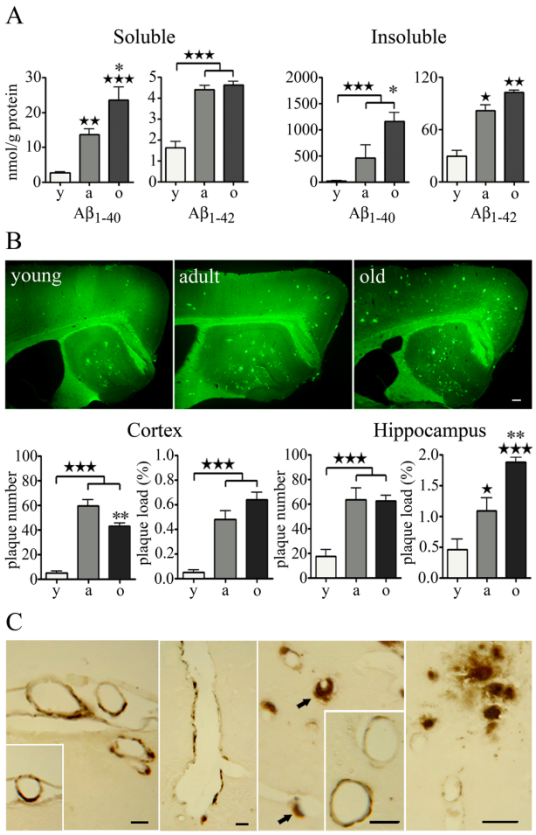

Figure 3. Progressive amyloidosis in A/T mice. ***A,*** Levels of soluble and insoluble $A\beta_{1-40}$ and $A\beta_{1-42}$ increased as a function of age in A/T mice, as assayed in hemicortices by ELISA. ***B,*** Gradual increase in the number and load (percent surface area) of Thioflavine S-positive amyloid plaques in the cortex and hippocampus of A/T mice. No such deposits were seen in wild-type (WT) animals (not shown). y, young; a, adult; o, old. ***C,*** Extensive CAA in the vasculature of aged A/T mice, as respectively seen from left to right, in surface pial vessels, a penetrating cortical artery, arterioles with associated extraluminal deposits (arrows) and hippocampal arteries (inset), and in hippocampal arterioles and capillaries, next to which parenchymal Aβ plaques can be seen. Scale bars, 20μm. Error bars represent SEM (n=4 mice/group). ★p<0.05, ★★p<0.01, ★★★p<0.001 for comparison to young mice or *p<0.05, **p<0.01 for comparison to adult mice using one-way ANOVA followed by Newman-Keuls post-hoc test.

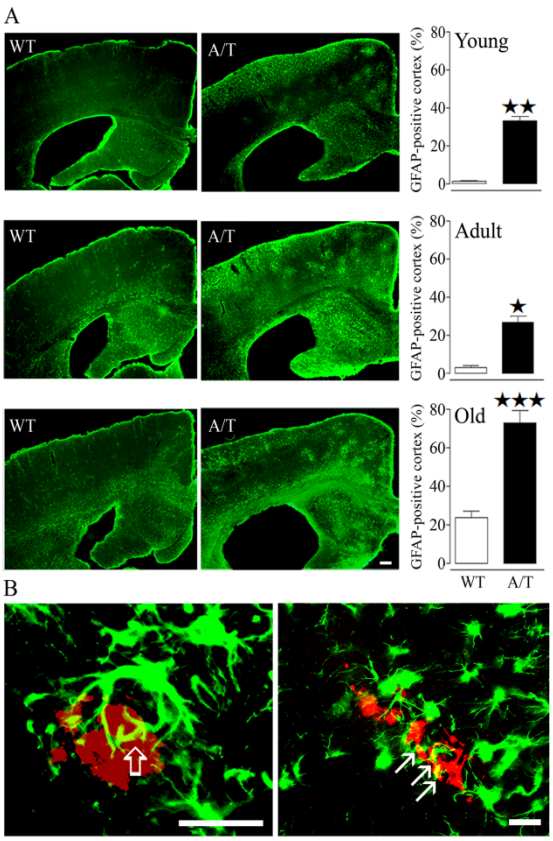

Figure 4. Astrogliosis. ***A,*** Enhanced astrocyte activation seen as clusters and diffuse GFAP-positive material in the brains of A/T mice with a smaller age-related activation also detectable in wild-type (WT) littermates. Astrocyte activation was expressed as the percent cortical area occupied by GFAP-positive cells. Scale bar, 20μm. ***B,*** Activated astrocytes (green) were found associated with Aβ deposits (red) in the parenchyma (left) and with cerebral vessels (right). Note, in yellow, the contact points between astrocytic processes and an Aβ plaque (open big arrow) or an amyloid-laden vessel (CAA) (thin arrows) (n=3-7 mice/group). Scale bars, left, 40μm; right, 20μm. Error bars represent SEM. ★p<0.05, ★★p<0.01, ★★★p<0.001 when compared with WT using Student's *t* test.

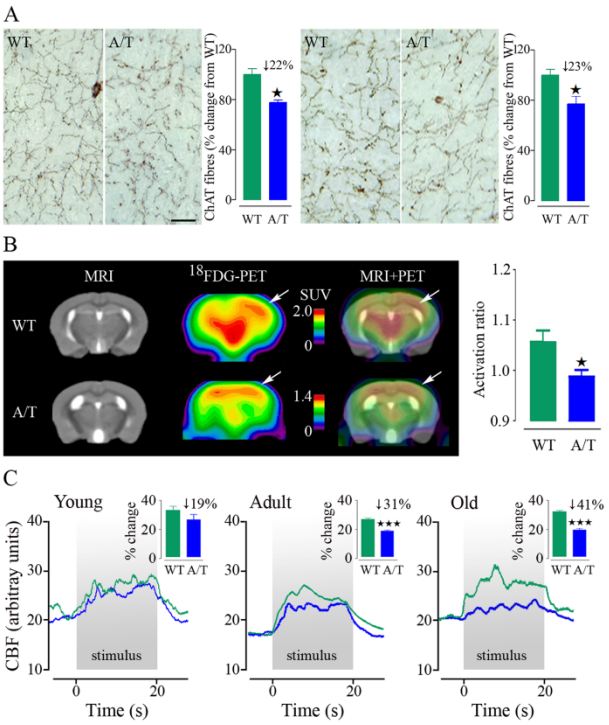

Figure 5. Neuronal dysfunction in A/T mice. ***A,*** Decline in the number of cortical cholinergic fibres in paraffin sections from adult (left panel) and old (right panel) A/T mice, relative to wild-type (WT) littermates, as detected with ChAT immunohistochemistry. Scale bar, 20µm. Values above histograms indicate the percent fibre loss compared to control animals ***B,*** Decrease in the CGU response to whisker stimulation in the somatosensory cortex (arrows) of 18 month-old A/T relative to WT mice (n=3-5 mice/group). SUV scales were adjusted to match the local activation spots in the two groups rather than the global brain uptake. The activation ratio is the corrected standard uptake value (SUV) in the activated contralateral relative to the ipsilateral somatosensory cortex. ***C,*** Gradual decline in the activity-driven hemodynamic response to whisker stimulation in A/T mice (blue) compared to age-matched WT controls (green), as measured by LDF (n=4-5 mice/group). Values above histograms indicate the percent loss of the response compared to control animals. Error bars represent SEM. Comparisons to WT, ★$p<0.05$, ★★★$p<0.001$ using Student's *t* test.

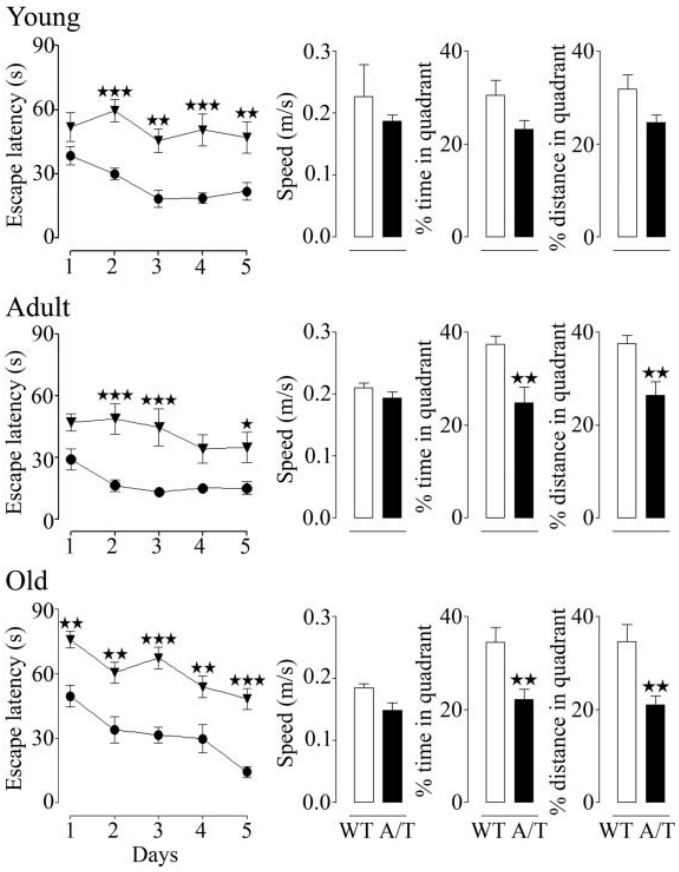

Figure 6. Progressive decline in Morris water maze performance in A/T mice (inverted triangle) compared to aged-matched wild-type (WT) counterparts (circle). Young mice featured impaired acquisition during hidden-platform testing, but only a trend towards decline in memory retention during the probe trial. Significant probe trial deficits appeared in adult and old A/T mice. Error bars represent SEM (n=7-16 mice/group). Comparisons to WT, ★p<0.05, ★★p<0.01, ★★★p<0.001 using two-way ANOVA followed by Bonferroni post-hoc test (latency curves) or using Student's *t* test (probe trial histograms).

Table 1 (suppl). Cerebrovascular responses to ACh, CGRP, ET-1, and NOS inhibition with L-NNA in A/T mice and wild-type (WT) littermates and, for comparison, in APP and TGF mice.

Young		**WT**	**A/T**	**APP**	**TGF**
		(n=3-4)	(n=6-7)	(n=4-6)	(n=7-13)
ACh	*EAmax*	38.5 ± 1.9	20.0 ± 1.3★★	28.0 ± 1.7	26.9 ± 1.7
	pD_2	8.26 ± 0.14	8.70 ± 0.21	8.51 ± 0.19	8.97 ± 0.20
CGRP	*EAmax*	39.4 ± 4.0	21.5 ± 0.8★★	18.8 ± 2.2	34.7 ± 3.6
	pD_2	7.97 ± 0.33	8.60 ± 0.11	7.94 ± 0.27	8.34 ± 0.26
ET-1	*EAmax*	44.8 ± 3.3	41.1 ± 3.6	40.3 ± 2.8	43.7 ± 4.0
	pD_2	8.19 ± 0.23	7.60 ± 0.26	8.72 ± 0.25	8.25 ± 0.31
L-NNA	*EAmax*	39.6 ± 5.7	37.6 ± 10.1	18.5 ± 6.6	18.6 ± 2.6

Adult		**WT**	**A/T**	**APP**	**TGF**
		(n=3-6)	(n=4-7)	(n=14-39)	(n=10-16)
ACh	*EAmax*	45.9 ± 1.6	24.7 ± 1.4★★	25.6 ± 0.7	22.3 ± 0.8
	pD_2	8.17 ± 0.10	7.84 ± 0.15	8.39 ± 0.08	8.45 ± 0.12
CGRP	*EAmax*	50.4 ± 2.1	21.2 ± 3.4★	20.5 ± 1.2	13.3 ± 2.4
	pD_2	8.11 ± 0.10	8.32 ± 0.41	8.73 ± 0.16	8.84 ± 0.49
ET-1	*EAmax*	58.9 ± 5.5	61.6 ± 5.3	43.9 ± 2.1	42.6 ± 2.5
	pD_2	7.38 ± 0.24	7.93 ± 0.25	8.71 ± 0.17	7.92 ± 0.18
L-NNA	*EAmax*	51.5 ± 4.5	38.9 ± 7.0	26.0 ± 2.0	21.0 ± 3.2

Old		WT	A/T	APP	TGF
		(n=3-7)	(n=4-8)	(n=5-10)	(n=17-20)
ACh	*EAmax*	41.6 ± 2.7	17.2 ± 1.3★★	22.7 ± 1.4	12.9 ± 1.2
	pD_2	8.07 ± 0.18	8.37 ± 0.23	8.16 ± 0.17	8.92 ± 0.29
CGRP	*EAmax*	43.9 ± 1.7	23.6 ± 1.8★★	25.0 ± 1.5	11.3 ± 1.4
	pD_2	8.64 ± 0.10	8.16 ± 0.18	8.77 ± 0.16	8.86 ± 0.33
ET-1	*EAmax*	52.0 ± 5.3	47.2 ± 2.7	50.5 ± 5.3	35.0 ± 2.9
	pD_2	7.76 ± 0.30	7.78 ± 0.16	8.05 ± 0.32	7.97 ± 0.27
L-NNA	*EAmax*	55.5 ± 2.0	28.9 ± 4.3★★★	27.4 ± 8.5	31.2 ± 2.9

Data are means ± SEM of the number (n) of animals in parentheses, and represent the best fitted values of maximal agonist response (EAmax) or potency (pD_2, -[logEC_{50}]). E_{Amax} is the percent maximal dilatation to ACh and CGRP, constriction to ET-1 or percent maximal diameter decrease after 35 min inhibition of NOS with 10^{-5}M L-NNA. WT, Wild-type. ★p<0.05, ★★p<0.01, ★★★p<0.001 when comparing A/T with WT mice using Student's *t* test. Data from APP (blue) and TGF (red) mice pooled from new and previously published studies (for significance, refer to original publications listed below) are illustrated for qualitative comparison to the present A/T and WT data set. These were not compared statistically as mice were not littermates, and sample sizes varied greatly in some cases.

Table 2 (suppl). Comparative decrease in the hemodynamic response to whisker stimulation in young, adult and old APP, TGF and A/T mice.

	APP (n=3-7)	TGF (n=7-11)	A/T (n=4-5)
Young (6-8 mo)	35.4 ± 3.2% ($p<0.001$)	37.5 ± 7.4% ($p<0.01$)	19.2 ± 6.3% ns
Adult (12-15 mo)	42.3 ± 4.0% ($p<0.001$)[a]	27.2 ± 8.3% ($p=0.057$)	31.2 ± 2.7% ($p<0.001$)
Old (18 mo)	43.9 ± 6.6% ($p<0.05$)	26.9 ± 3.3% ($p<0.001$)[b]	41.1 ± 3.3% ($p<0.001$)

Percentages indicate the reduction in evoked CBF response in the various transgenic lines compared to respective age-matched wild-type littermates by Student's *t* tests. Number of animals (n) is indicated within parentheses. ns, non-significant. [a]Values from reference 1. [b]Pooled values from references 2 and 3.

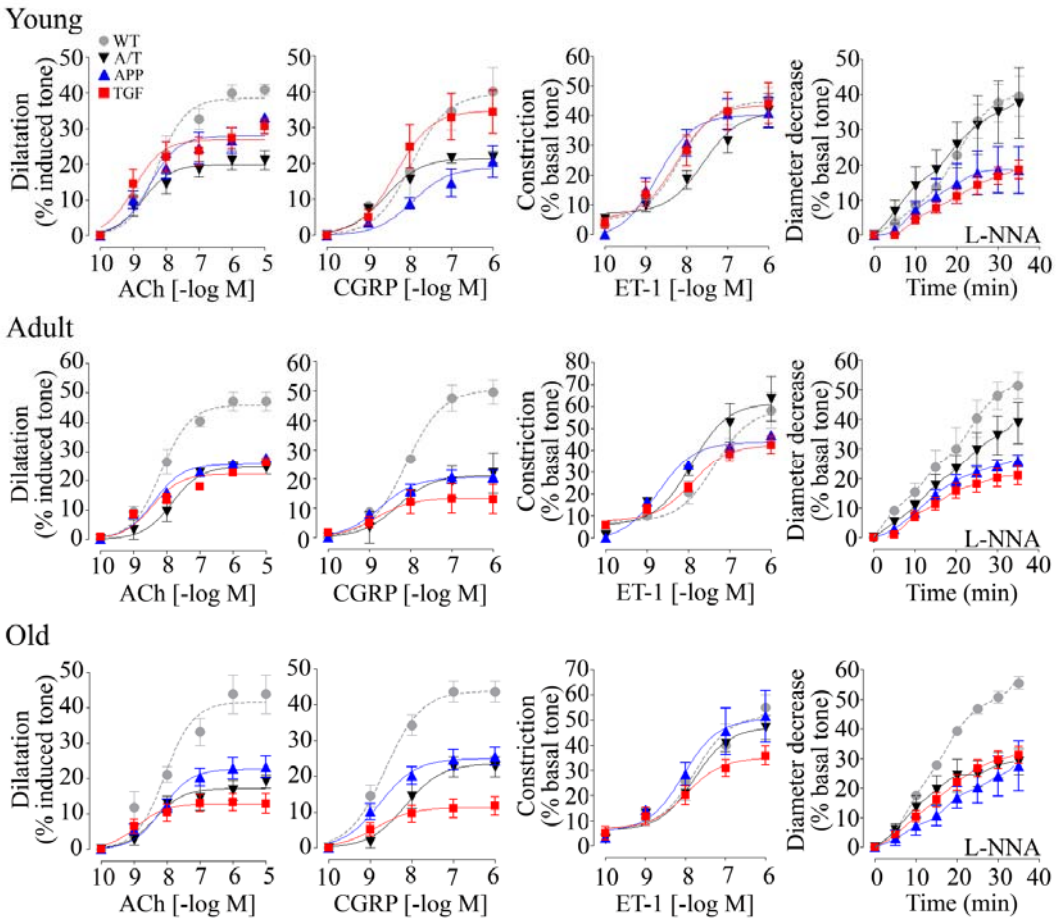

Figure 1 (suppl). Age-related impairment in cerebrovascular reactivity in A/T mice compared to similarly aged APP and TGF mice. Responses of WT mice from Fig.1 are illustrated for reference. Data from APP (blue) and TGF (red) mice were pooled from new and previously published studies. WT littermates of the singly transgenic lines had analogous responses to those of WT mice illustrated here, and were omitted for clarity. Statistical differences between singly transgenic mice and respective WT littermates can be found in the original publications listed below. There was no synergistic effect of Aβ and TGF-β1 overproduction on A/T responses, which were largely comparable to those of APP and TGF arteries. However, in A/T arteries, the intact ET-1-mediated contraction and impaired CGRP-induced dilatation compared better to those of APP mice, as these responses were respectively impaired and deficit delayed, but more severe in TGF mice (for significance, refer to original publications listed below). Also, A/T mice displayed a later decline in constitutive NO synthesis, measured during L-NNA-mediated NOS inhibition (10^{-5}M), compared to both APP and TGF mice. Number of animals is indicated in Supplemental Table 1. No statistical analysis was performed between the APP and TGF responses and those of A/T mice, as animals were from different litters and sample size often varied greatly. Statistical comparison between A/T and WT mice is shown in Fig. 1 of the manuscript.

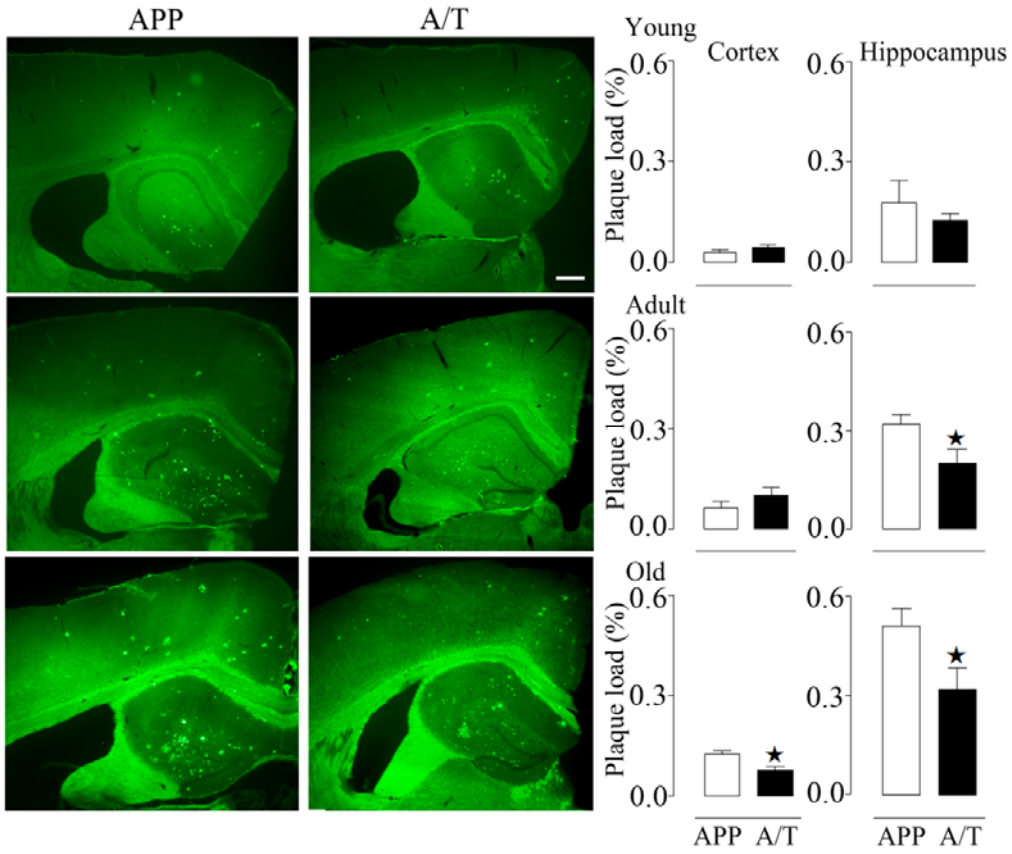

Figure 2 (suppl). Comparison of amyloid plaque load in the cortex and hippocampus of age-matched A/T and APP mice. Relative to APP mice, adult A/T mice featured a significantly reduced Thioflavine S-positive plaque area (load) in the hippocampus, and this extended to the cortex in old A/T animals (★$p<0.05$, Student's *t* test). Error bars represent SEM (n=7-8 mice/group). Scale bar, 20μm.

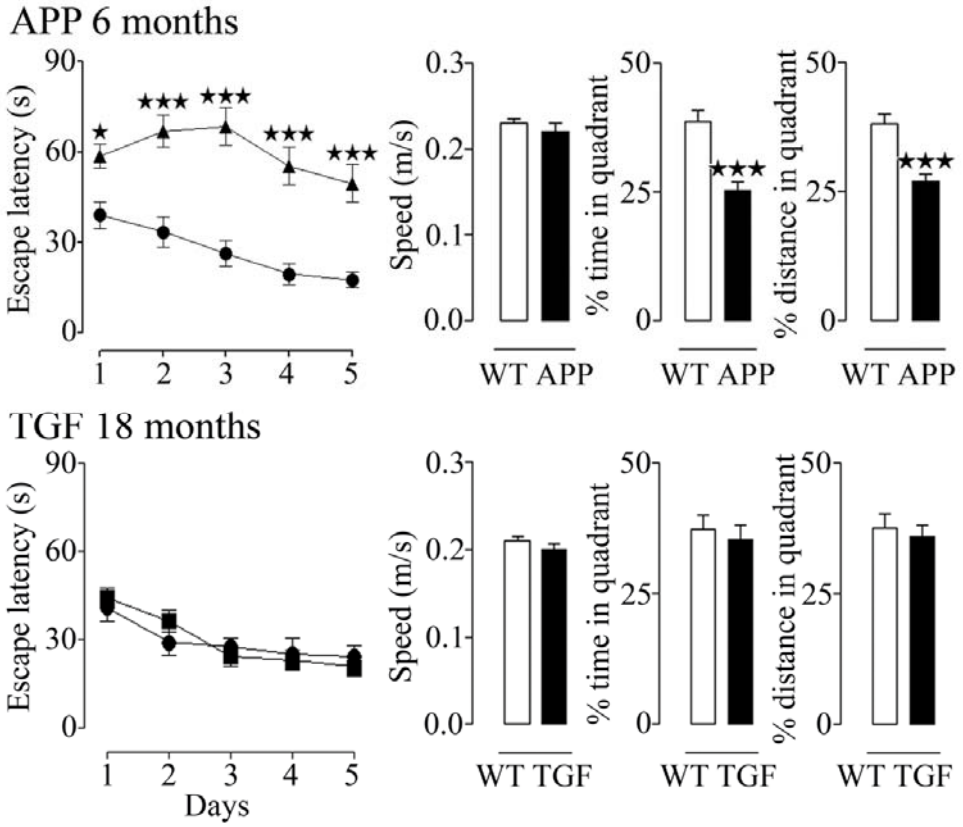

Figure 3 (suppl). Early spatial memory deficits in the Morris water maze in 6 month-old APP mice (triangles) are contrasted with the lack of impairment in TGF mice (squares) even at 18 months of age. This suggests Aβ-driven cognitive dysfunction in bitransgenic A/T mice (refer to Fig. 6). Error bars represent SEM (n=12-17 mice/group). ★★p<0.01, ★★★p<0.001 for comparison to age-matched wild-type (WT, circles) littermates mice using two-way ANOVA followed by Bonferroni post-hoc test (latency curves) or using Student's *t* test (probe trial histograms).

Preface to Chapter 3

In the previous chapter, we demonstrated that A/T mice displayed a progressive decline in spatial learning and memory, evoked cerebral blood flow and glucose uptake during brain activation, and cerebrovascular function, along with a progressive increase in astrocytic activation and Aβ pathology. In the following chapter, we sought to verify whether the abovementioned clinical outcomes could be rescued following chronic *in vivo* therapy administered to adult and aged A/T mice with fully-expressed neuronal, behavioural and cerebrovascular deficits, hence best representing AD patients with a TGF-β1-mediated vascular pathology who may receive diagnosis at an advanced stage.

We selected the PPARγ agonist pioglitazone (20mg/kg/day) based on its transcriptional control over inflammatory, metabolic, amyloidogenic and vascular pathways implicated in AD. It was preferred over rosiglitazone, another compound of the same thiazolidinediones class which cannot cross the BBB, whereas pioglitazone can, which could likely remedy neurons and glial cells of the diseased AD brain. We also chose pioglitazone as it was effective against specific AD pathologies – but not in Aβ-mediated cognitive loss – in singly ~14 months-old APP and ~18 months-old TGF mice (treated for 6-8 weeks). We hypothesized that longer treatment duration and/or starting at a younger age would facilitate memory recovery in A/T mice. We found that pioglitazone benefited selective AD hallmarks, precluding cognition, in a complex AD mouse model despite negative effects on dilatory function. Together, our results suggested a potential benefit of pioglitazone to protect the brain against neuroinflammation, cerebral perfusion and glucose metabolism in AD patients devoid of cerebrovascular pathology.

Chapter 3

Cerebrovascular and anti-inflammatory benefits of pioglitazone in bitransgenic APP/TGF-β1 mice with reversal memory improvement

Panayiota PAPADOPOULOS, Pedro ROSA-NETO, and Edith HAMEL

Abstract

Animal models of Alzheimer's disease (AD) have been invaluable in dissecting the pathogenic mechanisms and assessing the efficacy of potential therapies. Here, we used the peroxisome proliferator-activated receptor gamma agonist pioglitazone in an attempt to rescue the pathogenic phenotype in adult (12 months) and aged (>18 months) bitransgenic A/T mice that overexpress a mutated human amyloid precursor protein ($APP_{Swe,Ind}$) and a constitutively active form of transforming growth factor-β1 (TGF-β1). A/T mice display age-related cognitive deficits, amyloid-β (Aβ) pathology, altered metabolic and vascular coupling responses to increased neuronal activity, and a cerebrovascular pathology. Pioglitazone normalized neurometabolic and neurovascular coupling responses to sensory stimulation, and reduced cortical astroglial activation at both ages. Spatial learning and memory in the Morris watermaze were not normalized by pioglitazone, but reversal learning was improved in the adult cohort despite unaltered elevated Aβ levels or plaque load. Pioglitazone, however, failed to restore cerebrovascular reactivity in A/T mice, but rather exacerbated the vasodilatory deficit. These data demonstrate pioglitazone's efficacy on selective AD hallmarks in a complex AD mouse model despite negative effects on dilatory function. They further suggest a potential benefit of pioglitazone in managing neuroinflammation, cerebral perfusion and glucose metabolism in AD patients devoid of cerebrovascular pathology.

Introduction

Alzheimer's disease (AD), the most common form of senile dementia in the elderly, is characterized by high levels of amyloid-β (Aβ) peptide, neurofibrillary tangles, and neuroinflammation. It is also marked by early decreases in cerebral glucose uptake (CGU) and cerebral blood flow (CBF), and a cerebrovascular pathology (Bell and Zlokovic, 2009). The latter is multifaceted and involves a vascular fibrosis with thickening of the basement membrane, which has been imputed to increased levels of transforming growth factor-β1 (TGF-β1) (Wyss-Coray et al., 2000, Grammas and Ovase, 2002, Tesseur and Wyss-Coray, 2006). Hence, in order to better recapitulate the complexity of the AD pathology, a double transgenic mouse model that concurrently overproduces Aβ and TGF-β1 (A/T mice) has recently been characterized (Ongali et al., 2010). A/T mice display the broad spectrum of cerebrovascular, neuronal, glial, and cognitive alterations found in AD patients, thereby integrating the comorbid factor of cerebrovascular pathology to that of increased amyloidosis in the pathogenesis of AD (Zlokovic, 2010).

Pioglitazone is a peroxisome proliferator-activated receptor-γ (PPARγ) agonist that remains a potential candidate for AD therapy (Geldmacher et al., 2011, Sato et al., 2011). This interest was originally sparked by pioglitazone ability to cross the blood-brain-barrier (BBB) (Maeshiba et al., 1997) and subsequent findings of its benefits against multiple features of AD pathology. In APP mice, pioglitazone reduced glial inflammation, normalized CGU and cerebrovascular function, despite limited or no effect on Aβ processing and deposition (Yan et al., 2003, Heneka et al., 2005, Nicolakakis et al., 2008). Pioglitazone was similarly effective in restoring CGU and cerebrovascular

function in mice that overexpress TGF-β1 (Gaertner et al., 2005, Nicolakakis et al., 2011), faithfully reproducing the AD cerebrovascular pathology (Wyss-Coray et al., 2000). However, validation of pioglitazone therapy in AD might gain from a thorough examination of its efficacy in a more complex model, such as the A/T mice.

Hence, we investigated the effects of pioglitazone in adult and aged A/T mice on AD hallmarks including impaired neuronally-induced CGU and CBF responses, astroglial activation, amyloidosis and hippocampus-based learning and memory deficits. Cerebral arterial responsiveness and proteins regulating vascular structure or function were also evaluated. Despite aggravating effects of pioglitazone on vasodilatory responses, our findings support the use of pioglitazone as a strategy to delay the progression of the disease, particularly in AD patients free of vascular diseases, by demonstrating efficacy on AD-related neuroinflammation, hypoperfusion and hypometabolism together with benefits on cognitive flexibility.

Methods

Animals. A/T mice (Ongali et al., 2010) overexpress a mutated form of the human amyloid precursor protein ($APP_{Swe,Ind}$) driven by the platelet-derived growth factor β promoter (line J20) (Mucke et al., 2000) and a constitutively active form of TGF-β1 under the control of the glial fibrillary acidic protein (GFAP) promoter on a C57BL/6J background (line T64) (Wyss-Coray et al., 2000). The expression of both transgenes was identified by touchdown PCR using tail-extracted DNA (Ongali et al., 2010). Adult (12 months old at endpoint; treated for 6 months, N=8-11/group) and aged (18-21 months old at endpoint; treated for 3 months N=5-7/group) A/T mice and wild-type (WT) littermates

(body weight, ~30-60g) were treated or not with pioglitazone (20mg/kg/day in chow) with males and females evenly distributed in each group. Water and chow were available *ad libitum*. At the end of treatment, pioglitazone treated-A/T mice of both cohorts had gained more weight compared to age-matched WT or untreated A/T mice [adult (g): WT: 12.5 ± 1.0; WTpio: 8.6 ± 0.9; A/T: 11.7 ± 0.9; A/Tpio 21.6 ± 1.1; $p<0.05$; aged (g): WT: 2.5 ± 1.5; WTpio: 5.2 ± 2.3; A/T: 2.6 ± 0.5 vs A/Tpio 10.0 ± 0.9; $p < 0.05$]. Fasting glycemia measured with a commercial glucometer (One Touch Ultra, LifeScan, Burnaby, BC, Canada) using blood collected from the mouse's tail vein was not altered by treatment at any age [adult (mmol/L): WT 9.5 ± 0.4, WTpio 9.0 ± 0.3, A/T 8.7 ± 0.5, A/Tpio 8.8 ± 0.4; aged (mmol/L): WT 9.5 ± 0.5; WTpio 8.8 ± 0.3; A/T 9.2 ± 0.3; A/Tpio 8.4 ± 0.2]. All experiments were approved by the Animal Ethics Committee of the Montreal Neurological Institute, and abided by the guidelines of the Canadian Council on Animal Care.

Morris Watermaze. (i) Learning and Spatial Memory. Mice were trained to escape onto a platform located in a circular pool (1.4 m diameter) filled with opaque water (18±1°C) and located in a room with visual wall cues. The pool was subdivided into four quadrants numbered in a clockwise order – quadrant #1 being located north-east. There were two platform locations: (1) the visible platform (original quadrant; south-east quadrant #2) for a three-day training session, and (2) the hidden platform (target quadrant; north-west quadrant #4) submerged ~1cm below the surface of the water for a five-day training session. The location of the distal wall cues was changed between the visible and hidden platform sessions, as previously described (Deipolyi et al., 2008). Mice were given three trials daily (spaced 45min apart) with a maximum duration of

60s/trial and 90s/trial for the visible and hidden platform training sessions, respectively. On the first day of each session, mice that failed to locate the platform in the allotted time were guided to and allowed to stay on it for 10s. Spatial memory was tested during the probe trial (60s, platform removed) 24h after the last hidden platform trial (day 9). Mice were kept warm with a heating lamp and testing began at the same time every day. Subsequent experiments resumed 2 days later. Escape latencies and probe trial were recorded with the 2020 Plus tracking system and Water 2020 software (Ganz FC62D video camera; HVS Image, Buckingham, UK) (Nicolakakis et al., 2011). The parameters of the probe trial were: percent time spent and distance traveled in target quadrant, average distance to platform location and swim speed. The probe trial analysis was additionally subdivided in temporal patterns of search in the target quadrant presented in slices of 15s each (Maei et al., 2009). **(ii) Cognitive flexibility.** The inability to switch to a new focus or strategy (platform location) while failing to suppress the execution of a previously learned task is a correlate of impaired cognitive flexibility (Chen et al., 2000a, Seeger et al., 2004). To examine such possible alterations, the probe trial analysis was further extended to the assessment of the same abovementioned parameters in the original quadrant.

Cerebral glucose uptake (CGU). This test was performed only in mice from the aged cohort. Mice were fasted for 12h before being scanned for CGU of 2-deoxy-2-[^{18}F]fluoro-D-glucose ([^{18}F]FDG) under isoflurane (1–2% in medical air) anesthesia in a CTI Concorde R4 micropositron emission tomography (microPET) scanner (Siemens Preclinical Solutions, Knoxville, TN, USA). Mice were injected with 100-150 μCi (100 μl) of [^{18}F]FDG into the tail vein prior to a 45min uninterrupted whisker stimulation (8–

10 Hz, electrical toothbrush) followed by a 25min PET acquisition (15min emission/10min transmission scan using a [^{57}Co] point source). Physiological parameters (body temperature, cardiac rate and respiration) were constantly monitored (Biopac Systems, Goleta, CA, USA), and remained stable throughout the experiment. The reconstruction of the functional metabolic images was generated based on a maximum a posteriori probability algorithm for the [^{18}F]FDG standard uptake values (SUV) adjusted according to body weight, injected dose of radioligand and fasting glycemia measurements taken before and after the scanning. Images were superimposed on average magnetic resonance imaging (MRI) templates generated on a 7-T Bruker Pharmascan system (Bruker Biospin, Ettlingen, Germany) from similarly aged WT and A/T mice (n = 5 per group) (for details, (Nicolakakis et al., 2011, Tong et al., 2012)). The areas of interest for this study were drawn on the somatosensory cortices (Franklin and Paxinos, 1997). Metabolic activation was then defined as the percentage of ([^{18}F]FDG) SUV ratio between the maximally activated contralateral vs ipsilateral somatosensory cortex upon whisker stimulation. Final images were adjusted to animal body weight and injected radioactivity dose.

Cerebral blood flow (CBF). CBF increases induced by unilateral (right side) whisker stimulation were measured using laser Doppler flowmetry (Transonic Systems Inc, Ithaca, NY) two days following the Morris watermaze (adult mice) or PET session (aged mice). Mice were anesthetised with ketamine (85 mg/kg, intramuscularly (i.m.); Bioniche, Belleville, ON) and xylazine (3 mg/kg i.m.; Haver, Etobicoke, ON), and fixed in a stereotaxic frame. The bone over the left barrel cortex was thinned to translucency for positioning of the laser probe, as previously described (Nicolakakis et al., 2011).

Body temperature was kept stable throughout the experiment with a heating pad. CBF was measured before, during and after whisker stimulation (4-5 stimulations, 20s each, 8-10 Hz, electric toothbrush), and averaged for each mouse. Results are expressed as percentage increase of CBF from baseline. Experiments lasted ~20min/mouse and were performed blind to the identity of the mouse.

Tissue collection and preparation. At the end of the *in vivo* testing, a subset of mice from both cohorts was sacrificed by cervical dislocation for functional reactivity of the middle cerebral artery (MCA) (see below). The remaining vessels of the circle of Willis, together with cortex and hippocampus from one hemibrain were removed, frozen on dry ice and stored (-80°C) for subsequent ELISA and Western blot experiments. The other hemisphere was immersion-fixed (4% paraformaldehyde (PFA) in 0.1 M phosphate buffer (PB), pH 7.4, overnight, 4°C), cryoprotected overnight (4°C in 30% sucrose 0.1 M PB), frozen in isopentane (-45°C) and stored (-80°C) until cutting of free-floating thick sections (25 μm) on a freezing-microtome. The remaining mice from each group were anesthetized with pentobarbital (80 mg/kg, i.p.) and perfused transcardially with a 4% PFA solution. The brains were prepared as above, except that one hemisphere was processed for paraffin sectioning (5 μm-thick).

Vascular reactivity. MCA segments (40–70 μm average intraluminal diameter) were cannulated, pressurized (60 mm Hg) and superfused with oxygenated Krebs solution (~37°C) for reactivity studies using online videomicroscopy (Tong et al., 2005). Dilatory responses to acetylcholine (ACh; 10^{-10}-10^{-5} M), calcitonin gene-related peptide (CGRP; 10^{-10}-10^{-6} M) were tested on vessels pre-constricted submaximally with serotonin (5-HT; 2×10^{-7} M). Contractile responses to endothelin-1 (ET-1; 10^{-10}-10^{-6} M), 5-HT (10^{-10}-10^{-6}

M) and to inhibition of nitric oxide synthase (NOS) with N_{ω}-nitro-L-arginine (L-NNA; 10^{-5} M; 35min) were tested on vessels at basal tone. Responses to 5-HT (10^{-10}-10^{-6} M) and NO donor sodium nitroprusside (SNP; 10^{-10} - 10^{-4} M) were also tested in the adult cohort only. Changes in vessel diameter from either the basal or pre-constricted tone were expressed in percentage and plotted as a function of agonist concentration or time course of L-NNA incubation. Agonist efficacy and potency were compared using the maximal response (EA_{max}) and half maximal effective agonist concentration [EC_{50} value or pD_2=-(log EC_{50})], respectively.

ELISA measurement of $A\beta_{1-40}$ and $A\beta_{1-42}$. Soluble and insoluble $A\beta_{1-40}$ and $A\beta_{1-42}$ levels in cortex and hippocampus from hemibrains of adult and aged A/T mice were measured using an enzyme-linked immunosorbent assay (ELISA; BioSource International), as previously described (Nicolakakis et al., 2008). Results are expressed as micrograms per gram (μg/g) of protein in the supernatant (soluble Aβ species) or formic acid fractions (insoluble Aβ species).

Western blot. Proteins extracted from cerebral cortex and hippocampus (~20μg) were loaded onto a 15% Tris/tricine SDS PAGE and transferred to nitrocellulose membranes. Total soluble Aβ levels were detected with a mouse anti-Aβ1-16 antibody (6E10, 1:1000, Covance, Emeryville, CA, USA). Levels of proteins involved in vascular function and structure were also assessed in pial vessel extracts. Proteins (12-15 μg) loaded onto 10% SDS PAGE were probed with the following antibodies: goat anti-connective tissue growth factor (CTGF; 1:400; Abcam, San Francisco, CA, USA), -matrix metalloproteinase 9 (MMP9; 1:2000; Millipore, Temecula, CA, USA), -cyclooxygenase-

2 (COX-2; 1:200; Cayman, Ann Arbor, MI, USA), rabbit anti-vascular endothelial growth factor (VEGF; 1:500; Santa Cruz Biotechnology, Santa Cruz, CA, USA), or -actin (1:8000; Santa Cruz Biotechnology A5441, Santa Cruz, CA, USA). Membranes were incubated (1h) with horseradish peroxidase-conjugated secondary antibodies (1:2000; Jackson ImmunoResearch, West Grove, PA, USA), and visualized with Enhanced ChemiLuminescence (ECL Plus kit; Amersham, Baie d'Urfé, QC, Canada) using phosphorImager (Scanner STORM 860; GE Healthcare, Baie d'Urfé, QC, Canada). Quantification was performed with ImageQuant 5.0 (Molecular Dynamics, Sunnyvale, CA, USA).

Histochemical and Immunohistochemical stainings. Mature, dense core Aβ plaques were stained in 25μm-thick sections with 1% thioflavin S (8min). Activated astrocytes were immunodetected in similar sections with a rabbit anti-GFAP antibody (1:1000; DAKO), followed by a donkey anti-rabbit Cy2-conjugated secondary antibody (1:400; Jackson ImmunoResearch). Dewaxed thin paraffin sections (5 μm) were stained with 6E10 to quantify Aβ plaque load (1:2000). Sections were observed under a Leitz Aristoplan light microscope equipped with epifluorescence using an FITC filter (Leica). Pictures were taken with a Nikon digital camera (Coolpix 4500), and the percent area occupied by GFAP-, thioflavin S- and 6E10-positive immunostaining in cortex and/or hippocampus were quantified with MetaMorph 6.1r3 program (Universal Imaging).

Statistical analysis. Data are expressed as means ± SEM and were analyzed by two-way ANOVA with genotype and treatment as variables, followed by Newman-Keuls post-hoc multiple comparison test (Statistica for Academia, Tulsa, OK, USA). P values were reported if the interaction or at least one factor was significant. Two-group comparisons

were analyzed by Student's *t* test (GraphPad Prism 4, San Diego, CA, USA). A $p < 0.05$ was significant.

Results

Pioglitazone normalized neurovascular and neurometabolic coupling responses

The CBF response to increased neuronal activity induced by whisker stimulation was significantly reduced in adult (18.7±1.7%; p<0.01) and aged (18.3±1.2%; p<0.01) A/T mice compared to age-matched WT controls (adult: 24.6±1.0% and aged: 29.3±0.7%), as shown in the adult cohort (Figure 1A). Similarly, in aged A/T mice, the selective increase in CGU induced by whisker stimulation in the contralateral somatosensory cortex was significantly less than in WT littermates (% activation ratio: 1.3 ± 1.1 vs 8.4 ± 1.7 respectively; $p < 0.05$) (Figure 1B). Pioglitazone normalized the evoked CBF response to increased neuronal activity in both adult (Figure 1A) and aged (data not shown) A/T mice to levels comparable to their control counterparts. The CGU response was also significantly improved by pioglitazone in aged A/T mice (A/Tpio: 6.4 ± 1.3; Figure 1B). Treatment had no effect on WT controls for both responses.

Pioglitazone did not rescue spatial learning and memory – target quadrant #4

Adult and aged A/T mice displayed significantly increased escape latencies in finding the hidden platform compared to treated and untreated WT mice (Figure 2A). A/T mice also had a decreased inclination for the target quadrant during the probe trial, as shown for the adult cohort by the reduced time spent in this quadrant (#4) and greater average distance to the platform location (Figure 2B). These changes are indicative of impaired spatial learning and memory compared to their age-matched WT controls. These deficits could

not be explained by visual or motor disabilities as all groups had comparable swim speeds (data not shown) and similar abilities to find the visible platform (days 1-3, Figure 2A). Further analysis of the search patterns in slices of 15s (Figure 2C) revealed that WT controls focused on the target quadrant throughout the probe trial with minimal navigation elsewhere (including in the original quadrant #2) (Figure 2B), as also depicted by their representative swim patterns (Figure 2F). In contrast, A/T mice searched non-selectively and both the percent time spent (Figure 2B) and distance traveled in the target quadrant were significantly less than WT controls (WT 36.2±3.8% vs. A/T 13.8±3.3%, $p<0.01$). Average distance to the platform was also significantly larger in A/T mice for the majority of the 15s segments (Figure 2C). Pioglitazone treatment did not improve performance of A/T mice of either age during the learning phase or probe trial, as shown in the adult cohort (Figure 2A-C). Notably, spatial memory in adult and aged pioglitazone-treated WT mice was slightly, but significantly, deteriorated ($p<0.05$, Figure 2), an effect not seen in previous WT cohorts (Nicolakakis et al., 2008, Nicolakakis et al., 2011).

Pioglitazone and cognitive inflexibility – original quadrant #2

In contrast to WT controls, both adult and aged A/T mice targeted the original quadrant (#2) throughout the probe trial, as shown here in adult mice by both increased percent time spent (Figure 2D) and distance traveled (WT 20.5±2.8% vs. A/T 42.6±4.5, $p<0.01$) in this quadrant. Their erroneous persistence for the original platform location was apparent throughout the probe trial, despite a brief within-session extinction, and was significant in the last 15s segmentation analysis for all parameters assessed including average distance from platform, percent time spent (Figure 2E), and distance travelled

(WT 20.4±2.9% vs. A/T 54.7±8.8%, $p<0.01$). The preference of A/T mice for the original quadrant was obvious compared to any other quadrant, including the target quadrant (Figure 2F), pointing to their cognitive inflexibility or inability to inhibit a previously learned task for a new one (Whishaw and Tomie, 1997).

In adult, but not aged, A/T mice, pioglitazone had a positive effect in decreasing their time spent in the original quadrant and the average distance to platform (Figure 2D), specifically in the last quarter of the probe trial (Figure 2E). Similarly, the pioglitazone-treated adult A/T spent significantly less time (Figure 2E) and traveled less distance (A/T 42.6±4.5% vs. A/Tpio 24.5±5.2%, $p<0.01$) in the original quadrant during the last 15s-segment relative to untreated-A/T mice. However, this delayed yet significantly improved understanding of the platform relocation was not sufficient to redirect them to the target quadrant. Instead they predominantly navigated in quadrant #3 (adjacent to target quadrant #4) (Figure 2E, F), as seen by their swimming patterns (Figure 2F).

Pioglitazone effects on brain vessel reactivity and fibrosis

In agreement with previous studies, adult and aged A/T mice (Ongali et al. 2010) displayed significantly decreased dilatory responses to ACh and CGRP compared to their age-matched WT controls, as shown in the adult group (Figure 3A). Reduced diameter decrease during NOS inhibition with L-NNA was also observed in A/T mice of both age groups, confirming a diminished constitutive NO synthesis. Despite these alterations in vascular reactivity, receptor desensitization was ruled out, as the agonist potencies at vascular receptors were strictly comparable between all groups (Tables 1 and 2). Arterial relaxation to the NO donor SNP and the constriction induced by ET-1 were normal in

A/T mice, indicative of preserved contractile capacity, as also supported by the unaltered pre-constriction response to 5-HT (tested in the adult cohort only) (Figure 3A). Pioglitazone treatment partially (aged) or fully (adult) restored constitutive NO synthesis in A/T mice depending on age (Figure 3A, Tables 1, 2), and did not alter the contractile responses to 5-HT and ET-1. However, pioglitazone significantly deteriorated the dilatory responses to ACh and CGRP, resulting in no dilatation and weak contractile responses at high agonist concentrations (Figure 3A). Similarly, the NO donor SNP elicited vasoconstrictions at low doses that reverted to dilatations at higher concentrations (Figure 3A). These worsened responses were observed in both adult (Figure 3A) and aged (data not shown) pioglitazone-treated A/T mice, although they were less pronounced in the adult cohort. Pioglitazone did not alter the cerebrovascular reactivity of WT mice (Figure 3C). The cerebrovascular levels of the prostaglandin-synthesizing enzyme COX-2 (Figure 3B) and of the pro-fibrotic proteins CTGF, VEGF or MMP9 were not altered by pioglitazone, as shown in the adult cohort (Figure 3B).

Pioglitazone and amyloidosis

Pioglitazone had no effect on soluble and insoluble $A\beta_{1-40}$ and $A\beta_{1-42}$ levels measured by ELISA in cortex and hippocampus of adult (Figure 4A) and aged (data not shown) A/T mice. Increased total soluble Aβ levels were also detected in cortex and hippocampus of adult and aged A/T by Western blot and, similarly, pioglitazone had no benefit at either age, as shown in cortex of adult A/T mice (Figure 4B). Plaque load of thioflavin S-positive dense core plaques was unaltered by pioglitazone in cortex and hippocampus from A/T mice irrespective of age and length of treatment (Figure 4C). This was further confirmed by the unaltered load of diffuse and dense core immunopositive Aβ plaques

measured in thin sections (Figure 4D). Together, these results demonstrate that pioglitazone does not counter the amyloid pathology in A/T mice, in line with previous studies in APP mice (Yan et al., 2003, Nicolakakis et al., 2008).

Pioglitazone and neuroinflammation

Both adult and aged A/T mice exhibited a significant increase in GFAP-positive area in cortex and hippocampus compared to their age-matched WT controls ($p<0.001$) (adult cohort, Figure 5), GFAP being a marker of neuroinflammation. In both age cohorts, pioglitazone significantly reduced astroglial activation only in the cortex where activation was not as severe as in the hippocampus (Figure 5).

Discussion

This study demonstrates positive effects of pioglitazone on neurometabolic and neurovascular coupling responses, and on neuroinflammation in a complex AD mouse model of amyloidosis and cerebrovascular pathology. A modest improvement in reversal learning favouring cognitive flexibility was also observed in the adult, but not in the aged cohort, notwithstanding persistent memory deficits and amyloidosis in both age groups. The promoting contractile tone of brain vessels from A/T mice by pioglitazone treatment, however, pointed to possible detrimental effects in AD patients with vascular diseases.

Pioglitazone on neurometabolic and neurovascular coupling responses: a role for astrocytes

Early decreases in resting CGU have been reported in the parietotemporal and posterior cingulate cortex in AD patients (Fukuyama et al., 1994, Mosconi et al., 2004, Langbaum et al., 2009) and in various cortical areas in APP mice (Niwa et al., 2002) using FDG-

PET and autoradiography, respectively. Altered neurometabolic coupling in response to increased neuronal activity has also been reported in AD patients (Melrose et al., 2009), APP mice (Nicolakakis et al., 2008) and aged A/T mice (Ongali et al., 2010). The finding that pioglitazone improved CGU during activation of the somatosensory cortex in the combined Aβ- and TGF-β1-burdened brain of aged A/T mice underscored the high efficacy of pioglitazone in restoring brain glucose metabolism. *In vivo* experiments in healthy rat brain showed that glucose preferentially fuels astrocytes during neuronal activity even though neurons have greater metabolic needs (Chuquet et al., 2010). Astrocytes then supply neurons with glycolytic products, particularly lactate, for use in oxidative metabolism (Pellerin and Magistretti, 2003). Hence, our FDG-PET results may predominantly reflect restored astrocytic glucose metabolic activity by pioglitazone and, to a lesser extent, oxidative metabolism in neurons, similar to what has been demonstrated *in vitro* (Dello Russo et al., 2003, Izawa et al., 2009). In support of restored astrocytic function by pioglitazone is our finding of normalized cortical GFAP-immunostaining intensity, a marker of increased astrocytic-reactive inflammatory response (Wyss-Coray, 2006). Restored astroglial homeostasis could also explain the normalization of the functional hyperemic response that requires the concerted action of neurons, astrocytes and vascular cells (Zonta et al., 2003, Koehler et al., 2009). Particularly, PPARγ activation may have facilitated the ability of astrocytes to synthesize arachidonic acid derivatives, primarily the vasodilatory epoxyeicosatrienoic acids (EETs) that mediate a large part of the neurovascular coupling response to whisker stimulation (Niwa et al., 2001a, Lecrux and Hamel, 2011), which is severely affected in APP and A/T mice (Niwa et al., 2001b, Ongali et al., 2010). However, the pioglitazone-mediated

silencing of cortical astrocytes did not impact on either soluble Aβ species or Aβ plaque load. This finding is in line with some studies in APP mice (Yan et al., 2003, Nicolakakis et al., 2008), but not with others that reported decreased plaque load or Aβ processing (Sastre et al., 2003, Heneka et al., 2005).

Pioglitazone and spatial memory

Despite the beneficial effects of pioglitazone highlighted above, spatial learning and memory in adult or aged A/T mice was not improved, as in our previous findings in aged APP mice (Nicolakakis et al., 2008). This may indicate that, despite hypoperfusion (de la Torre, 1999, Farkas and Luiten, 2001) and hypometabolism (Melrose et al., 2009) being good correlates of memory decline in AD, local recovery of CBF and CGU responses in the somatosensory cortex are not good surrogates for hippocampus-based mnemonic function. Since brain glucose metabolism is heterogeneous, pioglitazone may have failed to normalize the metabolic deficit in the limbic system in A/T mice, as previously reported in TGF mice (Galea et al., 2006). Indeed, in contrast to its beneficial effects in cortex, pioglitazone did not reduce astrocytic activation in the hippocampus. Since astrocytes are important in maintaining hippocampal homeostasis, which is critical for memory formation (Santello and Volterra, 2010), we suggest that their persistent activated state might contribute to the lack of memory rescue in treated A/T mice. Future investigations should ideally evaluate the evoked CGU or CBF responses in the hippocampus, and use hippocampus-specific stimulation paradigms that would better correlate with memory performances.

In a study on a small population of mild AD patients with type II diabetes treated with pioglitazone, resting CBF improvement in the parietal lobe – including the post-central gyrus (encompassing the somatosensory cortex) – was accompanied by cognitive improvement (Sato et al., 2011). This beneficial effect was also concurrent with an increase in insulin-mediated glucose uptake (Sato et al., 2011), a known mechanism of action for PPARγ (Nicolakakis and Hamel, 2010). However, aside from one additional study showing cognitive improvement in diabetic AD patients with pioglitazone (Hanyu et al., 2009), all other clinical trials of AD patients failed to demonstrate benefit (Geldmacher et al., 2011). It is thus tempting to speculate that pioglitazone may confer cognitive protection only in AD patients with diabetes.

Pioglitazone and cognitive flexibility

Our data demonstrated that A/T mice exhibited a strong inclination for the original quadrant during the probe trial, as opposed to the target quadrant. Our protocol consisted of a single visible-to-hidden platform relocation and, as such, was less robust than the memory flexibility test of Chen and colleagues who used a series of hidden-platform relocation trials for the measurement of hippocampal-based learning deficits (Chen et al., 2000). Nevertheless, our data clearly showed that pioglitazone exerted beneficial effects on the reversal learning of A/T mice favoring an adaptation to the new contingency (target quadrant) and this, only in the adult cohort. These data point to age and treatment duration being both important elements in this beneficial effect of pioglitazone. Interestingly, rosiglitazone, another PPARγ agonist, similarly enhanced cognitive flexibility in APP/PS1 mice (Toledo and Inestrosa, 2010). Hence, this new therapeutic potential uncovered for pioglitazone in adult A/T mice may bear clinical significance for

AD patients in light of their reported impaired reversal learning (Levy-Gigi et al., 2011), but benefit could be highly dependent on the stage of the disease and time of treatment initiation.

Pioglitazone and cerebrovascular reactivity

Recovery of cerebrovascular reactivity with pioglitazone was anticipated based on its proven benefit in aged APP (Nicolakakis et al., 2008) and TGF (Nicolakakis et al., 2011) mice. While vasoconstriction to ET-1 and 5-HT remained unaffected, ACh- and CGRP-mediated dilations, on the contrary, were abolished or reversed to small constrictions in pioglitazone-treated A/T brain vessels. Although counterintuitive, this worsening behavior might be related to the reported ability of pioglitazone to directly elicit concentration-dependent dilations through endothelium-mediated NO release and gyanylyl cyclase activation, as recently shown in retinal arteries (Omae et al., 2011) and in rat aorta (Nomura et al., 2008). The adverse effects on CGRP may additionally be due to inhibition of ATP-sensitive K^+ (K_{ATP}) channels by pioglitazone, as shown in the coronary circulation (Yu et al., 2011). Although pioglitazone produced modest inhibitions compared to rosiglitazone, another PPARγ agonist recently prohibited from use in diabetic patients for its high risk cardiovascular profile (Kaul et al., 2010), the study points to the deleterious effects of pioglitazone on vasodilatory function. The ability of pioglitazone to activate SMC voltage gated K^+ (Kv) channels (Omae et al., 2011) may have also played a role even though these channels are less involved in CGRP vasorelaxation (Vedernikov et al., 2002). It is thus possible that chronic pioglitazone treatment in A/T mice exacerbated the NO signaling cascade or K^+ channel activation required for ACh- and CGRP-mediated dilatations (Mathie et al., 1991, Kitazono et al.,

1993, Tong et al., 2009). This possibility is reinforced by the failure of the NO donor SNP to induce dilation, pointing to mechanisms downstream of NO production being implicated in the failure of pioglitazone-treated vessels to dilate. Baseline NO production, however, was not altered by pioglitazone, which further suggested dysfunction in receptor-mediated NO signaling. Damaged smooth muscle cells and inability to dilate appear unlikely based on the preserved responses of arteries to various constrictors (ET-1, 5-HT).

Conclusion

Our results show that pioglitazone exerts beneficial effects on specific AD hallmarks in a complex AD mouse model that recapitulates the cerebrovascular, amyloidosis, cognitive and neuroinflammatory alterations seen in AD. Although area-specific, pioglitazone countered neuroinflammation, and subsequently CGU and CBF with age-dependent improvement in reversal learning, pointing to benefits at multiple levels. However, the A/T mouse model unmasked previously unrecognized, possibly deleterious, effect of chronic pioglitazone therapy on dilatory function, particularly those involving NO signaling. This finding may be relevant to AD patients with comorbid cardiovascular diseases even though pioglitazone may have a better cardiovascular safety profile than rosiglitazone (Lincoff et al., 2007, Ciudin et al., 2012).

Acknowledgements We thank Dr. L. Mucke (Gladstone Institute of Neurological Disease and Department of Neurology, UCSF, CA) and the J. David Gladstone Institutes for providing us $hAPP_{Swe,Ind}$ and TGF-β1 transgenic mouse breeders, Mr A. Aliaga for the PET scans, Mr J. Cakiroglu and Dr. B. Bedell (Small Animal Imaging Laboratory, SAIL, Montreal Neurological Institute) for generating the MRI templates, Drs. X.-K .Tong and

N. Nicolakakis for their invaluable technical training and support, Dr. Joseph Rochford for his input regarding the Morris watermaze analysis and Ms. P. Fernandes for the laser Doppler flowmetry experiments.

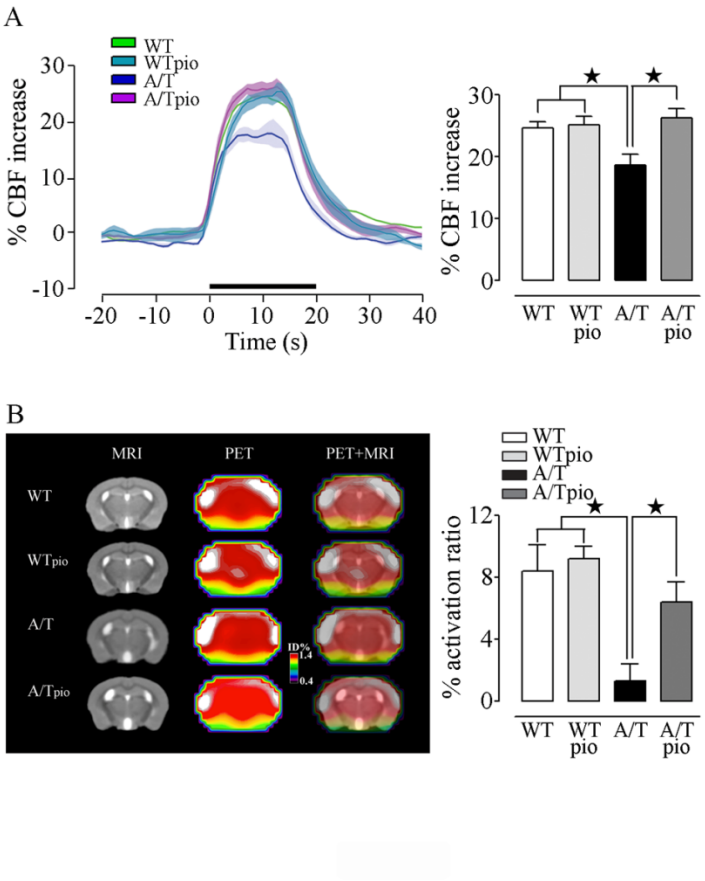

Figure 1. Pioglitazone restored stimulus-evoked CBF and CGU in A/T mice. ***A,*** The impaired hyperemic response to whisker stimulation in adult A/T mice was rescued by pioglitazone compared to age-matched WT controls, as measured by LDF (n=4 mice/group) (traces, green: WT; turquoise: WTpio; violet: A/T and pink: A/Tpio). Values represent the percent increase in CBF induced by whisker stimulation relative to baseline. ***B,*** Pioglitazone also improved the decreased CGU response to whisker stimulation in the somatosensory cortex of aged A/T compared to WT mice (n=3-6 mice/group). The % activation ratio denotes the percentage of corrected standard uptake value (SUV) in the activated contralateral vs. ipsilateral somatosensory cortex. Error bars represent SEM. ★p<0.05, ★★p<0.01, ★★★p<0.001 using two-way ANOVA followed by Newman-Keuls post-hoc test.

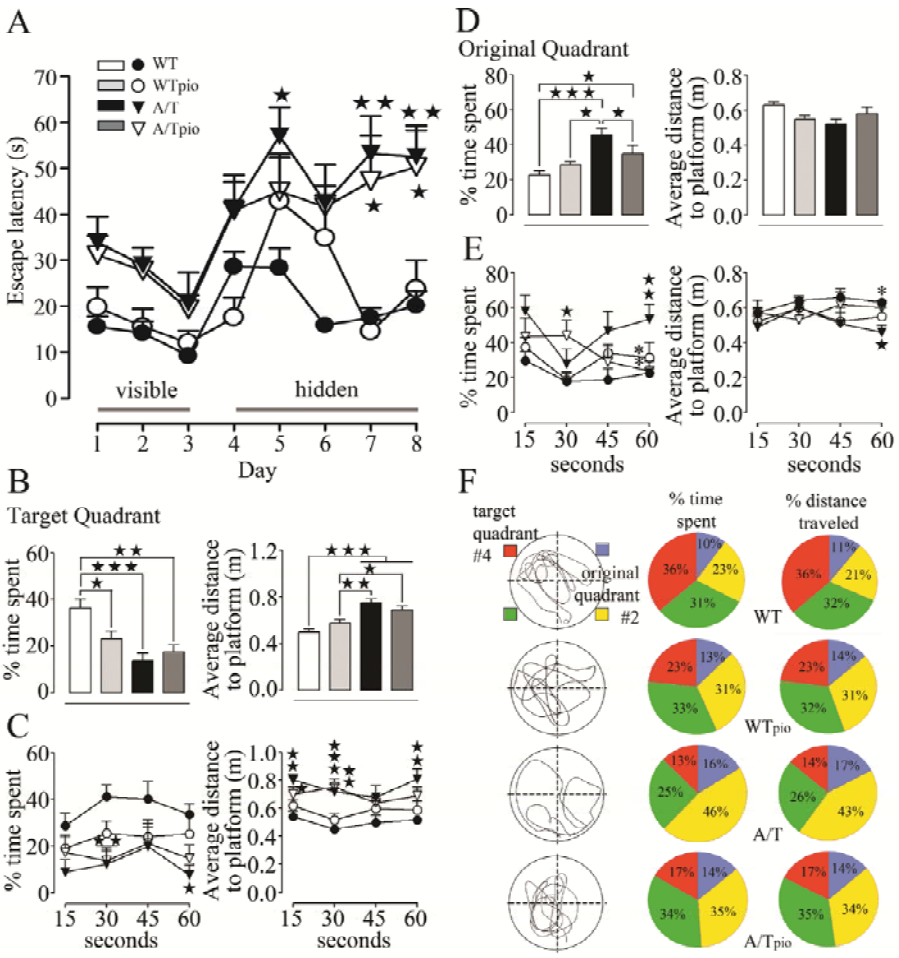

Figure 2. Spatial learning and memory in adult A/T mice in the Morris watermaze. ***A,*** Adult A/T mice (▼) displayed impaired learning during hidden-platform testing compared to aged-matched wild-type (WT) littermates (●). These deficits may not be explained by visual or motor disabilities as all groups had similar abilities to find the visible platform (days 1-3). Pioglitazone did not improve this deficit in A/T mice (▽) and did not affect the performance of pioglitazone-treated WT controls (○). ***B,*** A/T mice, treated and non-treated with pioglitazone displayed significant deficit in memory retention as assessed during the probe trial in the target quadrant. **C,** When the probe trial was subdivided in 15s segments for better understanding of the pattern of behavior throughout the 60s-long probe trial in target quadrant, pioglitazone did not exert any benefit. ***D,*** A/T mice showed an inclination for the original quadrant during the probe trial, as shown by the increased time spent in this quadrant and smaller average distance to the platform location. ***E,*** Patterns of behaviour in original quadrant segmented in 4 slices of 15s each during the probe trial showed that pioglitazone had a positive effect in increasing percent time spent and average distance to platform during in the last quarter of the probe trial. ***F,*** Pie-representation of typical swimming patterns of % time spent and % distance traveled in target quadrant during the probe trial. Error bars represent SEM (n=6-9 mice/group). ★p<0.05, ★★, ** p<0.01, ★★★p<0.001 when compared to untreated WT controls (★) or A/T mice (*) using two-way ANOVA followed by Newman-Keuls post-hoc test.

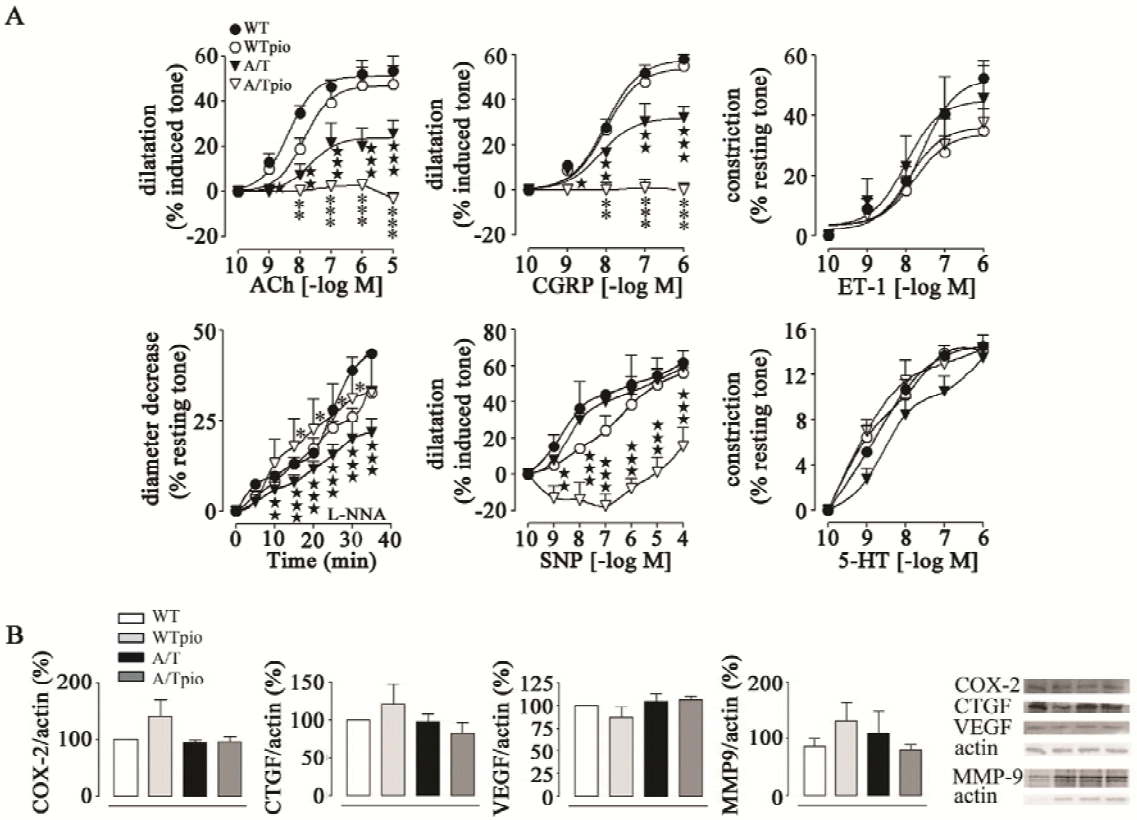

Figure 3. Cerebrovascular reactivity and protein alterations in adult A/T mice. ***A,*** The impaired cerebrovascular dilatations to acetylcholine (ACh) and calcitonin gene-related peptide (CGRP) in A/T mice (▼) were reversed to weak constrictions by pioglitazone (▽), accompanied by a partial or full recovery of baseline NO synthesis measured during NOS inhibition (L-NNA, 10^{-5}M). Dilatations induced by the NO donor SNP were impaired in A/T treated with pioglitazone. Contractile response to ET-1 and 5-HT were unaltered in A/T mice and pioglitazone had no detrimental effects. Error bars represent SEM. (n=4 for each group). ***B,*** Vasodilator synthesizing enzyme COX-2 and proteins associated with vascular fibrosis VEGF, CTGF and MMP-9 were not significantly altered by genotype or treatment, as measured by Western blot in pial vessels of adult A/T mice relative to their treated counterparts and WT mice. Actin was used as a reference for loading (n=4 mice/group). Similar results were obtained in the aged cohort, but data were not illustrated for clarity purposes. Error bars represent SEM. ★ $p<0.05$, ★★, ** $p<0.01$, ★★★, *** $p<0.001$ when compared to untreated WT controls (★) or A/T mice (*) using two-way ANOVA followed by Newman-Keuls post-hoc test.

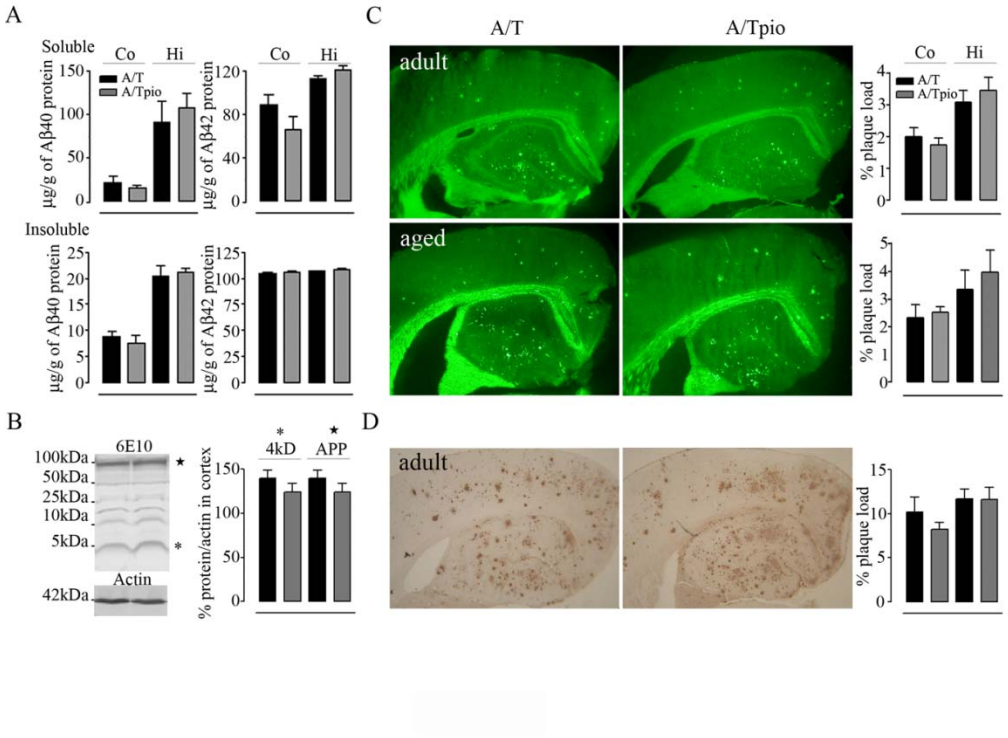

Figure 4. Pioglitazone had no effect on amyloidosis in A/T mice. ***A,*** Soluble and insoluble $A\beta_{1\text{-}40}$ and $A\beta_{1\text{-}42}$ in adult A/T mice, as assayed in cortex and hippocampus by ELISA. ***B,*** Western blot analysis with 6E10 antibody confirmed no effect of pioglitazone on soluble Aβ species of cortex in adult A/T mice. On the gel, (★) represents the APP band and (*), the 4kDa band of monomeric Aβ including $A\beta_{1\text{-}40}$ and $A\beta_{1\text{-}42}$. ***C,*** Thioflavin S-stained Aβ plaque load in cortex and hippocampus were unaltered by pioglitazone in adult A/T mice. ***D,*** Similarly, 6E10-immunostaining of diffuse and dense-core Aβ plaques measured in 5µm-thick paraffin sections (n=4 mice/group) showed no effect of pioglitazone on cortical and hippocampal Aβ plaque load in adult A/T mice. Error bars represent SEM (n=4 mice/group).

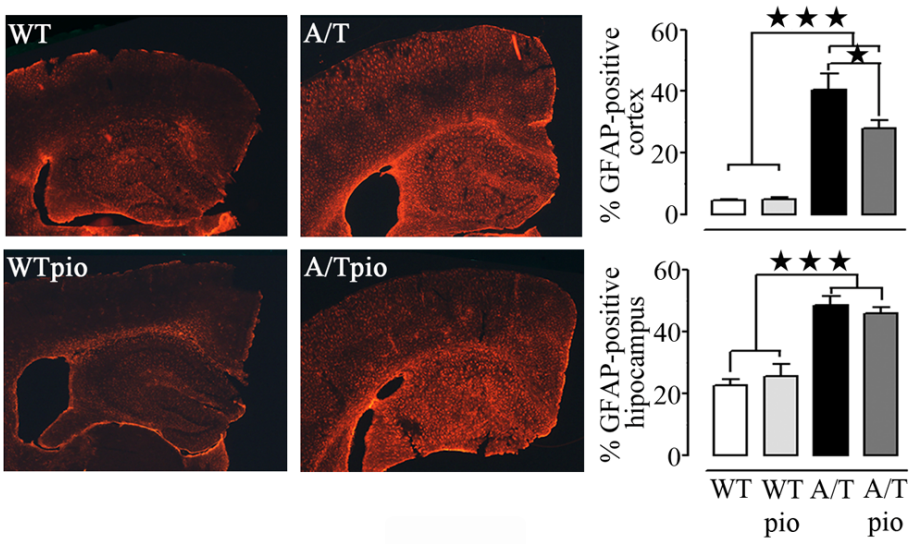

Figure 5. Pioglitazone selectively reduced astroglial activation. In the cortex (but not in the hippocampus) of adult A/T mice, pioglitazone significantly reduced the increase in GFAP-positive surface area relative to WT controls. (n=4 mice/group). Error bars represent SEM. ★$p<0.05$, ★★★$p<0.001$ using two-way ANOVA followed by Newman-Keuls post-hoc test.

Table 1. Effect of pioglitazone on cerebrovascular responses of adult A/T mice

Agonist		WT	WTpio	A/T	A/Tpio
ACh	E_{Amax}	51.2 ± 2.5	46.7 ± 4.0	23.7±3.6★★★	-3.1± 3.6★★★, ***
	pD_2	8.4 ± 0.2	7.9 ± 0.2	7.7 ± 0.4	ND
CGRP	E_{Amax}	57.6 ± 2.0	54.0 ± 3.6	31.9 ± 3.2★★★	-0.4 ± 2.0★★★, ***
	pD_2	8.0 ± 0.1	8.0 ± 0.2	8.2 ± 0.2	ND
SNP	E_{Amax}	62.0 ± 6.1	56.1 ± 3.0	59.5 ± 3.2	15.5 ± 10.1
5-HT	E_{Amax}	14.6 ± 0.2	14.2 ± 0.5	13.5 ± 1.3	14.3 ± 1.2
ET-1	E_{Amax}	52.3 ± 2.4	33.8 ± 4.1	44.9 ± 7.5	36.1 ± 5.0
	pD_2	7.6 ± 0.1	7.8 ± 0.3	8.0 ± 0.5	7.9 ± 0.4
L-NNA	E_{Amax}	43.7 ± 0.1	32.7 ± 1.9	21.8 ± 3.7★★★	32.8 ± 11.1 *

Data are means ± SEM (n=3-6 mice per group) and are expressed as the agonist maximal response (EAmax) or potency (pD_2, -[logEC_{50}]). EAmax is the percent maximal dilatation to ACh, CGRP and SNP or the percent maximal diameter decrease to ET-1, 5-HT or after 35min inhibition with 10^{-5}M L-NNA. ND: not determined. ★,* $p<0.05$, ★★,** $p<0.01$, ★★★ $p<0.001$ when compared to untreated WT controls (★) or A/T mice (*) by two way ANOVA followed by Newman-Keuls post-hoc multiple comparison test.

Table 2. Effect of pioglitazone on cerebrovascular responses of aged A/T mice

Agonist		WT	WTpio	A/T	A/Tpio
ACh	E_{Amax}	52.7 ± 2.0	54.5 ± 2.4	26.0±1.3★★★	16.0 ± 2.2★★★, ***
	pD_2	8.4 ± 0.1	8.3 ± 0.1	8.0 ± 0.1	ND
CGRP	E_{Amax}	54.1 ± 1.6	55.6 ± 3.0	25.3 ± 1.4★★★	9.9 ± 2.1★★★, ***
	pD_2	8.8 ± 0.1	8.4 ± 0.1	8.3 ± 0.1	ND
ET-1	E_{Amax}	58.3 ± 5.0	42.7 ± 3.6	53.4 ± 3.8	45.7 ± 4.0
	pD_2	8.2 ± 0.2	8.3 ± 0.3	8.4 ± 0.2	8.2 ± 0.2
L-NNA	E_{Amax}	52.3 ± 0.5	53.5 ± 5.1	15.1 ± 1.0★★★	28.7 ± 6.3★★

Data are means ± SEM (n=3-4 mice per group) and are expressed as the agonist maximal response (EAmax) or potency (pD_2, -[$logEC_{50}$]). EAmax is the percent maximal dilatation to ACh and CGRP or the percent maximal diameter decrease to ET-1 or after 35min inhibition with 10^{-5}M L-NNA. ND: not determined. ★,* $p<0.05$, ★★,** $p<0.01$, ★★★ $p<0.001$ when compared to untreated WT controls (★) or A/T mice (*) by two way ANOVA followed by Newman-Keuls post-hoc multiple comparison test.

Preface to Chapter 4

In Chapter 3, the cognitive deficits of adult and aged A/T mice could not be normalized by pioglitazone therapy, and the cerebrovascular dysfunction was worsened. We concluded that the age of treatment was too advanced for any effects in cognition, and that the complexity of the model was too severe, as per the worsened cerebrovascular function. We therefore proceeded to verify this conclusion in the chapter that follows using *in vivo* hydroxyl-methyl coA enzyme reductase inhibitor, simvastatin in young A/T mice.

Here, the choice to use BBB-penetrant simvastatin (40mg/kg/day) was incited by its superior efficacy over spatial learning and memory in adult (treated for 3 months, ~6 months old at endpoint) but not aged (treated for 6 months, ~12 months old at endpoint) APP mice, along with its capacity in normalizing the vascular deficits at both ages. Furthermore, the reported beneficial effects of statins in AD also prompted us to investigate neuronal and cognitive parameters in young A/T mice (treated for 3 months, ~6 months old at endpoint). We found that simvastatin was ineffective at improving learning and memory in A/T mice, despite a doubled treatment duration compared to APP mice. The decreased hemodynamic response to whisker stimulation in A/T mice was not normalized by treatment, and simvastatin not only failed to restore cerebrovascular reactivity in A/T mice, but rather exacerbated the dilatory deficit. Based on this data, we concluded that the concurrent upregulation of Aβ and TGF-β1 in A/T mice may represent a late stage of the pathology, at which point simvastatin is not efficacious.

Chapter 4

Lack of therapeutic benefit on spatial memory and cerebrovascular function by simvastatin in the Alzheimer's disease APP/TGF-β1 mouse model

Panayiota PAPADOPOULOS, Xin-Kang TONG, and Edith HAMEL

Abstract

Cognitive and cerebrovascular deficits are two manifestations of Alzheimer's disease (AD) to consider when aiming for effective therapy. Here, we used bitransgenic A/T mice overexpressing a mutated form of the human amyloid precursor protein ($APP_{Swe,Ind}$) and a constitutively active form of transforming growth factor-β1 (TGF), which recapitulate several AD cerebrovascular and cognitive deficits, to evaluate the therapeutic efficacy of simvastatin. Simvastatin (40mg/kg/day) failed to improve learning and memory in 6 and 9 month-old A/T mice treated for 3 and 6 months, respectively. The decreased hemodynamic response to whisker stimulation in A/T mice was not normalized by treatment, and simvastatin failed to restore cerebrovascular reactivity in A/T mice, but rather exacerbated the dilatory deficit. Simvastatin significantly lowered brain levels of insoluble amyloid-beta (Aβ) peptide and Aβ plaque load, without altering the protein levels of Aβ-degrading enzymes neprilysin and β-site-APP cleaving enzyme (BACE). Similarly, the decreased baseline levels of memory-related protein Egr1 in the CA1 hippocampal area were not normalized by simvastatin. In brain vessels, proteins involved in fibrosis or synthesis of the vasodilator nitric oxide were unaltered by treatment. Together, these findings demonstrate that the therapeutic benefits of simvastatin in A/T mice are not as readily obtained as in APP mice (Li et al., 2006, Tong et al., 2012). Since A/T mice combine the cerebrovascular and neuronal alterations of AD, these findings may reflect the complexity that one faces when attempting to counter the disease in AD patients, as suggested by the divergent results obtained with statins.

Introduction

Memory loss is an early symptom of Alzheimer's disease (AD), the most common form of progressive dementia with increasing age. Post-mortem, the AD brain is characterized by amyloid-beta (Aβ) plaques, neurofibrillary tangles, synaptic loss, glial cell activation and a vascular pathology (Zlokovic, 2011). The latter is defined by cerebral amyloid angiopathy (CAA) and thickening of the vascular basement membrane due to accumulation of extracellular matrix proteins, a fibrotic process imputed to increased levels of transforming growth factor-beta 1 (TGF-β1) (Wyss-Coray et al., 2000). AD is also associated with a chronic cerebral hypoperfusion and decreased brain metabolism (Iadecola, 2004).

Statins have demonstrated promise in decreasing the incidence of AD among statin-prescribed patients (Jick et al., 2000, Wolozin et al., 2000, Yaffe et al., 2002, Cramer et al., 2008, Haag et al., 2009). Statins positive effects on cognition in mild to moderate AD patients (Sparks et al., 2005) and normocholesterolemic AD patients (Simons et al., 2002) have been imputed to their pleitropic effects rather than their ability to lower cholesterol. In support of these reported benefits in man, studies in AD mouse models showed that statins normalized several AD hallmarks such as impaired brain glucose metabolism, glial activation, cerebrovascular dysfunction and most importantly, memory deficits depending on age and duration of treatment (Li et al., 2006, Tong et al., 2009, Kurata et al., 2011, Tong et al., 2012). However, studies in AD patients have generated mixed results (Arvanitakis et al., 2008, Butterfield et al., 2011, Sano et al., 2011), and it was argued that statins may exert benefits only if administered early in the disease process (Sano et al., 2011, Shepardson et al., 2011b, a, Sparks, 2011). These

studies point to the need for a better understanding of statin efficacy in AD mouse models that recapitulate the complexity of the human disease.

Here, we investigated the therapeutic value of simvastatin in bitransgenic mice that display concurrent overexpression of the human amyloid precursor protein ($hAPP_{Swe,Ind}$, line J20) and a constitutively active form of TGF-β1 (line T64) (A/T mice), thereby mimicking the Aβ-associated neuronal deficits and the comorbid TGF-β1-induced AD cerebrovascular pathology (Wyss-Coray et al., 2000, Grammas and Ovase, 2002, Ongali et al., 2010). We assessed the capacity of simvastatin (40mg/kg/day) in rescuing spatial learning and memory in adult A/T mice (3 month-old, tested after 3 and 6 months of treatment), and the evoked CBF responses to increased neuronal activity as an index of functional hyperemia. Cerebral arterial reactivity, astroglial and microglial activation, amyloidosis and proteins regulating vascular structure or function were evaluated at endpoint (9 month-old A/T mice). The data show that simvastatin, in contrast to its high efficacy in singly APP mice (Li et al., 2006, Tong et al., 2012), failed to rescue cerebrovascular and memory deficits in A/T mice even after extended treatment (6 months). Together, these findings highlight the importance of testing potentially promising therapies in experimental models that recapitulate multiple facets of AD as they may better predict efficacy in a disease as complex as AD.

Methods

Animals. Bitransgenic A/T mice (Ongali et al., 2010) concomitantly overexpress a mutated form of the human amyloid precursor protein ($APP_{Swe,Ind}$) driven by the platelet-derived growth factor β promoter (line J20, (Mucke et al., 2000), and the constitutively active form of TGF-β1 driven by glial fibrillary acidic protein (GFAP) promoter on a

C57BL/6J background (line T64, (Wyss-Coray et al., 1995). Transgene expression was confirmed by touchdown PCR using tail-extracted DNA (Wyss-Coray et al., 1995). Three-month-old A/T mice and wildtype (WT) littermates (body weight, ~30g) were treated or not for 6 months (9 months old at endpoint) with simvastatin (40mg/kg/day in water). Males and females were randomly and equally assigned in each group. Water and chow were available *ad libitum*. There was no significant body weight change over time (in g: WT: 13.8±2.0, WTsv: 10.0±1.7, A/T: 9.6±1.3, A/Tsv: 7.1±2.4), or total blood cholesterol levels: (in mmol/L: WT: 4.25±0.07, WTsv: 4.19±0.04, A/T: 4.20±0.05, A/Tsv: 4.19±0.05) among all groups as measured in blood collected from the tail tip with a commercial cholesterol meter Accutrend® GC meter (Roche Diagnostic, Laval, Canada). Animal use was in accordance to the Animal Ethics Committee of the Montreal Neurological Institute, and abided by the guidelines of the Canadian Council on Animal Care.

Morris watermaze. After 3 and 6 months of treatment, mice were tested in the Morris watermaze. The first test was performed at the age of 6 months: mice were trained to locate a visible platform during a 3-day session (days 1-3, familiarization session), followed by a 5-day-hidden platform training session (platform submerged ~1cm below the surface of the water, learning phase of the test, days 4-8) in a 1.4 m circular pool filled with opaque water (18±1°C). The location of the platform and of the distal visual cues was changed between the two training sessions, as previously described (Deipolyi et al., 2008). Three trials were performed on each day of the visible (60s each) and hidden (90s each) platform sessions, with a 45min inter-trial interval. Mice that passed the time limit were directed to the platform, and all mice were given 10s on the platform on the

first day of each training session. Spatial memory was evaluated 24h after the last hidden platform session in the probe trial (day 9, platform removed, 60s). Performances were compared using escape latencies (days 4-8) and percent time spent and distance traveled, as well as the number of crossings over the previous location of the platform in the probe trial (day 9). All parameters together with swim speed were recorded with the 2020 Plus tracking system and Water 2020 software (Ganz FC62D video camera; HVS Image, Buckingham, UK). The visible platform session allowed to control for visual acuity, motor ability and motivation to perform the task. Mice were kept warm throughout the sessions with a heating lamp and subsequently left to rest for 2 days before further experiments resumed. Three months later, the same mice underwent a second Morris watermaze. As the mice were already familiar with the task, only the hidden platform session was performed (day 1-5), whereby the location of the platform and that of the distal visual cues differed from those used in the first Morris watermaze test. A probe trial was performed 24h later (day 6).

Cerebral blood flow (CBF). CBF increases during whisker stimulation were measured using laser Doppler flowmetry (Transonic Systems Inc, Ithaca, NY). Mice anesthetised with ketamine (85 mg/kg, intramuscularly (i.m.); Bioniche, Belleville, ON) and xylazine (3 mg/kg, Haver, Etobicoke, ON) were fixed in a stereotaxic frame for thinning the bone to translucency over the left barrel cortex with a dental drill. Whiskers on the right snout were stimulated with an electric toothbrush (8-10 Hz, 4-5 stimulation blocks of 20s each interspaced by ~30 sec). Increases in CBF were recorded with a laser probe positioned on the thinned bone over the barrel cortex. Body temperature was monitored and kept stable at 37°C with a heating pad throughout the experiment. Results are expressed as percent

increase over baseline and represent averages of all evoked CBF responses acquired during the stimulation blocks. The identity of the mouse was unknown to the experimenter. Total duration of experiment was ~20min/mouse.

Tissue collection and preparation. Upon completion of the *in vivo* experiments, a subset of mice was sacrificed by cervical dislocation for reactivity studies of the posterior cerebral artery (PCA) (see below). The remaining arteries of the circle of Willis together with their small branches and the attached pial membrane were removed, together with the cortex and hippocampus of one hemibrain. These tissues were frozen on dry ice and stored at -80°C for subsequent ELISA and Western blot experiments. The other hemibrain was immersion-fixed overnight in 4% paraformaldehyde (PFA; in 0.1 M phosphate buffer (PB), pH 7.4, 4°C), cryoprotected overnight (30% sucrose 0.1 M PB, 4°C), and then frozen in isopentane and stored at -80°C until cutting into free-floating thick sections (25 μm) on a freezing-microtome. The other subset of mice was anesthetised with pentobarbital (80 mg/kg, i.p.) and perfused transcardially (4% PFA solution at 4°C, ~200ml/mouse). One brain hemisphere was used for thick-sections as described above, whereas the other was embedded in paraffin for sectioning of thin (5 μm-thick) brain sections.

Vascular reactivity. PCA segments (40–70 μm average intraluminal diameter) were cannulated, pressurized (60 mmHg) and superfused with Krebs solution (37°C) for measurement of vasomotor function using online videomicroscopy (Tong et al., 2005). Vessels were pre-constricted sub-maximally with serotonin (5-HT; 2×10^{-7}M) for the measurement of dilatory responses to acetylcholine (ACh; 10^{-10}-10^{-5}M), calcitonin gene-related peptide (CGRP; 10^{-10}-10^{-6}M), and the NO donor sodium nitroprusside (SNP,

10^{-10}-10^{-4}M). Contractile responses to endothelin-1 (ET-1; 10^{-10}-10^{-6} M) and 5-HT (10^{-10}-10^{-6} M), and the tonic production of NO evaluated under inhibition of nitric oxide synthase (NOS) with Nω-nitro-L-arginine (L-NNA; 10^{-5} M, for 35min) were measured on vessels at basal tone. Vessel diameter changes were expressed in percentage relative to either the basal or pre-constricted tone, and plotted as a function of agonist concentration or time for L-NNA superfusion. The maximal vessel response (EA_{max}) and half maximal effective concentration [EC_{50} value or pD_2=−(log EC_{50})] were used to compare agonist's efficacy and potency, respectively.

ELISA. An enzyme-linked immunosorbent assay (ELISA) (BioSource International) was used to measure the levels of insoluble $A\beta_{1-40}$ and $A\beta_{1-42}$ species in cortex and hippocampus from treated- and untreated-A/T mice. Tissue was homogenized by sonication (~20s in 20mM Tris buffer containing 1 mM EDTA, 1 mM EGTA, 250 mM sucrose, and protease inhibitors) and centrifuged (100,000 *g*, 60 min, 4°C). The pellet containing insoluble Aβ was then sonicated (~20s) in 70% formic acid (FA) and centrifuged (100,000 *g*, 60min, 4°C). The Aβ levels were measured as per the manufacturer (BioSource International), and were expressed as micrograms per gram (μg/g) of protein in formic acid (FA)-insoluble fraction.

Western blot. The levels of total soluble Aβ species were measured in protein extracts (20 μg) from cerebral cortex and hippocampus loaded onto a 15% Tris/tricine SDS PAGE, transferred to nitrocellulose membranes and detected with a mouse anti-$A\beta_{1-16}$ antibody (6E10, 1:1000, Covance, Emeryville, CA, USA). The same protein extracts were used to measure the levels of the anti-β-site APP cleaving enzyme 1 (BACE) and neprilysin (1:2000; Santa Cruz Biotechnology and Chemicon, respectively).

Cerebrovascular proteins (12-15 μg) were loaded onto 10% SDS PAGE and probed with goat anti-connective tissue growth factor (CTGF; 1:400; Abcam), rabbit anti-vascular endothelial growth factor (VEGF; 1:500; Santa Cruz Biotechnology), mouse anti-actin (1:8000; Santa Cruz Biotechnology A5441, Santa Cruz, CA, USA), or anti-endothelial nitric oxide synthase (eNOS; 1:500; BD Transduction) (for details, (Tong et al., 2009)). Blots were incubated (1h) with horseradish peroxidase-conjugated secondary antibodies (1:2000; Jackson ImmunoResearch, West Grove, PA, USA) and visualized with Enhanced ChemiLuminescence (ECL Plus kit; Amersham, Baie d'Urfé QC, Canada) using phosphorImager (Scanner STORM 860; GE Healthcare, Baie d'Urfé QC, Canada). Bands were quantified using ImageQuant 5.0 (Molecular Dynamics, Sunnyvale, CA, USA) using actin for loading normalization.

Immunohistochemical and histochemical stainings. Thick sections were immunostained with a rabbit anti-glial fibrillary acidic protein (GFAP) antibody, a marker of astrocyte activation (1:1000; DAKO), visualized with a donkey anti-rabbit cyanin 2 (Cy2)-conjugated secondary antibody (1:400; Jackson ImmunoResearch, West Grove, PA, USA). Thioflavin S (1%, 8 min) staining of mature, dense core Aβ plaques was also performed on thick sections. Dewaxed paraffin sections were used for immunostaining of diffuse and dense-core Aβ plaques (6E10, 1:2000), the memory-linked immediate early gene Egr-1/Zif268 (1:200; Santa Cruz, Santa Cruz, CA, USA) and the marker of microglial activation ionized calcium binding adaptor molecule 1 (Iba-1, 1: 300; Wako Chemicals, Cedarlane). These were detected with species-specific biotinylated IgGs (1h30, Vector lab) and the AB Complex (1h15, Vector Labs), and the

reaction visualized with 3,3'-diaminobenzidine (DAB, brown precipitate, 6E10, Iba-1, Vector labs) or the SG kit (blue-gray precipitate, Egr-1, Vector Labs).

Data analysis. Brain sections (2 to 3 sections/mouse, 4 mice/group) were observed under a Leitz Aristoplan light microscope either using bright field or epifluorescence and an FITC filter (Leica, Montréal, QC, Canada). Digital pictures were taken with a Nikon camera (Coolpix 4500, Montréal, QC, Canada) and used for quantification using MetaMorph 6.1r3 (Universal Imaging, Downingtown, PA, U.S.A). The areas of interest (cingulate and somatosensory cortex, hippocampus) were manually outlined to quantify the percent area occupied by GFAP-, thioflavin S-, and 6E10-immunostaining. The number of immunopositive Egr-1 nuclei in the CA1 area of the hippocampus was counted in a 0.062mm^2 surface area. The intensity of Egr-1-positive nuclei in the CA1 region of the hippocampus was measured as total gray level using MetaMorph. The surface area of individual Iba-1-positive microglial cells and extensions (1 section/mouse, ~20 microglial cells/section, 4 mice/group) was quantified with ImageJ (Image Processing and Analysis in Java, NIH) and expressed as a percent of WT.

Statistical analysis. Data are expressed as means ± SEM. They were analyzed by two-way analysis of variance (ANOVA) with genotype and treatment as the two variables followed by Newman-Keuls post-hoc multiple comparison test (Statistica Academic, Tulsa, OK, USA). Newman-Keuls's *p* values were indicated when the interaction or at least one factor was significant. Student's t-test was used when two groups were compared (GraphPad Prism 4, San Diego, CA, USA). A $p \leq 0.05$ was considered significant.

Results

Simvastatin and spatial memory

A/T mice were tested twice in the Morris watermaze (test 1: after 3 months of treatment; test 2: at endpoint after 6 months treatment). In test 1, all animals located the visible platform with ease ruling out visual or motor disabilities, and any possible lack of motivation. During the 5 days of hidden platform training (days 4-8), A/T mice exhibited learning impairments as depicted by their increase escape latencies relative to age-matched WT controls (Figure 1A). This deficit, however, did not reach statistical significance despite a clear trend on days 7 and 8. Performances during the probe trial (day 9) indicated memory deficits of A/T mice, as illustrated by the decreased percent time spent and distance traveled in the target quadrant, as well as the smaller number of platform crossings (Figure 1B). These deficits occurred despite unaltered swim speed, in agreement with previous studies (Ongali et al., 2010). In test 2, only the 5 days of hidden platform were conducted. A/T mice were significantly impaired in both the learning and memory phases of the test (Figure 1C, D). Simvastatin failed to improve learning and memory performance in A/T mice treated for either 3 (Figures 1A, B) or 6 (Figures 1C, D) months. These findings contrast with the previously reported benefit of simvastatin in singly APP mice (Li et al., 2006, Tong et al., 2012), and indicate that memory deficits in A/T mice are not as readily rescued, which suggests that the concurrent increases in Aβ and TGF-β1 in brain parenchyma added a level of complexity in the cognitive deficits of A/T mice compared to singly APP mice.

Simvastatin and baseline protein levels of Egr-1

The immediate early gene Egr-1 is critical for normal memory function. Its baseline (Dickey et al., 2003, Tong et al., 2012) or induced (Blanchard et al., 2008) mRNA or protein levels are decreased at baseline in APP mice. Consistent with these findings, baseline levels of Egr-1 in the CA1 area of the hippocampus were lower in A/T mice compared to WT controls, as shown by the significantly decreased number and weaker staining intensity of Erg-1 immunostained nuclei (Figure 2). Recently, upregulation of baseline levels of Egr-1 in the CA1 area was found to correlate with memory improvements in adult APP mice treated with simvastatin whereas aged APP mice that did not recover memory did not display normalization of Egr-1 protein levels (Tong et al., 2012). Correspondingly, we found that simvastatin failed to improve Egr-1-immunoreactivity in CA1 neurons of A/T mice with persistent memory deficits (Figure 2).

Simvastatin decreased insoluble Aβ species and Aβ plaque load

In line with previous studies (Ongali et al., 2010), A/T mice featured increased levels of Aβ species and Aβ plaque load (Figure 3). Simvastatin significantly reduced the levels of insoluble $A\beta_{1-40}$ and $A\beta_{1-42}$ in cortex and hippocampus of A/T mice, as measured by ELISA (Figure 3A). Accordingly, total Aβ plaque load determined by 6E10 immunolabeling on thin sections was significantly decreased in cortex and hippocampus (-59% and -53%, $p<0.05$, respectively) (Figure 3D, E), whereas the small decreases in dense-core Aβ plaques detected with thioflavin-S staining did not reach significance in either brain region (Figure 3B, C). The levels of soluble Aβ species measured by Western blot remained unchanged after simvastatin treatment (Figure 3F), including the 4kDa

band of monomeric Aβ. The protein levels of BACE and Aβ-degrading enzyme neprilysin were similarly not altered by simvastatin (Figure 3G). Together, these results indicate that simvastatin promoted a decrease in parenchymal amyloidosis in A/T mice, in line with some (Shinohara et al., 2010, Tamboli et al., 2010), but not all studies (Li et al., 2006, Tong et al., 2009, Tong et al., 2012) in APP mice.

Simvastatin effects on neurovascular coupling upon whisker stimulation

Impaired functional hyperemia upon sensory activation, indicative of an imbalance between neuronal demand and blood supply to the activated brain area, has been reported in A/T mice of different ages (Ongali et al., 2010). We confirmed that the CBF response to whisker stimulation was significantly impaired in A/T mice at 9 months of age compared to WT controls, and we found that simvastatin treatment did not improve this deficit (Figure 4). Surprisingly, there was a slight although significant deterioration in the evoked CBF response in simvastatin-treated WT mice compared to untreated controls (WT: 22.0±1.9% vs WTsv: 16.6±1.2%, $p<0.05$), an effect that was not observed in previous cohorts of adult or aged WT mice treated with simvastatin (Tong et al., 2009, Tong et al., 2012).

Simvastatin and neuroinflammation

Astrocytes and microglia are critical in orchestrating the immunity of the brain in response to pathogenic molecules such as Aβ (Rivest, 2011). A/T mice displayed increased GFAP immunoreactive material in cortex and hippocampus compared to WT ($p<0.001$), and simvastatin did not reduce such astroglial activation in either region (Figure 5). Microglia was also highly activated in A/T mouse brain as evidenced by the marked swelling of microglial cell bodies and the large extent of their ramifications

(Figure 6). Simvastatin failed to exert any protective effects in minimizing microglial activation in both the cortex and the hippocampus of A/T mice (Figure 6).

Simvastatin, cerebrovascular reactivity and fibrosis

As reported before (Ongali et al., 2010), cerebral arteries of A/T mice featured intact contractile responses, as shown here for ET-1, but were significant impaired in their dilatory capacity compared to their control counterparts, as determined for ACh- and CGRP-induced dilatations (Figure 7, Table 1). A small decrease in baseline NO synthesis was also evidenced by the smaller diameter decrease induced by NOS inhibition with L-NNA superfusion. However, dilatory responses to the NO donor SNP were intact in A/T mice, indicative of a preserved capacity of the smooth muscle cells to dilate (Figure 7). Simvastatin fully normalized constitutive NO-mediated tone by the end of L-NNA incubation time (Figure 7), and did not affect the contractile responses induced by ET-1. However, simvastatin significantly worsened the dilatory deficits to ACh and CGRP. Indeed, the dilatory responses were completely abolished at low agonist concentrations and reversed to small contractions at higher concentrations (Figure 7). Likewise, the response to the NO donor SNP was altered in simvastatin-treated A/T mice and resulted in constriction at low concentrations that tended towards dilatation at higher concentrations (Figure 7). Simvastatin did not alter the arterial responses in WT mice (Figure 7).

In search for an explanation for the aggravated cerebrovascular function in simvastatin-treated A/T mice, we assessed simvastatin effects on markers of vascular fibrosis and on the NO synthesizing enzyme eNOS in protein extracts of pial vessels. We found that the levels of these proteins did not differ between 9 month-old A/T mice and

WT controls, and that simvastatin, despite its capacity to worsen vasomotor function, did not alter any of these proteins (Figure 8).

Discussion

We report the failure of simvastatin to salvage mnemonic, hemodynamic and neuroinflammatory function in adult A/T mice. Interestingly, the persistent learning and memory deficits occurred despite significant decreases in insoluble Aβ species and in 6E10 immunodetected Aβ plaque load, but with persistent elevated soluble Aβ species. The results also show that simvastatin had no beneficial effects on cerebrovascular function in A/T mice, but rather exerted aggravating effects on vasodilatory function. These findings highlight the potential limitations for simvastatin therapy in AD patients with a pathology not limited to Aβ but also encompassing TGF-β1-mediated inflammation, cerebrovascular fibrosis and neuronal alterations.

TGF-β1 as an exacerbating factor in memory

Unlike our recent findings in adult APP mice (Tong et al., 2012), simvastatin did not protect spatial learning and memory in adult A/T mice despite extension of treatment duration to 6 months. These findings suggest that chronic upregulation of TGF-β1 added a level of complexity to the Aβ-mediated neuronal pathology and rendered A/T mice resistant to a pharmacological therapy proven effective in singly APP mice (Li et al., 2006, Tong et al., 2012). Interestingly, while neuroprotective effects of TGF-β1 in AD mice or patients have been reported (Chao et al., 1994, Tesseur and Wyss-Coray, 2006, Tesseur et al., 2006, Caraci et al., 2008), it has also been identified as an important contributor to AD pathogenesis (van der Wal et al., 1993, Flanders et al., 1995, Wyss-Coray et al., 1997, Wyss-Coray et al., 2000). Particularly, chronic increases of TGF-β1

have been associated with age-related reductions of hippocampal neurogenesis with up to a 60% decrease in the number of immature neurons (Buckwalter et al., 2006). Although newly-born neurons recruited into the existing neuronal circuits of the adult dentate gyrus only account for ~10% of the granule cell population (Imayoshi et al., 2008), they substantially contribute to hippocampal-dependent learning and memory processes (Kee et al., 2007, Dupret et al., 2008, Deng et al., 2009). A similar causal relationship between Aβ-induced neurogenesis and memory deficits has been shown in various AD mouse models (Haughey et al., 2002, Drapeau et al., 2003, Donovan et al., 2006, Verret et al., 2007, Lazarov et al., 2010, Valero et al., 2011), This interrelationship was further highlighted by improved memory following neurogenesis-targeted pharmacological stimulation in AD mice (Chen et al., 2000b, Butovsky et al., 2006, Rockenstein et al., 2006, Fiorentini et al., 2010). TGF-β1 upregulation did not induce spatial memory impairments in singly TGF mice (Papadopoulos et al., 2010, Nicolakakis et al., 2011) nor did it result in more severe learning and memory deficits in the A/T mouse model compared to age-matched APP mice (data not shown). Hence, TGF-mediated inhibition of adult neurogenesis may not be sufficient to harm memory processes, but may act as an exacerbating factor to the already impaired neurogenesis by Aβ in AD mice (Lazarov et al., 2010, Valero et al., 2011), reducing neurogenesis in A/T mice to levels unresponsive to pharmacotherapy.

Indeed, simvastatin has been shown to promote neurogenesis and improve cognitive function through activation of the PI3k/Akt pathway (Wu et al., 2008) in experimental models of stroke (Chen et al., 2003, Karki et al., 2009) and traumatic brain injury (Lu et al., 2007, Wu et al., 2008). Simvastatin-mediated PI3k/Akt pathway

activation was also suggested as a possible mechanism for memory normalization in APP mice (Li et al., 2006, Tong et al., 2012). Since the PI3k/Akt signaling cascade is also activated by TGF-β1 in the hippocampus (Zhu et al., 2004), it may have been overstimulated in A/T mice due to chronic TGF-β1 overproduction, which might have prevented the neuroprotective effects of simvastatin. Such hypothesis would be compatible with simvastatin's inability to upregulate baseline protein levels of the memory-related immediate early gene Egr-1 in A/T mice, Egr-1 being downstream from the PI3K-Akt signaling cascade (Jones et al., 2001, Bozon et al., 2003, Davis et al., 2003). Baseline Egr-1 was upregulated in the CA1 area of simvastatin-treated APP with preserved memory (Tong et al., 2012). Moreover, Egr-1 was induced in new granule neurons of the dentate gyrus of adult mice after testing for remote spatial memory (Trouche et al., 2009), further reinforcing the notion that incorporation of these neurons into functional hippocampal networks is required for spatial memory processing.

Insoluble Aβ reduction and persistent memory deficits

Simvastatin failed to normalize cognitive performance despite significantly reduced brain levels of insoluble Aβ and Aβ plaque load, in agreement with previous studies (Fassbender et al., 2001, Petanceska et al., 2002). However, this finding is not undisputed since other simvastatin studies found cognitive improvement in Tg2576 (Li et al., 2006) and $APP_{Swe/Ind}$ (Tong et al., 2012) mice, as well as in asymptomatic middle-aged adults at risk for AD (Carlsson et al., 2008), independently from any Aβ plaque load reductions. Cognitively intact elderly individuals having equivalent Aβ plaque densities as AD patients further support the notion that Aβ plaques may be necessary for initiation but not maintenance of progressive neurodegeneration (Davis et al., 1999). It could be argued

that the sustained high levels of soluble Aβ species in simvastatin-treated A/T mice may explain their persistent memory deficit as Aβ oligomers are the most harmful to neuronal and synaptic function (Mucke et al., 2000, Lesne et al., 2008). Yet, simvastatin-treated APP mice recovered memory without any reduction in soluble Aβ (Li et al., 2006, Tong et al., 2012), and aged Tg2576 mice lacking the catalytic subunit of NADPH oxidase (Park et al., 2008) or treated with COX-2 inhibitors (Kotilinek et al., 2008) had preserved memory despite high levels of soluble and insoluble Aβ, further pointing to the dichotomy between memory impairment and amyloidosis.

Simvastatin and neuroinflammation

The abnormal production of pro-inflammatory cytokines and chemokines by glial cells can disrupt nerve terminal activity causing dysfunction and loss of synapses, and eventually memory decline (Popovich and Longbrake, 2008, Frank-Cannon et al., 2009, Ferretti and Cuello, 2011, Rao et al., 2012). Furthermore, astrocytes could be activated by TGFβ-1 to generate more Aβ further aggravating the pathology (Burton et al., 2002). Thus, treatments directed at controlling the glial cell activation may be valuable to counter AD neurodegeneration. In A/T mice, simvastatin did not display anti-inflammatory properties as it was ineffective in silencing Aβ plaque-associated microglia and astrocytes. This contrasted with our previous study in APP mice (Tong et al., 2009), and may have thus contributed to the persistent memory deficit in treated-A/T mice. Persistent glial activation may also account for the drug's failure to normalize the neurovascular coupling response to whisker stimulation that highly depends on astrocytes for the synthesis and release of vasoactive messengers (Koehler et al., 2009).

Simvastatin and cerebrovascular reactivity

We anticipated normalization of cerebrovascular function with simvastatin based on its significant benefits in adult and aged APP (Tong et al., 2009, Tong et al., 2012) or TGF (Tong et al. *in preparation*) mice. The most surprising finding was that incubation of cerebral arteries from simvastatin-treated A/T mice with the vasodilators ACh and CGRP induced no response or a small constriction at high concentrations. This unexpected response indicated a deleterious effect of simvastation of receptor-mediated vasodilatory responses through both endothelial and smooth muscle cells. This finding, however, was not exclusive to simvastatin as pioglitazone-treated A/T mice similarly displayed worsened cerebrovascular dilatory function (Papadopoulos et al. *in preparation*, Chapter 2 of this thesis), an effect imputed to the ability of pioglitazone to dilate blood vessels through both endothelial and smooth muscle mechanisms. Interestingly, simvastatin also can elicit NO-mediated dilations via direct activation of soluble guanylyl cyclase (sGC) in retinal arteries (Nagaoka et al., 2007), and it may thus have acted as a competitive agonist for the ACh-mediated NO signalling cascade thereby chronically exhausting the sGC/cGMP pathway. The vasoconstriction observed during incubation with the NO donor SNP further supports a disruption of sGC signalling as it required higher concentrations of SNP to get activated. Whether similar effects of simvastatin on K^+ channels that mediate the CGRP-induced dilation (Vedernikov et al., 2002) are involved in A/T mouse diseased vessels will require further investigations. Upregulation of the protein levels of the NO synthesizing enzyme eNOS has been reported in brain of APP mice treated with simvastatin (Li et al., 2006). We did not find such an effect in A/T mice, further pointing to the complexity of their cerebrovascular pathology.

Conclusion

Simvastatin efficacy on neuronal pathways in APP mice is protective rather than restorative (Tong et al., 2012) and simvastatin therapy in man has been recommended at early stages of the disease (Arvanitakis and Knopman, 2010, Shepardson et al., 2011b). Our results suggest that the concurrent upregulation of Aβ and TGF-β1 in A/T mice may represent an advanced stage of the disease, which is beyond the therapeutic window for simvastatin efficacy (Li et al., 2010a, Butterfield et al., 2011), when Aβ and TGF-β1 interactions have become irreversible and resistant to therapy. Our findings further highlight the importance of studying drug efficacy in animal models that reproduce multiple aspects of the human AD pathology for a reliable screening of potential new treatment strategies.

Acknowledgements: This work was supported by the Canadian Institutes of Health Research (CIHR grant MOP-84275 to EH) and a Jeanne Timmins Costello Fellowship (PP). We are grateful to Dr. Lennart Mucke (Gladstone Institute of Neurological Disease and Department of Neurology, UCSF, CA) and the J. David Gladstone Institutes for the $hAPP_{Swe,Ind}$ and TGF-β1 transgenic mouse breeders.

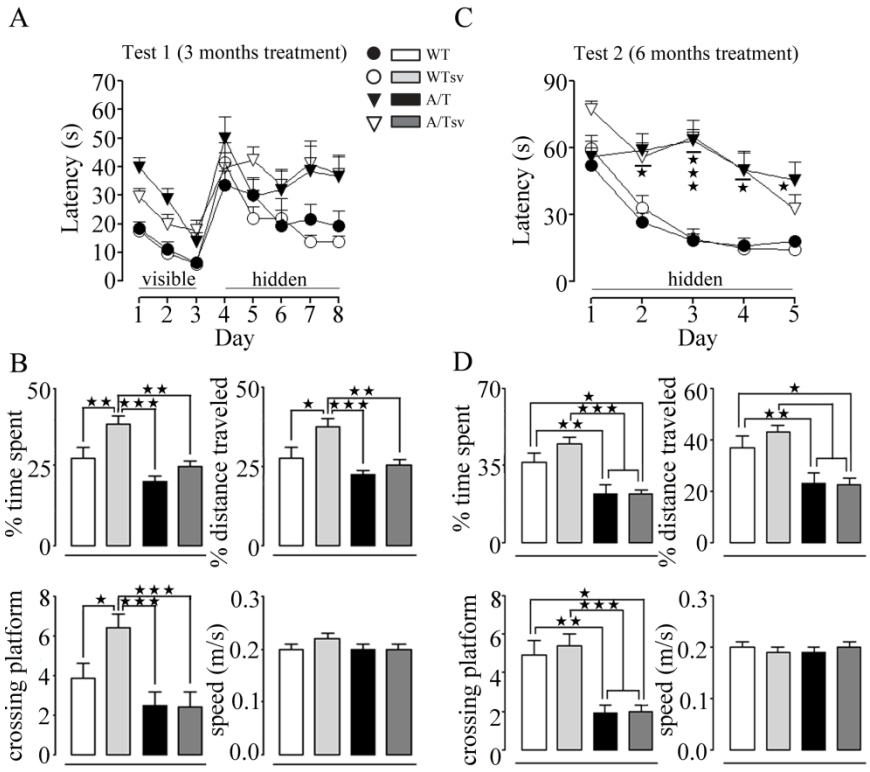

Figure 1. Simvastatin (SV) did not improve spatial learning and memory in A/T mice. ***A,*** A/T mice (6 month-old, ▼) had no deficit in the visible platform session, but displayed impaired learning during the hidden-platform testing compared to wild-type (WT) littermates (●). Simvastatin did not improve the learning deficit in A/T mice (treated for 3 months, ▽) and did not affect performance in WT mice (○). ***B,*** A/T mice treated for 3 months displayed significant deficit in spatial memory as indicated by the reduced percent time spent and distance travelled in the target quadrant, and fewer crossings over the previously located platform during the probe trial. ***C,*** Extended simvastatin treatment (6 months, ▽) did not improve the learning deficit in A/T mice (9 month-old, ▼) and did not affect that of WT mice (○). ***D,*** Spatial memory deficits during the probe trial were not recovered even after this extended simvastatin treatment. Error bars represent SEM (n=9-13 mice/group). ★$p<0.05$, ★★$p<0.01$, ★★★$p<0.001$ using two-way ANOVA followed by Newman-Keuls post-hoc test.

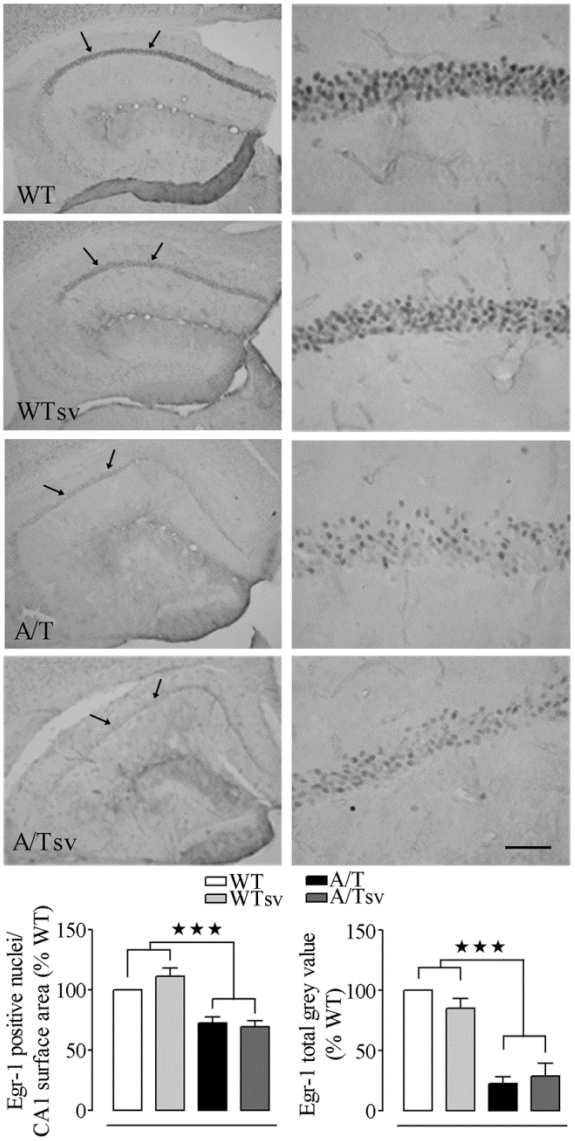

Figure 2. Simvastatin (SV) did not upregulate baseline Egr-1 protein levels in A/T mice. Egr-1 immunopositive nuclei were significantly decreased in the CA1 area of the hippocampus of A/T mice relative to WT controls (delineated by arrows in left panels and magnified in right panels). Simvastatin failed to normalize the number and intensity of Egr-1-positive nuclei even after 6 months treatment (n=4 mice/group). ★★★$p<0.001$ using two-way ANOVA followed by Newman-Keuls post-hoc test. Scale bar, 50μm.

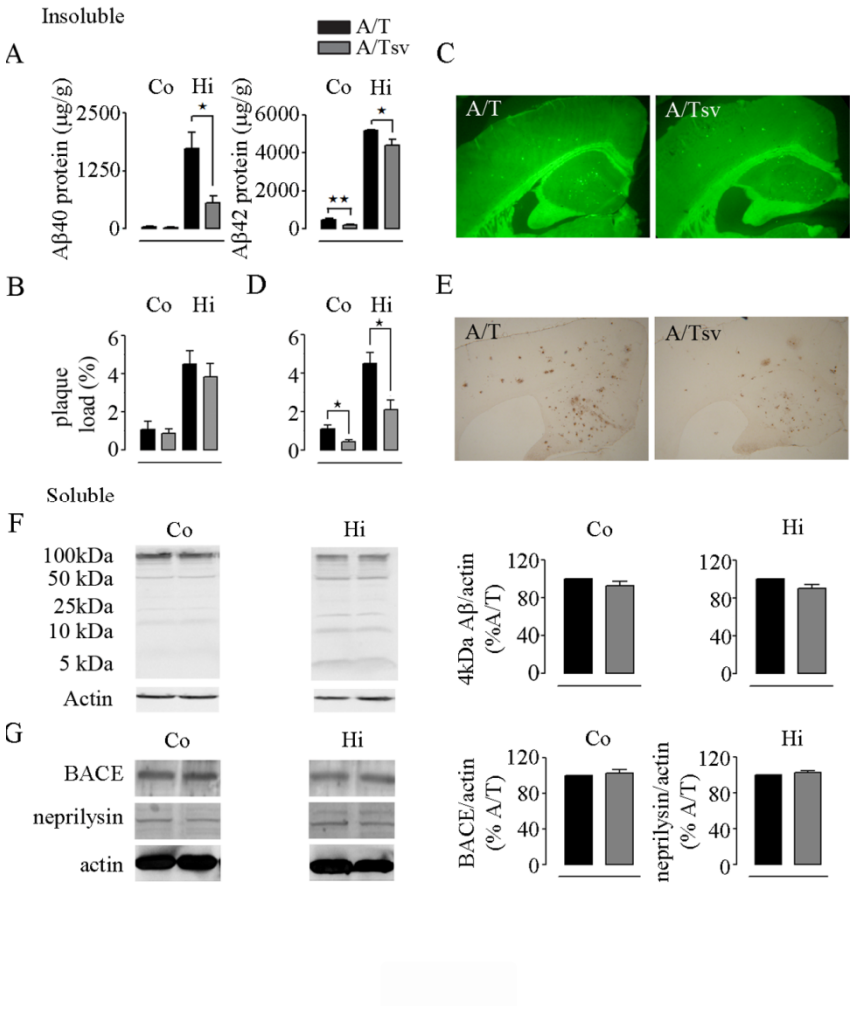

Figure 3. Simvastatin (SV) selectively reduced insoluble Aβ levels and Aβ plaque load in A/T mice. ***A,*** The levels of insoluble $A\beta_{1\text{-}40}$ and $A\beta_{1\text{-}42}$ were significantly reduced in simvastatin- treated A/T mice, as assayed in cortex and hippocampus by ELISA. ***B,*** Thioflavin S-stained dense-core Aβ plaque load was unaltered by simvastatin in cortex and hippocampus of A/T mice (***C)***. ***D,*** However, diffuse and dense-core Aβ plaques immunostained with the 6E10-antibody in 5μm-thick paraffin sections (***E***) were significantly reduced in simvastatin-treated A/T mice (n=4 mice/group). ***F,*** Western blot analysis with 6E10 antibody revealed no effect of simvastatin on soluble Aβ species in cortex and hippocampus of A/T mice. ***G,*** Similarly, BACE and neprilysin protein levels were not altered by treatment, as measured by Western blot in cortex and hippocampus of A/T mice compared to their treated counterparts. Actin was used as a reference for loading (n=4 mice/group). Error bars represent SEM (n=4 mice/group). ★$p<0.05$, ★★$p<0.01$ for comparison to A/T mice using two-way ANOVA followed by Newman-Keuls post-hoc test.

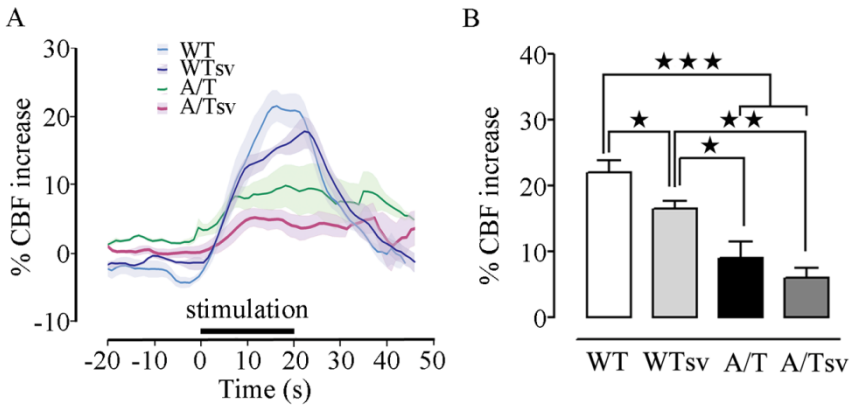

Figure 4. Simvastatin (SV) did not restore the stimulus-evoked CBF increase in A/T mice. ***A,*** Traces of averaged evoked CBF responses acquired before, during and after whisker stimulation (WT: blue, WTsv: purple, A/T: green and A/Tsv: pink). ***B,*** Histogram representing the maximum values of the evoked CBF responses for each group (4-5 stimulations), as measured by LDF. The impaired hyperemic response to whisker stimulation in A/T mice was not rescued by simvastatin (n=4 mice/group). Values represent the percent increase of CBF response relative to baseline. Error bars represent SEM. ★$p<0.05$, ★★$p<0.01$, ★★★$p<0.001$ using two-way ANOVA followed by Newman-Keuls post-hoc test.

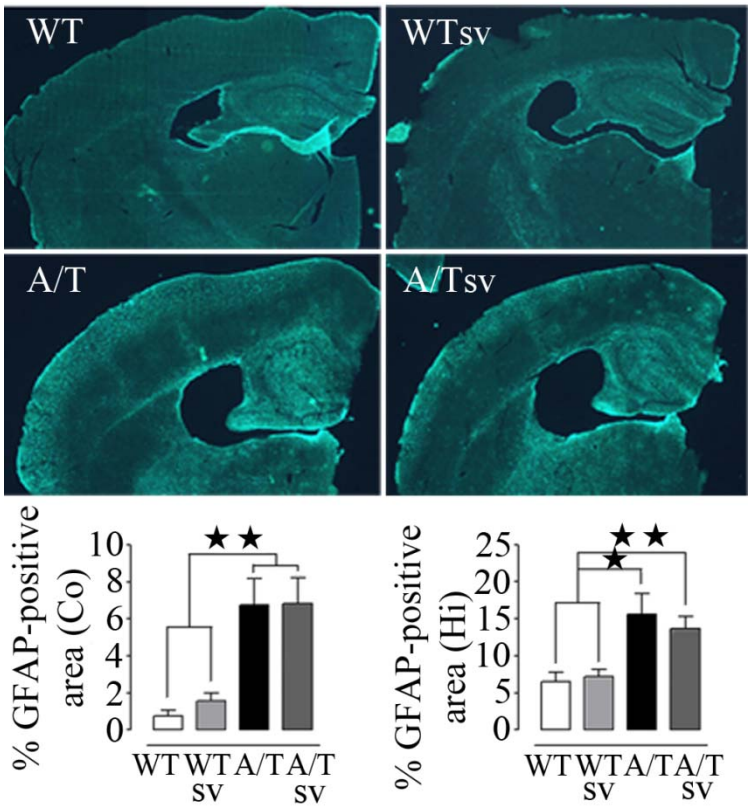

Figure 5. Simvastatin (SV) did not reduce astrocytosis. Percent area occupied by GFAP-positive astrocytes in cortex and hippocampus of A/T mice compared WT littermates remained elevated after simvastatin treatment. (n=4 mice/group). ★$p<0.05$, ★★$p<0.01$ using two-way ANOVA followed by Newman-Keuls post-hoc test.

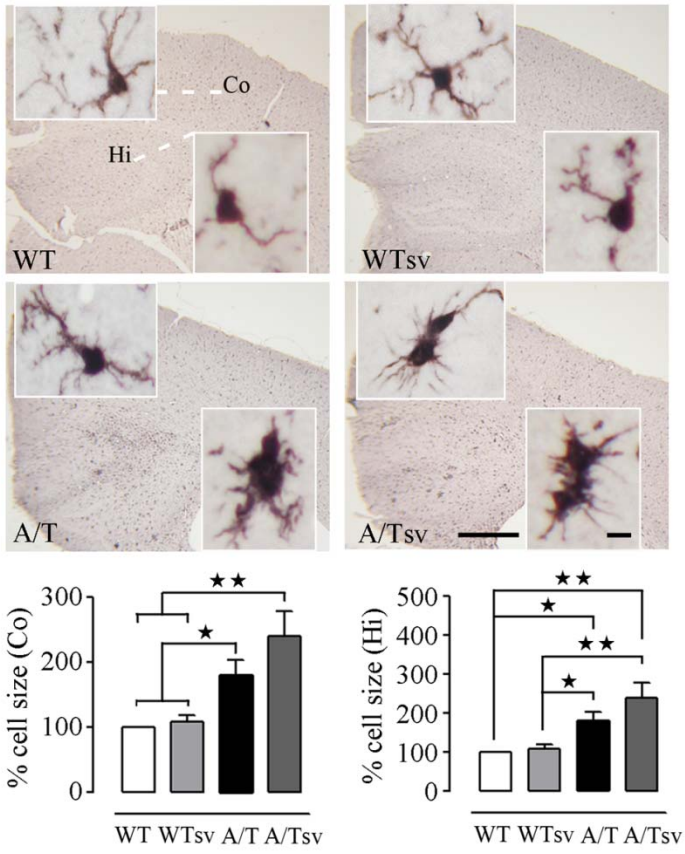

Figure 6. Simvastatin (SV) did not reduce microgliosis. Simvastatin had no reducing effects on the cell body expansion of Iba-1-positive microglial cells in cortex (Co) and hippocampus (Hi) of A/T mice compared to WT (n=4 mice/group). Error bars represent SEM. ★$p<0.05$, ★★$p<0.01$ using two-way ANOVA followed by Newman-Keuls post-hoc test. Right scale bar, 50μm. Left scale bar, 10μm.

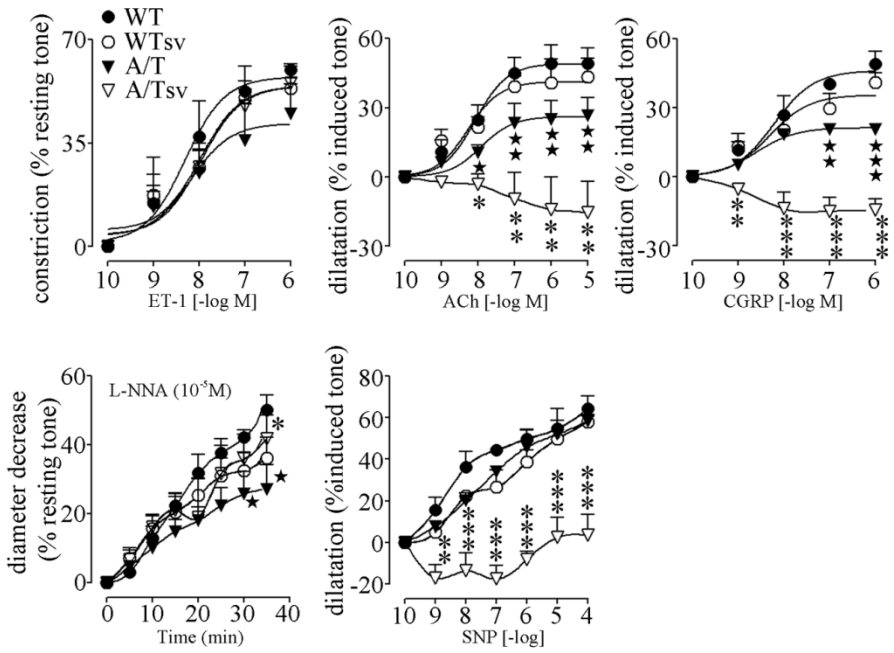

Figure 7. Simvastatin (SV) worsened dilatory function in A/T mice. Concentration-dependent contractile responses to ET-1 were unaltered in treated- (▽) and untreated- (▼) A/T mice compared to treated- (●) and untreated- (○) WT controls. In contrast, the impaired cerebrovascular dilatations to ACh and CGRP in A/T mice (▼) were reversed to weak constrictions by increasing concentrations of simvastatin (▽). Baseline NO synthesis and release measured during NOS inhibition (L-NNA, 10^{-5}M) were fully recovered in simvastatin-treated A/T mice (▽), whereas the dilatations induced by the NO donor SNP remained impaired in simvastatin-treated A/T mice. Error bars represent SEM. N=4 for each group. ★$p<0.05$, ★★$p<0.01$, ★★★$p<0.001$ when compared to WT using two-way ANOVA followed by Newman-Keuls post-hoc test.

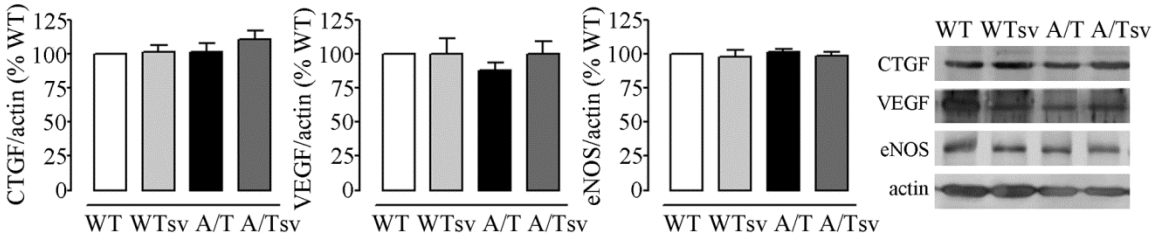

Figure 8. Simvastatin (SV) had no effect on profibrotic and eNOS protein levels. Protein levels of VEGF, CTGF and eNOS were not altered in pial vessels from A/T mice compared to WT controls, and simvastatin did not alter any of these proteins in either A/T or WT mice, as measured by Western blot. Actin was used as a reference for loading (n=4 mice/group). Error bars represent SEM. ★$p<0.05$, ★★$p<0.01$, ★★★$p<0.001$ using two-way ANOVA followed by Newman-Keuls post-hoc test.

Table 1. Effect of simvastatin on cerebrovascular responses of A/T mice

		WT	WTsv	A/T	A/Tsv
ACh	E_{Amax}	49.1±3.6	41.3±3.7	26.1±3.3★★	16.6 ±13.6★★,**
	pD_2	8.1±0.2	8.3±0.3	7.9±0.4	ND
CGRP	E_{Amax}	46.0±3.7	35.5±4.1	21.3±1.0★★★	14.4±3.9★★★,***
	pD_2	8.2±0.2	8.3±0.3	8.6±0.1	ND
SNP	E_{Amax}	64.1±6.1	57.8±3.0	58.4±3.2	3.4±10.1***
ET-1	E_{Amax}	57.3±7.0	54.2±4.2	41.6±6.8	54.1±4.7
	pD_2	8.3±0.4	8.0±4.2	8.2±0.5	8.0±0.3
L-NNA	E_{Amax}	50.0±4.3	36.1±6.0	27.2±6.9★	41.8±6.8*

Data are means ± SEM (n=3-4 mice per group) and are expressed as the agonist maximal response (EAmax) or potency (pD_2, -[logEC_{50}]). EAmax is the percent maximal dilatation to ACh, CGRP and SNP or the percent maximal diameter decrease to ET-1, 5-HT or after 35 min inhibition with 10^{-5}M L-NNA. ND: not determined, ★,* $p<0.05$, ★★,** $p<0.01$, ★★★ $p<0.001$ when compared to untreated WT controls (★) or A/T mice (*) by two way ANOVA followed by Newman-Keuls post-hoc multiple comparison test.

Preface to Chapter 5

In the previous chapter, the cognitive deficits and the evoked hemodynamic response to whisker stimulation of young A/T mice could not be normalized by *in vivo* simvastatin therapy, despite extension of treatment duration. In addition, the cerebrovascular dysfunction was worsened. We proposed that A/T mice may represent a late stage of the AD pathology past the therapeutic window of simvastatin efficacy. We therefore proceeded to verify this conclusion in the chapter that follows, as a preliminary study, using *in vivo* angiotensin II type 1 receptor (AT1R) antagonist, losartan in young A/T mice. We also used two treatment doses (10 and 25 mg/kdg/day) to see if one would play in our favour more than the other.

A rationale for angiotensin II type 1 receptor blockade was encouraged by the capacity of AT1R antagonists to improve cognition in young (2-3 months old) but most importantly in adult mice (12 months old) Tg2576 mice. Moreoever, previous studies have shown the loss of cerebrovascular dilatory capacity associated with aging was prevented in AT1-deficient mice. As you will read in this last chapter, a most exciting finding was that losartan was modestly effective in improving spatial learning and memory in young A/T mice, and this with the low dose. We also found that losartan displayed dose-dependent rescuing effects on cerebrovascular reactivity, particularly on vasodilatory responses. Nevertheless, losartan did not improve the lessened neurovascular coupling response to sensory stimulation. Together, the positive findings with the low dose losartan on spatial memory suggest that a longer treatment duration could potentially result in a more complete rescue of cognitive deficits. AT1R antagonists may be a promising therapeutic avenue for AD.

Chapter 5

Losartan rescued vasodilatory function and cognitive deficits in a mouse model of Alzheimer's disease with combined overproduction of amyloid-β and transforming growth factor-β1

Panayiota PAPADOPOULOS, Xin-Kang TONG, and Edith HAMEL

Abstract

Alterations of the renin-angiotensin system (RAS) are thought to be involved in the pathogenesis of Alzheimer's disease (AD). Here, we used A/T mice that overexpress a mutated form of the human amyloid precursor protein $APP_{Swe,Ind}$ and a constitutively active form of transforming growth factor-β1 (TGF-β1) to test the efficacy of losartan, a selective angiotensin II type 1 receptor (AT1R) antagonist, in alleviating cognitive and cerebrovascular deficits. Losartan exerted dose-related benefits on cognitive function, with significantly improved spatial memory at the low, but not the high dose treatment (10 and 25mg/kg/day, respectively) with limited benefits on spatial learning. Losartan also displayed dose-related rescuing effects on cerebrovascular reactivity, particularly on vasodilatory responses despite no improvement in the tonic production of nitric oxide. Nevertheless, losartan did not improve the lessened neurovascular coupling response to sensory stimulation, and did not reduce the brain levels of soluble and insoluble $A\beta_{1-40}$ and $A\beta_{1-42}$, or those of TGF-β1. Together, the positive findings with the low dose losartan on spatial memory suggest that an extended treatment duration could potentially result in a more complete rescue of cognitive deficits. Furthermore, these results demonstrate the capacity of losartan to improve cerebrovascular reactivity in a model of combined amyloid-β and TGF-β1-induced cerebrovascular dysfunction. They further suggest that losartan and, possibly, other AT1R antagonists, may be a promising therapeutic avenue for patients with vascular diseases at high risk of developing AD, or for AD patients with cardiovascular diseases.

Introduction

Vascular risk factors in midlife have been linked to an increased incidence of dementia (Launer et al., 2000, Whitmer et al., 2005) and cognitive decline in later life (Launer et al., 1995, Carmelli et al., 1998). Particularly, hypertension has been associated with cognitive failure and increased risk for Alzheimer's disease (AD) (Kivipelto et al., 2001). Interestingly, as series of epidemiological and clinical studies have reported mixed results on the association between the use of antihypertensive drugs targeting the altered brain renin-angiotensin system (RAS) and the incidence of AD (Guo et al., 1999, in't Veld et al., 2001, Forette et al., 2002, Khachaturian et al., 2006). Hence, additional investigations are needed to clarify the impact of antihypertensive therapy on AD pathogenesis.

Antihypertensive drugs such as angiotensin II type 1 receptor (AT1R) antagonists selectively obstruct the actions of angiotensin II on its hypertension-linked AT1R sparing those of its type 2 receptor (AT2R), both receptors being present in the brain parenchyma. Exclusive AT2R stimulation reportedly leads to improvements of cerebral blood flow (CBF) (Maxwell and Hogan, 2010) and neuroprotective effects on learning and memory (Maul et al., 2008) thus demonstrating potential benefit in the context of AD. In AD mouse models, a range of AT1R antagonists showed efficacy in improving cognition independently or not of amyloidosis (Wang et al., 2007, Mogi et al., 2008, Takeda et al., 2009, Tsukuda et al., 2009). However, these studies were conducted in $A\beta_{1-40}$ infused mice, or singly Tg2576 transgenic AD mice that recapitulate the amyloid (Aβ)-induced pathology of AD. Studies have yet to investigate the possibility of reversing cerebrovascular and mnemonic impairments in mice that combine amyloidogenic pathology with the vascular comorbidities imputed to transforming growth factor-beta 1

(TGF-β1) (Ongali et al., 2010) as seen in AD patients (Wyss-Coray et al., 1997, Wyss-Coray et al., 2000, Grammas and Ovase, 2002). It is therefore important that the reported benefits of selective AT1R antagonists be further assessed in mouse models with higher relevance to the multifaceted human pathology.

Here, we examined the therapeutic effectiveness of two doses (10mg/kg/day and 25mg/kg/day, 3 month treatment) of losartan in ~6 month-old bitransgenic A/T mice concurrently overproducing Aβ and TGF-β1 (Ongali et al., 2010), thereby integrating the comorbid factor of cerebrovascular pathology to that of enhanced amyloidosis (Zlokovic, 2010). Specific AD landmarks were evaluated such as spatial learning and memory, amyloidosis, functional hyperemia and cerebrovascular reactivity. Our findings underscore the efficacy of the low dose losartan in partly improving cognitive and cerebrovascular function, despite persistent amyloidosis, elevated TGF-β1 expression and functional hyperemic deficits. Enhancement of losartan therapeutic efficacy may be possible with increased treatment duration. Together, our results bring to light the therapeutic value of targeting the RAS and support losartan for further testing in AD models.

Methods

Animals. Bitransgenic A/T mice (Ongali et al., 2010) co-overexpress a mutated form of the human amyloid precursor protein ($APP_{Swe,Ind}$) driven by the platelet-derived growth factor β promoter (line J20) (Mucke et al., 2000) and a constitutively active form of TGF-β1 driven by the glial fibrillary acidic protein (GFAP) promoter (line T64) (Wyss-Coray et al., 1995) on a C57BL/6J background. Identification of transgenes was done touchdown PCR using tail-extracted DNA (Ongali et al., 2010). Three-month-old A/T

mice and wildtype (WT) littermates (body weight, ~30-50g) were used for this study, and they were treated for a period of 3 months (6 months old at endpoint) with either a low (10mg/kg/day) or a high (25mg/kg/day) dose of losartan in drinking water. Untreated WT and A/T mice were the same for both cohorts. All animals were randomly assigned and males and females were distributed equally in each group. Water and chow were available *ad libitum* for all mice. No significant difference in body weight between the groups was observed during the treatment period (weight gain in g: WT: 8.6±1.2 WT10: 6.2±1.5 WT25: 3.9±0.8 A/T: 5.6±1.5 A/T10: 4.4±1.6 A/T25: 3.8±0.9; 10 and 25 referring respectively to 10 or 25mg/kg/day of losartan). Experiments were approved by the Animal Ethics Committee of the Montreal Neurological Institute and complied with local and national regulations in accordance to the Canadian Council on Animal Care Institute.

Morris Watermaze. Spatial learning and memory were tested in a modified version of the Morris watermaze (Deipolyi et al., 2008). The paradigm consisted of 8 days of 2 training sessions in a 1.4 m circular pool filled with opaque water (18±1°C) located in a quiet room with distal visual cues, followed by a probe trial on day 9. Mice were first familiarized with the test by searching for a visible platform (days 1-3, 3 trials/day, 60s/trial), followed by a 5 day training session whereby mice have to learn the location of a hidden platform submerged ~1cm below the surface of the water (days 4-8, 3 trials/day, 90s/trial). Platform location and distribution of visual cues were changed between the two training sessions. A 45 min inter-trial interval was respected. Spatial memory was evaluated during the probe trial (platform removed) on day 9 (60s/trial, 1 trial). Escape latencies and probe trial parameters (percent time spent and distance traveled in the target quadrant where the platform used to be located, number of platform crossings above the

previously located platform and swim speed) were recorded with the 2020 Plus tracking system and Water 2020 software (Ganz FC62D video camera; HVS Image, Buckingham, UK) (Ongali et al., 2010). Additionally, the slope of the learning curve (days 5-8) was calculated as an index of the learning capacity of each group (Drouin et al., 2011). Swim speeds were the same for all groups (data not shown). Mice were kept warm with a heating lamp throughout the paradigm to avoid hypothermia. Subsequent experiments started 2 days later.

Cerebral blood flow (CBF). Functional hyperemia or the tight coupling between CBF and increased neuronal activity induced by whisker stimulation in the somatosensory cortex was measured with laser Doppler flowmetry (Transonic Systems Inc, Ithaca, NY). Mice were anesthetised with ketamine (85 mg/kg, intramuscularly (i.m.); Bioniche, Belleville, ON, Canada) and xylazine (3 mg/kg, Haver, Etobicoke, ON) and fixed in a stereotaxic frame. The laser doppler probe was placed on the bone of the left barrel cortex which was thinned to translucency with a dental drill. An electric toothbrush was used to stimulate (8-10 Hz, 20 sec) the mouse whiskers on the right snout. Body temperature was kept stable at 37°C with a heating pad. Four to five stimulations were performed for each mouse with ~30s interval, and the evoked CBF responses were acquired and expressed as percent average increase relative to baseline. The experimenter was blind to the identity of the mouse and the entire procedure lasted about 20min/mouse.

Mean arterial blood pressure: Mice except WT-treated were anesthetized with isofluorane (5% in medical air during 2-min induction, 1.5-2%), and a small incision was performed under local analgesia (2% xylocaine) from the third superior part to the midline of the hindpaw, for insertion of a small catheter (SAI, catalogue #: MAC-01) in

the femoral artery. Mice were then placed in a small restraining cylinder, anesthesia was switched off and mean arterial blood pressure (MAP), heart rate and body temperature were acquired for a period of 30min (Powerlab, ADinstruments, St.-Laurent QC, Canada). Losartan did not alter these parameters and, particularly MAP (in mmHg) at any dose (WT: 104.8±5.9, A/T: 108.8±4.8, A/T10: 99.5±2.3, A/T25: 106.2±4.8).

Tissue collection and preparation. Upon completion of *in vivo* experiments, mice were sacrificed by cervical dislocation for functional reactivity of the posterior cerebral artery (PCA) (see below). The remaining vessels from the circle of Willis were isolated, frozen on dry ice and stored at -80°C, together with the cortex and hippocampus from one hemibrain for subsequent use for ELISA and western blot experiments. The other hemibrain was immersion-fixed in 4% paraformaldehyde (PFA in 0.1 M phosphate buffer (PB), pH 7.4; 4°C) overnight, cryoprotected (30% sucrose in 0.1 M PB; 4°C) overnight, frozen in isopentane and stored (-80°C) until sectioning (25 μm-thick sections) on a freezing-microtome.

Vascular reactivity. Vascular reactivity was measured in cannulated and pressurized (60 mm Hg) segments (40–70 μm of intraluminal diameter) of the PCA superfused with Krebs solution (37°C) using online videomicroscopy (Tong et al., 2005). Vasodilations to acetylcholine (ACh; 10^{-10}-10^{-5} M), calcitonin gene-related peptide (CGRP; 10^{-10}-10^{-6} M) or to the NO donor sodium nitroprusside (SNP, 10^{-10} - 10^{-4} M) were measured on vessels slightly pre-constricted with serotonin (5-HT; 2×10^{-7} M). Contractile responses to endothelin-1 (ET-1; 10^{-10}-10^{-6} M) and to inhibition to the tonic production of the vasodilator nitric oxide (NO) by superfusion of the NO synthase (NOS) inhibitor Nω-nitro-L-arginine (L-NNA; 10^{-5} M, for 35 min) were performed on vessels at basal tone.

Changes in vessel diameter are presented in percent change from the basal or pre-constricted tone. Results were plotted as a function of agonist concentration or time for L-NNA superfusion. The maximal response (EA_{max}) and half maximal effective concentration (EC_{50} value or $pD_2 = -(\log EC_{50})$) were determined to compare agonist efficacy and potency respectively.

ELISA measurement of Aβ species. Insoluble $A\beta_{1-40}$ and $A\beta_{1-42}$ levels in cortex and hippocampus from one hemibrain were measured using an enzyme-linked immunosorbent assay (ELISA) (BioSource International, Camarillo, CA, USA), as described by the manufacturer (for details, (Ongali et al., 2010)). Data are presented in micrograms per gram (μg/g) of protein in formic acid insoluble Aβ-fraction.

Western blot. Cortical and hippocampal protein (~20 μg of ELISA supernatant) were loaded onto a 15% Tris/tricine SDS PAGE and transferred to nitrocellulose membranes for the detection of total levels of soluble Aβ species using a mouse anti-Aβ1-16 antibody (6E10, 1:1000, Covance, Emeryville, CA, USA). Hippocampal proteins (~35μg) were also used for the detection of TGF-β1 (1:1200; Cell Sciences, Canton, MA). Membranes were subsequently incubated (1h) with horseradish peroxidase-conjugated secondary antibodies (1:2000; Jackson ImmunoResearch, West Grove, PA, USA) in TBST blocking buffer (50mM Tris-HCl, pH = 7.5; 150mM NaCl; 0.1% Tween 20) containing 5% skim milk. They were visualized with Enhanced ChemiLuminescence (ECL Plus kit; Amersham, Baie d'Urfé, QC, Canada) using phosphorImager (Scanner STORM 860; GE Healthcare, Baie d'Urfé, QC, Canada). Band intensity was quantifed by densitometry with ImageQuant 5.0 (Molecular Dynamics, Sunnyvale, CA, USA) by densitometry.

Histochemical staining. Thioflavin S (1%, 8 min) staining of mature, dense core Aβ plaques was performed on thick sections (3 sections per mouse, five mice per group), which were observed under a Leitz Aristoplan light microscope using epifluorescence and an FITC filter (Leica). Pictures were taken with a Nikon digital camera (Coolpix 4500), and were used for quantification using MetaMorph 6.1r3 (Universal Imaging). The areas of interest (cingulate and somatosensory cortex, hippocampus) were manually outlined for percent area occupied by thioflavin S-positive staining.

Statistical analysis. Data are expressed as means ± SEM, and were analyzed by two-way analysis of variance (ANOVA) with genotype and treatment as the two variables, followed by Newman-Keuls post-hoc multiple comparison test (Statistica Academic, Tulsa, OK, USA). Student's t-test was used to determine significance between two groups (GraphPad Prism 4, San Diego, CA, USA). A p value ≤ 0.05 was considered significant.

Results

Losartan and spatial learning and memory

WT and A/T mice required comparable time to locate the visible platform in the Morris watermaze (days 1-3) ruling out visual and motor disabilities, and lack of motivation. However, A/T mice were severely impaired in finding the hidden platform, as depicted by their elevated escape latencies compared to age-matched WT controls (days 4-8) (Figures 1A, D). The learning slope between days 5 and 8 (WT: -4.17±2.03, A/T: 2.46±3.13) further demonstrated their reduced learning capacity. A/T mice also displayed memory deficits in the probe trial as illustrated by the decreased percent time spent and distance traveled in the target quadrant, and by the few platform crossings over the

previously located platform (Figures 1C, F). These findings are in line with our previous studies (Ongali et al., 2010). The low and the high doses of losartan did not exert any significant beneficial effects on spatial learning measured with the escape latencies (Figures 1A, D). However, the learning slope of A/T-treated mice with the low – but not high – dose of losartan equated to that of WT control littermates, indicative of improved learning capacity although it did not reach statistical significance (A/T10: -4.57±2.97, A/T25: -1.44±2.04) (Figures 1B, E). Moreover, the low dose of losartan, but not the high dose, significantly improved spatial memory with slightly but significantly more time and distance travelled in the target quadrant, despite a persistent lack of precision evidenced by the remaining low platform crossings even after losartan (Figures 1B, D). Together, these findings indicate that the low dose of losartan exerted beneficial effects on spatial learning and memory in A/T mice.

Losartan did not restore functional hyperemia

The evoked CBF response induced by whisker stimulation was reduced in A/T mice compared to WT controls (WT: 26.4±3.7% vs. A/T: 8.6±1.0%, $p<0.01$) (Figure 2). Losartan failed to improve this evoked response in both the low (11.0±3.1%, $p<0.01$) and high dose cohorts (6.9±2.0%, $p<0.01$). Interestingly, the low dose losartan slightly, but significantly, potentiated the hyperemic response in WT mice compared to non-treated controls (WT: 26.4±3.7% vs. WT_{10}: 36.2±6.5%, $p<0.01$) (Figure 2).

Losartan improved cerebrovascular reactivity in A/T mice

Isolated PCA of A/T mice displayed significantly reduced dilatory responses to ACh and CGRP relative to WT controls (Figures 3-4), in line with previous data (Ongali et al., 2010). Receptor desensitization did not account for these alterations since agonist

potencies at vascular receptors were comparable between WT and A/T mice (Tables 1-2). Baseline NO synthesis was also decreased compared to WT controls, as shown by the smaller diameter decrease during L-NNA superfusion (Figures 3-4; Table 1-2). In contrast, dilations induced by the NO donor SNP were not altered in A/T mice, indicative of preserved integrity of the smooth muscle, as also demonstrated by the intact contractile response to ET-1 (Figures 3-4; Table 1-2). Losartan, irrespective of the dose, normalized the ACh- and CGRP-mediated dilatory responses in A/T mice, although the recovery in ACh-mediated dilations did not reach significance at the high dose. Losartan failed to normalize constitutive NO release essential for maintaining resting tone (Figures 3-4, Tables 1-2), and did not alter the contractile ET-1 and dilatory SNP responses. Losartan did not affect vasomotor responses in WT mice (Figures 3-4, Tables 1-2).

Losartan and amyloidosis

As expected, A/T displayed high levels of soluble and insoluble Aβ species in cortex and hippocampus (Figure 5), and these remained unchanged after losartan therapy at either dose as measured by Western blot (Figure 5A) or ELISA (Figure 5B). Accordingly, Aβ plaque load was not reduced among groups as determined by thioflavin-S staining of dense-core Aβ plaques, although the high dose showed a trend toward a decrease which did not reach significance (Figure 5C). These results show that losartan did not alter the progression of the amyloidogenic process in A/T mice. Interestingly, neither dose of losartan exerted any effect on hippocampal protein levels of TGF-β1 (Figure 5D).

Discussion

The present study highlights the unique capacity of a low dose of losartan to exert selective beneficial effects on spatial learning and memory in 6 month-old A/T mice.

Furthermore, both the low and high doses of losartan improved arterial responsiveness to vasodilatory agonists, despite no change in the decreased tonic production of NO in the vessel wall. These cognitive and cerebrovascular benefits occurred with persistent amyloidosis and lessened hemodynamic responses to increased neuronal activity.

Specific beneficial effects of losartan on cognitive function

We found that the low dose of losartan conferred some protection against the onset of cognitive dysfunction in adult A/T mice. This cognitive beneficial effect of losartan is highly promising as it is the first time that losartan is being tested in a complex AD mouse model of combined amyloidosis and cerebrovascular pathology. Indeed, previous studies that showed neuroprotective effects of losartan (Mogi et al., 2008) or other AT1R antagonists such as olmesartan (Takeda et al., 2009) and telmisartan (Tsukuda et al., 2009) did so using $A\beta_{1\text{-}40}$-injected mice. Only one other study (Wang et al., 2007) used a transgenic APP mouse model, the Tg2576 model, which bears the Swedish APP mutation (Westerman et al., 2002).. Hence, our study supports the use of AT1R antagonism for cognitive improvements, but is the first to additionally extend it to transgenic animals with an AD-associated cerebrovascular pathology.

Chronic upregulation of TGF-β1, a key extracellular matrix regulator, has been documented in the brain and the cerebral vasculature of AD patients (Wyss-Coray et al., 1997, Grammas and Ovase, 2002, Tesseur and Wyss-Coray, 2006), as well as in patients with ischemic stroke (Krupinski et al., 1996), hypertension and diabetes who are at increased risk for AD (Peterson, 2005). Furthermore, studies have evidenced the deleterious effects of chronic TGF-β1 upregulation on neurogenesis (Buckwalter et al., 2006), a process known to substantially contribute to hippocampal-dependent learning

and memory (Kee et al., 2007, Dupret et al., 2008, Deng et al., 2009). The harmful contribution of long-term TGF-β1 to neuronal and cerebrovascular function is further supported by the lack of beneficial effects of simvastatin found in A/T mice on both spatial memory and cerebrovascular function (see Chapter 3 of this thesis), while it was highly effective in rescuing both deficits in singly APP mice (Tong et al., 2012). Therefore, our results with losartan bear great therapeutic significance for AD patients overexpressing TGF-β1 and at risk for AD.

Attenuation of TGF-β1 expression by losartan has been proposed as a possible mechanism of action in preventing or reversing disease progression in animal models of chronic renal insufficiency (Lavoie et al., 2005), cardiomyopathy (Lim et al., 2001), and in Duchenne muscular dystrophy (Cohn et al., 2007), all accompanied by increases of TGF-β1 expression. However, in our study, losartan did not decrease TGF-β1 protein levels in hippocampus, not even at the high dose, suggesting that chronic TGF-β1 overexpression in A/T mice overpowered this potential effect of losartan. Therefore, TGF inhibition likely did not account for the learning and memory improvements seen at the low dose of losartan.

Another possible explanation resulting from AT1R blockade may be accredited to a concomitant restoration of memory-enhancing AT2R (Tsutsumi and Saavedra, 1991, Maul et al., 2008) or, possibly, AT4R (Gard, 2008, Wright and Harding, 2010) to which angiotensin IV, an active metabolite of angiotensin II, binds with high affinity. Both receptor subtypes are distributed in cognitive-processing areas including the hippocampus (Maul et al., 2008, Wright and Harding, 2008, 2010), and their role in memory processes has been confirmed in AT2R-KO (Maul et al., 2008) and AT4R-KO (Albiston et al.,

2010) mice that both featured spatial memory decline. Although the mechanisms by which learning and memory are facilitated are still unclear, long term potentiation (LTP) stimulation in hippocampal CA1 is thought to be involved (Wayner et al., 2001). In contrast to previous studies with valsartan (10 and 40mg/kg/day) on aged 11 month-old Tg2576 mice treated for 5 months (Wang et al., 2007), we did not find a dose-dependent effect of losartan on cognitive performance.

An unexpected finding was the failure of losartan to normalize the evoked neurovascular coupling in A/T mice, suggesting a persistent reduced delivery of oxygen and glucose by the cerebral circulation to activated neurons of the somatosensory cortex. As this hemodynamic response depends on thalamocortical glutamatergic afferents and astrocytic signaling (Carmignoto and Gomez-Gonzalo, 2010), it may suggest that the astrocytic function was still impaired after losartan, despite the reported anti-inflammatory effects of AT1R including telmisartan in Aβ1-40 infused mice (Tsukuda et al., 2009) or adult C57BL/6J male mice subjected to bilateral common carotid artery stenosis (Washida et al., 2010).

Normalized vascular reactivity

A most fascinating finding from our current study was that both the low and high doses of losartan improved endothelium-dependent dilatations to ACh and CGRP. This was achieved despite no recovery of baseline NO synthesis, a response dependent on endothelial nitric oxide synthase (eNOS), which have been reported to be increased by losartan (Miatello et al., 2003, Taguchi et al., 2011) or valsartan via Src/PI3K/Akt-dependent signaling cascade (Su et al., 2009). Although such effects were not detected on baseline NO levels, the improved Ach and CGRP-mediated dilations may suggest

normalization of receptor-mediated NO-dependent responses or, alternatively, that other dilatory pathways are involved on which losartan also exert beneficial effects. Indeed, cerebrovascular dilatation to ACh occurs through NO release upon m5 muscarinic receptor activation (Elhusseiny and Hamel, 2000, Yamada et al., 2001), but also via hydrogen peroxide (H_2O_2) (Drouin et al., 2007), likely following activation of soluble guanylate cyclase (sGC) as in peripheral arteries (Iesaki et al., 1999). Similarly, CGRP-induced dilatations in mouse brain arteries are primarily mediated by smooth muscle K+ channels including K_{ATP} (Kitazono et al., 1993, Tong et al., 2009) and Ca^{2+}-activated K^+ (K_{Ca2+}) channels (Hong et al., 1996, Vedernikov et al., 2002), both types of channels being normalized by losartan, in conditions such as diabetes type 2 (Matsumoto et al., 2010), renal failure (Koobi et al., 2003) or following AngII inhibition (Hayabuchi et al., 2001).

Aβ induces cerebrovascular dysfunction primarily through increased reactive oxygen species, particularly O_2^- ions that trap NO, making it unavailable for dilatation (Iadecola et al., 1999; Park et al., 2005, 2008; Tong et al., 2005). Although antioxidants applied *in vitro* on cerebral arteries of A/T mice did not suggest a major role for oxidative stress in their impaired dilatory capacity (Ongali et al., 2010), it is still possible that the downregulation exerted *in vivo* by losartan on the p47phox subunit of NADPH oxidase (Zhu et al., 2007), the main source of free radical production in brain vessels, may have contributed to the protective effects. Although we did not seek to further explore the exact mechanisms underlying cerebrovascular recovery, our results unequivocally demonstrate the effectiveness of losartan on the combined Aβ and TGF-β1 cerebrovascular pathology, thus strongly supporting its use in countering AD

cerebrovascular dysfunction imputed to alterations in both Aβ and TGF-β1 (Grammas and Ovase, 2002, Peterson, 2005)

Losartan and amyloidosis

Brain levels of insoluble Aβ remained unchanged with losartan therapy, in contrast to other studies that showed significant reductions in soluble or deposited Aβ in $A\beta_{1-40}$-injected (Mogi et al., 2008, Tsukuda et al., 2009), APP/PS1 (Danielyan et al., 2010) and Tg2576 (Wang et al., 2007) mice. However, a clear tendency for reduction with the higher dose was apparent, by both Elisa and Thioflavin-S-stained plaque load quantification. However, since soluble Aβ oligomer levels which reportedly are the most detrimental to neuronal and synaptic function (Mucke et al., 2000, Lesne et al., 2008) remained unchanged, even at the low dose losartan that exerted beneficial effects on cognitive function, these findings underscore the lack of correlation between amyloidosis and behavioral recovery (Mogi et al., 2008, Park et al., 2008, Tong et al., 2012). Studies showing cognitively unaffected elderly individuals having equivalent Aβ plaque densities as AD patients further support the notion that Aβ plaques are not good correlates of dementia (Davis et al., 1999).

Conclusion

The therapeutic efficacy of low dose losartan against spatial memory and cerebrovascular reactivity of A/T mice at 6 months of age highlights the possible involvement of the brain RAS in the neuronal and vascular aspects of AD pathology. Moreover, its failure to fully normalize the cognitive deficit and the functional hemodynamic response may suggest that longer treatment may be more effective. Overall, our findings in A/T mice with

losartan would be supportive of the benefits reported for this type of compounds in preventing AD (Ohrui et al., 2004, Hajjar et al., 2008).

Acknowledgements: This work was supported by the Canadian Institutes of Health Research (CIHR grant MOP-84275 to EH) and a Jeanne Timmins Costello Fellowship (PP). We thank Dr. Lennart Mucke (Gladstone Institute of Neurological Disease and Department of Neurology, UCSF, CA) and the J. David Gladstone Institutes for the $hAPP_{Swe,Ind}$ and TGF-β1 transgenic mouse breeders.

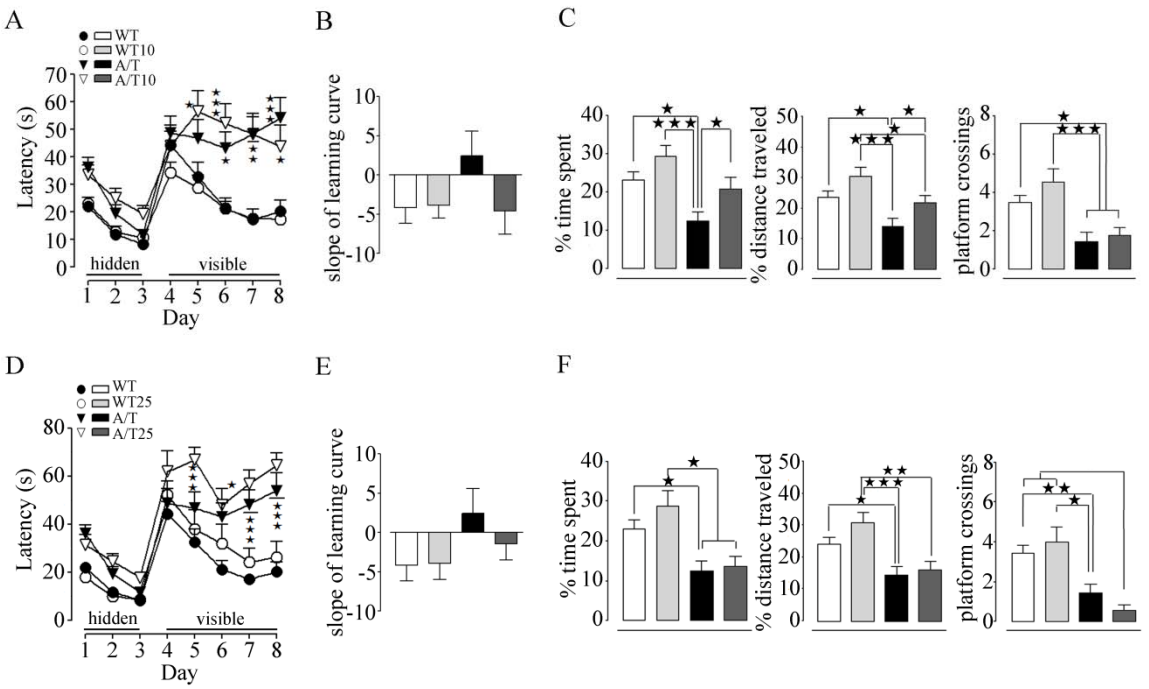

Figure 1. Losartan on spatial learning and memory in A/T mice in the Morris watermaze. ***A,*** A/T mice at 6 months of age (▼) displayed impaired learning during hidden-platform testing compared to aged-matched wild-type (WT) littermates (●). Low dose of losartan did not improve the learning deficit in A/T-treated mice (▽) nor change that of the WT-treated mice (○). Visibile-platform session demonstrated proper visual acuity and motivation levels for each group. ***B,*** The learning slope between days 5 and 8 demonstrated the reduced learning capacity of A/T compared to WT mice. The learning slope of A/T-treated mice with the low dose of losartan equated to that of their control littermates, indicative of a learning process. ***C,*** Low-dose-losartan exerted significant effects on spatial memory relative to the untreated A/T mice as evidenced by the improved percent time spent and distance travelled as well as fewer crossings over the previously located platform during the probe trial. ***D,*** Losartan did not improve the learning deficit in the high-dose in the target quadrant treated-A/T mice (▼) nor change that of the WT-treated mice (●). ***E,*** The learning slope of A/T-treated mice with the high dose of losartan differed from that of their control littermates, demonstrating a lack of learning process among these mice. ***F,*** Spatial memory deficits during the probe trial were not recovered by high dose losartan treatment. Error bars represent SEM (n=10-12 mice/group). ★$p<0.05$, ★★$p<0.01$, ★★★$p<0.001$ using two-way ANOVA followed by Newman-Keuls post-hoc test.

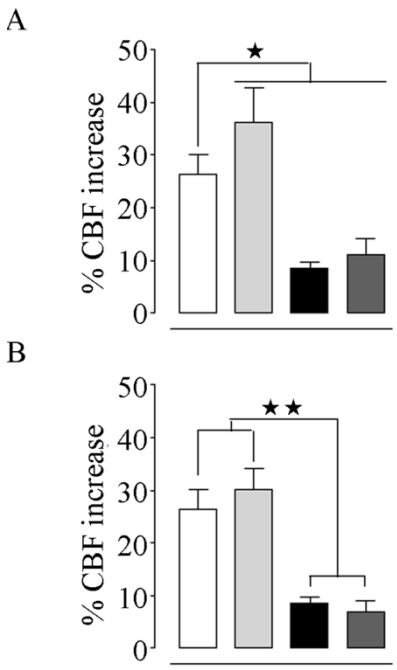

Figure 2. Losartan did not restore stimulus-evoked CBF in A/T mice. The impaired hyperemic response to whisker stimulation in A/T mice was not restored by the low **(A)** or the high dose **(B)** of losartan, and remained reduced compared to the WT controls, as measured by LDF (n=4 mice/group). Values represent the percent increase of CBF response relative to baseline. Error bars represent SEM. ★$p<0.05$, ★★$p<0.01$ using two-way ANOVA followed by Newman-Keuls post-hoc test.

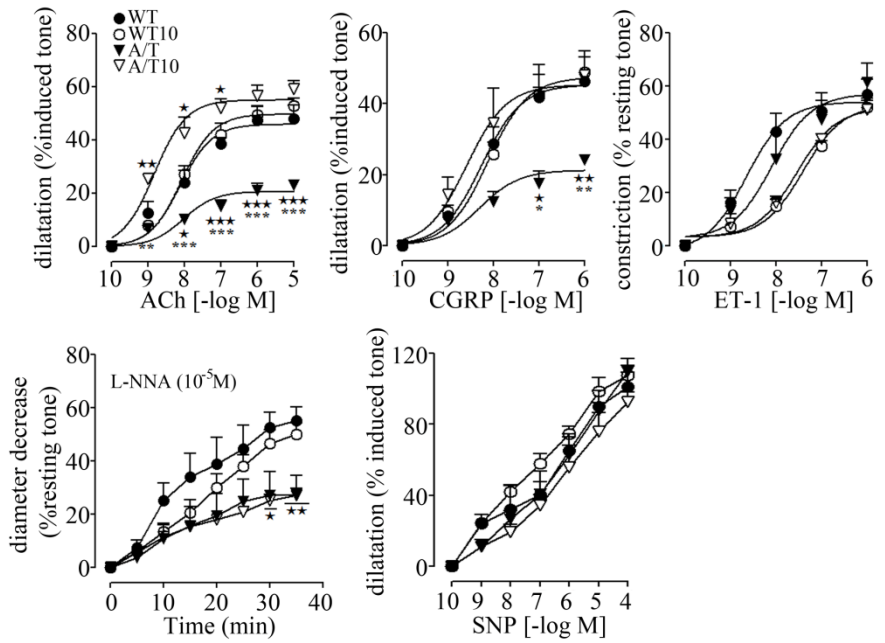

Figure 3. Low dose losartan normalized vasodilatory function of A/T mice. The impaired cerebrovascular dilatations to ACh and CGRP in A/T mice (▼) were normalized by losartan (▽), but this was not accompanied by a recovery of baseline NO synthesis during NOS inhibition (L-NNA, 10^{-5}M). Dilatations induced by the NO donor SNP remained unchanged in A/T treated with losartan. Contractile response to ET-1 remained unaltered in both treated- and untreated-A/T mice. Error bars represent SEM. n=4 for each group. ★,* $p<0.05$, ★★, ** $p<0.01$, ★★★, *** $p<0.001$ when compared to untreated WT controls (★) or A/T mice (*) using two-way ANOVA followed by Newman-Keuls post-hoc test.

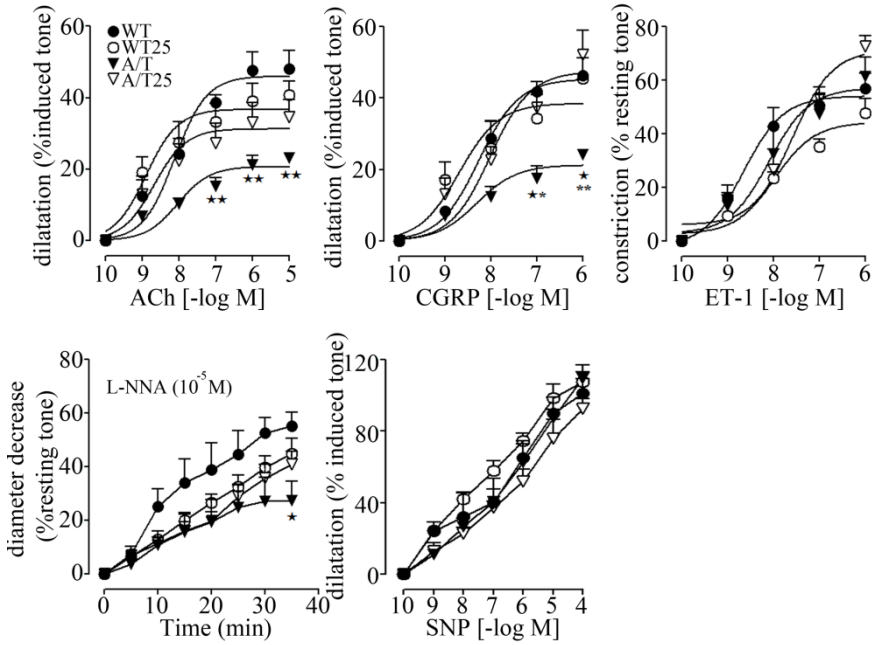

Figure 4. High dose losartan improved vasodilatory function of A/T mice. Losartan partially and fully reversed the impaired cerebrovascular dilatations to ACh and CGRP, respectively, in losartan-treated A/T mice (▽), with no recovery of baseline NO synthesis. Similarly, dilatations induced by the NO donor SNP, remained unaltered as contractile response to ET-1 in both treated- and untreated-A/T mice. Error bars represent SEM. n=4 for each group. The same vessels of WT (●) and A/T (▼) mice described in figure 2 were also utilized in this figure. ★,* $p<0.05$, ★★, ** $p<0.01$, ★★★ $p<0.001$ when compared to untreated WT controls (★) or A/T mice (*) using two-way ANOVA followed by Newman-Keuls post-hoc test.

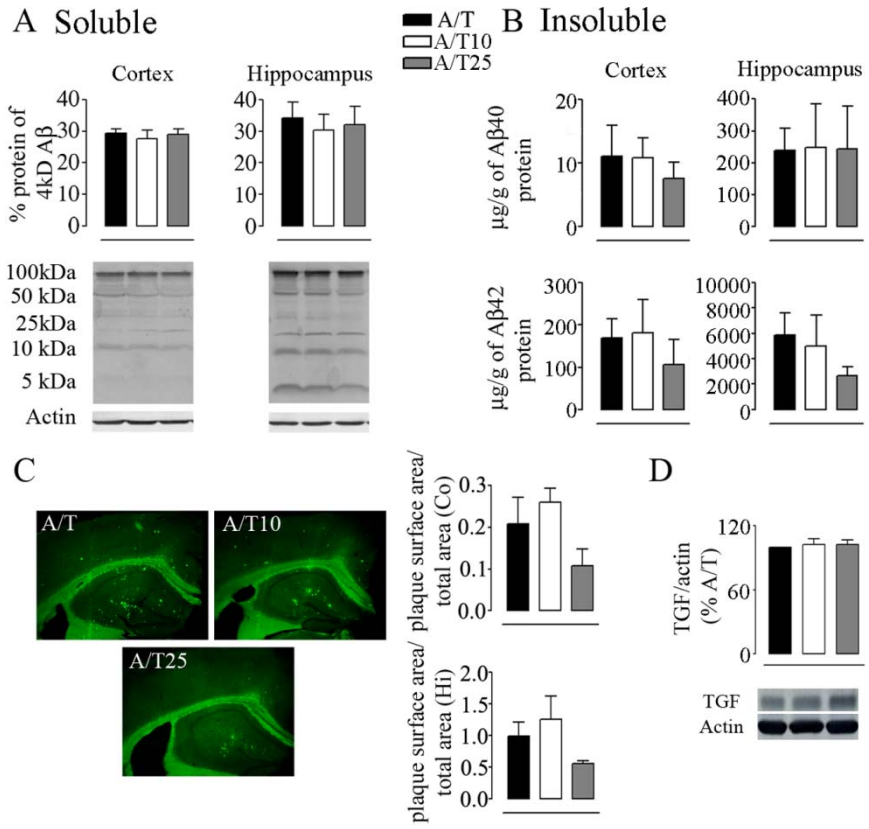

Figure 5. Losartan, amyloidosis and TGF-β1 expression in A/T mice. ***A,*** Western blot analysis with 6E10 antibody revealed no effect of losartan on soluble Aβ species in cortex and hippocampus of A/T mice. Actin was used as a reference for loading. ***B,*** Insoluble $A\beta_{1\text{-}40}$ and $A\beta_{1\text{-}42}$ levels in treated-A/T mice remained unchanged as assayed in half-brain of cortex and hippocampus by ELISA, although the high dose showed a clear trend towards decreased levels. ***C,*** The surface area occupied by Aβ plaque load was not changed among groups as determined by thioflavin-S staining of dense-core Aβ plaques in both cortex and hippocampus. Nevertheless, the high dose losartan also showed a strong trend towards a decrease, but did not reach significance. ***D,*** Losartan did not yield any changes in protein levels of TGF-β1 irrespective of the dose. Actin was used as a reference for loading. Error bars represent SEM (n=4 mice/group). Error bars represent SEM (n=4 mice/group). ★$p<0.05$, ★★$p<0.01$, ★★★$p<0.001$ for comparison to A/T mice using two-way ANOVA followed by Newman-Keuls post-hoc test.

Table 1. Effect of 10mg/kg/day losartan on cerebrovascular responses of A/T mice

		WT	WT10	A/T	A/T10
ACh	E_{Amax}	46.0±2.6	49.8±1.8	20.7±1.3★★	55.1±2.1★★,**
	pD_2	8.1±0.2	8.1±0.1	8.0±0.2	8.8±0.1
CGRP	E_{Amax}	45.3±1.9	47.4±2.9	21.2±1.7★★★	45.3±4.7★★★,***
	pD_2	8.3±0.1	8.1±0.1	8.3±0.2	8.6±0.3
SNP	E_{Amax}	101.3±8.3	107.8±9.2	110.7±3.4	92.7±5.5***
ET-1	E_{Amax}	54.1±3.3	52.9±2.7	57.1±6.0	51.8 ±2.9
	pD_2	8.7±0.2	7.4±0.1	8.1±0.3	7.6±0.1
L-NNA	E_{Amax}	55.1±5.2	50.0±4.4	27.6±7.2★	27.3±2.5*

Data are means ± SEM (n=4 mice per group) and are expressed as the agonist maximal response (EAmax) or potency (pD_2, -[logEC_{50}]). EAmax is the percent maximal dilatation to ACh, CGRP and SNP or the percent maximal diameter decrease to ET-1, 5-HT or after 35 min inhibition with 10^{-5}M L-NNA. ★,* $p<0.05$, ★★,** $p<0.01$, ★★★,*** $p<0.001$ when compared to untreated WT controls (★) or A/T mice (*) by two way ANOVA followed by Newman-Keuls post-hoc multiple comparison test.

Table 2. Effect of 25mg/kg/day losartan on cerebrovascular responses of A/T mice

		WT	WT25	A/T	A/T25
ACh	E_{Amax}	46.0±2.6	36.8±2.4	20.7±1.3★★	31.3±2.5
	pD_2	8.1±0.2	8.9±0.3	8.0±0.2	8.7±0.3
CGRP	E_{Amax}	45.3±1.9	38.5±4.0	21.2±1.7★★★	47.4±4.0★★★,***
	pD_2	8.3±0.1	8.7±0.3	8.3±0.2	8.0±0.2
SNP	E_{Amax}	101.3±8.3	107.8±9.2	110.7±3.4	92.7±5.5***
ET-1	E_{Amax}	54.1±3.3	44.3±2.8	57.1±6.0	71.4±5.0
	pD_2	8.7±0.2	8.0±0.2	8.1±0.3	7.6±0.2
L-NNA	E_{Amax}	55.1±5.2	45.0±5.6	27.6±7.2★	41.0±4.8*

Data are means ± SEM (n=4 mice per group) and are expressed as the agonist maximal response (EAmax) or potency (pD_2, -[logEC_{50}]). EAmax is the percent maximal dilatation to ACh, CGRP and SNP or the percent maximal diameter decrease to ET-1, 5-HT or after 35 min inhibition with 10^{-5}M L-NNA. ★,* $p<0.05$, ★★,** $p<0.01$, ★★★,*** $p<0.001$ when compared to untreated WT controls (★) or A/T mice (*) by two way ANOVA followed by Newman-Keuls post-hoc multiple comparison test.

General Discussion

Summary and interpretation of results

We hypothesized that A/T bitransgenic mice, which feature cognitive, cerebrovascular and glial deficits may represent a more accurate model for AD pathology. These deficits may be reversible or curable by therapeutic intervention. If so, the effective compounds may bear promise in AD patients. Using A/T mice, we evaluated the efficacy of pioglitazone (20mg/kg/day), simvastatin (40mg/kg/day) and losartan (10 and 25mg/kg/day) on key clinical outcomes including spatial learning and memory (Morris watermaze), evoked neurovascular and/or neurometabolic coupling responses, cerebrovascular reactivity, amyloidosis and glial activation.

We provide evidence that:

[1] Concomitant overexpression of Aβ and TGF-β1 in A/T mice was associated with spatial memory deficits as well as arterial and hemodynamic dysfunction (Chapter 2).

[2] The PPARγ agonist pioglitazone exerted positive effects on neurometabolic and neurovascular coupling responses to sensory stimulation, and reduced cortical astroglial activation. Nevertheless, pioglitazone worsened vasodilatory function in A/T mice. Spatial learning and memory in the Morris watermaze were not normalized although modest, but significant, improvements were seen in reversal learning in the adult cohort despite unaltered Aβ levels (Chapter 3).

[3] The HMG-CoA reductase inhibitor simvastatin failed to normalize spatial learning and memory, the evoked CBF to sensory stimulation, glial activation, and it worsened vasodilatory function in A/T mice. However, simvastatin significantly lowered brain levels of insoluble Aβ and Aβ plaque load (Chapter 4).

[4] The AT1R antagonist losartan at a low dose only was able to confer some cognitive protection as evidenced by the improved learning capacity and spatial memory and this, despite persistent amyloidosis. Both doses of losartan tested exerted beneficial effects on cerebrovascular reactivity, although the neurovascular coupling to sensory stimulation was not normalized by either dose (Chapter 5).

The following sections discuss the relevance of these main findings to AD.

1. Characterizing an AD model

We investigated in chapter 2, the interactive effects of APP and TGF-β1 overexpression in young, adult and old A/T mice on cerebrovascular reactivity, inflammation, evoked CGU and CBF, and spatial memory. A/T mice featured progressive cerebrovascular dysfunction insensitive to *in vitro* antioxidant treatment. In addition, A/T mice displayed progressive astrocytic activation, Aβ pathology and impairment in evoked cerebral blood flow and glucose uptake along with a spatial memory decline, thus bringing together cerebrovascular, glial and cognitive aspects of AD pathophysiology.

2. Effects of pioglitazone in A/T mice

Pioglitazone reversed the impaired CBF and CGU deficits of aged A/T mice, in line with the recovered astroglial function in the activated somatosensory area. The decreased release of inflammatory cytokines by these astrocytic elements was suggested to also partake to the recovery. Particularly, PPARγ activation may have facilitated the ability of astrocytes to synthesize arachidonic acid derivatives, primarily the vasodilatory epoxyeicosatrienoic acids (EETs) that mediate a large part of the neurovascular coupling response to whisker stimulation (Lecrux and Hamel, 2011). Together, these findings support the hypothesis that pioglitazone can reverse glial alterations even at an advanced

stage of the pathology benefiting neurovascular and neurometabolic coupling, responses that depend on a healthy neurogliovascular unit (Carmignoto and Gomez-Gonzalo, 2010, Lecrux and Hamel, 2011).

Nevertheless, as discussed in chapter 3, recovery of neurovascular coupling response in the somatosensory cortex did not necessarily mirror that of the hippocampus. Not only does this response depend on the associated perivascular astrocytic endfeet, but also on specific neuronal networks within each activated area including local excitatory–inhibitory pathways (Logothetis, 2008). As such, because of possible regional CBF heterogeneity (Sloan et al., 2010), CBF evaluations should ideally be performed in the hippocampus for a direct link with memory performances. However, such approaches are invasive and perturb the brain parenchyma (Barretto et al., 2011) and because of this, we used the whisker-to-barrel pathway, which is a well-established pathway with reduced functional hyperemia in APP mice (Niwa et al., 2000). The same applies to the neurometabolic coupling response (Chuquet et al., 2010). We suggest that future investigations should include stimulation paradigms for CGU evaluations in the hippocampus for better associative power between alterations in glucose metabolism and cognition. For instance, instead of stimulating the whiskers for 45 min post-FDG injection, mice may perform the probe trial of the watermaze for direct stimulation of the hippocampus (among other areas). Limitations in terms of feasibility to this experimental approach may exist like the physical stamina of a mouse which may require an increased FDG-injection dose for a decreased stimulation time.

The fact that pioglitazone failed to decrease astrogliosis in the hippocampus, in contrast to its positive effects on the cortex, may even suggest that there was no

hippocampal CBF and CGU recovery. Such possibility could very well explain why pioglitazone failed to recover spatial memory in A/T mice, hypoperfusion and hypometabolism being good correlates of AD memory decline (de la Torre, 1999, Melrose et al., 2009). Even more, astrocytes have been associated to hippocampal homeostasis required for memory formation (Santello and Volterra, 2010). The fact that the prolonged treatment duration demonstrated modest reversal memory benefits may hint two things: [1] Memory recovery could have been possible if the allotted time of the probe trial was more than 60s, i.e. prolonged to 90s like in the hidden-platform learning session. With a delayed yet significantly improved understanding of the platform relocation, the extended time may have been favourable for the pioglitazone-treated-A/T mice to redirect themselves to the target quadrant. [2] The Morris watermaze paradigm, considered stringent and stressful (Van Dam and De Deyn, 2006) may have masked understated behavioural improvements that may have been apparent in other paradigms like the Y-maze (Van Dam and De Deyn, 2006).

Perhaps future experimental studies attempting to normalize memory with pioglitazone should be directed on AD-associated insulin-resistant *db/db* mice with hippocampus-dependent mnemonic impairments (Takeda et al., 2010) and pathological AD features (Jolivalt et al., 2008). Indeed, pioglitazone is primarily effective against insulin resistance (Mrak and Landreth, 2004), an AD accelerator (Zhao et al., 2004) partly because of its effects on synaptic plasticity (Gasparini et al., 2002). As such, hemodynamic rescue by pioglitazone in the somatosensory cortex of *db/db* mice might be enough for behavioral improvement, unlike in A/T (here) and APP (Nicolakakis et al., 2008), but like in the human study of diabetic AD patients by Sato et al. 2011. The data

may even call for a higher pioglitazone dose, like that used by Heneka et al. (2005) for increased potency (40mg/kg/day). A treatment starting point at a younger age, i.e. 2 months of age instead of 6 months (here), may also prove to be beneficial for this A/T mouse model, which may well exhibit memory impairment earlier than 6 months of age.

The findings therefore point to earlier therapeutic intervention with, possibly, a higher pioglitazone dose, in the A/T mouse model or even more, a redirected interest towards diabetic mice to assess the cognitive potential of pioglitazone therapy. Indeed, the latest pioglitazone clinical trials in AD patients failed to demonstrate any efficacy (Geldmacher et al., 2011) which, together with our findings, may disprove the hypothesis that cognitive dysfunction is reversible with PPARγ agonist therapy. Clinical and preclinical testing should be henceforth aimed at diabetic AD patients, like in Sato et al. 2011.

3. Effects of simvastatin in A/T mice

Simvastatin was inefficient in restoring mnemonic, cerebrovascular and neuroinflammatory function in adult A/T mice, despite a significant decrease in parenchymal insoluble Aβ (Chapter 4). Simvastatin also failed to rescue neurovascular coupling and silence activated astrocytes and reactive microglia. These findings show limitations for simvastatin therapy on specific indexes of clinical outcome in A/T mice, and possibly in AD patients with vascular diseases defined by TGF-β1 upregulation.

As discussed in Chapter 4, some studies have shown TGF-β1-mediated neuroprotective effects against injury, ischemia and AD pathology in mice or AD patients (Tesseur and Wyss-Coray, 2006, Caraci et al., 2008), but others suggest # neurodegenerative-promoting effects, reduction in hippocampal neurogenesis

(Buckwalter et al., 2006), and impairment of spatial learning in AD mouse models (Town et al., 2005, Salins et al., 2008). A study pointed to the distinction between a temporarily limited and prolonged TGF-β1 augmentation using a tetracycline-regulated gene expression system on a transgenic mouse model with inducible neuron-specific expression of TGF-β1 (Ueberham et al., 2005). Neuroprotective effects were observed after short-term expression of TGF-β1 whereas the consequences of a chronic upregulation, like in our mouse model, were detrimental (Ueberham et al., 2005). Still, TGF mice do not exhibit spatial learning and memory deficits (Papadopoulos et al., 2010, Nicolakakis et al., 2011). As neurogenesis substantially contributes to hippocampal-dependent learning and memory processes (Kee et al., 2007, Dupret et al., 2008, Deng et al., 2009), TGF-β1 overexpression may have aggravated the already reduced neurogenesis primed by the Aβ pathology (Verret et al., 2007, Valero et al., 2011) and decreased the threshold of cognitive activation of A/T mice. Such statement may partly explain why simvastatin was effective in restoring memory in singly APP (Tong et al., 2012) but not A/T-treated mice (Chapter 4).

Another possible explanation, as mentioned in Chapter 4, may pertain to the concurrent stimulation of the survival-related PI3k/Akt pathway by both simvastatin (Wu et al., 2008) and TGF-β1 (Zhu et al. 2004). The overexpression of the latter though may have chronically exacerbated this signaling cascade preventing in turn simvastatin from exerting its neuroprotective effects. Thus, simvastatin and TGF-β1 may have competed for the PI3k/Akt pathway in the expense of memory recovery of A/T mice.

3.1 TGF-β1, a vascular obstacle? Critic of the A/T model

The Rotterdam (Ruitenberg et al., 2005) and Honolulu-Asia Aging (Freitag et al., 2006) studies with respectively lower MCA blood flow velocity or midlife hypertension are examples demonstrating a link between cerebrovascular insults and an increased incidence of dementia in subjects. Vessel occlusion in rats (Farkas et al., 2007, Barros et al., 2009) and vessel stenosis in mice (Miki et al., 2009) have induced impairments in procedural and reference memory tasks, respectively. Nevertheless, the vascular pathology in AD has not earned a causal role in cognitive failure. Instead, it is recognized as an aggravating factor as highlighted by the worsening of memory deficits induced by hypoxia in 8 month-old APP mice chronically exposed to a low-oxygen (8% O2) environment (Sun et al., 2006). Also, rescuing the hemodynamic responses alone with pioglitazone or together with cerebrovascular reactivity as seen after simvastatin treatment supplemented with chitin, a natural biopolymer of N-acetylglucosamine known to reduce CAA (supplemental Figures 1-4) did not suffice to restore cognitive function.

Vascular risk factors have been associated with cognitive decline as early as middle age (Knopman et al., 2009). Chronic TGF-β1 overexpression in mice mimics several aspects of the cerebrovascular AD pathology, justifying TGF-β1 overexpression as our choice for studying the vascular comorbidity added to the amyloidosis pathology of APP mice. The resulting cerebrovascular disturbances in TGF mice include arterial dysfunction as early as 4 months of age (Tong et al., 2005), chronic hypoperfusion at baseline (Gaertner et al., 2005), and impaired neurovascular coupling (Papadopoulos et al., 2010, Nicolakakis et al., 2011). In AD patients, increased levels of TGF-β1 have been reported at a relatively advanced age, the youngest subject being 64 years old and the

oldest, 88 (Wyss-Coray et al., 1997, Grammas and Ovase, 2002). Therefore, bitransgenic A/T mice with an elevated burden of vascular pathology may represent an advanced stage of the human AD pathology and may, possibly, have passed the critical window of opportunity for statin efficacy.

Noteworthily, clinical studies suggest that the onset of treatment and clinical status of the patients are important determinants of statin effectiveness in AD (Wolozin et al., 2000, Wolozin et al., 2007, Arvanitakis and Knopman, 2010). In other words, statins may prove to have a therapeutically favourable impact on AD only if taken early enough in life, such as decades before the clinical manifestations of AD (Arvanitakis and Knopman, 2010).

Nevertheless, aged Tg2576 mice (Li et al., 2006) substantially benefited from a higher dose (50mg/kg/day vs 40mg/kg/day in our study) of simvastatin treatment, a finding that was not reproduced by our group in aged APP mice treated with 40mg/kg/day for 6 months (Tong et al., 2012). As the Tg2576 mouse model carries only the Swedish mutation (Westerman et al., 2002), as opposed to the APP J20 line and the A/T mice that carry the double Swedish and Indiana mutations, the Tg2576 mice may be more amenable to therapeutic benefits, which may point to a possible therapeutic efficacy with simvastatin at a higher dose and/or following earlier and longer interventions. Then again, future preclinical studies should focus on normalizing memory with simvastatin in APP mice with diet-induced hypercholesterolemia, which exhibit worsened hippocampus-dependent mnemonic impairments (Umeda et al., 2012) and AD features (Refolo et al., 2000, Shie et al., 2002) compared to control transgenic mice. As a primary target of statin therapy, but also an AD risk factor and accelerator (Refolo et al., 2000,

Umeda et al., 2012), this study may shed light on the benefits of providing statins to mild to moderate AD patients with elevated cholesterol or triglycerides, which are excluded from clinical studies for safety and ethical reasons (Arvanitakis and Knopman, 2010).

4. Effects of losartan in A/T mice

A most fascinating finding from our study was the mnemonic effectiveness, although modest, exerted by losartan (Chapter 5). Losartan efficacy was dose-specific as only the low dose (10mg/kg/day) significantly improved spatial memory with limited benefit on the learning capacity. Whereas neurovascular coupling to sensory stimulation was not normalized by either dose, the low and high doses demonstrated partial beneficial effects in cerebrovascular reactivity, and no change in amyloidosis was apparent. It remains to be determined whether extension of treatment with the most effective dose may demonstrate complete rescue of both cognitive and cerebrovascular deficits.

As an altered system in dementia (Kehoe et al., 2009), it appears that targeting the RAS comes with great benefits for dementia and warrants further investigation. Losartan was previously evaluated in other studies (Wang et al., 2007, Mogi et al., 2008, Takeda et al., 2009), but none demonstrated its restorative effects in mice recapitulating the broad spectrum of cerebrovascular, neuronal, glial, and cognitive alterations found in AD patients, thereby integrating the comorbid factor of cerebrovascular pathology to that of increased amyloidosis (van der Wal et al., 1993, Zlokovic, 2010). Further, our study emphasized that losartan intervention is feasible in a disease associated with advanced age. Indeed, as mentioned above, we suggest that A/T mice represent a late stage of the pathology since TGF-β1 cytokine has only been reported in patients older than 69, and on average 80 years of age (Flanders et al., 1995, Grammas and Ovase, 2002). Our findings

of losartan therapeutic benefit in A/T mice are in agreement with two clinical studies that highlighted the importance of selectively blocking AT1R as opposed to working upstream from this receptor, with angiotensin converting enzyme (ACE) inhibitors. Indeed, compared to ACE inhibitor lisinopril, telmisartan significantly improved episodic memory and visuospatial abilities in elderly subjects, in parallel to lowering blood pressure (Fogari et al., 2006). Aged subjects taking angiotensin receptor blockers (ARBs) – including losartan – compared to those taking ACE inhibitors had greater reduction in incidence of AD (Li et al., 2010b). Even more, those who switched from an ACE inhibitor to an ARB were at significantly lower risk of incident dementia than those who did not switch further strengthening the therapeutic value of the ARBs assessed (Li et al., 2010b). Noteworthily, these were normotensive subjects, as were our mice (Chapter 5), and so blood pressure changes likely do not account for these beneficial effects.

5. Amyloidosis, a bad correlate of memory recovery

The failure of simvastatin (Chapter 4) to normalize behaviour in A/T mice occurred with significantly reduced brain levels of insoluble Aβ and parenchymal Aβ plaque load. In contrast, losartan (Chapter 5) improved spatial memory despite persistent amyloidosis. On the basis of these results, the lack of relationship between Aβ plaque load and cognitive failure was substantiated. Moreover, these findings evidence that reducing amyloidosis is not necessarily a protective mechanism in halting AD progression, as reinforced in AD patients who underwent $A\beta_{42}$ immunization (Holmes et al., 2008). Studies showing cognitively unaffected elderly individuals having equivalent Aβ plaque densities as AD patients further support the notion that Aβ plaques are not exclusive to cognitively impaired AD patients (Davis et al., 1999). Actually, while reductions of

insoluble Aβ by simvastatin (Chapter 4) occurred despite no behavioral improvement, memory recovery occurred in simvastatin-treated APP mice with persistent amyloidosis (Li et al., 2006, Tong et al., 2012) .

Although not undisputed (Pedersen et al., 2006), soluble Aβ levels may also be considered bad correlates of memory recovery. They not only remained elevated in pioglitazone- and simvastatin- treated A/T mice that did not recover memory, but also in losartan-treated A/T mice (Chapter 5) and simvastatin-treated APP mice (Li et al., 2006, Tong et al., 2012), which displayed spatial learning and memory improvements. Similarly, the Morris watermaze performance of aged Tg2576-treated mice with COX-2 inhibitors was improved, despite no reductions in soluble and insoluble Aβ40, Aβ42 or Aβ56 levels (Kotilinek et al., 2008), the latter oligomer being associated with memory deficits in Tg2576 mice (Lesne et al., 2006).

6. Effects of therapies on vascular reactivity in A/T mice

In A/T mice, decreases in vasodilatory capacity in response to ACh and CGRP incubation were present in all age groups, but showed resistance to antioxidants SOD or apocynin as assessed *ex vivo*, in contrast to APP mice (Nicolakakis et al., 2008). A/T mice also showed a preserved contractile response to ET-1, and a decreased constitutive NO synthesis (Chapter 2).

We anticipated normalization of cerebrovascular function with pioglitazone and simvastatin based on their significant benefits in adult and aged APP (Nicolakakis et al., 2008, Tong et al., 2009, Tong et al., 2012) or TGF (Nicolakakis et al., 2011)(Tong et al. *in preparation*) mice. However, whereas pioglitazone normalized the basal levels of NO, both pioglitazone and simvastatin worsened cerebrovascular dilatory function in treated

A/T mice, and losartan was the only treatment to improve the dilatory responses to ACh and CGRP. The deleterious effects of pioglitazone and simvastatin may result from their ability to dilate blood vessels through direct activation of vasodilatory pathways shared by ACh (Nagaoka et al., 2007, Omae et al., 2011) or blockade of K+ channels through which CGRP induces dilatation (Vedernikov et al., 2002, Yu et al., 2011). The delayed dilatation observed only with the high doses of the NO donor SNP further supports a disruption of dilatory sGC signalling. The question then arises as to why were these negative effects not seen in singly APP or TGF mice? Is there an exacerbation or desensitization of the signaling pathways when both Aβ and TGF-β1 are combined? Could it be that interactions of synergistic effects between Aβ and TGF-β1 increase the complexity of the cerebrovascular alterations making them irresponsive to therapies effective in singly transgenic models? Further investigations are clearly needed to decipher the underlying mechanisms, but these findings likely point to the complexity of the cerebrovascular pathology in the human disease.

Yet, losartan demonstrated positive effects on dilatory function even though the baseline NO production was not rescued by treatment. As discussed in Chapter 5, the multifaceted actions of losartan on oxidative stress, K+ channel signaling and several other channels involved in vascular function (Morel et al., 1996, Akerman et al., 2003) may contribute to these benefits.

Conclusion

As vascular risk factors in midlife have been linked to an increased incidence of dementia (Launer et al., 2000, Whitmer et al., 2005) and cognitive decline in later life (Launer et al., 1995, Carmelli et al., 1998), the use of A/T mice may increase the predictive value of

compounds for AD patients with vascular pathology. As such, based on our results, pioglitazone emerged as a promising strategy to protect altered brain hemodynamics and glucose metabolism, but only in AD patients free of vascular pathology in view of its negative effects on vascular reactivity. Further, our results agree with the growing appreciation that statin efficacy is dependent on the timing of exposure to the patient. The positive outcome of losartan incites further studies to confirm the encouraging losartan-based improvements in cognitive and cerebrovascular function that agree with the benefits reported in clinical studies (Fogari et al., 2006, Li et al., 2010b).

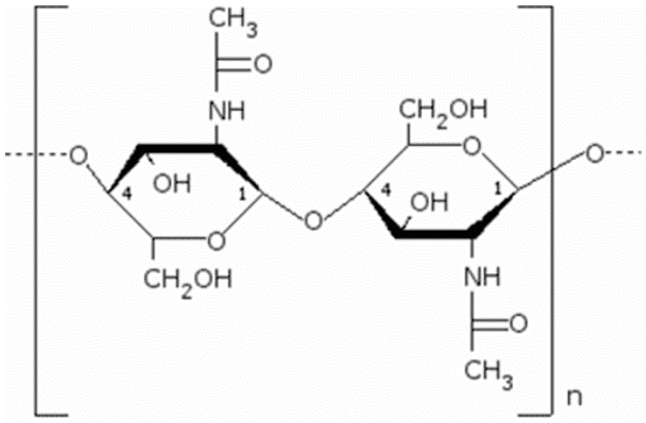

Figure 1 supplemental: As a preliminary study, chitin (1 mg/ml solution) (Hawkes and McLaurin, 2009) or vehicle (0.1 M phosphate buffered saline, PBS) was injected into the lateral ventricle (icv, 10 µl delivered over 20 min) at the stereotaxic coordinates (AP: 0.46 mm, L: 1.1mm and V: 2.2 mm) of WT and simvastatin-treated A/T mice (Chapter 3), while they were anesthetized with ketamine (85 mg/kg, intramuscularly) and xylazine (3 mg/kg). The injection syringe was left in place for 10min. Icv injections were performed twice in 1 month with a 2-week interval, once in each brain hemisphere. Fourteen days after the last injection, mice were used to assess CBF and vascular reactivity.

Chitin, a natural biopolymer of N-acetylglucosamine expressed in the cell walls of fungi, crustaceans, insects, and worms, has recently been shown to decrease CAA in TgCRND 8 APP mice that carry the APP$_{Swe,Ind}$ mutations.

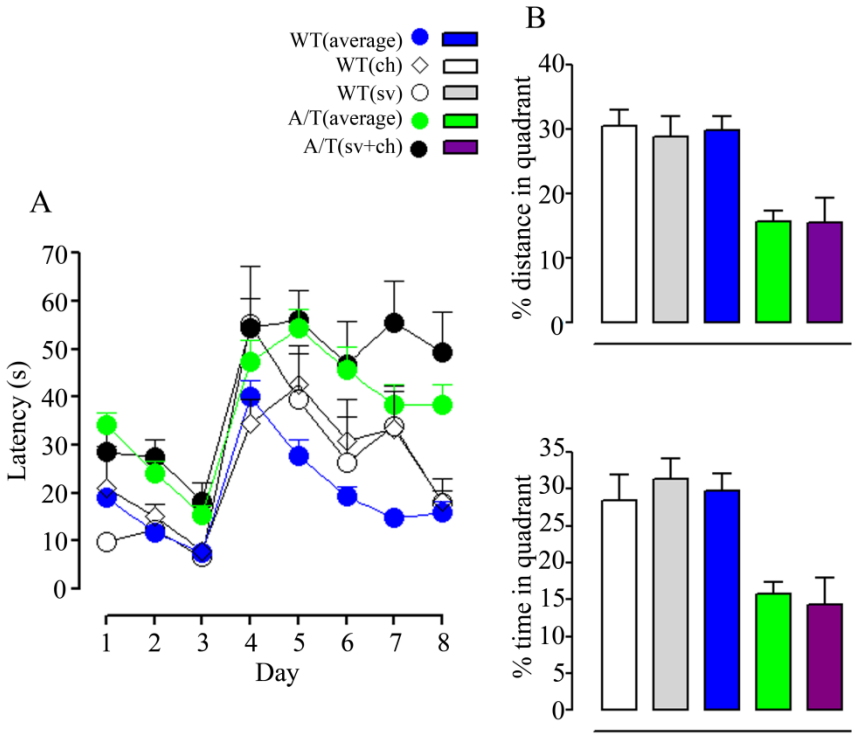

Figure 2 supplemental. Combined simvastatin (sv) and chitin (ch) treatment did not improve spatial learning and memory in A/T mice. ***A,*** All groups of mice had a similar ability in finding the visible platform session (days 1-3). A/T mice (●) displayed impaired learning during hidden-platform testing compared to aged-matched wild-type (WT) mice (●). Sv+ch did not improve this deficit of A/T-treated mice (6 month-old, treated for 3 months,●), and simvastatin (◇) or chitin (○) alone did not affect the performance of WT mice. ***B,*** A/T mice, treated and non-treated with sv+ch displayed significant deficit in memory retention as assessed during the probe trial in the target quadrant. Error bars represent SEM. Averaged escape latencies from previous groups of WT and A/T mice were used (n=10 mice/group).

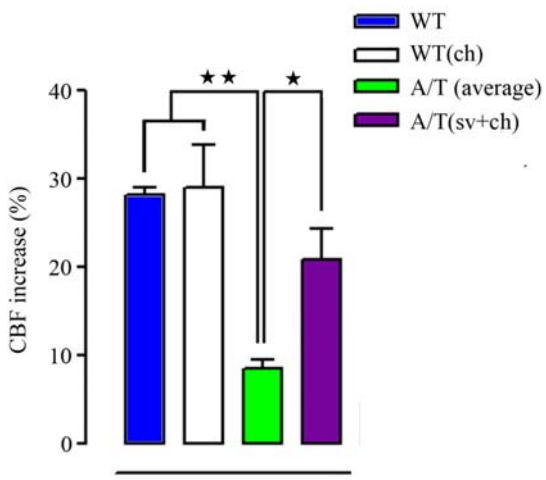

Figure 3 supplemental. Simvastatin+chitin (sv+ch) restored neurovascular coupling in A/T mice. ***A,*** Histogram representing the maximum values of the evoked CBF responses for each group (4-5 stimulations), as measured by LDF. The impaired hyperemic response to whisker stimulation in A/T mice was rescued by simvastatin+chitin. (n=4 mice/group). Values represent the percent increase of CBF response relative to baseline. ★$p<0.05$, ★★$p<0.01$ using two-way ANOVA followed by Newman-Keuls post-hoc test.

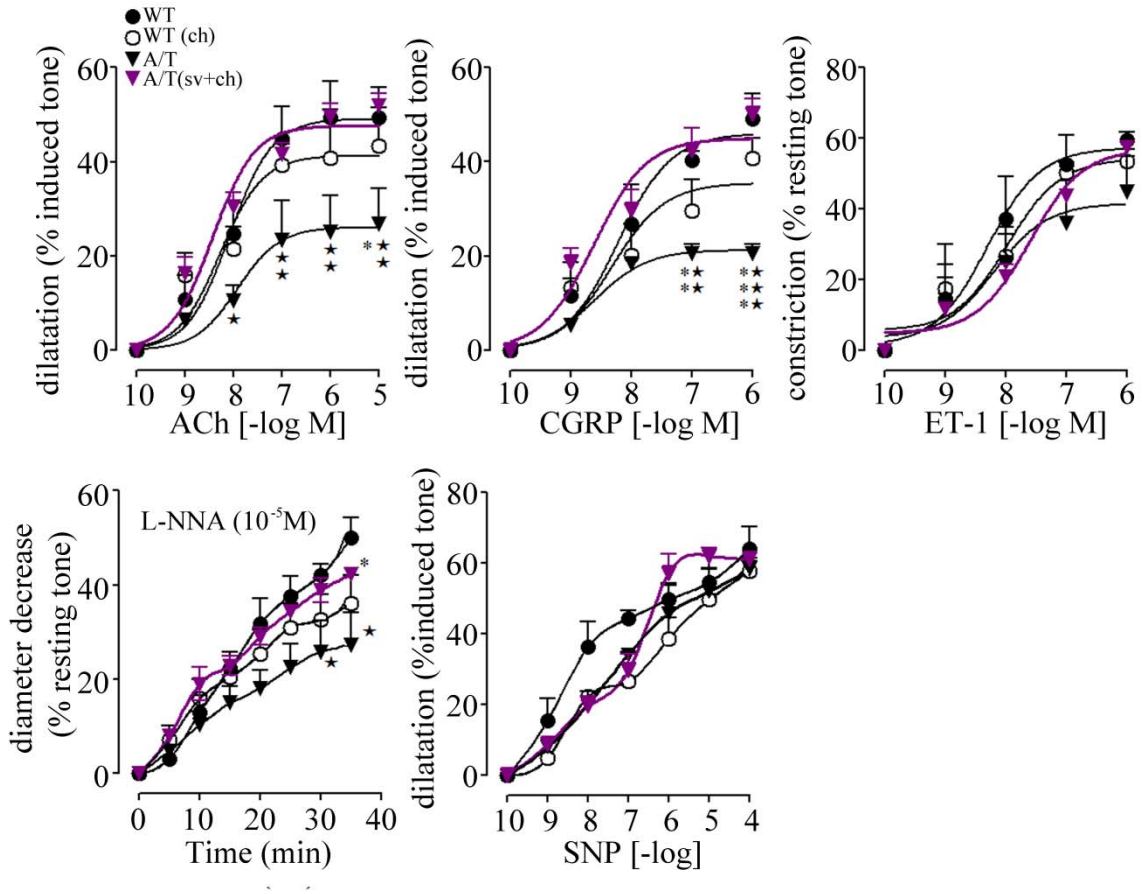

Figure 4 supplemental. Simvastatin+chitin (sv+ch) normalized dilatory function in A/T mice. The impaired dilatations to acetylcholine (ACh) and calcitonin gene-related peptide CGRP in A/T mice (▼) were normalized by sv+ch (▼). Concentration-dependent contractile responses to ET-1 were unaltered in treated- (▼) and untreated- (▼) A/T mice compared to treated- (●) and untreated- (○) WT controls. Baseline NO synthesis and release measured during NOS inhibition (L-NNA, 10^{-5}M) were recovered in sv+ch-treated A/T mice (▼). The dilatations induced by the NO donor SNP were not affected by sv+ch treatment Error bars represent SEM (n=4 for each group). ★$p<0.05$, ★★$p<0.01$, ★★★$p<0.001$ for comparison to WT mice, *$p<0.05$, **$p<0.01$, ***$p<0.001$ for comparison to untreated-A/T mice using two-way ANOVA followed by Newman-Keuls post-hoc test.

References

Abramov AY, Canevari L, Duchen MR (2004) Beta-amyloid peptides induce mitochondrial dysfunction and oxidative stress in astrocytes and death of neurons through activation of NADPH oxidase. The Journal of neuroscience : the official journal of the Society for Neuroscience 24:565-575.

Akerman S, Williamson DJ, Goadsby PJ (2003) Voltage-dependent calcium channels are involved in neurogenic dural vasodilatation via a presynaptic transmitter release mechanism. British journal of pharmacology 140:558-566.

Albiston AL, Fernando RN, Yeatman HR, Burns P, Ng L, Daswani D, Diwakarla S, Pham V, Chai SY (2010) Gene knockout of insulin-regulated aminopeptidase: loss of the specific binding site for angiotensin IV and age-related deficit in spatial memory. Neurobiology of learning and memory 93:19-30.

Annes JP, Munger JS, Rifkin DB (2003) Making sense of latent TGFbeta activation. Journal of cell science 116:217-224.

Arnaiz E, Jelic V, Almkvist O, Wahlund LO, Winblad B, Valind S, Nordberg A (2001) Impaired cerebral glucose metabolism and cognitive functioning predict deterioration in mild cognitive impairment. Neuroreport 12:851-855.

Arnold SE, Hyman BT, Flory J, Damasio AR, Van Hoesen GW (1991) The topographical and neuroanatomical distribution of neurofibrillary tangles and neuritic plaques in the cerebral cortex of patients with Alzheimer's disease. Cereb Cortex 1:103-116.

Arvanitakis Z, Knopman DS (2010) Clinical trial efforts in Alzheimer disease: why test statins? Neurology 74:945-946.

Arvanitakis Z, Schneider JA, Wilson RS, Bienias JL, Kelly JF, Evans DA, Bennett DA (2008) Statins, incident Alzheimer disease, change in cognitive function, and neuropathology. Neurology 70:1795-1802.

Attems J, Quass M, Jellinger KA, Lintner F (2007) Topographical distribution of cerebral amyloid angiopathy and its effect on cognitive decline are influenced by Alzheimer disease pathology. Journal of the neurological sciences 257:49-55.

Aucoin JS, Jiang P, Aznavour N, Tong XK, Buttini M, Descarries L, Hamel E (2005) Selective cholinergic denervation, independent from oxidative stress, in a mouse model of Alzheimer's disease. Neuroscience 132:73-86.

Auld DS, Kornecook TJ, Bastianetto S, Quirion R (2002) Alzheimer's disease and the basal forebrain cholinergic system: relations to beta-amyloid peptides, cognition, and treatment strategies. Progress in neurobiology 68:209-245.

Bagi Z, Koller A, Kaley G (2004) PPARgamma activation, by reducing oxidative stress, increases NO bioavailability in coronary arterioles of mice with Type 2 diabetes. American journal of physiology Heart and circulatory physiology 286:H742-748.

Balducci C, Forloni G (2011) APP transgenic mice: their use and limitations. Neuromolecular medicine 13:117-137.

Bancher C, Braak H, Fischer P, Jellinger KA (1993) Neuropathological staging of Alzheimer lesions and intellectual status in Alzheimer's and Parkinson's disease patients. Neuroscience letters 162:179-182.

Barger SW (2005) Vascular consequences of passive Abeta immunization for Alzheimer's disease. Is avoidance of "malactivation" of microglia enough? Journal of neuroinflammation 2:2.

Barretto RP, Ko TH, Jung JC, Wang TJ, Capps G, Waters AC, Ziv Y, Attardo A, Recht L, Schnitzer MJ (2011) Time-lapse imaging of disease progression in deep brain areas using fluorescence microendoscopy. Nature medicine 17:223-228.

Barros CA, Ekuni R, Moro MA, Pereira FM, Dos Santos Pereira MA, Milani H (2009) The cognitive and histopathological effects of chronic 4-vessel occlusion in rats depend on the set of vessels occluded and the age of the animals. Behavioural brain research 197:378-387.

Bartus RT, Dean RL, Pontecorvo MJ, Flicker C (1985) The cholinergic hypothesis: a historical overview, current perspective, and future directions. Annals of the New York Academy of Sciences 444:332-358.

Bateman GA, Levi CR, Schofield P, Wang Y, Lovett EC (2006) Quantitative measurement of cerebral haemodynamics in early vascular dementia and Alzheimer's disease. Journal of clinical neuroscience : official journal of the Neurosurgical Society of Australasia 13:563-568.

Bell RD, Zlokovic BV (2009) Neurovascular mechanisms and blood-brain barrier disorder in Alzheimer's disease. Acta neuropathologica 118:103-113.

Bennett SA, Pappas BA, Stevens WD, Davidson CM, Fortin T, Chen J (2000) Cleavage of amyloid precursor protein elicited by chronic cerebral hypoperfusion. Neurobiology of aging 21:207-214.

Berchtold NC, Cotman CW (1998) Evolution in the conceptualization of dementia and Alzheimer's disease: Greco-Roman period to the 1960s. Neurobiology of aging 19:173-189.

Bishop-Bailey D, Hla T (1999) Endothelial cell apoptosis induced by the peroxisome proliferator-activated receptor (PPAR) ligand 15-deoxy-Delta12, 14-prostaglandin J2. The Journal of biological chemistry 274:17042-17048.

Blanchard J, Martel G, Guillou JL, Nogues X, Micheau J (2008) Impairment of spatial memory consolidation in APP(751SL) mice results in cue-guided response. Neurobiology of aging 29:1011-1021.

Blessed G, Tomlinson BE, Roth M (1968) The association between quantitative measures of dementia and of senile change in the cerebral grey matter of elderly subjects. The British journal of psychiatry : the journal of mental science 114:797-811.

Bliss TVP, Collingridge GL (1993) A Synaptic Model of Memory - Long-Term Potentiation in the Hippocampus. Nature 361:31-39.

Boche D, Cunningham C, Gauldie J, Perry VH (2003) Transforming growth factor-beta 1-mediated neuroprotection against excitotoxic injury in vivo. Journal of cerebral blood flow and metabolism : official journal of the International Society of Cerebral Blood Flow and Metabolism 23:1174-1182.

Boche D, Zotova E, Weller RO, Love S, Neal JW, Pickering RM, Wilkinson D, Holmes C, Nicoll JA (2008) Consequence of Abeta immunization on the vasculature of human Alzheimer's disease brain. Brain : a journal of neurology 131:3299-3310.

Bolmont T, Haiss F, Eicke D, Radde R, Mathis CA, Klunk WE, Kohsaka S, Jucker M, Calhoun ME (2008) Dynamics of the microglial/amyloid interaction indicate a

role in plaque maintenance. The Journal of neuroscience : the official journal of the Society for Neuroscience 28:4283-4292.
Bottinger EP, Letterio JJ, Roberts AB (1997) Biology of TGF-beta in knockout and transgenic mouse models. Kidney international 51:1355-1360.
Bozon B, Davis S, Laroche S (2003) A requirement for the immediate early gene zif268 in reconsolidation of recognition memory after retrieval. Neuron 40:695-701.
Braak E, Griffing K, Arai K, Bohl J, Bratzke H, Braak H (1999) Neuropathology of Alzheimer's disease: what is new since A. Alzheimer? European archives of psychiatry and clinical neuroscience 249 Suppl 3:14-22.
Brain SD, Grant AD (2004) Vascular actions of calcitonin gene-related peptide and adrenomedullin. Physiological reviews 84:903-934.
Brion JP, Couck AM, Passareiro E, Flament-Durand J (1985) Neurofibrillary tangles of Alzheimer's disease: an immunohistochemical study. Journal of submicroscopic cytology 17:89-96.
Buckner RL, Andrews-Hanna JR, Schacter DL (2008) The brain's default network: anatomy, function, and relevance to disease. Annals of the New York Academy of Sciences 1124:1-38.
Buckner RL, Wheeler ME (2001) The cognitive neuroscience of remembering. Nature reviews Neuroscience 2:624-634.
Buckwalter MS, Wyss-Coray T (2004) Modelling neuroinflammatory phenotypes in vivo. Journal of neuroinflammation 1:10.
Buckwalter MS, Yamane M, Coleman BS, Ormerod BK, Chin JT, Palmer T, Wyss-Coray T (2006) Chronically increased transforming growth factor-beta1 strongly inhibits hippocampal neurogenesis in aged mice. The American journal of pathology 169:154-164.
Burton T, Liang B, Dibrov A, Amara F (2002) Transcriptional activation and increase in expression of Alzheimer's beta-amyloid precursor protein gene is mediated by TGF-beta in normal human astrocytes. Biochemical and biophysical research communications 295:702-712.
Butovsky O, Koronyo-Hamaoui M, Kunis G, Ophir E, Landa G, Cohen H, Schwartz M (2006) Glatiramer acetate fights against Alzheimer's disease by inducing dendritic-like microglia expressing insulin-like growth factor 1. Proceedings of the National Academy of Sciences of the United States of America 103:11784-11789.
Butterfield DA, Barone E, Mancuso C (2011) Cholesterol-independent neuroprotective and neurotoxic activities of statins: perspectives for statin use in Alzheimer disease and other age-related neurodegenerative disorders. Pharmacological research : the official journal of the Italian Pharmacological Society 64:180-186.
Butterfield DA, Drake J, Pocernich C, Castegna A (2001) Evidence of oxidative damage in Alzheimer's disease brain: central role for amyloid beta-peptide. Trends in molecular medicine 7:548-554.
Buxbaum JD, Christensen JL, Ruefli AA, Greengard P, Loring JF (1993) Expression of APP in brains of transgenic mice containing the entire human APP gene. Biochemical and biophysical research communications 197:639-645.

Bye N, Zieba M, Wreford NG, Nichols NR (2001) Resistance of the dentate gyrus to induced apoptosis during ageing is associated with increases in transforming growth factor-beta1 messenger RNA. Neuroscience 105:853-862.

Cao X, Sudhof TC (2001) A transcriptionally [correction of transcriptively] active complex of APP with Fe65 and histone acetyltransferase Tip60. Science 293:115-120.

Caraci F, Battaglia G, Busceti C, Biagioni F, Mastroiacovo F, Bosco P, Drago F, Nicoletti F, Sortino MA, Copani A (2008) TGF-beta 1 protects against Abeta-neurotoxicity via the phosphatidylinositol-3-kinase pathway. Neurobiology of disease 30:234-242.

Carlsson CM, Gleason CE, Hess TM, Moreland KA, Blazel HM, Koscik RL, Schreiber NT, Johnson SC, Atwood CS, Puglielli L, Hermann BP, McBride PE, Stein JH, Sager MA, Asthana S (2008) Effects of simvastatin on cerebrospinal fluid biomarkers and cognition in middle-aged adults at risk for Alzheimer's disease. Journal of Alzheimer's disease : JAD 13:187-197.

Carmelli D, Swan GE, Reed T, Miller B, Wolf PA, Jarvik GP, Schellenberg GD (1998) Midlife cardiovascular risk factors, ApoE, and cognitive decline in elderly male twins. Neurology 50:1580-1585.

Carmignoto G, Gomez-Gonzalo M (2010) The contribution of astrocyte signalling to neurovascular coupling. Brain research reviews 63:138-148.

Castillo GM, Ngo C, Cummings J, Wight TN, Snow AD (1997) Perlecan binds to the beta-amyloid proteins (A beta) of Alzheimer's disease, accelerates A beta fibril formation, and maintains A beta fibril stability. Journal of neurochemistry 69:2452-2465.

Chao CC, Hu S, Frey WH, 2nd, Ala TA, Tourtellotte WW, Peterson PK (1994) Transforming growth factor beta in Alzheimer's disease. Clinical and diagnostic laboratory immunology 1:109-110.

Chartier-Harlin MC, Crawford F, Houlden H, Warren A, Hughes D, Fidani L, Goate A, Rossor M, Roques P, Hardy J, et al. (1991) Early-onset Alzheimer's disease caused by mutations at codon 717 of the beta-amyloid precursor protein gene. Nature 353:844-846.

Chauhan NB, Siegel GJ, Feinstein DL (2004) Effects of lovastatin and pravastatin on amyloid processing and inflammatory response in TgCRND8 brain. Neurochemical research 29:1897-1911.

Chen G, Chen KS, Knox J, Inglis J, Bernard A, Martin SJ, Justice A, McConlogue L, Games D, Freedman SB, Morris RG (2000a) A learning deficit related to age and beta-amyloid plaques in a mouse model of Alzheimer's disease. Nature 408:975-979.

Chen G, Rajkowska G, Du F, Seraji-Bozorgzad N, Manji HK (2000b) Enhancement of hippocampal neurogenesis by lithium. Journal of neurochemistry 75:1729-1734.

Chen J, Zhang ZG, Li Y, Wang Y, Wang L, Jiang H, Zhang C, Lu M, Katakowski M, Feldkamp CS, Chopp M (2003) Statins induce angiogenesis, neurogenesis, and synaptogenesis after stroke. Annals of neurology 53:743-751.

Cheng IH, Scearce-Levie K, Legleiter J, Palop JJ, Gerstein H, Bien-Ly N, Puolivali J, Lesne S, Ashe KH, Muchowski PJ, Mucke L (2007) Accelerating amyloid-beta

fibrillization reduces oligomer levels and functional deficits in Alzheimer disease mouse models. The Journal of biological chemistry 282:23818-23828.

Cheng JS, Dubal DB, Kim DH, Legleiter J, Cheng IH, Yu GQ, Tesseur I, Wyss-Coray T, Bonaldo P, Mucke L (2009) Collagen VI protects neurons against Abeta toxicity. Nature neuroscience 12:119-121.

Chishti MA, Yang DS, Janus C, Phinney AL, Horne P, Pearson J, Strome R, Zuker N, Loukides J, French J, Turner S, Lozza G, Grilli M, Kunicki S, Morissette C, Paquette J, Gervais F, Bergeron C, Fraser PE, Carlson GA, George-Hyslop PS, Westaway D (2001) Early-onset amyloid deposition and cognitive deficits in transgenic mice expressing a double mutant form of amyloid precursor protein 695. The Journal of biological chemistry 276:21562-21570.

Christie R, Yamada M, Moskowitz M, Hyman B (2001) Structural and functional disruption of vascular smooth muscle cells in a transgenic mouse model of amyloid angiopathy. The American journal of pathology 158:1065-1071.

Chuquet J, Quilichini P, Nimchinsky EA, Buzsaki G (2010) Predominant enhancement of glucose uptake in astrocytes versus neurons during activation of the somatosensory cortex. The Journal of neuroscience : the official journal of the Society for Neuroscience 30:15298-15303.

Cimino M, Gelosa P, Gianella A, Nobili E, Tremoli E, Sironi L (2007) Statins: multiple mechanisms of action in the ischemic brain. The Neuroscientist : a review journal bringing neurobiology, neurology and psychiatry 13:208-213.

Ciudin A, Hernandez C, Simo R (2012) Update on Cardiovascular safety of PPARgamma agonists and relevance to medicinal chemistry and clinical pharmacology. Current topics in medicinal chemistry.

Cohn RD, van Erp C, Habashi JP, Soleimani AA, Klein EC, Lisi MT, Gamradt M, ap Rhys CM, Holm TM, Loeys BL, Ramirez F, Judge DP, Ward CW, Dietz HC (2007) Angiotensin II type 1 receptor blockade attenuates TGF-beta-induced failure of muscle regeneration in multiple myopathic states. Nature medicine 13:204-210.

Cole AJ, Saffen DW, Baraban JM, Worley PF (1989) Rapid increase of an immediate early gene messenger RNA in hippocampal neurons by synaptic NMDA receptor activation. Nature 340:474-476.

Coleman P, Federoff H, Kurlan R (2004) A focus on the synapse for neuroprotection in Alzheimer disease and other dementias. Neurology 63:1155-1162.

Cook DG, Leverenz JB, McMillan PJ, Kulstad JJ, Ericksen S, Roth RA, Schellenberg GD, Jin LW, Kovacina KS, Craft S (2003) Reduced hippocampal insulin-degrading enzyme in late-onset Alzheimer's disease is associated with the apolipoprotein E-epsilon4 allele. The American journal of pathology 162:313-319.

Cordle A, Landreth G (2005) 3-Hydroxy-3-methylglutaryl-coenzyme A reductase inhibitors attenuate beta-amyloid-induced microglial inflammatory responses. The Journal of neuroscience : the official journal of the Society for Neuroscience 25:299-307.

Cote S, Carmichael PH, Verreault R, Lindsay J, Lefebvre J, Laurin D (2012) Nonsteroidal anti-inflammatory drug use and the risk of cognitive impairment and

Alzheimer's disease. Alzheimer's & dementia : the journal of the Alzheimer's Association 8:219-226.

Courtney C, Farrell D, Gray R, Hills R, Lynch L, Sellwood E, Edwards S, Hardyman W, Raftery J, Crome P, Lendon C, Shaw H, Bentham P (2004) Long-term donepezil treatment in 565 patients with Alzheimer's disease (AD2000): randomised double-blind trial. Lancet 363:2105-2115.

Cramer C, Haan MN, Galea S, Langa KM, Kalbfleisch JD (2008) Use of statins and incidence of dementia and cognitive impairment without dementia in a cohort study. Neurology 71:344-350.

Cummings JL (2004) Alzheimer's disease. The New England journal of medicine 351:56-67.

D'Hooge R, De Deyn PP (2001) Applications of the Morris water maze in the study of learning and memory. Brain research Brain research reviews 36:60-90.

Danielyan L, Klein R, Hanson LR, Buadze M, Schwab M, Gleiter CH, Frey WH (2010) Protective effects of intranasal losartan in the APP/PS1 transgenic mouse model of Alzheimer disease. Rejuvenation research 13:195-201.

Davis DG, Schmitt FA, Wekstein DR, Markesbery WR (1999) Alzheimer neuropathologic alterations in aged cognitively normal subjects. Journal of neuropathology and experimental neurology 58:376-388.

Davis HP, Squire LR (1984) Protein-Synthesis and Memory - a Review. Psychol Bull 96:518-559.

Davis S, Bozon B, Laroche S (2003) How necessary is the activation of the immediate early gene zif268 in synaptic plasticity and learning? Behavioural brain research 142:17-30.

de la Torre JC (1999) Critical threshold cerebral hypoperfusion causes Alzheimer's disease? Acta neuropathologica 98:1-8.

de la Torre JC (2004) Is Alzheimer's disease a neurodegenerative or a vascular disorder? Data, dogma, and dialectics. Lancet neurology 3:184-190.

Deane R, Du Yan S, Submamaryan RK, LaRue B, Jovanovic S, Hogg E, Welch D, Manness L, Lin C, Yu J, Zhu H, Ghiso J, Frangione B, Stern A, Schmidt AM, Armstrong DL, Arnold B, Liliensiek B, Nawroth P, Hofman F, Kindy M, Stern D, Zlokovic B (2003) RAGE mediates amyloid-beta peptide transport across the blood-brain barrier and accumulation in brain. Nature medicine 9:907-913.

Deipolyi AR, Fang S, Palop JJ, Yu GQ, Wang X, Mucke L (2008) Altered navigational strategy use and visuospatial deficits in hAPP transgenic mice. Neurobiology of aging 29:253-266.

Dello Russo C, Gavrilyuk V, Weinberg G, Almeida A, Bolanos JP, Palmer J, Pelligrino D, Galea E, Feinstein DL (2003) Peroxisome proliferator-activated receptor gamma thiazolidinedione agonists increase glucose metabolism in astrocytes. The Journal of biological chemistry 278:5828-5836.

Deng W, Saxe MD, Gallina IS, Gage FH (2009) Adult-born hippocampal dentate granule cells undergoing maturation modulate learning and memory in the brain. The Journal of neuroscience : the official journal of the Society for Neuroscience 29:13532-13542.

Deshpande A, Mina E, Glabe C, Busciglio J (2006) Different conformations of amyloid beta induce neurotoxicity by distinct mechanisms in human cortical neurons. The

Journal of neuroscience : the official journal of the Society for Neuroscience 26:6011-6018.
Deutsch JA (1971) The cholinergic synapse and the site of memory. Science 174:788-794.
Deutsch JA, Hamburg MD, Dahl H (1966) Anticholinesterase-induced amnesia and its temporal aspects. Science 151:221-223.
Dhandapani KM, Brann DW (2003) Transforming growth factor-beta: a neuroprotective factor in cerebral ischemia. Cell biochemistry and biophysics 39:13-22.
Dickerson BC, Eichenbaum H (2010) The episodic memory system: neurocircuitry and disorders. Neuropsychopharmacology : official publication of the American College of Neuropsychopharmacology 35:86-104.
Dickey CA, Loring JF, Montgomery J, Gordon MN, Eastman PS, Morgan D (2003) Selectively reduced expression of synaptic plasticity-related genes in amyloid precursor protein + presenilin-1 transgenic mice. The Journal of neuroscience : the official journal of the Society for Neuroscience 23:5219-5226.
Diep QN, Amiri F, Touyz RM, Cohn JS, Endemann D, Neves MF, Schiffrin EL (2002) PPARalpha activator effects on Ang II-induced vascular oxidative stress and inflammation. Hypertension 40:866-871.
Dodart JC, May P (2005) Overview on rodent models of Alzheimer's disease. Current protocols in neuroscience / editorial board, Jacqueline N Crawley [et al] Chapter 9:Unit 9 22.
Donovan MH, Yazdani U, Norris RD, Games D, German DC, Eisch AJ (2006) Decreased adult hippocampal neurogenesis in the PDAPP mouse model of Alzheimer's disease. The Journal of comparative neurology 495:70-83.
Drapeau E, Mayo W, Aurousseau C, Le Moal M, Piazza PV, Abrous DN (2003) Spatial memory performances of aged rats in the water maze predict levels of hippocampal neurogenesis. Proceedings of the National Academy of Sciences of the United States of America 100:14385-14390.
Drouin A, Bolduc V, Thorin-Trescases N, Belanger E, Fernandes P, Baraghis E, Lesage F, Gillis MA, Villeneuve L, Hamel E, Ferland G, Thorin E (2011) Catechin treatment improves cerebrovascular flow-mediated dilation and learning abilities in atherosclerotic mice. American journal of physiology Heart and circulatory physiology 300:H1032-1043.
Drouin A, Thorin-Trescases N, Hamel E, Falck JR, Thorin E (2007) Endothelial nitric oxide synthase activation leads to dilatory H2O2 production in mouse cerebral arteries. Cardiovascular research 73:73-81.
Drzezga A, Grimmer T, Riemenschneider M, Lautenschlager N, Siebner H, Alexopoulus P, Minoshima S, Schwaiger M, Kurz A (2005) Prediction of individual clinical outcome in MCI by means of genetic assessment and (18)F-FDG PET. Journal of nuclear medicine : official publication, Society of Nuclear Medicine 46:1625-1632.
Dupret D, Revest JM, Koehl M, Ichas F, De Giorgi F, Costet P, Abrous DN, Piazza PV (2008) Spatial relational memory requires hippocampal adult neurogenesis. PloS one 3:e1959.
Duron E, Hanon O (2008) Vascular risk factors, cognitive decline, and dementia. Vascular health and risk management 4:363-381.

Duron E, Rigaud AS, Dubail D, Mehrabian S, Latour F, Seux ML, Hanon O (2009) Effects of antihypertensive therapy on cognitive decline in Alzheimer's disease. American journal of hypertension 22:1020-1024.

Elhusseiny A, Hamel E (2000) Muscarinic--but not nicotinic--acetylcholine receptors mediate a nitric oxide-dependent dilation in brain cortical arterioles: a possible role for the M5 receptor subtype. Journal of cerebral blood flow and metabolism : official journal of the International Society of Cerebral Blood Flow and Metabolism 20:298-305.

Esch FS, Keim PS, Beattie EC, Blacher RW, Culwell AR, Oltersdorf T, McClure D, Ward PJ (1990) Cleavage of amyloid beta peptide during constitutive processing of its precursor. Science 248:1122-1124.

Escribano L, Simon AM, Gimeno E, Cuadrado-Tejedor M, Lopez de Maturana R, Garcia-Osta A, Ricobaraza A, Perez-Mediavilla A, Del Rio J, Frechilla D (2010) Rosiglitazone rescues memory impairment in Alzheimer's transgenic mice: mechanisms involving a reduced amyloid and tau pathology. Neuropsychopharmacology : official publication of the American College of Neuropsychopharmacology 35:1593-1604.

Farkas E, Luiten PG (2001) Cerebral microvascular pathology in aging and Alzheimer's disease. Progress in neurobiology 64:575-611.

Farkas E, Luiten PG, Bari F (2007) Permanent, bilateral common carotid artery occlusion in the rat: a model for chronic cerebral hypoperfusion-related neurodegenerative diseases. Brain research reviews 54:162-180.

Farris W, Schutz SG, Cirrito JR, Shankar GM, Sun X, George A, Leissring MA, Walsh DM, Qiu WQ, Holtzman DM, Selkoe DJ (2007) Loss of neprilysin function promotes amyloid plaque formation and causes cerebral amyloid angiopathy. The American journal of pathology 171:241-251.

Fassbender K, Simons M, Bergmann C, Stroick M, Lutjohann D, Keller P, Runz H, Kuhl S, Bertsch T, von Bergmann K, Hennerici M, Beyreuther K, Hartmann T (2001) Simvastatin strongly reduces levels of Alzheimer's disease beta -amyloid peptides Abeta 42 and Abeta 40 in vitro and in vivo. Proceedings of the National Academy of Sciences of the United States of America 98:5856-5861.

Feldman HH, Doody RS, Kivipelto M, Sparks DL, Waters DD, Jones RW, Schwam E, Schindler R, Hey-Hadavi J, DeMicco DA, Breazna A (2010) Randomized controlled trial of atorvastatin in mild to moderate Alzheimer disease: LEADe. Neurology 74:956-964.

Fellows LK (2011) Orbitofrontal contributions to value-based decision making: evidence from humans with frontal lobe damage. Annals of the New York Academy of Sciences 1239:51-58.

Ferretti MT, Cuello AC (2011) Does a pro-inflammatory process precede Alzheimer's disease and mild cognitive impairment? Current Alzheimer research 8:164-174.

Fiala M, Lin J, Ringman J, Kermani-Arab V, Tsao G, Patel A, Lossinsky AS, Graves MC, Gustavson A, Sayre J, Sofroni E, Suarez T, Chiappelli F, Bernard G (2005) Ineffective phagocytosis of amyloid-beta by macrophages of Alzheimer's disease patients. Journal of Alzheimer's disease : JAD 7:221-232; discussion 255-262.

Finch CE, Laping NJ, Morgan TE, Nichols NR, Pasinetti GM (1993) TGF-beta 1 is an organizer of responses to neurodegeneration. Journal of cellular biochemistry 53:314-322.

Fiorentini A, Rosi MC, Grossi C, Luccarini I, Casamenti F (2010) Lithium improves hippocampal neurogenesis, neuropathology and cognitive functions in APP mutant mice. PloS one 5:e14382.

Flanders KC, Lippa CF, Smith TW, Pollen DA, Sporn MB (1995) Altered expression of transforming growth factor-beta in Alzheimer's disease. Neurology 45:1561-1569.

Fogari R, Mugellini A, Zoppi A, Lazzari P, Destro M, Rinaldi A, Preti P (2006) Effect of telmisartan/hydrochlorothiazide vs lisinopril/hydrochlorothiazide combination on ambulatory blood pressure and cognitive function in elderly hypertensive patients. Journal of human hypertension 20:177-185.

Forette F, Seux ML, Staessen JA, Thijs L, Babarskiene MR, Babeanu S, Bossini A, Fagard R, Gil-Extremera B, Laks T, Kobalava Z, Sarti C, Tuomilehto J, Vanhanen H, Webster J, Yodfat Y, Birkenhager WH (2002) The prevention of dementia with antihypertensive treatment: new evidence from the Systolic Hypertension in Europe (Syst-Eur) study. Archives of internal medicine 162:2046-2052.

Frank-Cannon TC, Alto LT, McAlpine FE, Tansey MG (2009) Does neuroinflammation fan the flame in neurodegenerative diseases? Molecular neurodegeneration 4:47.

Franklin KBJ, Paxinos G (1997) The mouse brain in stereotaxic coordinates. San Diego: Academic Press.

Freeman FM, Rose SP, Scholey AB (1995) Two time windows of anisomycin-induced amnesia for passive avoidance training in the day-old chick. Neurobiology of learning and memory 63:291-295.

Freitag MH, Peila R, Masaki K, Petrovitch H, Ross GW, White LR, Launer LJ (2006) Midlife pulse pressure and incidence of dementia: the Honolulu-Asia Aging Study. Stroke; a journal of cerebral circulation 37:33-37.

Frey U, Krug M, Reymann KG, Matthies H (1988) Anisomycin, an inhibitor of protein synthesis, blocks late phases of LTP phenomena in the hippocampal CA1 region in vitro. Brain research 452:57-65.

Friedhoff LT, Cullen EI, Geoghagen NS, Buxbaum JD (2001) Treatment with controlled-release lovastatin decreases serum concentrations of human beta-amyloid (A beta) peptide. Int J Neuropsychopharmacol 4:127-130.

Fu M, Zhang J, Zhu X, Myles DE, Willson TM, Liu X, Chen YE (2001) Peroxisome proliferator-activated receptor gamma inhibits transforming growth factor beta-induced connective tissue growth factor expression in human aortic smooth muscle cells by interfering with Smad3. The Journal of biological chemistry 276:45888-45894.

Fukuyama H, Ogawa M, Yamauchi H, Yamaguchi S, Kimura J, Yonekura Y, Konishi J (1994) Altered cerebral energy metabolism in Alzheimer's disease: a PET study. Journal of nuclear medicine : official publication, Society of Nuclear Medicine 35:1-6.

Gaertner RF, Wyss-Coray T, Von Euw D, Lesne S, Vivien D, Lacombe P (2005) Reduced brain tissue perfusion in TGF-beta 1 transgenic mice showing

Alzheimer's disease-like cerebrovascular abnormalities. Neurobiology of disease 19:38-46.
Galea E, Feinstein DL, Lacombe P (2006) Pioglitazone does not increase cerebral glucose utilisation in a murine model of Alzheimer's disease and decreases it in wild-type mice. Diabetologia 49:2153-2161.
Gard PR (2008) Cognitive-enhancing effects of angiotensin IV. BMC neuroscience 9 Suppl 2:S15.
Gasparini L, Netzer WJ, Greengard P, Xu H (2002) Does insulin dysfunction play a role in Alzheimer's disease? Trends in pharmacological sciences 23:288-293.
Geldmacher DS, Fritsch T, McClendon MJ, Landreth G (2011) A randomized pilot clinical trial of the safety of pioglitazone in treatment of patients with Alzheimer disease. Archives of neurology 68:45-50.
Geula C, Mesulam MM (1989) Cortical cholinergic fibers in aging and Alzheimer's disease: a morphometric study. Neuroscience 33:469-481.
Giannakopoulos P, Herrmann FR, Bussiere T, Bouras C, Kovari E, Perl DP, Morrison JH, Gold G, Hof PR (2003) Tangle and neuron numbers, but not amyloid load, predict cognitive status in Alzheimer's disease. Neurology 60:1495-1500.
Girouard H, Iadecola C (2006) Neurovascular coupling in the normal brain and in hypertension, stroke, and Alzheimer disease. J Appl Physiol 100:328-335.
Glenner GG, Wong CW (1984a) Alzheimer's disease and Down's syndrome: sharing of a unique cerebrovascular amyloid fibril protein. Biochemical and biophysical research communications 122:1131-1135.
Glenner GG, Wong CW (1984b) Alzheimer's disease: initial report of the purification and characterization of a novel cerebrovascular amyloid protein. Biochemical and biophysical research communications 120:885-890.
Goate A, Chartier-Harlin MC, Mullan M, Brown J, Crawford F, Fidani L, Giuffra L, Haynes A, Irving N, James L, et al. (1991) Segregation of a missense mutation in the amyloid precursor protein gene with familial Alzheimer's disease. Nature 349:704-706.
Goedert M, Spillantini MG (2006) A century of Alzheimer's disease. Science 314:777-781.
Goldgaber D, Lerman MI, McBride OW, Saffiotti U, Gajdusek DC (1987) Characterization and chromosomal localization of a cDNA encoding brain amyloid of Alzheimer's disease. Science 235:877-880.
Grammas P, Ovase R (2002) Cerebrovascular transforming growth factor-beta contributes to inflammation in the Alzheimer's disease brain. The American journal of pathology 160:1583-1587.
Grundke-Iqbal I, Iqbal K, Quinlan M, Tung YC, Zaidi MS, Wisniewski HM (1986a) Microtubule-associated protein tau. A component of Alzheimer paired helical filaments. The Journal of biological chemistry 261:6084-6089.
Grundke-Iqbal I, Iqbal K, Tung YC, Quinlan M, Wisniewski HM, Binder LI (1986b) Abnormal phosphorylation of the microtubule-associated protein tau (tau) in Alzheimer cytoskeletal pathology. Proceedings of the National Academy of Sciences of the United States of America 83:4913-4917.

Guo Z, Viitanen M, Winblad B, Fratiglioni L (1999) Low blood pressure and incidence of dementia in a very old sample: dependent on initial cognition. Journal of the American Geriatrics Society 47:723-726.

Guzowski JF, Setlow B, Wagner EK, McGaugh JL (2001) Experience-dependent gene expression in the rat hippocampus after spatial learning: a comparison of the immediate-early genes Arc, c-fos, and zif268. The Journal of neuroscience : the official journal of the Society for Neuroscience 21:5089-5098.

Haag MD, Hofman A, Koudstaal PJ, Stricker BH, Breteler MM (2009) Statins are associated with a reduced risk of Alzheimer disease regardless of lipophilicity. The Rotterdam Study. Journal of neurology, neurosurgery, and psychiatry 80:13-17.

Haass C, Schlossmacher MG, Hung AY, Vigo-Pelfrey C, Mellon A, Ostaszewski BL, Lieberburg I, Koo EH, Schenk D, Teplow DB, et al. (1992) Amyloid beta-peptide is produced by cultured cells during normal metabolism. Nature 359:322-325.

Hajjar IM, Keown M, Lewis P, Almor A (2008) Angiotensin converting enzyme inhibitors and cognitive and functional decline in patients with Alzheimer's disease: an observational study. American journal of Alzheimer's disease and other dementias 23:77-83.

Hall J, Thomas KL, Everitt BJ (2001) Cellular imaging of zif268 expression in the hippocampus and amygdala during contextual and cued fear memory retrieval: selective activation of hippocampal CA1 neurons during the recall of contextual memories. The Journal of neuroscience : the official journal of the Society for Neuroscience 21:2186-2193.

Hamel E (2004) Cholinergic modulation of the cortical microvascular bed. Progress in brain research 145:171-178.

Hamel E (2006) Perivascular nerves and the regulation of cerebrovascular tone. J Appl Physiol 100:1059-1064.

Hamel E, Nicolakakis N, Aboulkassim T, Ongali B, Tong XK (2008) Oxidative stress and cerebrovascular dysfunction in mouse models of Alzheimer's disease. Experimental physiology 93:116-120.

Hampel H, Blennow K, Shaw LM, Hoessler YC, Zetterberg H, Trojanowski JQ (2010) Total and phosphorylated tau protein as biological markers of Alzheimer's disease. Experimental gerontology 45:30-40.

Han BH, Zhou ML, Abousaleh F, Brendza RP, Dietrich HH, Koenigsknecht-Talboo J, Cirrito JR, Milner E, Holtzman DM, Zipfel GJ (2008) Cerebrovascular dysfunction in amyloid precursor protein transgenic mice: contribution of soluble and insoluble amyloid-beta peptide, partial restoration via gamma-secretase inhibition. The Journal of neuroscience : the official journal of the Society for Neuroscience 28:13542-13550.

Hanyu H, Sato T, Kiuchi A, Sakurai H, Iwamoto T (2009) Pioglitazone improved cognition in a pilot study on patients with Alzheimer's disease and mild cognitive impairment with diabetes mellitus. Journal of the American Geriatrics Society 57:177-179.

Hardy J, Selkoe DJ (2002) The amyloid hypothesis of Alzheimer's disease: progress and problems on the road to therapeutics. Science 297:353-356.

Harrison FE, Hosseini AH, McDonald MP (2009) Endogenous anxiety and stress responses in water maze and Barnes maze spatial memory tasks. Behavioural brain research 198:247-251.

Harrison FE, Reiserer RS, Tomarken AJ, McDonald MP (2006) Spatial and nonspatial escape strategies in the Barnes maze. Learn Mem 13:809-819.

Harrison RV, Harel N, Panesar J, Mount RJ (2002) Blood capillary distribution correlates with hemodynamic-based functional imaging in cerebral cortex. Cereb Cortex 12:225-233.

Haughey NJ, Nath A, Chan SL, Borchard AC, Rao MS, Mattson MP (2002) Disruption of neurogenesis by amyloid beta-peptide, and perturbed neural progenitor cell homeostasis, in models of Alzheimer's disease. Journal of neurochemistry 83:1509-1524.

Hawkes CA, McLaurin J (2009) Selective targeting of perivascular macrophages for clearance of beta-amyloid in cerebral amyloid angiopathy. Proceedings of the National Academy of Sciences of the United States of America 106:1261-1266.

Hayabuchi Y, Davies NW, Standen NB (2001) Angiotensin II inhibits rat arterial KATP channels by inhibiting steady-state protein kinase A activity and activating protein kinase Ce. The Journal of physiology 530:193-205.

Haydon PG, Carmignoto G (2006) Astrocyte control of synaptic transmission and neurovascular coupling. Physiological reviews 86:1009-1031.

Hebb DO (1949) The organization of behavior; a neuropsychological theory. New York,: Wiley.

Heneka MT, Sastre M, Dumitrescu-Ozimek L, Hanke A, Dewachter I, Kuiperi C, O'Banion K, Klockgether T, Van Leuven F, Landreth GE (2005) Acute treatment with the PPARgamma agonist pioglitazone and ibuprofen reduces glial inflammation and Abeta1-42 levels in APPV717I transgenic mice. Brain : a journal of neurology 128:1442-1453.

Herzig MC, Van Nostrand WE, Jucker M (2006) Mechanism of cerebral beta-amyloid angiopathy: murine and cellular models. Brain Pathol 16:40-54.

Herzig MC, Winkler DT, Burgermeister P, Pfeifer M, Kohler E, Schmidt SD, Danner S, Abramowski D, Sturchler-Pierrat C, Burki K, van Duinen SG, Maat-Schieman ML, Staufenbiel M, Mathews PM, Jucker M (2004) Abeta is targeted to the vasculature in a mouse model of hereditary cerebral hemorrhage with amyloidosis. Nature neuroscience 7:954-960.

Hilgetag CC, Barbas H (2009) Are there ten times more glia than neurons in the brain? Brain structure & function 213:365-366.

Ho L, Fukuchi K, Younkin SG (1996) The alternatively spliced Kunitz protease inhibitor domain alters amyloid beta protein precursor processing and amyloid beta protein production in cultured cells. The Journal of biological chemistry 271:30929-30934.

Hock C, Villringer K, Muller-Spahn F, Wenzel R, Heekeren H, Schuh-Hofer S, Hofmann M, Minoshima S, Schwaiger M, Dirnagl U, Villringer A (1997) Decrease in parietal cerebral hemoglobin oxygenation during performance of a verbal fluency task in patients with Alzheimer's disease monitored by means of near-infrared spectroscopy (NIRS)--correlation with simultaneous rCBF-PET measurements. Brain research 755:293-303.

Hoffman JM, Welsh-Bohmer KA, Hanson M, Crain B, Hulette C, Earl N, Coleman RE (2000) FDG PET imaging in patients with pathologically verified dementia. Journal of nuclear medicine : official publication, Society of Nuclear Medicine 41:1920-1928.

Holmes C, Boche D, Wilkinson D, Yadegarfar G, Hopkins V, Bayer A, Jones RW, Bullock R, Love S, Neal JW, Zotova E, Nicoll JA (2008) Long-term effects of Abeta42 immunisation in Alzheimer's disease: follow-up of a randomised, placebo-controlled phase I trial. Lancet 372:216-223.

Hong KW, Yoo SE, Yu SS, Lee JY, Rhim BY (1996) Pharmacological coupling and functional role for CGRP receptors in the vasodilation of rat pial arterioles. The American journal of physiology 270:H317-323.

Hsia AY, Masliah E, McConlogue L, Yu GQ, Tatsuno G, Hu K, Kholodenko D, Malenka RC, Nicoll RA, Mucke L (1999) Plaque-independent disruption of neural circuits in Alzheimer's disease mouse models. Proceedings of the National Academy of Sciences of the United States of America 96:3228-3233.

Hsiao KK, Borchelt DR, Olson K, Johannsdottir R, Kitt C, Yunis W, Xu S, Eckman C, Younkin S, Price D, et al. (1995) Age-related CNS disorder and early death in transgenic FVB/N mice overexpressing Alzheimer amyloid precursor proteins. Neuron 15:1203-1218.

Hunyady L, Catt KJ (2006) Pleiotropic AT1 receptor signaling pathways mediating physiological and pathogenic actions of angiotensin II. Mol Endocrinol 20:953-970.

Iadecola C (2004) Neurovascular regulation in the normal brain and in Alzheimer's disease. Nature reviews Neuroscience 5:347-360.

Iadecola C, Nedergaard M (2007) Glial regulation of the cerebral microvasculature. Nature neuroscience 10:1369-1376.

Iadecola C, Zhang F, Niwa K, Eckman C, Turner SK, Fischer E, Younkin S, Borchelt DR, Hsiao KK, Carlson GA (1999) SOD1 rescues cerebral endothelial dysfunction in mice overexpressing amyloid precursor protein. Nature neuroscience 2:157-161.

Iesaki T, Gupte SA, Kaminski PM, Wolin MS (1999) Inhibition of guanylate cyclase stimulation by NO and bovine arterial relaxation to peroxynitrite and H2O2. The American journal of physiology 277:H978-985.

Ignotz RA, Massague J (1986) Transforming growth factor-beta stimulates the expression of fibronectin and collagen and their incorporation into the extracellular matrix. The Journal of biological chemistry 261:4337-4345.

Imayoshi I, Sakamoto M, Ohtsuka T, Takao K, Miyakawa T, Yamaguchi M, Mori K, Ikeda T, Itohara S, Kageyama R (2008) Roles of continuous neurogenesis in the structural and functional integrity of the adult forebrain. Nature neuroscience 11:1153-1161.

in't Veld BA, Ruitenberg A, Hofman A, Stricker BH, Breteler MM (2001) Antihypertensive drugs and incidence of dementia: the Rotterdam Study. Neurobiology of aging 22:407-412.

Iqbal K, Grundke-Iqbal I, Smith AJ, George L, Tung YC, Zaidi T (1989) Identification and localization of a tau peptide to paired helical filaments of Alzheimer disease.

Proceedings of the National Academy of Sciences of the United States of America 86:5646-5650.
Itoh A, Akaike T, Sokabe M, Nitta A, Iida R, Olariu A, Yamada K, Nabeshima T (1999) Impairments of long-term potentiation in hippocampal slices of beta-amyloid-infused rats. European journal of pharmacology 382:167-175.
Itoh S, Itoh F, Goumans MJ, Ten Dijke P (2000) Signaling of transforming growth factor-beta family members through Smad proteins. European journal of biochemistry / FEBS 267:6954-6967.
Izawa Y, Takahashi S, Suzuki N (2009) Pioglitazone enhances pyruvate and lactate oxidation in cultured neurons but not in cultured astroglia. Brain research 1305:64-73.
Jaffar S, Counts SE, Ma SY, Dadko E, Gordon MN, Morgan D, Mufson EJ (2001) Neuropathology of mice carrying mutant APP(swe) and/or PS1(M146L) transgenes: alterations in the p75(NTR) cholinergic basal forebrain septohippocampal pathway. Experimental neurology 170:227-243.
Jagust W, Reed B, Mungas D, Ellis W, Decarli C (2007) What does fluorodeoxyglucose PET imaging add to a clinical diagnosis of dementia? Neurology 69:871-877.
Janus C, Westaway D (2001) Transgenic mouse models of Alzheimer's disease. Physiology & behavior 73:873-886.
Jhoo JH, Kim HC, Nabeshima T, Yamada K, Shin EJ, Jhoo WK, Kim W, Kang KS, Jo SA, Woo JI (2004) Beta-amyloid (1-42)-induced learning and memory deficits in mice: involvement of oxidative burdens in the hippocampus and cerebral cortex. Behavioural brain research 155:185-196.
Jick H, Zornberg GL, Jick SS, Seshadri S, Drachman DA (2000) Statins and the risk of dementia. Lancet 356:1627-1631.
Johnston MV, McKinney M, Coyle JT (1981) Neocortical cholinergic innervation: a description of extrinsic and intrinsic components in the rat. Experimental brain research Experimentelle Hirnforschung Experimentation cerebrale 43:159-172.
Jolivalt CG, Lee CA, Beiswenger KK, Smith JL, Orlov M, Torrance MA, Masliah E (2008) Defective insulin signaling pathway and increased glycogen synthase kinase-3 activity in the brain of diabetic mice: parallels with Alzheimer's disease and correction by insulin. Journal of neuroscience research 86:3265-3274.
Jones MW, Errington ML, French PJ, Fine A, Bliss TV, Garel S, Charnay P, Bozon B, Laroche S, Davis S (2001) A requirement for the immediate early gene Zif268 in the expression of late LTP and long-term memories. Nature neuroscience 4:289-296.
Kalaria RN (2000) The role of cerebral ischemia in Alzheimer's disease. Neurobiology of aging 21:321-330.
Kalaria RN, Harik SI (1989) Reduced glucose transporter at the blood-brain barrier and in cerebral cortex in Alzheimer disease. Journal of neurochemistry 53:1083-1088.
Kalaria RN, Maestre GE, Arizaga R, Friedland RP, Galasko D, Hall K, Luchsinger JA, Ogunniyi A, Perry EK, Potocnik F, Prince M, Stewart R, Wimo A, Zhang ZX, Antuono P (2008) Alzheimer's disease and vascular dementia in developing countries: prevalence, management, and risk factors. Lancet neurology 7:812-826.
Kalaria RN, Pax AB (1995) Increased collagen content of cerebral microvessels in Alzheimer's disease. Brain research 705:349-352.

Kalueff AV, Wheaton M, Murphy DL (2007) What's wrong with my mouse model? Advances and strategies in animal modeling of anxiety and depression. Behavioural brain research 179:1-18.

Kamenetz F, Tomita T, Hsieh H, Seabrook G, Borchelt D, Iwatsubo T, Sisodia S, Malinow R (2003) APP processing and synaptic function. Neuron 37:925-937.

Kandel ER (2001a) The molecular biology of memory storage: A dialog between genes and synapses. Bioscience Rep 21:565-611.

Kandel ER (2001b) Neuroscience - The molecular biology of memory storage: A dialogue between genes and synapses. Science 294:1030-1038.

Kang J, Lemaire HG, Unterbeck A, Salbaum JM, Masters CL, Grzeschik KH, Multhaup G, Beyreuther K, Muller-Hill B (1987) The precursor of Alzheimer's disease amyloid A4 protein resembles a cell-surface receptor. Nature 325:733-736.

Karki K, Knight RA, Han Y, Yang D, Zhang J, Ledbetter KA, Chopp M, Seyfried DM (2009) Simvastatin and atorvastatin improve neurological outcome after experimental intracerebral hemorrhage. Stroke; a journal of cerebral circulation 40:3384-3389.

Kaul S, Bolger AF, Herrington D, Giugliano RP, Eckel RH (2010) Thiazolidinedione drugs and cardiovascular risks: a science advisory from the American Heart Association and American College Of Cardiology Foundation. Journal of the American College of Cardiology 55:1885-1894.

Kee N, Teixeira CM, Wang AH, Frankland PW (2007) Preferential incorporation of adult-generated granule cells into spatial memory networks in the dentate gyrus. Nature neuroscience 10:355-362.

Kehoe AD, Nikiforov AM, Alexanin SS, Neronov EG, Tikhomirova OV, Shun'kov VB, Makarova NV, Rabinovich E, Usmanova NM, Kazakov VI, Slozina NM, Montgomery HE (2009) Angiotensin-converting enzyme genotype and encephalopathy in Chernobyl cleanup workers. European journal of neurology : the official journal of the European Federation of Neurological Societies 16:95-100.

Khachaturian AS, Zandi PP, Lyketsos CG, Hayden KM, Skoog I, Norton MC, Tschanz JT, Mayer LS, Welsh-Bohmer KA, Breitner JC (2006) Antihypertensive medication use and incident Alzheimer disease: the Cache County Study. Archives of neurology 63:686-692.

Kidd M (1964) Alzheimer's Disease--an Electron Microscopical Study. Brain : a journal of neurology 87:307-320.

Kitagawa K, Matsumoto M, Yang G, Mabuchi T, Yagita Y, Hori M, Yanagihara T (1998) Cerebral ischemia after bilateral carotid artery occlusion and intraluminal suture occlusion in mice: evaluation of the patency of the posterior communicating artery. Journal of cerebral blood flow and metabolism : official journal of the International Society of Cerebral Blood Flow and Metabolism 18:570-579.

Kitazono T, Heistad DD, Faraci FM (1993) Role of ATP-sensitive K+ channels in CGRP-induced dilatation of basilar artery in vivo. The American journal of physiology 265:H581-585.

Kivipelto M, Helkala EL, Laakso MP, Hanninen T, Hallikainen M, Alhainen K, Soininen H, Tuomilehto J, Nissinen A (2001) Midlife vascular risk factors and Alzheimer's disease in later life: longitudinal, population based study. BMJ 322:1447-1451.

Klingner M, Apelt J, Kumar A, Sorger D, Sabri O, Steinbach J, Scheunemann M, Schliebs R (2003) Alterations in cholinergic and non-cholinergic neurotransmitter receptor densities in transgenic Tg2576 mouse brain with beta-amyloid plaque pathology. International journal of developmental neuroscience : the official journal of the International Society for Developmental Neuroscience 21:357-369.

Klyubin I, Walsh DM, Lemere CA, Cullen WK, Shankar GM, Betts V, Spooner ET, Jiang L, Anwyl R, Selkoe DJ, Rowan MJ (2005) Amyloid beta protein immunotherapy neutralizes Abeta oligomers that disrupt synaptic plasticity in vivo. Nature medicine 11:556-561.

Knopman DS, Mosley TH, Catellier DJ, Coker LH (2009) Fourteen-year longitudinal study of vascular risk factors, APOE genotype, and cognition: the ARIC MRI Study. Alzheimer's & dementia : the journal of the Alzheimer's Association 5:207-214.

Koehler RC, Roman RJ, Harder DR (2009) Astrocytes and the regulation of cerebral blood flow. Trends in neurosciences 32:160-169.

Kolb-Bachofen V, Kuhn A, Suschek CV (2006) The role of nitric oxide. Rheumatology (Oxford) 45 Suppl 3:iii17-19.

Koobi P, Kalliovalkama J, Jolma P, Rysa J, Ruskoaho H, Vuolteenaho O, Kahonen M, Tikkanen I, Fan M, Ylitalo P, Porsti I (2003) AT1 receptor blockade improves vasorelaxation in experimental renal failure. Hypertension 41:1364-1371.

Kornblum HI, Araujo DM, Annala AJ, Tatsukawa KJ, Phelps ME, Cherry SR (2000) In vivo imaging of neuronal activation and plasticity in the rat brain by high resolution positron emission tomography (microPET). Nature biotechnology 18:655-660.

Kosik KS, Joachim CL, Selkoe DJ (1986) Microtubule-associated protein tau (tau) is a major antigenic component of paired helical filaments in Alzheimer disease. Proceedings of the National Academy of Sciences of the United States of America 83:4044-4048.

Kotilinek LA, Westerman MA, Wang Q, Panizzon K, Lim GP, Simonyi A, Lesne S, Falinska A, Younkin LH, Younkin SG, Rowan M, Cleary J, Wallis RA, Sun GY, Cole G, Frautschy S, Anwyl R, Ashe KH (2008) Cyclooxygenase-2 inhibition improves amyloid-beta-mediated suppression of memory and synaptic plasticity. Brain : a journal of neurology 131:651-664.

Krupinski J, Kumar P, Kumar S, Kaluza J (1996) Increased expression of TGF-beta 1 in brain tissue after ischemic stroke in humans. Stroke; a journal of cerebral circulation 27:852-857.

Kurata T, Miyazaki K, Kozuki M, Panin VL, Morimoto N, Ohta Y, Nagai M, Ikeda Y, Matsuura T, Abe K (2011) Atorvastatin and pitavastatin improve cognitive function and reduce senile plaque and phosphorylated tau in aged APP mice. Brain research 1371:161-170.

Lacombe P, Mathews PM, Schmidt SD, Breidert T, Heneka MT, Landreth GE, Feinstein DL, Galea E (2004) Effect of anti-inflammatory agents on transforming growth

factor beta over-expressing mouse brains: a model revised. Journal of neuroinflammation 1:11.

Lamb BT, Sisodia SS, Lawler AM, Slunt HH, Kitt CA, Kearns WG, Pearson PL, Price DL, Gearhart JD (1993) Introduction and expression of the 400 kilobase amyloid precursor protein gene in transgenic mice [corrected]. Nature genetics 5:22-30.

Lanahan A, Worley P (1998) Immediate-early genes and synaptic function. Neurobiology of learning and memory 70:37-43.

Langbaum JB, Chen K, Lee W, Reschke C, Bandy D, Fleisher AS, Alexander GE, Foster NL, Weiner MW, Koeppe RA, Jagust WJ, Reiman EM (2009) Categorical and correlational analyses of baseline fluorodeoxyglucose positron emission tomography images from the Alzheimer's Disease Neuroimaging Initiative (ADNI). NeuroImage 45:1107-1116.

Lau JC, Lerch JP, Sled JG, Henkelman RM, Evans AC, Bedell BJ (2008) Longitudinal neuroanatomical changes determined by deformation-based morphometry in a mouse model of Alzheimer's disease. NeuroImage 42:19-27.

Launer LJ, Masaki K, Petrovitch H, Foley D, Havlik RJ (1995) The association between midlife blood pressure levels and late-life cognitive function. The Honolulu-Asia Aging Study. JAMA : the journal of the American Medical Association 274:1846-1851.

Launer LJ, Ross GW, Petrovitch H, Masaki K, Foley D, White LR, Havlik RJ (2000) Midlife blood pressure and dementia: the Honolulu-Asia aging study. Neurobiology of aging 21:49-55.

Lavoie P, Robitaille G, Agharazii M, Ledbetter S, Lebel M, Lariviere R (2005) Neutralization of transforming growth factor-beta attenuates hypertension and prevents renal injury in uremic rats. Journal of hypertension 23:1895-1903.

Lazarov O, Mattson MP, Peterson DA, Pimplikar SW, van Praag H (2010) When neurogenesis encounters aging and disease. Trends in neurosciences 33:569-579.

Leask A, Abraham DJ (2004) TGF-beta signaling and the fibrotic response. The FASEB journal : official publication of the Federation of American Societies for Experimental Biology 18:816-827.

Lecrux C, Hamel E (2011) The neurovascular unit in brain function and disease. Acta Physiol (Oxf) 203:47-59.

Lee JL, Di Ciano P, Thomas KL, Everitt BJ (2005) Disrupting reconsolidation of drug memories reduces cocaine-seeking behavior. Neuron 47:795-801.

Lee JL, Everitt BJ, Thomas KL (2004) Independent cellular processes for hippocampal memory consolidation and reconsolidation. Science 304:839-843.

Lee VM, Goedert M, Trojanowski JQ (2001) Neurodegenerative tauopathies. Annual review of neuroscience 24:1121-1159.

Lesne S, Docagne F, Gabriel C, Liot G, Lahiri DK, Buee L, Plawinski L, Delacourte A, MacKenzie ET, Buisson A, Vivien D (2003) Transforming growth factor-beta 1 potentiates amyloid-beta generation in astrocytes and in transgenic mice. The Journal of biological chemistry 278:18408-18418.

Lesne S, Koh MT, Kotilinek L, Kayed R, Glabe CG, Yang A, Gallagher M, Ashe KH (2006) A specific amyloid-beta protein assembly in the brain impairs memory. Nature 440:352-357.

Lesne S, Kotilinek L, Ashe KH (2008) Plaque-bearing mice with reduced levels of oligomeric amyloid-beta assemblies have intact memory function. Neuroscience 151:745-749.

Levy-Gigi E, Kelemen O, Gluck MA, Keri S (2011) Impaired context reversal learning, but not cue reversal learning, in patients with amnestic mild cognitive impairment. Neuropsychologia 49:3320-3326.

Levy-Lahad E, Wasco W, Poorkaj P, Romano DM, Oshima J, Pettingell WH, Yu CE, Jondro PD, Schmidt SD, Wang K, et al. (1995) Candidate gene for the chromosome 1 familial Alzheimer's disease locus. Science 269:973-977.

Levy E, Carman MD, Fernandez-Madrid IJ, Power MD, Lieberburg I, van Duinen SG, Bots GT, Luyendijk W, Frangione B (1990) Mutation of the Alzheimer's disease amyloid gene in hereditary cerebral hemorrhage, Dutch type. Science 248:1124-1126.

Li G, Shofer JB, Rhew IC, Kukull WA, Peskind ER, McCormick W, Bowen JD, Schellenberg GD, Crane PK, Breitner JC, Larson EB (2010a) Age-varying association between statin use and incident Alzheimer's disease. Journal of the American Geriatrics Society 58:1311-1317.

Li L, Cao D, Kim H, Lester R, Fukuchi K (2006) Simvastatin enhances learning and memory independent of amyloid load in mice. Annals of neurology 60:729-739.

Li NC, Lee A, Whitmer RA, Kivipelto M, Lawler E, Kazis LE, Wolozin B (2010b) Use of angiotensin receptor blockers and risk of dementia in a predominantly male population: prospective cohort analysis. BMJ 340:b5465.

Lim DS, Lutucuta S, Bachireddy P, Youker K, Evans A, Entman M, Roberts R, Marian AJ (2001) Angiotensin II blockade reverses myocardial fibrosis in a transgenic mouse model of human hypertrophic cardiomyopathy. Circulation 103:789-791.

Lin AH, Luo J, Mondshein LH, ten Dijke P, Vivien D, Contag CH, Wyss-Coray T (2005) Global analysis of Smad2/3-dependent TGF-beta signaling in living mice reveals prominent tissue-specific responses to injury. J Immunol 175:547-554.

Lincoff AM, Wolski K, Nicholls SJ, Nissen SE (2007) Pioglitazone and risk of cardiovascular events in patients with type 2 diabetes mellitus: a meta-analysis of randomized trials. JAMA : the journal of the American Medical Association 298:1180-1188.

Logothetis NK (2008) What we can do and what we cannot do with fMRI. Nature 453:869-878.

Lu D, Qu C, Goussev A, Jiang H, Lu C, Schallert T, Mahmood A, Chen J, Li Y, Chopp M (2007) Statins increase neurogenesis in the dentate gyrus, reduce delayed neuronal death in the hippocampal CA3 region, and improve spatial learning in rat after traumatic brain injury. Journal of neurotrauma 24:1132-1146.

Luchsinger JA (2008) Adiposity, hyperinsulinemia, diabetes and Alzheimer's disease: an epidemiological perspective. European journal of pharmacology 585:119-129.

Luchsinger JA, Reitz C, Honig LS, Tang MX, Shea S, Mayeux R (2005) Aggregation of vascular risk factors and risk of incident Alzheimer disease. Neurology 65:545-551.

Lue LF, Kuo YM, Roher AE, Brachova L, Shen Y, Sue L, Beach T, Kurth JH, Rydel RE, Rogers J (1999) Soluble amyloid beta peptide concentration as a predictor of

synaptic change in Alzheimer's disease. The American journal of pathology 155:853-862.

Luedecking EK, DeKosky ST, Mehdi H, Ganguli M, Kamboh MI (2000) Analysis of genetic polymorphisms in the transforming growth factor-beta1 gene and the risk of Alzheimer's disease. Human genetics 106:565-569.

Luterman JD, Haroutunian V, Yemul S, Ho L, Purohit D, Aisen PS, Mohs R, Pasinetti GM (2000) Cytokine gene expression as a function of the clinical progression of Alzheimer disease dementia. Archives of neurology 57:1153-1160.

Maei HR, Zaslavsky K, Teixeira CM, Frankland PW (2009) What is the Most Sensitive Measure of Water Maze Probe Test Performance? Frontiers in integrative neuroscience 3:4.

Maeshiba Y, Kiyota Y, Yamashita K, Yoshimura Y, Motohashi M, Tanayama S (1997) Disposition of the new antidiabetic agent pioglitazone in rats, dogs, and monkeys. Arzneimittel-Forschung 47:29-35.

Malaguarnera L, Motta M, Di Rosa M, Anzaldi M, Malaguarnera M (2006) Interleukin-18 and transforming growth factor-beta 1 plasma levels in Alzheimer's disease and vascular dementia. Neuropathology : official journal of the Japanese Society of Neuropathology 26:307-312.

Mancardi GL, Perdelli F, Rivano C, Leonardi A, Bugiani O (1980) Thickening of the basement membrane of cortical capillaries in Alzheimer's disease. Acta neuropathologica 49:79-83.

Mandell JW, Banker GA (1996) Microtubule-associated proteins, phosphorylation gradients, and the establishment of neuronal polarity. Perspectives on developmental neurobiology 4:125-135.

Mandrekar S, Jiang Q, Lee CY, Koenigsknecht-Talboo J, Holtzman DM, Landreth GE (2009) Microglia mediate the clearance of soluble Abeta through fluid phase macropinocytosis. The Journal of neuroscience : the official journal of the Society for Neuroscience 29:4252-4262.

Martens FM, Visseren FL, de Koning EJ, Rabelink TJ (2005) Short-term pioglitazone treatment improves vascular function irrespective of metabolic changes in patients with type 2 diabetes. Journal of cardiovascular pharmacology 46:773-778.

Masters CL, Simms G, Weinman NA, Multhaup G, McDonald BL, Beyreuther K (1985) Amyloid plaque core protein in Alzheimer disease and Down syndrome. Proceedings of the National Academy of Sciences of the United States of America 82:4245-4249.

Mathie RT, Ralevic V, Alexander B, Burnstock G (1991) Nitric oxide is the mediator of ATP-induced dilatation of the rabbit hepatic arterial vascular bed. British journal of pharmacology 103:1602-1606.

Matsumoto T, Ishida K, Taguchi K, Kobayashi T, Kamata K (2010) Losartan normalizes endothelium-derived hyperpolarizing factor-mediated relaxation by activating Ca2+-activated K+ channels in mesenteric artery from type 2 diabetic GK rat. Journal of pharmacological sciences 112:299-309.

Maul B, von Bohlen und Halbach O, Becker A, Sterner-Kock A, Voigt JP, Siems WE, Grecksch G, Walther T (2008) Impaired spatial memory and altered dendritic spine morphology in angiotensin II type 2 receptor-deficient mice. J Mol Med (Berl) 86:563-571.

Maxwell CJ, Hogan DB (2010) Antihypertensive agents and prevention of dementia. BMJ 340:b5409.
McGeer PL, McGeer E (2004) Immunotherapy for Alzheimer's disease. Science of aging knowledge environment : SAGE KE 2004:pe29.
McGowan E, Eriksen J, Hutton M (2006) A decade of modeling Alzheimer's disease in transgenic mice. Trends in genetics : TIG 22:281-289.
McKhann G, Drachman D, Folstein M, Katzman R, Price D, Stadlan EM (1984) Clinical diagnosis of Alzheimer's disease: report of the NINCDS-ADRDA Work Group under the auspices of Department of Health and Human Services Task Force on Alzheimer's Disease. Neurology 34:939-944.
Meilandt WJ, Cisse M, Ho K, Wu T, Esposito LA, Scearce-Levie K, Cheng IH, Yu GQ, Mucke L (2009) Neprilysin overexpression inhibits plaque formation but fails to reduce pathogenic Abeta oligomers and associated cognitive deficits in human amyloid precursor protein transgenic mice. The Journal of neuroscience : the official journal of the Society for Neuroscience 29:1977-1986.
Melrose RJ, Campa OM, Harwood DG, Osato S, Mandelkern MA, Sultzer DL (2009) The neural correlates of naming and fluency deficits in Alzheimer's disease: an FDG-PET study. International journal of geriatric psychiatry 24:885-893.
Mesulam M (2004) The cholinergic lesion of Alzheimer's disease: pivotal factor or side show? Learn Mem 11:43-49.
Mesulam MM (1999) Neuroplasticity failure in Alzheimer's disease: bridging the gap between plaques and tangles. Neuron 24:521-529.
Miatello R, Risler N, Castro C, Cruzado M, Gonzalez S, Zumino AP (2003) Chronic administration of losartan reverses cardiovascular changes in hypertensive fructose-fed rats. Cell Mol Biol (Noisy-le-grand) 49:945-952.
Mielke R, Schroder R, Fink GR, Kessler J, Herholz K, Heiss WD (1996) Regional cerebral glucose metabolism and postmortem pathology in Alzheimer's disease. Acta neuropathologica 91:174-179.
Miki K, Ishibashi S, Sun L, Xu H, Ohashi W, Kuroiwa T, Mizusawa H (2009) Intensity of chronic cerebral hypoperfusion determines white/gray matter injury and cognitive/motor dysfunction in mice. Journal of neuroscience research 87:1270-1281.
Milbrandt J (1987) A nerve growth factor-induced gene encodes a possible transcriptional regulatory factor. Science 238:797-799.
Moechars D, Dewachter I, Lorent K, Reverse D, Baekelandt V, Naidu A, Tesseur I, Spittaels K, Haute CV, Checler F, Godaux E, Cordell B, Van Leuven F (1999) Early phenotypic changes in transgenic mice that overexpress different mutants of amyloid precursor protein in brain. The Journal of biological chemistry 274:6483-6492.
Mogi M, Li JM, Tsukuda K, Iwanami J, Min LJ, Sakata A, Fujita T, Iwai M, Horiuchi M (2008) Telmisartan prevented cognitive decline partly due to PPAR-gamma activation. Biochemical and biophysical research communications 375:446-449.
Molinuevo JL, Llado A, Rami L (2005) Memantine: targeting glutamate excitotoxicity in Alzheimer's disease and other dementias. American journal of Alzheimer's disease and other dementias 20:77-85.

Morel JL, Macrez-Lepretre N, Mironneau J (1996) Angiotensin II-activated Ca2+ entry-induced release of Ca2+ from intracellular stores in rat portal vein myocytes. British journal of pharmacology 118:73-78.

Morelli L, Llovera RE, Mathov I, Lue LF, Frangione B, Ghiso J, Castano EM (2004) Insulin-degrading enzyme in brain microvessels: proteolysis of amyloid {beta} vasculotropic variants and reduced activity in cerebral amyloid angiopathy. The Journal of biological chemistry 279:56004-56013.

Moreno MJ, Cohen Z, Stanimirovic DB, Hamel E (1999) Functional calcitonin gene-related peptide type 1 and adrenomedullin receptors in human trigeminal ganglia, brain vessels, and cerebromicrovascular or astroglial cells in culture. Journal of cerebral blood flow and metabolism : official journal of the International Society of Cerebral Blood Flow and Metabolism 19:1270-1278.

Morgan JI, Curran T (1991) Stimulus-transcription coupling in the nervous system: involvement of the inducible proto-oncogenes fos and jun. Annual review of neuroscience 14:421-451.

Morris M, Maeda S, Vossel K, Mucke L (2011) The many faces of tau. Neuron 70:410-426.

Morris R (1984) Developments of a water-maze procedure for studying spatial learning in the rat. Journal of neuroscience methods 11:47-60.

Mosconi L, Perani D, Sorbi S, Herholz K, Nacmias B, Holthoff V, Salmon E, Baron JC, De Cristofaro MT, Padovani A, Borroni B, Franceschi M, Bracco L, Pupi A (2004) MCI conversion to dementia and the APOE genotype: a prediction study with FDG-PET. Neurology 63:2332-2340.

Mrak RE, Landreth GE (2004) PPARgamma, neuroinflammation, and disease. Journal of neuroinflammation 1:5.

Mucke L, Masliah E, Yu GQ, Mallory M, Rockenstein EM, Tatsuno G, Hu K, Kholodenko D, Johnson-Wood K, McConlogue L (2000) High-level neuronal expression of abeta 1-42 in wild-type human amyloid protein precursor transgenic mice: synaptotoxicity without plaque formation. The Journal of neuroscience : the official journal of the Society for Neuroscience 20:4050-4058.

Nader K, Schafe GE, Le Doux JE (2000) Fear memories require protein synthesis in the amygdala for reconsolidation after retrieval. Nature 406:722-726.

Nagaoka T, Hein TW, Yoshida A, Kuo L (2007) Simvastatin elicits dilation of isolated porcine retinal arterioles: role of nitric oxide and mevalonate-rho kinase pathways. Investigative ophthalmology & visual science 48:825-832.

Nichols NR (1999) Glial responses to steroids as markers of brain aging. Journal of neurobiology 40:585-601.

Nicolakakis N, Aboulkassim T, Aliaga A, Tong XK, Rosa-Neto P, Hamel E (2011) Intact memory in TGF-beta1 transgenic mice featuring chronic cerebrovascular deficit: recovery with pioglitazone. Journal of cerebral blood flow and metabolism : official journal of the International Society of Cerebral Blood Flow and Metabolism 31:200-211.

Nicolakakis N, Aboulkassim T, Ongali B, Lecrux C, Fernandes P, Rosa-Neto P, Tong XK, Hamel E (2008) Complete rescue of cerebrovascular function in aged Alzheimer's disease transgenic mice by antioxidants and pioglitazone, a

peroxisome proliferator-activated receptor gamma agonist. The Journal of neuroscience : the official journal of the Society for Neuroscience 28:9287-9296.
Nicolakakis N, Hamel E (2010) The Nuclear Receptor PPARgamma as a Therapeutic Target for Cerebrovascular and Brain Dysfunction in Alzheimer's Disease. Frontiers in aging neuroscience 2.
Nishimura N, Schaffer CB, Friedman B, Lyden PD, Kleinfeld D (2007) Penetrating arterioles are a bottleneck in the perfusion of neocortex. Proceedings of the National Academy of Sciences of the United States of America 104:365-370.
Nissen SE, Wolski K (2010) Rosiglitazone revisited: an updated meta-analysis of risk for myocardial infarction and cardiovascular mortality. Archives of internal medicine 170:1191-1201.
Nitta A, Fukuta T, Hasegawa T, Nabeshima T (1997) Continuous infusion of beta-amyloid protein into the rat cerebral ventricle induces learning impairment and neuronal and morphological degeneration. Japanese journal of pharmacology 73:51-57.
Nitta A, Itoh A, Hasegawa T, Nabeshima T (1994) beta-Amyloid protein-induced Alzheimer's disease animal model. Neuroscience letters 170:63-66.
Niwa K, Haensel C, Ross ME, Iadecola C (2001a) Cyclooxygenase-1 participates in selected vasodilator responses of the cerebral circulation. Circulation research 88:600-608.
Niwa K, Kazama K, Younkin SG, Carlson GA, Iadecola C (2002) Alterations in cerebral blood flow and glucose utilization in mice overexpressing the amyloid precursor protein. Neurobiology of disease 9:61-68.
Niwa K, Porter VA, Kazama K, Cornfield D, Carlson GA, Iadecola C (2001b) A beta-peptides enhance vasoconstriction in cerebral circulation. American journal of physiology Heart and circulatory physiology 281:H2417-2424.
Niwa K, Younkin L, Ebeling C, Turner SK, Westaway D, Younkin S, Ashe KH, Carlson GA, Iadecola C (2000) Abeta 1-40-related reduction in functional hyperemia in mouse neocortex during somatosensory activation. Proceedings of the National Academy of Sciences of the United States of America 97:9735-9740.
Nixon RA (2007) Autophagy, amyloidogenesis and Alzheimer disease. Journal of cell science 120:4081-4091.
Nomura H, Yamawaki H, Mukohda M, Okada M, Hara Y (2008) Mechanisms underlying pioglitazone-mediated relaxation in isolated blood vessel. Journal of pharmacological sciences 108:258-265.
Nukina N, Ihara Y (1986) One of the antigenic determinants of paired helical filaments is related to tau protein. Journal of biochemistry 99:1541-1544.
O'Donovan KJ, Tourtellotte WG, Millbrandt J, Baraban JM (1999) The EGR family of transcription-regulatory factors: progress at the interface of molecular and systems neuroscience. Trends in neurosciences 22:167-173.
Oddo S, Caccamo A, Kitazawa M, Tseng BP, LaFerla FM (2003) Amyloid deposition precedes tangle formation in a triple transgenic model of Alzheimer's disease. Neurobiology of aging 24:1063-1070.
Ohrui T, Tomita N, Sato-Nakagawa T, Matsui T, Maruyama M, Niwa K, Arai H, Sasaki H (2004) Effects of brain-penetrating ACE inhibitors on Alzheimer disease progression. Neurology 63:1324-1325.

Omae T, Nagaoka T, Tanano I, Yoshida A (2011) Pioglitazone, a peroxisome proliferator-activated receptor-gamma agonist, induces dilation of isolated porcine retinal arterioles: role of nitric oxide and potassium channels. Investigative ophthalmology & visual science 52:6749-6756.

Ongali B, Nicolakakis N, Lecrux C, Aboulkassim T, Rosa-Neto P, Papadopoulos P, Tong XK, Hamel E (2010) Transgenic mice overexpressing APP and transforming growth factor-beta1 feature cognitive and vascular hallmarks of Alzheimer's disease. The American journal of pathology 177:3071-3080.

Palop JJ, Jones B, Kekonius L, Chin J, Yu GQ, Raber J, Masliah E, Mucke L (2003) Neuronal depletion of calcium-dependent proteins in the dentate gyrus is tightly linked to Alzheimer's disease-related cognitive deficits. Proceedings of the National Academy of Sciences of the United States of America 100:9572-9577.

Papadopoulos P, Ongali B, Hamel E (2010) Selective in vivo antagonism of endothelin receptors in transforming growth factor-beta1 transgenic mice that mimic the vascular pathology of Alzheimer's disease. Canadian journal of physiology and pharmacology 88:652-660.

Park L, Anrather J, Zhou P, Frys K, Pitstick R, Younkin S, Carlson GA, Iadecola C (2005) NADPH-oxidase-derived reactive oxygen species mediate the cerebrovascular dysfunction induced by the amyloid beta peptide. The Journal of neuroscience : the official journal of the Society for Neuroscience 25:1769-1777.

Park L, Zhou P, Pitstick R, Capone C, Anrather J, Norris EH, Younkin L, Younkin S, Carlson G, McEwen BS, Iadecola C (2008) Nox2-derived radicals contribute to neurovascular and behavioral dysfunction in mice overexpressing the amyloid precursor protein. Proceedings of the National Academy of Sciences of the United States of America 105:1347-1352.

Pedersen WA, McMillan PJ, Kulstad JJ, Leverenz JB, Craft S, Haynatzki GR (2006) Rosiglitazone attenuates learning and memory deficits in Tg2576 Alzheimer mice. Experimental neurology 199:265-273.

Pellerin L, Bouzier-Sore AK, Aubert A, Serres S, Merle M, Costalat R, Magistretti PJ (2007) Activity-dependent regulation of energy metabolism by astrocytes: an update. Glia 55:1251-1262.

Pellerin L, Magistretti PJ (2003) How to balance the brain energy budget while spending glucose differently. The Journal of physiology 546:325.

Perlmutter LS, Chui HC (1990) Microangiopathy, the vascular basement membrane and Alzheimer's disease: a review. Brain research bulletin 24:677-686.

Petanceska SS, DeRosa S, Olm V, Diaz N, Sharma A, Thomas-Bryant T, Duff K, Pappolla M, Refolo LM (2002) Statin therapy for Alzheimer's disease: will it work? Journal of molecular neuroscience : MN 19:155-161.

Peterson MC (2005) Circulating transforming growth factor beta-1: a partial molecular explanation for associations between hypertension, diabetes, obesity, smoking and human disease involving fibrosis. Medical science monitor : international medical journal of experimental and clinical research 11:RA229-232.

Phillips JW, Barringhaus KG, Sanders JM, Yang Z, Chen M, Hesselbacher S, Czarnik AC, Ley K, Nadler J, Sarembock IJ (2003) Rosiglitazone reduces the accelerated neointima formation after arterial injury in a mouse injury model of type 2 diabetes. Circulation 108:1994-1999.

Pihlaja R, Koistinaho J, Malm T, Sikkila H, Vainio S, Koistinaho M (2008) Transplanted astrocytes internalize deposited beta-amyloid peptides in a transgenic mouse model of Alzheimer's disease. Glia 56:154-163.

Poirier J, Davignon J, Bouthillier D, Kogan S, Bertrand P, Gauthier S (1993) Apolipoprotein E polymorphism and Alzheimer's disease. Lancet 342:697-699.

Popovich PG, Longbrake EE (2008) Can the immune system be harnessed to repair the CNS? Nature reviews Neuroscience 9:481-493.

Priller C, Bauer T, Mitteregger G, Krebs B, Kretzschmar HA, Herms J (2006) Synapse formation and function is modulated by the amyloid precursor protein. The Journal of neuroscience : the official journal of the Society for Neuroscience 26:7212-7221.

Probstfield JL, O'Brien KD (2010) Progression of cardiovascular damage: the role of renin-angiotensin system blockade. The American journal of cardiology 105:10A-20A.

Rao JS, Kellom M, Kim HW, Rapoport SI, Reese EA (2012) Neuroinflammation and synaptic loss. Neurochemical research 37:903-910.

Refolo LM, Malester B, LaFrancois J, Bryant-Thomas T, Wang R, Tint GS, Sambamurti K, Duff K, Pappolla MA (2000) Hypercholesterolemia accelerates the Alzheimer's amyloid pathology in a transgenic mouse model. Neurobiology of disease 7:321-331.

Reisberg B, Doody R, Stoffler A, Schmitt F, Ferris S, Mobius HJ (2003) Memantine in moderate-to-severe Alzheimer's disease. The New England journal of medicine 348:1333-1341.

Richardson CL, Tate WP, Mason SE, Lawlor PA, Dragunow M, Abraham WC (1992) Correlation between the induction of an immediate early gene, zif/268, and long-term potentiation in the dentate gyrus. Brain research 580:147-154.

Risner ME, Saunders AM, Altman JF, Ormandy GC, Craft S, Foley IM, Zvartau-Hind ME, Hosford DA, Roses AD (2006) Efficacy of rosiglitazone in a genetically defined population with mild-to-moderate Alzheimer's disease. The pharmacogenomics journal 6:246-254.

Rivest S (2011) The promise of anti-inflammatory therapies for CNS injuries and diseases. Expert review of neurotherapeutics 11:783-786.

Robakis NK, Ramakrishna N, Wolfe G, Wisniewski HM (1987) Molecular cloning and characterization of a cDNA encoding the cerebrovascular and the neuritic plaque amyloid peptides. Proceedings of the National Academy of Sciences of the United States of America 84:4190-4194.

Rockenstein E, Torrance M, Mante M, Adame A, Paulino A, Rose JB, Crews L, Moessler H, Masliah E (2006) Cerebrolysin decreases amyloid-beta production by regulating amyloid protein precursor maturation in a transgenic model of Alzheimer's disease. Journal of neuroscience research 83:1252-1261.

Rogaev EI, Sherrington R, Rogaeva EA, Levesque G, Ikeda M, Liang Y, Chi H, Lin C, Holman K, Tsuda T, et al. (1995) Familial Alzheimer's disease in kindreds with missense mutations in a gene on chromosome 1 related to the Alzheimer's disease type 3 gene. Nature 376:775-778.

Roher AE, Kuo YM, Esh C, Knebel C, Weiss N, Kalback W, Luehrs DC, Childress JL, Beach TG, Weller RO, Kokjohn TA (2003) Cortical and leptomeningeal

cerebrovascular amyloid and white matter pathology in Alzheimer's disease. Mol Med 9:112-122.

Roher AE, Lowenson JD, Clarke S, Woods AS, Cotter RJ, Gowing E, Ball MJ (1993) beta-Amyloid-(1-42) is a major component of cerebrovascular amyloid deposits: implications for the pathology of Alzheimer disease. Proceedings of the National Academy of Sciences of the United States of America 90:10836-10840.

Rosen WG, Mohs RC, Davis KL (1984) A new rating scale for Alzheimer's disease. The American journal of psychiatry 141:1356-1364.

Rosengarten B, Paulsen S, Molnar S, Kaschel R, Gallhofer B, Kaps M (2006) Acetylcholine esterase inhibitor donepezil improves dynamic cerebrovascular regulation in Alzheimer patients. Journal of neurology 253:58-64.

Ruitenberg A, den Heijer T, Bakker SL, van Swieten JC, Koudstaal PJ, Hofman A, Breteler MM (2005) Cerebral hypoperfusion and clinical onset of dementia: the Rotterdam Study. Annals of neurology 57:789-794.

Saheki A, Terasaki T, Tamai I, Tsuji A (1994) In vivo and in vitro blood-brain barrier transport of 3-hydroxy-3-methylglutaryl coenzyme A (HMG-CoA) reductase inhibitors. Pharmaceutical research 11:305-311.

Salins P, He Y, Olson K, Glazner G, Kashour T, Amara F (2008) TGF-beta1 is increased in a transgenic mouse model of familial Alzheimer's disease and causes neuronal apoptosis. Neuroscience letters 430:81-86.

Sano M, Bell KL, Galasko D, Galvin JE, Thomas RG, van Dyck CH, Aisen PS (2011) A randomized, double-blind, placebo-controlled trial of simvastatin to treat Alzheimer disease. Neurology 77:556-563.

Santello M, Volterra A (2010) Neuroscience: Astrocytes as aide-memoires. Nature 463:169-170.

Sastre M, Dewachter I, Landreth GE, Willson TM, Klockgether T, van Leuven F, Heneka MT (2003) Nonsteroidal anti-inflammatory drugs and peroxisome proliferator-activated receptor-gamma agonists modulate immunostimulated processing of amyloid precursor protein through regulation of beta-secretase. The Journal of neuroscience : the official journal of the Society for Neuroscience 23:9796-9804.

Sato T, Hanyu H, Hirao K, Kanetaka H, Sakurai H, Iwamoto T (2011) Efficacy of PPAR-gamma agonist pioglitazone in mild Alzheimer disease. Neurobiology of aging 32:1626-1633.

Schreurs BG (2010) The effects of cholesterol on learning and memory. Neuroscience and biobehavioral reviews 34:1366-1379.

Seeger T, Fedorova I, Zheng F, Miyakawa T, Koustova E, Gomeza J, Basile AS, Alzheimer C, Wess J (2004) M2 muscarinic acetylcholine receptor knock-out mice show deficits in behavioral flexibility, working memory, and hippocampal plasticity. The Journal of neuroscience : the official journal of the Society for Neuroscience 24:10117-10127.

Selkoe DJ (2001) Alzheimer's disease results from the cerebral accumulation and cytotoxicity of amyloid beta-protein. Journal of Alzheimer's disease : JAD 3:75-80.

Selkoe DJ (2011) Alzheimer's disease. Cold Spring Harbor perspectives in biology 3.

Seubert P, Vigo-Pelfrey C, Esch F, Lee M, Dovey H, Davis D, Sinha S, Schlossmacher M, Whaley J, Swindlehurst C, et al. (1992) Isolation and quantification of soluble Alzheimer's beta-peptide from biological fluids. Nature 359:325-327.

Shepardson NE, Shankar GM, Selkoe DJ (2011a) Cholesterol level and statin use in Alzheimer disease: I. Review of epidemiological and preclinical studies. Archives of neurology 68:1239-1244.

Shepardson NE, Shankar GM, Selkoe DJ (2011b) Cholesterol level and statin use in Alzheimer disease: II. Review of human trials and recommendations. Archives of neurology 68:1385-1392.

Sherrington R, Rogaev EI, Liang Y, Rogaeva EA, Levesque G, Ikeda M, Chi H, Lin C, Li G, Holman K, Tsuda T, Mar L, Foncin JF, Bruni AC, Montesi MP, Sorbi S, Rainero I, Pinessi L, Nee L, Chumakov I, Pollen D, Brookes A, Sanseau P, Polinsky RJ, Wasco W, Da Silva HA, Haines JL, Perkicak-Vance MA, Tanzi RE, Roses AD, Fraser PE, Rommens JM, St George-Hyslop PH (1995) Cloning of a gene bearing missense mutations in early-onset familial Alzheimer's disease. Nature 375:754-760.

Shie FS, Jin LW, Cook DG, Leverenz JB, LeBoeuf RC (2002) Diet-induced hypercholesterolemia enhances brain A beta accumulation in transgenic mice. Neuroreport 13:455-459.

Shimohama S, Tanino H, Kawakami N, Okamura N, Kodama H, Yamaguchi T, Hayakawa T, Nunomura A, Chiba S, Perry G, Smith MA, Fujimoto S (2000) Activation of NADPH oxidase in Alzheimer's disease brains. Biochemical and biophysical research communications 273:5-9.

Shinohara M, Sato N, Kurinami H, Takeuchi D, Takeda S, Shimamura M, Yamashita T, Uchiyama Y, Rakugi H, Morishita R (2010) Reduction of brain beta-amyloid (Abeta) by fluvastatin, a hydroxymethylglutaryl-CoA reductase inhibitor, through increase in degradation of amyloid precursor protein C-terminal fragments (APP-CTFs) and Abeta clearance. The Journal of biological chemistry 285:22091-22102.

Simard AR, Soulet D, Gowing G, Julien JP, Rivest S (2006) Bone marrow-derived microglia play a critical role in restricting senile plaque formation in Alzheimer's disease. Neuron 49:489-502.

Simons M, Schwarzler F, Lutjohann D, von Bergmann K, Beyreuther K, Dichgans J, Wormstall H, Hartmann T, Schulz JB (2002) Treatment with simvastatin in normocholesterolemic patients with Alzheimer's disease: A 26-week randomized, placebo-controlled, double-blind trial. Annals of neurology 52:346-350.

Simpson IA, Chundu KR, Davies-Hill T, Honer WG, Davies P (1994) Decreased concentrations of GLUT1 and GLUT3 glucose transporters in the brains of patients with Alzheimer's disease. Annals of neurology 35:546-551.

Skinner J, Carvalho JO, Potter GG, Thames A, Zelinski E, Crane PK, Gibbons LE (2012) The Alzheimer's Disease Assessment Scale-Cognitive-Plus (ADAS-Cog-Plus): an expansion of the ADAS-Cog to improve responsiveness in MCI. Brain imaging and behavior.

Sloan HL, Austin VC, Blamire AM, Schnupp JW, Lowe AS, Allers KA, Matthews PM, Sibson NR (2010) Regional differences in neurovascular coupling in rat brain as determined by fMRI and electrophysiology. NeuroImage 53:399-411.

Solomon A, Kivipelto M (2009) Cholesterol-modifying strategies for Alzheimer's disease. Expert review of neurotherapeutics 9:695-709.

Sparks DL (2011) Alzheimer disease: Statins in the treatment of Alzheimer disease. Nature reviews Neurology.

Sparks DL, Sabbagh MN, Connor DJ, Lopez J, Launer LJ, Browne P, Wasser D, Johnson-Traver S, Lochhead J, Ziolwolski C (2005) Atorvastatin for the treatment of mild to moderate Alzheimer disease: preliminary results. Archives of neurology 62:753-757.

Squire LR, Barondes SH (1972) Variable decay of memory and its recovery in cycloheximide-treated mice. Proceedings of the National Academy of Sciences of the United States of America 69:1416-1420.

Stalder M, Phinney A, Probst A, Sommer B, Staufenbiel M, Jucker M (1999) Association of microglia with amyloid plaques in brains of APP23 transgenic mice. The American journal of pathology 154:1673-1684.

Stefani M, Liguri G (2009) Cholesterol in Alzheimer's disease: unresolved questions. Current Alzheimer research 6:15-29.

Strittmatter WJ, Saunders AM, Schmechel D, Pericak-Vance M, Enghild J, Salvesen GS, Roses AD (1993) Apolipoprotein E: high-avidity binding to beta-amyloid and increased frequency of type 4 allele in late-onset familial Alzheimer disease. Proceedings of the National Academy of Sciences of the United States of America 90:1977-1981.

Su KH, Tsai JY, Kou YR, Chiang AN, Hsiao SH, Wu YL, Hou HH, Pan CC, Shyue SK, Lee TS (2009) Valsartan regulates the interaction of angiotensin II type 1 receptor and endothelial nitric oxide synthase via Src/PI3K/Akt signalling. Cardiovascular research 82:468-475.

Sun X, He G, Qing H, Zhou W, Dobie F, Cai F, Staufenbiel M, Huang LE, Song W (2006) Hypoxia facilitates Alzheimer's disease pathogenesis by up-regulating BACE1 gene expression. Proceedings of the National Academy of Sciences of the United States of America 103:18727-18732.

Taguchi K, Kobayashi T, Takenouchi Y, Matsumoto T, Kamata K (2011) Angiotensin II causes endothelial dysfunction via the GRK2/Akt/eNOS pathway in aortas from a murine type 2 diabetic model. Pharmacological research : the official journal of the Italian Pharmacological Society 64:535-546.

Takeda S, Sato N, Takeuchi D, Kurinami H, Shinohara M, Niisato K, Kano M, Ogihara T, Rakugi H, Morishita R (2009) Angiotensin receptor blocker prevented beta-amyloid-induced cognitive impairment associated with recovery of neurovascular coupling. Hypertension 54:1345-1352.

Takeda S, Sato N, Uchio-Yamada K, Sawada K, Kunieda T, Takeuchi D, Kurinami H, Shinohara M, Rakugi H, Morishita R (2010) Diabetes-accelerated memory dysfunction via cerebrovascular inflammation and Abeta deposition in an Alzheimer mouse model with diabetes. Proceedings of the National Academy of Sciences of the United States of America 107:7036-7041.

Tamboli IY, Barth E, Christian L, Siepmann M, Kumar S, Singh S, Tolksdorf K, Heneka MT, Lutjohann D, Wunderlich P, Walter J (2010) Statins promote the degradation of extracellular amyloid {beta}-peptide by microglia via stimulation of exosome-

associated insulin-degrading enzyme (IDE) secretion. The Journal of biological chemistry 285:37405-37414.

Tanzi RE, Bertram L (2005) Twenty years of the Alzheimer's disease amyloid hypothesis: a genetic perspective. Cell 120:545-555.

Tanzi RE, Gusella JF, Watkins PC, Bruns GA, St George-Hyslop P, Van Keuren ML, Patterson D, Pagan S, Kurnit DM, Neve RL (1987) Amyloid beta protein gene: cDNA, mRNA distribution, and genetic linkage near the Alzheimer locus. Science 235:880-884.

Tarkowski E, Issa R, Sjogren M, Wallin A, Blennow K, Tarkowski A, Kumar P (2002) Increased intrathecal levels of the angiogenic factors VEGF and TGF-beta in Alzheimer's disease and vascular dementia. Neurobiology of aging 23:237-243.

Terry RD (1963) The Fine Structure of Neurofibrillary Tangles in Alzheimer's Disease. Journal of neuropathology and experimental neurology 22:629-642.

Tesseur I, Wyss-Coray T (2006) A role for TGF-beta signaling in neurodegeneration: evidence from genetically engineered models. Current Alzheimer research 3:505-513.

Tesseur I, Zou K, Esposito L, Bard F, Berber E, Can JV, Lin AH, Crews L, Tremblay P, Mathews P, Mucke L, Masliah E, Wyss-Coray T (2006) Deficiency in neuronal TGF-beta signaling promotes neurodegeneration and Alzheimer's pathology. The Journal of clinical investigation 116:3060-3069.

Toledo EM, Inestrosa NC (2010) Activation of Wnt signaling by lithium and rosiglitazone reduced spatial memory impairment and neurodegeneration in brains of an APPswe/PSEN1DeltaE9 mouse model of Alzheimer's disease. Molecular psychiatry 15:272-285, 228.

Tong XK, Hamel E (2007) Transforming growth factor-beta 1 impairs endothelin-1-mediated contraction of brain vessels by inducing mitogen-activated protein (MAP) kinase phosphatase-1 and inhibiting p38 MAP kinase. Molecular pharmacology 72:1476-1483.

Tong XK, Lecrux C, Hamel E (2012) Age-dependent rescue by simvastatin of Alzheimer's disease cerebrovascular and memory deficits. The Journal of neuroscience : the official journal of the Society for Neuroscience 32:4705-4715.

Tong XK, Nicolakakis N, Fernandes P, Ongali B, Brouillette J, Quirion R, Hamel E (2009) Simvastatin improves cerebrovascular function and counters soluble amyloid-beta, inflammation and oxidative stress in aged APP mice. Neurobiology of disease 35:406-414.

Tong XK, Nicolakakis N, Kocharyan A, Hamel E (2005) Vascular remodeling versus amyloid beta-induced oxidative stress in the cerebrovascular dysfunctions associated with Alzheimer's disease. The Journal of neuroscience : the official journal of the Society for Neuroscience 25:11165-11174.

Town T, Laouar Y, Pittenger C, Mori T, Szekely CA, Tan J, Duman RS, Flavell RA (2008) Blocking TGF-beta-Smad2/3 innate immune signaling mitigates Alzheimer-like pathology. Nature medicine 14:681-687.

Town T, Nikolic V, Tan J (2005) The microglial "activation" continuum: from innate to adaptive responses. Journal of neuroinflammation 2:24.

Trepanier CH, Milgram NW (2010) Neuroinflammation in Alzheimer's disease: are NSAIDs and selective COX-2 inhibitors the next line of therapy? Journal of Alzheimer's disease : JAD 21:1089-1099.

Trouche S, Bontempi B, Roullet P, Rampon C (2009) Recruitment of adult-generated neurons into functional hippocampal networks contributes to updating and strengthening of spatial memory. Proceedings of the National Academy of Sciences of the United States of America 106:5919-5924.

Tsukuda K, Mogi M, Iwanami J, Min LJ, Sakata A, Jing F, Iwai M, Horiuchi M (2009) Cognitive deficit in amyloid-beta-injected mice was improved by pretreatment with a low dose of telmisartan partly because of peroxisome proliferator-activated receptor-gamma activation. Hypertension 54:782-787.

Tsutsumi K, Saavedra JM (1991) Characterization and development of angiotensin II receptor subtypes (AT1 and AT2) in rat brain. The American journal of physiology 261:R209-216.

Ueberham U, Ueberham E, Bruckner MK, Seeger G, Gartner U, Gruschka H, Gebhardt R, Arendt T (2005) Inducible neuronal expression of transgenic TGF-beta1 in vivo: dissection of short-term and long-term effects. The European journal of neuroscience 22:50-64.

Umeda T, Tomiyama T, Kitajima E, Idomoto T, Nomura S, Lambert MP, Klein WL, Mori H (2012) Hypercholesterolemia accelerates intraneuronal accumulation of Abeta oligomers resulting in memory impairment in Alzheimer's disease model mice. Life sciences.

Unsicker K, Flanders KC, Cissel DS, Lafyatis R, Sporn MB (1991) Transforming growth factor beta isoforms in the adult rat central and peripheral nervous system. Neuroscience 44:613-625.

Valero J, Espana J, Parra-Damas A, Martin E, Rodriguez-Alvarez J, Saura CA (2011) Short-term environmental enrichment rescues adult neurogenesis and memory deficits in APP(Sw,Ind) transgenic mice. PloS one 6:e16832.

Van Dam D, De Deyn PP (2006) Drug discovery in dementia: the role of rodent models. Nature reviews Drug discovery 5:956-970.

van der Wal EA, Gomez-Pinilla F, Cotman CW (1993) Transforming growth factor-beta 1 is in plaques in Alzheimer and Down pathologies. Neuroreport 4:69-72.

Vassar R, Bennett BD, Babu-Khan S, Kahn S, Mendiaz EA, Denis P, Teplow DB, Ross S, Amarante P, Loeloff R, Luo Y, Fisher S, Fuller J, Edenson S, Lile J, Jarosinski MA, Biere AL, Curran E, Burgess T, Louis JC, Collins F, Treanor J, Rogers G, Citron M (1999) Beta-secretase cleavage of Alzheimer's amyloid precursor protein by the transmembrane aspartic protease BACE. Science 286:735-741.

Vedernikov YP, Fulep EE, Saade GR, Garfield RE (2002) Calcitonin gene-related peptide dilates the pregnant rat uterine vascular bed via guanylate cyclase, ATP- and Ca-sensitive potassium channels and gap junctions. Current medical research and opinion 18:465-470.

Verret L, Jankowsky JL, Xu GM, Borchelt DR, Rampon C (2007) Alzheimer's-type amyloidosis in transgenic mice impairs survival of newborn neurons derived from adult hippocampal neurogenesis. The Journal of neuroscience : the official journal of the Society for Neuroscience 27:6771-6780.

Vicenzini E, Ricciardi MC, Altieri M, Puccinelli F, Bonaffini N, Di Piero V, Lenzi GL (2007) Cerebrovascular reactivity in degenerative and vascular dementia: a transcranial Doppler study. European neurology 58:84-89.

Vinters HV, Wang ZZ, Secor DL (1996) Brain parenchymal and microvascular amyloid in Alzheimer's disease. Brain Pathol 6:179-195.

Wang J, Ho L, Chen L, Zhao Z, Zhao W, Qian X, Humala N, Seror I, Bartholomew S, Rosendorff C, Pasinetti GM (2007) Valsartan lowers brain beta-amyloid protein levels and improves spatial learning in a mouse model of Alzheimer disease. The Journal of clinical investigation 117:3393-3402.

Washida K, Ihara M, Nishio K, Fujita Y, Maki T, Yamada M, Takahashi J, Wu X, Kihara T, Ito H, Tomimoto H, Takahashi R (2010) Nonhypotensive dose of telmisartan attenuates cognitive impairment partially due to peroxisome proliferator-activated receptor-gamma activation in mice with chronic cerebral hypoperfusion. Stroke; a journal of cerebral circulation 41:1798-1806.

Watkins PB, Zimmerman HJ, Knapp MJ, Gracon SI, Lewis KW (1994) Hepatotoxic effects of tacrine administration in patients with Alzheimer's disease. JAMA : the journal of the American Medical Association 271:992-998.

Watson GS, Cholerton BA, Reger MA, Baker LD, Plymate SR, Asthana S, Fishel MA, Kulstad JJ, Green PS, Cook DG, Kahn SE, Keeling ML, Craft S (2005) Preserved cognition in patients with early Alzheimer disease and amnestic mild cognitive impairment during treatment with rosiglitazone: a preliminary study. The American journal of geriatric psychiatry : official journal of the American Association for Geriatric Psychiatry 13:950-958.

Wayner MJ, Armstrong DL, Phelix CF, Wright JW, Harding JW (2001) Angiotensin IV enhances LTP in rat dentate gyrus in vivo. Peptides 22:1403-1414.

Weller RO, Subash M, Preston SD, Mazanti I, Carare RO (2008) Perivascular drainage of amyloid-beta peptides from the brain and its failure in cerebral amyloid angiopathy and Alzheimer's disease. Brain Pathol 18:253-266.

Westerman MA, Cooper-Blacketer D, Mariash A, Kotilinek L, Kawarabayashi T, Younkin LH, Carlson GA, Younkin SG, Ashe KH (2002) The relationship between Abeta and memory in the Tg2576 mouse model of Alzheimer's disease. The Journal of neuroscience : the official journal of the Society for Neuroscience 22:1858-1867.

Whishaw IQ, Tomie J (1997) Piloting and dead reckoning dissociated by fimbria-fornix lesions in a rat food carrying task. Behavioural brain research 89:87-97.

Whitehouse PJ, Price DL, Clark AW, Coyle JT, DeLong MR (1981) Alzheimer disease: evidence for selective loss of cholinergic neurons in the nucleus basalis. Annals of neurology 10:122-126.

Whitmer RA, Sidney S, Selby J, Johnston SC, Yaffe K (2005) Midlife cardiovascular risk factors and risk of dementia in late life. Neurology 64:277-281.

Wilcock DM, Gharkholonarehe N, Van Nostrand WE, Davis J, Vitek MP, Colton CA (2009a) Amyloid reduction by amyloid-beta vaccination also reduces mouse tau pathology and protects from neuron loss in two mouse models of Alzheimer's disease. The Journal of neuroscience : the official journal of the Society for Neuroscience 29:7957-7965.

Wilcock DM, Vitek MP, Colton CA (2009b) Vascular amyloid alters astrocytic water and potassium channels in mouse models and humans with Alzheimer's disease. Neuroscience 159:1055-1069.

Wolozin B, Kellman W, Ruosseau P, Celesia GG, Siegel G (2000) Decreased prevalence of Alzheimer disease associated with 3-hydroxy-3-methyglutaryl coenzyme A reductase inhibitors. Archives of neurology 57:1439-1443.

Wolozin B, Wang SW, Li NC, Lee A, Lee TA, Kazis LE (2007) Simvastatin is associated with a reduced incidence of dementia and Parkinson's disease. BMC medicine 5:20.

Wong TP, Debeir T, Duff K, Cuello AC (1999) Reorganization of cholinergic terminals in the cerebral cortex and hippocampus in transgenic mice carrying mutated presenilin-1 and amyloid precursor protein transgenes. The Journal of neuroscience : the official journal of the Society for Neuroscience 19:2706-2716.

Wood JG, Mirra SS, Pollock NJ, Binder LI (1986) Neurofibrillary tangles of Alzheimer disease share antigenic determinants with the axonal microtubule-associated protein tau (tau). Proceedings of the National Academy of Sciences of the United States of America 83:4040-4043.

WorldAlzheimerReport (2011) http://www.alz.co.uk/research/WorldAlzheimerReport2011.pdf.

Wright JW, Harding JW (2008) The angiotensin AT4 receptor subtype as a target for the treatment of memory dysfunction associated with Alzheimer's disease. Journal of the renin-angiotensin-aldosterone system : JRAAS 9:226-237.

Wright JW, Harding JW (2010) The brain RAS and Alzheimer's disease. Experimental neurology 223:326-333.

Wu H, Lu D, Jiang H, Xiong Y, Qu C, Li B, Mahmood A, Zhou D, Chopp M (2008) Simvastatin-mediated upregulation of VEGF and BDNF, activation of the PI3K/Akt pathway, and increase of neurogenesis are associated with therapeutic improvement after traumatic brain injury. Journal of neurotrauma 25:130-139.

Wu Z, Guo H, Chow N, Sallstrom J, Bell RD, Deane R, Brooks AI, Kanagala S, Rubio A, Sagare A, Liu D, Li F, Armstrong D, Gasiewicz T, Zidovetzki R, Song X, Hofman F, Zlokovic BV (2005) Role of the MEOX2 homeobox gene in neurovascular dysfunction in Alzheimer disease. Nature medicine 11:959-965.

Wyss-Coray T (2006) Inflammation in Alzheimer disease: driving force, bystander or beneficial response? Nature medicine 12:1005-1015.

Wyss-Coray T, Feng L, Masliah E, Ruppe MD, Lee HS, Toggas SM, Rockenstein EM, Mucke L (1995) Increased central nervous system production of extracellular matrix components and development of hydrocephalus in transgenic mice overexpressing transforming growth factor-beta 1. The American journal of pathology 147:53-67.

Wyss-Coray T, Lin C, Sanan DA, Mucke L, Masliah E (2000) Chronic overproduction of transforming growth factor-beta1 by astrocytes promotes Alzheimer's disease-like microvascular degeneration in transgenic mice. The American journal of pathology 156:139-150.

Wyss-Coray T, Lin C, Yan F, Yu GQ, Rohde M, McConlogue L, Masliah E, Mucke L (2001) TGF-beta1 promotes microglial amyloid-beta clearance and reduces plaque burden in transgenic mice. Nature medicine 7:612-618.

Wyss-Coray T, Loike JD, Brionne TC, Lu E, Anankov R, Yan F, Silverstein SC, Husemann J (2003) Adult mouse astrocytes degrade amyloid-beta in vitro and in situ. Nature medicine 9:453-457.

Wyss-Coray T, Masliah E, Mallory M, McConlogue L, Johnson-Wood K, Lin C, Mucke L (1997) Amyloidogenic role of cytokine TGF-beta1 in transgenic mice and in Alzheimer's disease. Nature 389:603-606.

Yaffe K (2007) Metabolic syndrome and cognitive disorders: is the sum greater than its parts? Alzheimer disease and associated disorders 21:167-171.

Yaffe K, Barrett-Connor E, Lin F, Grady D (2002) Serum lipoprotein levels, statin use, and cognitive function in older women. Archives of neurology 59:378-384.

Yamada M, Lamping KG, Duttaroy A, Zhang W, Cui Y, Bymaster FP, McKinzie DL, Felder CC, Deng CX, Faraci FM, Wess J (2001) Cholinergic dilation of cerebral blood vessels is abolished in M(5) muscarinic acetylcholine receptor knockout mice. Proceedings of the National Academy of Sciences of the United States of America 98:14096-14101.

Yamaguchi F, Richards SJ, Beyreuther K, Salbaum M, Carlson GA, Dunnett SB (1991) Transgenic mice for the amyloid precursor protein 695 isoform have impaired spatial memory. Neuroreport 2:781-784.

Yan Q, Zhang J, Liu H, Babu-Khan S, Vassar R, Biere AL, Citron M, Landreth G (2003) Anti-inflammatory drug therapy alters beta-amyloid processing and deposition in an animal model of Alzheimer's disease. The Journal of neuroscience : the official journal of the Society for Neuroscience 23:7504-7509.

Yan SD, Chen X, Fu J, Chen M, Zhu H, Roher A, Slattery T, Zhao L, Nagashima M, Morser J, Migheli A, Nawroth P, Stern D, Schmidt AM (1996) RAGE and amyloid-beta peptide neurotoxicity in Alzheimer's disease. Nature 382:685-691.

Yasojima K, Akiyama H, McGeer EG, McGeer PL (2001) Reduced neprilysin in high plaque areas of Alzheimer brain: a possible relationship to deficient degradation of beta-amyloid peptide. Neuroscience letters 297:97-100.

Yong VW, Rivest S (2009) Taking advantage of the systemic immune system to cure brain diseases. Neuron 64:55-60.

Yu L, Jin X, Yang Y, Cui N, Jiang C (2011) Rosiglitazone inhibits vascular KATP channels and coronary vasodilation produced by isoprenaline. British journal of pharmacology 164:2064-2072.

Zarow C, Barron E, Chui HC, Perlmutter LS (1997) Vascular basement membrane pathology and Alzheimer's disease. Annals of the New York Academy of Sciences 826:147-160.

Zhao L, Teter B, Morihara T, Lim GP, Ambegaokar SS, Ubeda OJ, Frautschy SA, Cole GM (2004) Insulin-degrading enzyme as a downstream target of insulin receptor signaling cascade: implications for Alzheimer's disease intervention. The Journal of neuroscience : the official journal of the Society for Neuroscience 24:11120-11126.

Zhu WW, Liu XP, Wu N, Zhao TT, Zhao Y, Zhang J, Shao JH (2007) Beneficial effects of losartan on vascular injury induced by advanced glycosylation end products and their receptors in spontaneous hypertension rats. Molecular and cellular biochemistry 304:35-43.

Zhu Y, Culmsee C, Klumpp S, Krieglstein J (2004) Neuroprotection by transforming growth factor-beta1 involves activation of nuclear factor-kappaB through phosphatidylinositol-3-OH kinase/Akt and mitogen-activated protein kinase-extracellular-signal regulated kinase1,2 signaling pathways. Neuroscience 123:897-906.

Zlokovic BV (2005) Neurovascular mechanisms of Alzheimer's neurodegeneration. Trends in neurosciences 28:202-208.

Zlokovic BV (2010) Neurodegeneration and the neurovascular unit. Nature medicine 16:1370-1371.

Zlokovic BV (2011) Neurovascular pathways to neurodegeneration in Alzheimer's disease and other disorders. Nature reviews Neuroscience 12:723-738.

Zonta M, Angulo MC, Gobbo S, Rosengarten B, Hossmann KA, Pozzan T, Carmignoto G (2003) Neuron-to-astrocyte signaling is central to the dynamic control of brain microcirculation. Nature neuroscience 6:43-50.

Appendix

Selective in vivo antagonism of endothelin receptors in transforming growth factor-β1 transgenic mice that mimic the vascular pathology of Alzheimer's disease[1]

Panayiota Papadopoulos, Brice Ongali, and Edith Hamel

Abstract: Increased levels of transforming growth factor-β_1 (TGF-β_1) induce a vascular pathology that shares similarities with that seen in Alzheimer's disease, and which possibly contributes to the cognitive decline. In aged transgenic mice that overexpress TGF-β_1 (TGF mice), we previously found reduced dilatory function and selectively impaired endothelin-1 (ET-1)-induced contraction. Here we studied the effects of chronic treatments with selective ET_A (ABT-627) or ET_B (A-192621) receptor antagonist on cerebrovascular reactivity, cerebral perfusion, or memory performance. The dilatory deficit of TGF mice was not improved by either treatment, but both ET-1 contraction and basal nitric oxide (NO) production were distinctly altered. Although ABT-627 was devoid of any effect in TGF mice, it virtually abolished the ET-1-induced contraction and NO release in wild-type (WT) littermates. In contrast, A-192621 only acted upon TGF mice with full recovery of ET-1 contraction and baseline NO synthesis. TGF mice, treated or not, had no cognitive deficit in the Morris water maze, nor did ABT-627-treated WT controls despite severely impaired vasoreactivity. These findings confirm that ET_A receptors primarily mediate the ET-1-induced contraction. Further, they suggest that ET_B receptors play a detrimental role in conditions of increased TGF-β_1 and that vascular dysfunction does not inevitably lead to cognitive deficit.

Key words: endothelin-1, selective endothelin receptor antagonism, hypoperfusion, vasoreactivity, memory.

Résumé : Des niveaux élevés du transforming growth factor-β_1 (TGF-β_1) induisent une pathologie vasculaire semblable à celle observée dans la maladie d'Alzheimer, et qui pourrait contribuer au déficit cognitif. Nous avons préalablement observé une diminution de la fonction dilatatrice et une altération sélective de la contraction induite par l'endothéline-1 (ET-1) chez des souris transgéniques âgées surexprimant le TGF-β_1 (souris TGF). Dans la présente étude, nous examinons les effets de traitements chroniques avec des antagonistes sélectifs des récepteurs ET_A (ABT-627) ou ET_B (A-192621) sur la réactivité cérébrovasculaire, le débit sanguin cérébral ou la mémoire. Les traitements n'ont pas amélioré le déficit dilatateur des souris TGF, mais ils ont significativement modifié la contraction induite par l'ET-1 et la production basale de monoxyde d'azote (NO). ABT-167 n'a eu aucun effet chez les souris TGF alors qu'il a pratiquement supprimé la contraction induite par l'ET-1 et la libération de NO chez leurs témoins de type sauvage (TS) de même portée. Par contre, A-192621 n'a agi que chez les souris TGF, rétablissant la contraction induite par l'ET-1 et la synthèse basale de NO. Les souris TGF, traitées ou non traitées, n'ont montré aucun déficit cognitif dans la piscine de Morris. Il en a été de même des témoins TS traités par ABT-627, malgré l'altération importante de la vasoréactivité. Ces résultats confirment que les récepteurs ET_A sont les principaux médiateurs de la contraction induite par l'ET-1, soutiennent que les récepteurs ET_B ont un rôle néfaste en présence de niveaux élevés de TGF-β_1, et montrent que les dysfonctions vasculaires n'entraînent pas forcément un déficit cognitif.

Mots-clés : endothéline-1, antagonisme sélectif des récepteurs de l'endothéline, hypoperfusion, vasoréactivité, mémoire.

[Traduit par la Rédaction]

Introduction

The integrity of brain function requires an absolute maintenance of cerebral blood supply through a proficient vasculature. When compromised, the latter may induce chronic cerebral hypoperfusion, destabilizing substrate delivery and waste removal, hence resulting in a meaningful mnemonic decline (de la Torre et al. 1992; Ruitenberg et al. 2005). In Alzheimer's disease (AD), progressive dementia is accompanied by both neurodegenerative and cerebrovascular alter-

Received 23 October 2009. Accepted 3 February 2010. Published on the NRC Research Press Web site at cjpp.nrc.ca on 22 June 2010.

P. Papadopoulos,[2] B. Ongali,[2] and E. Hamel.[3] Laboratory of Cerebrovascular Research, Montreal Neurological Institute, McGill University, Montréal, QC H3A 2B4, Canada.

[1]This article is one of a selection of papers published in the two-part special issue entitled 20 Years of Endothelin Research.
[2]The first two authors contributed equally to this work.
[3]Corresponding author (e-mail: edith.hamel@mcgill.ca).

ations primarily characterized by amyloid β-peptide (Aβ) deposition within the vessel walls (cerebral amyloid angiopathy, CAA) and overexpression of inflammatory and basement membrane proteins (Zarow et al. 1997). The levels of transforming growth factor-β_1 (TGF-β_1) in AD patients have also generated interest for their potential role in the vascular pathology, as TGF-β_1 is increased in the serum (Malaguarnera et al. 2006), cerebrospinal fluid (Chao et al. 1994; Wyss-Coray et al. 1997), Aβ plaques (van der Wal et al. 1993), and brain vessels in these patients (Grammas and Ovase 2002). TGF-β_1 is also upregulated in a variety of conditions including mechanical injury (Lin et al. 2005) and ischemic stroke (Krupinski et al. 1996), consequently prompting fibrosis (Leask and Abraham 2004). Moreover, TGF-β_1 gene polymorphisms have been considered as a possible risk factor for developing AD (Luedecking et al. 2000).

Transgenic mice that overexpress a constitutive form of TGF-β_1 (TGF mice) in astrocytes mimic several aspects of the cerebrovascular pathology seen in AD. These include primarily structural abnormalities associated with increased levels of extracellular matrix proteins, such as collagen, perlecan, and fibronectin, thickening of the blood vessel walls, and microvascular degenerative changes (Kalaria and Pax 1995; Wyss-Coray et al. 2000; Tong et al. 2005). Additionally, TGF mice exhibit reduced resting cerebral perfusion (Gaertner et al. 2005) and glucose metabolism (Galea et al. 2006), two other landmarks of AD brain dysfunction. Functionally, TGF mice display progressive impairments in endothelium-dependent and -independent dilatations, as well as a selective reduction in endothelin-1 (ET-1) contractile response in elderly animals (Tong et al. 2005), the latter possibly reflecting an adapted response to the dilatory deficits. These dysfunctions have been associated with reduced synthesis of vasoactive molecules in the blood vessels, altered ET_A receptor signalling and upregulation of vascular ET_B receptor levels (Tong et al. 2005; Tong and Hamel 2007). Hence, a better understanding of these alterations and how TGF-β_1 selectively impairs the cerebrovascular effects of ET-1 could have significance for the vascular pathology in AD.

In the present study, we sought to elucidate the roles of ET_A and ET_B receptors in the impaired ET-1-mediated contractile response in aged TGF mice by assessing the cerebrovascular reactivity in TGF and wild-type (WT) controls treated in vivo with selective ET-1 receptor antagonists. In addition, we tested the outcome of ET_A receptor blockade on functional hyperemia and spatial memory.

Materials and methods

Animals

Experiments were approved by the Animal Ethics Committee of the Montreal Neurological Institute and complied with the guidelines of the Canadian Council on Animal Care. The animals used in the study were heterozygous transgenic mice overexpressing a constitutively active form of TGF-β_1 under the control of the glial fibrillary acidic protein (GFAP) promoter on a C57BL/6J background (line T64) (Wyss-Coray et al. 1995). Mice were screened for transgene expression by touchdown PCR using tail-extracted DNA (Wyss-Coray et al. 1997). TGF mice and control WT littermates were used at 16 months of age (body weight ~40 g), males and females being in approximately equal numbers in each group.

In vivo drug treatments

TGF mice and WT littermates were treated or not with selective ET_A (ABT-627 or atrasentan, 10 mg/kg per day) or ET_B (A-192621, 30 mg/kg per day) receptor antagonist for a period of 8 weeks. Both drugs were obtained from Abbott Laboratories, dissolved in water, and rendered basic with NaOH for a final pH of approximately 7.5. To mask the bitter taste of the solution, glucose was added to a final concentration of 2.5%, which did not affect cerebrovascular reactivity (data not shown). Mice had free access to water, water supplemented with glucose (control conditions), or water supplemented with glucose and either drug. No significant difference in body weight gain was observed across the different treatment groups throughout the study (data not shown).

Morris water maze

Spatial memory was tested in the Morris water maze (a 1.4 m diameter circular pool filled with opaque water at $17 \pm 1\,^{\circ}C$) only in mice treated with the ET_A receptor antagonist. The paradigm consisted of 3 successive days of visible-platform training followed by 5 days of hidden-platform trials in which the positions of the platform and wall cues were changed, as described previously (deIpolyi et al. 2008). On day 1, all mice unable to locate the hidden platform within the allotted 60 s were directed to it and allowed to rest upon it for 10 s. For the hidden platform training, mice were given 3 trials daily (90 s/trial, 45 min intertrial interval). On the last day, at least 2 h after the last hidden-platform trials, mice were given a probe trial (60 s), in which the platform was removed. Percentage time spent and distance traveled in the target quadrant (where the platform was initially located), swim speed, and swim pattern were recorded and analyzed with the 2020 Plus tracking system and Water 2020 software (Ganz FC62D video camera; HVS Image) (Nicolakakis et al. 2008; Tong et al. 2009). After each trial, animals were kept under a heating lamp to dry to prevent hypothermia.

Cerebral blood flow

Laser Doppler flowmetry (Transonic Systems, Ithaca, USA) measurements of cerebral blood flow (CBF) increases induced by whisker stimulation were carried out 3 days after the Morris water maze. Mice were anesthetized with ketamine (85 mg/kg i.p., Bioniche, Belleville, Canada) and xylazine (3 mg/kg i.p., Haver, Etobicoke, Canada), and fixed in a stereotaxic frame. The bone over the left barrel cortex was thinned to translucency, as described previously (Nicolakakis et al. 2008). Body temperature was kept stable ($37\,^{\circ}C$) with a heating pad. Four or 5 recordings of CBF were acquired before, during, and after stimulation of the whiskers on the right side of the snout (20 s, 8–10 Hz), and averaged for each mouse. Cortical CBF change was expressed as percent increase from baseline. The procedure lasted less than 75 min, and the experimenter was blind to the identities of the mice.

Fig. 1. Effects of ABT-627 (ET_A receptor antagonist) on cerebrovascular reactivity in aged TGF mice and WT controls. Aged TGF mice displayed impaired responses to ACh, CGRP, ET-1, and L-NNA relative to age-matched WT littermates. Chronic ABT-627 treatment almost completely ablated the ET-1 response and baseline NO release measured during NOS inhibition with L-NNA in treated WT mice, and slightly but significantly reduced the maximal dilatation to ACh and CGRP, as compared with untreated WT controls. In aged TGF mice treated with ABT-627, there was no improvement in any of the vasomotor deficits. Data are means ± SE, n = 3–7 mice per group. ★, Significant at $p < 0.05$, ★★, $p < 0.01$, and ★★★, $p < 0.001$ compared with untreated WT controls; *, $p < 0.05$, **, $p < 0.01$, and ***, $p < 0.001$ compared with untreated TGF (one-way ANOVA followed by Newman–Keuls post hoc multiple comparisons test). The vertical bar (|) across symbols indicates that all included groups differ from untreated WT controls. Definitions as shown in Table 1.

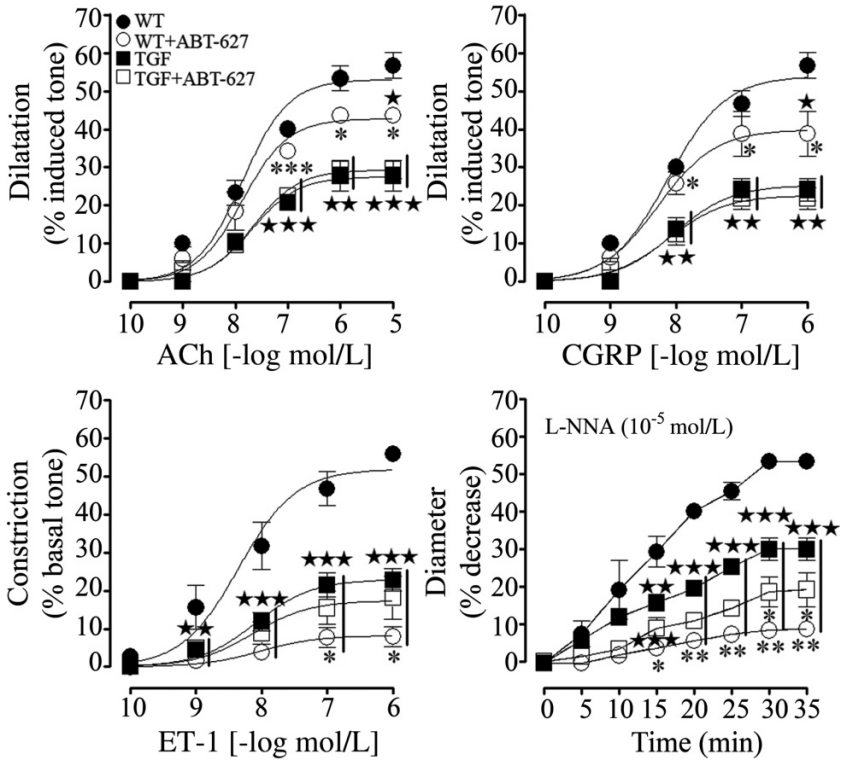

Vascular reactivity

At the end of the in vivo testing, mice were euthanized by cervical dislocation and the middle cerebral artery (MCA) was collected in cold Krebs solution (4 °C, pH 7.4 ± 0.1) containing the following: 118 mmol/L NaCl, 4.5 mmol/L KCl, 2.5 mmol/L $CaCl_2$, 1 mmol/L $MgSO_4$, 1 mmol/L KH_2PO_4, 25 mmol/L $NaHCO_3$, and 11 mmol/L glucose. MCA segments (40–70 μm average intraluminal diameter) were isolated, cannulated, pressurized (60 mm Hg), and superfused with a Krebs solution for evaluation of vascular reactivity using online videomicroscopy (Tong et al. 2005). Dilatory responses to acetylcholine (ACh; 10^{-10}–10^{-5} mol/L) and calcitonin gene-related peptide (CGRP; 10^{-10}–10^{-6} mol/L) were tested on vessels slightly preconstricted with serotonin (5-HT; 2×10^{-7} mol/L, to ~10% of the basal tone). Contractile responses to ET-1 (10^{-10}–10^{-6} mol/L) and the tonic production of nitric oxide (NO) were subsequently examined in vessels at basal tone, the latter assessing diameter reduction during inhibition of nitric oxide synthase (NOS) with N^{ω}-nitro-L-arginine (L-NNA; 10^{-5} mol/L, by superfusion for 35 min). Vasomotor responses, expressed as percent changes in vessel diameter from basal or preconstricted tone, were plotted as a function of agonist concentration or time course of NOS inhibition. The dose–response curves were fitted by using GraphPad Prism. The maximal response ($E_{A\,max}$) was used to determine the agonist efficacy, and the concentration eliciting half the $E_{A\,max}$ (EC_{50} value or $pD_2 = -\log EC_{50}$), the agonist potency.

Statistical analysis

Data are expressed as means ± standard error of the mean (SE) and were analyzed by one-way ANOVA followed by Newman–Keuls post hoc multiple comparisons test (GraphPad Prism 4). A p value of 0.05 was considered as significant.

Results

Cerebrovascular abnormalities in aged TGF mice

In agreement with our previous findings (Tong et al. 2005), cerebral arteries of aged TGF mice displayed a reduced capacity to dilate to ACh and CGRP, an attenuated baseline release of NO, as assessed by the lessened diameter reduction during NOS inhibition with L-NNA, and a reduced contractile response to ET-1, as compared to age-matched WT controls (Figs. 1, 4, and Tables 1, 2). The vasomotor deficits occurred without any change in agonist potencies between WT and TGF mice, ruling out the possibility of receptor desensitization (Tables 1, 2).

Table 1. Effects of ABT-627 (ET_A receptor antagonist) on cerebrovascular responses to ACh, CGRP, ET-1, and NOS inhibition with L-NNA in aged WT and TGF mice.

Agonist		WT	WT + ABT-627	TGF	TGF + ABT-627
ACh	$E_{A\,max}$	53.0±2.1	42.7±1.8★,*	27.5±1.5★★★	29.3±1.2★★★
	pD_2	7.86±0.10	7.86±0.11	7.68±0.15	7.65±0.11
CGRP	$E_{A\,max}$	53.9±2.0	39.8±2.9★,*	25.3±1.8★★	22.6±1.8★★
	pD_2	8.12±0.09	8.27±0.18	8.03±0.17	8.12±0.19
ET-1	$E_{A\,max}$	51.8±3.5	8.2±1.5★★★,*	22. 9±1.8★★★	17.3±2.7★★★
	pD_2	8.35±0.17	8.02±0.40	8.09±0.18	8.14±0.37
L-NNA	$E_{A\,max}$	52.8±1.4	8.9±1.0★★★,**	29.8±2.9★★★	19.2±4.5★★★,*

Note: Data are means ± SE (n = 3–7 mice per group) and are expressed as the agonist maximal response ($E_{A\,max}$) or potency (pD_2, $-\log EC_{50}$). $E_{A\,max}$ is the percent maximal dilatation to ACh and CGRP and the percent maximal diameter decrease either to ET-1 or after 35 min incubation with 10^{-5} mol/L L-NNA. ★, Significant at $p < 0.05$, ★★, $p < 0.01$, and ★★★, $p < 0.001$ compared with untreated WT controls; *, $p < 0.05$, **, $p < 0.01$ compared with untreated TGF (one-way ANOVA followed by Newman–Keuls post hoc multiple comparisons test). TGF mice, transgenic mice overexpressing a constitutive form of TGF-β_1; WT, wild type; ACh, acetylcholine; CGRP, calcitonin gene-related peptide; ET-1, endothelin-1; L-NNA, N^{ω}-nitro-L-arginine; NOS, nitric oxide synthase.

Fig. 2. Effects of ABT-627 (ET_A receptor antagonist) on the CBF response induced by whisker stimulation in aged WT and TGF mice. The colour version of this figure is available on the journal Web site at http://cjpp.nrc.ca. (A) Representative recordings of CBF measured before, during, and after whisker stimulation (shaded area, 20 s at 8–10 Hz) in treated and untreated WT and TGF mice. Tracings show that untreated TGF mice (lowest line in shaded area of panel A) displayed a reduced CBF response and that treatment with ABT-627 fully normalized this response. (B) Average increases in cortical CBF in the barrel cortex contralateral to whisker stimulation. ABT-627 had no effect on the hemodynamic response to whisker stimulation in WT mice, but it significantly improved the deficit in TGF mice. Data are means ± SE, n = 6 mice per group. ★★★, Significant at $p < 0.001$; **, $p < 0.01$ (one-way ANOVA followed by Newman–Keuls post hoc multiple comparisons test). CBF, cerebral blood flow; TPU, tissue perfusion units.

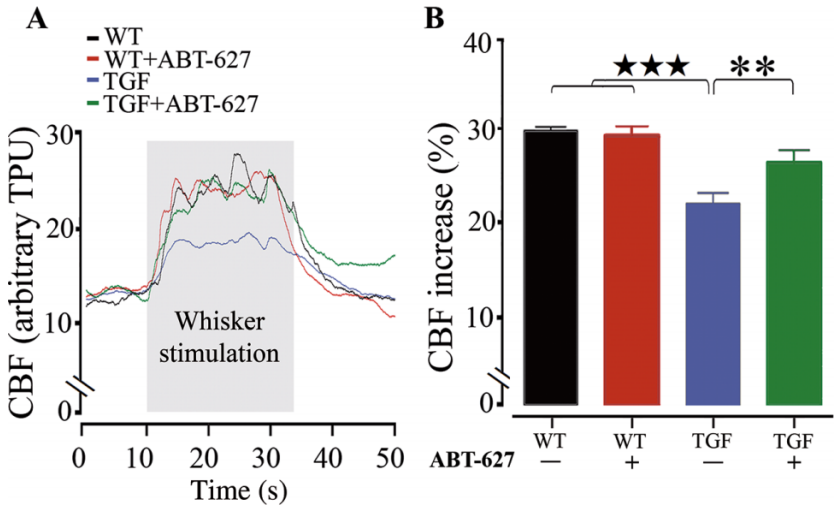

Effects of ET_A receptor antagonism (ABT-627) on cerebrovascular function

Chronic ET_A receptor antagonism with ABT-627 did not result in any additional deleterious effect on the impaired ET-1 response in the TGF mice. Similarly, the reduced basal NO release was not exacerbated by treatment, and there were no beneficial effects on the impaired ACh and CGRP vasodilatations (Fig. 1). However, such chronic ET_A receptor antagonism drastically reduced the ET-1-induced contraction in WT controls and the basal NO release measured during NOS inhibition with L-NNA, as compared with untreated controls (Fig. 1). Treatment did not generate any changes in agonist potencies (Table 1).

In WT controls, whisker stimulation elicited the characteristic increase in CBF in the barrel cortex, a response significantly reduced (22%; $p < 0.001$) in aged TGF mice (Fig. 2). Chronic ET_A receptor antagonism with ABT-627 did not alter this functional hyperemic response in WT controls, but it significantly improved it in aged TGF mice (Figs. 2A, 2B).

Effects of ET_A receptor antagonism (ABT-627) on spatial memory

Considering that aged TGF mice exhibited a reduced baseline perfusion (Gaertner et al. 2005), impaired cerebrovascular reactivity (Fig. 1), and decreased CBF response to increased neuronal activity (Fig. 2), conditions that can contribute or exacerbate mnemonic dysfunction in AD (de la Torre et al. 1992; Ruitenberg et al. 2005), we tested the outcome of these deficits on spatial learning and memory. In the visible platform pretraining, thought to reduce the stress

Fig. 3. Effects of ABT-627 (ET_A receptor antagonist) on spatial learning and memory in aged WT and TGF mice in the Morris water maze. (A) None of the groups displayed deficit in the time needed to find the visible (day 1–3) or hidden (day 4–8) platform. (B–D) Similarly, all groups exhibited comparable swim speed, swim time, and traveling distance in the target quadrant during the probe trial after removing the platform. Data are means ± SE, n = 9–12 mice per group.

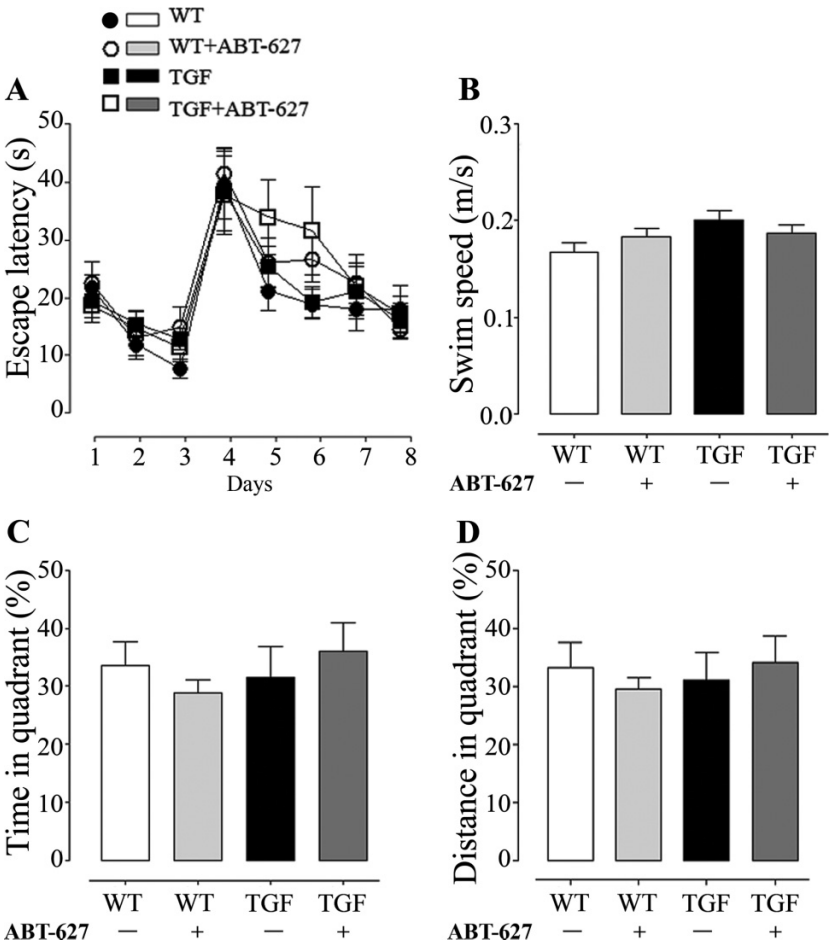

levels associated with the novelty of the task and environment, all mice performed identically, discarding visual or motor deficits in aged WT and TGF mice. In the hidden platform and probe trials, the escape latency curves and the inclination for the target quadrant (percentage time spent and distance traveled where the platform used to be located) did not differ between aged TGF mice and WT controls (Fig. 3). Chronic ET_A receptor blockade with ABT-627 did not affect any of the parameters in any of the groups (Fig. 3).

Effects of ET_B receptor antagonism (A-192621) on vasomotor reactivity

Chronic blockade of ET_B receptors with A-192621 had no effect on the ET-1-induced contraction or basal NO release in WT controls, and it only slightly but significantly reduced the response to ACh at high concentrations (Fig. 4). However, such treatment fully normalized the ET-1 contractile response and baseline NO release in aged TGF mice, the responses reaching levels equivalent to those of control WT littermates. In contrast, treatment did not improve the impaired vasodilatory responses to ACh and CGRP (Fig. 4). There were no agonist potency differences between any of the groups (Table 2).

Discussion

The results demonstrate that chronic ET_A receptor antagonism with ABT-627 drastically altered the contractile response to ET-1 and basal NO release of WT mice—two important regulators of cerebrovascular basal tone—to levels below those of aged TGF mice. The treatment, however, did not exacerbate the reduced ET-1-induced contraction or rescue the impaired endothelium-dependent and -independent dilatations of TGF mice, although it largely normalized the CBF response upon whisker stimulation. Despite severe vascular dysfunctions and suboptimal hemodynamic responses to increased neuronal activity, aged TGF mice did not display any learning or memory deficits in the Morris water maze. Importantly, chronic blockade of ET_B receptors with A-192621 in aged TGF mice selectively restored both ET-1 -induced contractions and basal NO release.

Effects of the ET_A receptor antagonist ABT-627 on cerebrovascular reactivity

The capacity of the ET_A receptor antagonist ABT-627 to ablate the ET-1 response and basal NO release in WT mice even more severely than the deficits seen in TGF mice unequivocally confirmed that ET_A receptors are the primary

Fig. 4. Effects of A-192621 (ET_B receptor antagonist) on cerebrovascular reactivity in aged TGF mice and WT controls. Chronic A-192621 treatment had no beneficial effect on the impaired dilatory responses to ACh and CGRP in aged TGF compared with WT littermates. However, A-192621 normalized the reduced ET-1 contractile response and basal NO release in TGF mice. In WT mice, A-192621 slightly but significantly reduced the dilatation to ACh. Data are means ± SE, $n = 5$ mice per group. ★, Significant at $p < 0.05$, ★★, $p < 0.01$, and ★★★, $p < 0.001$ compared with untreated WT controls; *, $p < 0.05$, **, $p < 0.01$, and ***, $p < 0.001$ compared with untreated TGF (one-way ANOVA followed by Newman–Keuls post hoc multiple comparisons test). The vertical bar (|) across symbols indicates that all included groups differ from untreated WT controls or TGF mice.

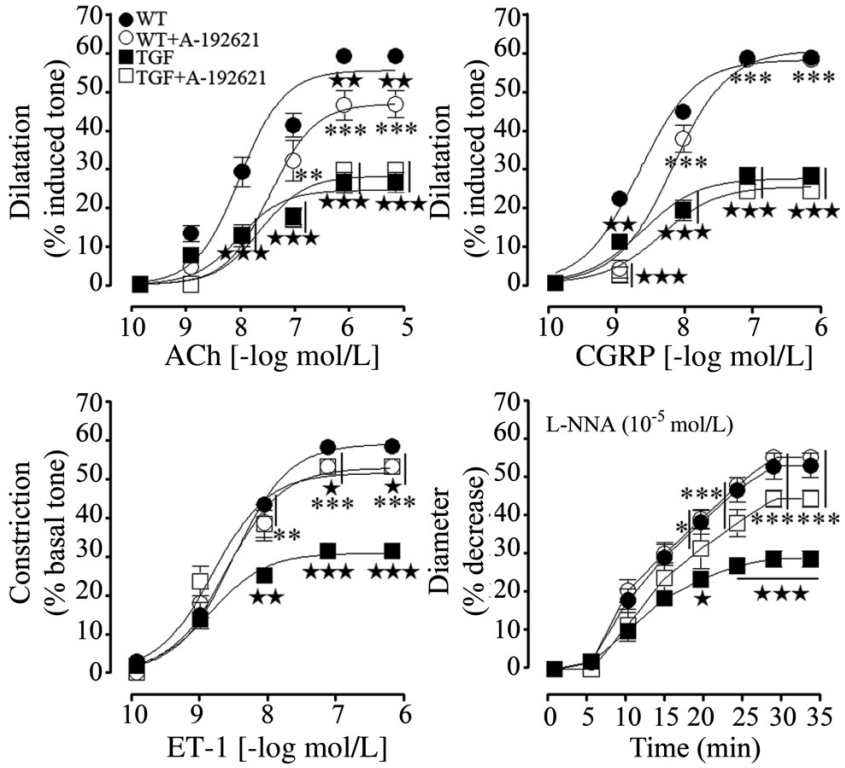

Table 2. Effects of A-192621 (ET_B receptor antagonist) on cerebrovascular responses to ACh, CGRP, ET-1, and NOS inhibition with L-NNA in aged WT and TGF mice.

Agonist		WT	WT + A-192621	TGF	TGF + A-192621
ACh	$E_{A\,max}$	58.8±2.3	49.6±2.4★★,***	25.9±1.7★★★	29.8±1.4★★★
	pD_2	8.04±0.11	7.45±0.13	8.06±0.18	7.64±0.12
CGRP	$E_{A\,max}$	61.2±1.5	63.8±1.8***	28.7±1.5★★★	26.5±1.5★★★
	pD_2	8.69±0.06	8.17±0.07	8.64±0.14	8.35±0.13
ET-1	$E_{A\,max}$	63.7±1.3	56.1±2.2★,***	32.7±1.1★★★	54.7±2.0★,***
	pD_2	8.48±0.06	8.59±0.11	8.85±0.09	8.80±0.10
L-NNA	$E_{A\,max}$	56.0±3.4	58.2±1.4***	30.3±2.2★★★	46.8±2.3***

Note: Data are means ± SE ($n = 5$ mice per group) and are expressed as the agonist maximal response ($E_{A\,max}$) or potency (pD_2, $-\log EC_{50}$). $E_{A\,max}$ is the percent maximal dilatation to ACh and CGRP and the percent maximal diameter decrease either to ET-1 or after 35 min incubation with 10^{-5} mol/L L-NNA. ★, Significant at $p < 0.05$, ★★, $p < 0.01$, and ★★★, $p < 0.001$ compared with untreated WT controls; ***, $p < 0.001$ compared with untreated TGF (one-way ANOVA followed by Newman–Keuls post hoc multiple comparisons test). Definitions as in Table 1.

mediators of the ET-1-induced contraction in cerebral blood vessels of several species, including human (Nilsson et al. 1997; Pierre and Davenport 1998; Widder et al. 2000; Tong and Hamel 2007). These results also indicate that ET_B receptors contribute insignificantly to the ET-1-mediated contraction in mouse cerebral arteries, thereby substantiating that they primarily correspond to endothelial receptors, as previously reported (Szok et al. 2001). Additionally, the fact that ABT-627 exerted a small, but significant, reducing effect on the maximal dilatory responses to ACh and CGRP in WT mice, responses that, respectively, depend entirely (Elhusseiny et al. 2000; Yamada et al. 2001) or partly (Rosenblum et al. 1993; Akerman et al. 2002) on endothelial NO, suggested that not only basal NO release, but also receptor-mediated dilatory responses, were altered by chronic ET_A receptor antagonism. These findings imply that chronic blockade of ET_A receptors diverted ET-1 towards endothelium ET_B receptor-mediated NO synthesis and release (Feger et al. 1997; Nilsson et al. 1997; Szok et al. 2001), resulting in a decreased capacity of NOS to produce NO upon

receptor activation. The fact that basal NO release was literally abolished in treated WT mice implies that reduction in endothelial NO synthase (eNOS) activity was exacerbated or eNOS protein levels were reduced by chronic ABT-627 treatment. Interestingly, in TGF mice that display decreased eNOS protein levels (Tong et al. 2005), the reduced ACh- and CGRP-mediated dilatations were not worsened by ABT-627 treatment, suggesting that eNOS-mediated functions were already maximally impaired. Previous studies with chronic ET_A receptor blockade in rat basilar arteries found an increased sensitivity to ET-1 and no effect on ACh dilatations (Widder et al. 2000; Harris et al. 2008). These apparent discrepancies could be explained by the use of different vessels, species, antagonists or, possibly, experimental protocols. Indeed, in contrast to our study in which receptor blockade was still effective during our reactivity measurements—on the basis of the plasma half-life of ABT-627 (Wessale et al. 2002)—other studies discontinued treatment 36 h before reactivity measurements, most likely clearing the antagonist from the receptor sites (Widder et al. 2000). In line with these dissimilarities, in diabetic rat basilar artery segments, ET_A receptor antagonism completely restored ACh-induced relaxation (Harris et al. 2008), a response not improved in TGF mice, further pointing to different effects dependent on models or pathology.

Effects of the ET_A receptor antagonist ABT-627 on hemodynamic responses and cognition

It has been previously reported that TGF mice display cerebral hypoperfusion at baseline in specific brain areas as early as 9 months of age (Gaertner et al. 2005). Here, we found that aged TGF mice also exhibited an impaired hyperemic response to whisker stimulation, reflecting dysfunction in the neurogliovascular unit responsible for coupling blood flow to increased neuronal activity (Hamel 2006; Haydon and Carmignoto 2006). As this glutamate-induced neurovascular coupling response is essentially mediated by dilatory arachidonic acid derivatives released from cortical neurons (Niwa et al. 2000) and astrocytes (Koehler et al. 2009) and modulated by neuronal NO (Dirnagl et al. 1993; Ayata et al. 1996), it is likely that the impaired response results from increased neuroinflammation in brains of TGF mice exemplified by astroglial activation (Lacombe et al. 2004). The capacity of chronic ET_A blockade to significantly improve this neurovascular coupling response in TGF mice, despite its failure to rescue vascular reactivity, may be due to a beneficial effect on astroglial activation, as shown in rat glial cell cultures (Filipovich and Fleisher-Berkovich 2008).

Although aged TGF mice exhibited cerebral hypoperfusion (Gaertner et al. 2005) and cerebrovascular dysfunction, they performed normally in both the learning and memory aspects of the Morris water maze. A previous study in 13-week-old rats with intracerebroventricular administration of TGF-β_1 for 3 months similarly found no impairment in the learning aspect of the test, but reported memory deficits in the probe trial (Nakazato et al. 2002). Chronic cerebral hypoperfusion appears as an early and important contributing factor to AD pathogenesis (Iadecola 2004). In animal models of cerebral hypoperfusion, recent studies indicated that the manifestation of cognitive impairments is highly dependent on the intensity of the perfusion deficit and the age of the animals (Farkas et al. 2007; Barros et al. 2009; Miki et al. 2009). Together with our findings, these observations point to an insufficient level of hypoperfusion in selected brain regions of aged TGF mice (at most 30%, Gaertner et al. 2005) to trigger the cascade of events that lead to cognitive dysfunction. Alternatively, reduced cerebral perfusion could be an aggravating factor of an already existing pathology, as suggested from studies in memory-impaired AD mice submitted to hypoxia (Sun et al. 2006). The fact that ABT-627-treated WT controls with severe impairments in vascular reactivity exhibited intact memory performance and functional hyperemic response to whisker stimulation further highlights the importance of other underlying pathology or more severe hypoperfusion to alter cognitive function.

Effects of the ET_B receptor antagonist A-192621 on cerebrovascular reactivity

In contrast to ET_A receptor antagonism, which had no beneficial effects in aged TGF mice and detrimental ones in WT controls, ET_B receptor antagonism fully normalized the ET-1 contractile response and largely restored the basal NO synthetic capacity of the vessels in TGF mice without altering these responses in WT controls. This treatment, however, did not rescue the impaired ACh and CGRP dilatations in TGF mice, and only slightly reduced the ACh response in controls. These data in TGF mice suggest that chronic blockade of ET_B receptors, which are increased in aged TGF mice, allows recovery of the ET_A receptor-mediated contractile response regardless of their impaired signalling (Tong and Hamel 2007), possibly by hindering the counteracting ET_B-mediated dilatation (Feger et al. 1997; Nilsson et al. 1997). The results further indicate that receptor-mediated NO synthesis and release, as required for ACh and, to some degree, CGRP dilatations, were not rescued by ET_B receptor blockade, pointing to incomplete normalization of endothelial NO functions. Alternatively, the lack of beneficial effects of chronic ET_A and ET_B receptor blockade on other mediators of vasodilation, such as hydrogen peroxide (H_2O_2) in the ACh response (Drouin et al. 2007) and smooth muscle ATP-sensitive K^+ channels that mediate most of the CGRP dilatory response (Kitazono et al. 1993; DeWitt et al. 2001), could explain the failure to restore these functions.

Conclusion

Together these findings underscore the importance of the ET_A receptor in maintaining homeostasis between ET-1-mediated contraction and basal NO dilatory tone in cerebral blood vessels. Our results showed that counteracting the ET_B-mediated NO production in brain vessels of aged TGF mice with reduced ET_A-induced contraction and basal NO release may provide a means to rescue this homeostasis. In the context of diseased vessels with increased TGF-β_1, altered ET_A receptor signalling, and increased ET_B receptor levels, as seen in TGF mice, these findings suggest that ET_B receptor antagonism may be able to restore the ET-1/NO balance. Moreover, the data imply that the cerebrovascular pathology in TGF mice, which bears similarities to that found in AD brains (Wyss-Coray et al. 2000; Tong et al. 2005), does not result in a cerebrovascular dysfunction that is severe enough to impair cognitive function.

Acknowledgements

Supported by research grants from the Canadian Institutes of Health Research (CIHR, MOP-62194 and MOP-84275), the Alzheimer Society of Canada, and a fellowship from les Fonds de la recherche en santé du Québec (B.O.). The authors thank Dr. L. Mucke (Gladstone Institute of Neurological Disease and Department of Neurology, University of California, San Francisco) for the TGF transgenic mouse breeders, and Abbott Laboratories for their generous supply of the ET_A and ET_B receptor antagonists. We also thank Dr. X.-K. Tong, P. Fernandes, and Dr. N. Nicolakakis for technical assistance.

References

Akerman, S., Williamson, D.J., Kaube, H., and Goadsby, P.J. 2002. Nitric oxide synthase inhibitors can antagonize neurogenic and calcitonin gene-related peptide induced dilation of dural meningeal vessels. Br. J. Pharmacol. **137**(1): 62–68. doi:10.1038/sj.bjp.0704842. PMID:12183331.

Ayata, C., Ma, J., Meng, W., Huang, P., and Moskowitz, M.A. 1996. L-NA-sensitive rCBF augmentation during vibrissal stimulation in type III nitric oxide synthase mutant mice. J. Cereb. Blood Flow Metab. **16**(4): 539–541. doi:10.1097/00004647-199607000-00002. PMID:8964791.

Barros, C.A., Ekuni, R., Moro, M.A., Pereira, F.M., Dos Santos Pereira, M.A., and Milani, H. 2009. The cognitive and histopathological effects of chronic 4-vessel occlusion in rats depend on the set of vessels occluded and the age of the animals. Behav. Brain Res. **197**(2): 378–387. doi:10.1016/j.bbr.2008.10.023. PMID:19007820.

Chao, C.C., Hu, S., Frey, W.H., 2nd, Ala, T.A., Tourtellotte, W.W., and Peterson, P.K. 1994. Transforming growth factor β in Alzheimer's disease. Clin. Diagn. Lab. Immunol. **1**(1): 109–110. PMID:7496909.

de la Torre, J.C., Fortin, T., Park, G.A., Butler, K.S., Kozlowski, P., Pappas, B.A., et al. 1992. Chronic cerebrovascular insufficiency induces dementia-like deficits in aged rats. Brain Res. **582**(2): 186–195. doi:10.1016/0006-8993(92)90132-S. PMID:1327402.

deIpolyi, A.R., Fang, S., Palop, J.J., Yu, G.Q., Wang, X., and Mucke, L. 2008. Altered navigational strategy use and visuospatial deficits in hAPP transgenic mice. Neurobiol. Aging, **29**(2): 253–266. doi:10.1016/j.neurobiolaging.2006.10.021. PMID:17126954.

DeWitt, D.S., Mathew, B.P., Chaisson, J.M., and Prough, D.S. 2001. Peroxynitrite reduces vasodilatory responses to reduced intravascular pressure, calcitonin gene-related peptide, and cromakalim in isolated middle cerebral arteries. J. Cereb. Blood Flow Metab. **21**(3): 253–261. doi:10.1097/00004647-200103000-00009. PMID:11295880.

Dirnagl, U., Lindauer, U., and Villringer, A. 1993. Role of nitric oxide in the coupling of cerebral blood flow to neuronal activation in rats. Neurosci. Lett. **149**(1): 43–46. doi:10.1016/0304-3940(93)90343-J. PMID:8469377.

Drouin, A., Thorin-Trescases, N., Hamel, E., Falck, J.R., and Thorin, E. 2007. Endothelial nitric oxide synthase activation leads to dilatory H2O2 production in mouse cerebral arteries. Cardiovasc. Res. **73**(1): 73–81. doi:10.1016/j.cardiores.2006.10.005. PMID:17113574.

Elhusseiny, A., and Hamel, E. 2000. Muscarinic – but not nicotinic – acetylcholine receptors mediate a nitric oxide-dependent dilation in brain cortical arterioles: a possible role for the M5 receptor subtype. J. Cereb. Blood Flow Metab. **20**(2): 298–305. doi:10.1097/00004647-200002000-00011. PMID:10698067.

Farkas, E., Luiten, P.G., and Bari, F. 2007. Permanent, bilateral common carotid artery occlusion in the rat: a model for chronic cerebral hypoperfusion-related neurodegenerative diseases. Brain Res. Brain Res. Rev. **54**(1): 162–180. doi:10.1016/j.brainresrev.2007.01.003. PMID:17296232.

Feger, G.I., Schilling, L., Ehrenreich, H., and Wahl, M. 1997. Endothelium-dependent relaxation counteracting the contractile action of endothelin-1 is partly due to ET_B receptor activation. Res. Exp. Med. (Berl.), **196**(6): 327–337. doi:10.1007/s004330050042. PMID:9089881.

Filipovich, T., and Fleisher-Berkovich, S. 2008. Regulation of glial inflammatory mediators synthesis: possible role of endothelins. Peptides, **29**(12): 2250–2256. doi:10.1016/j.peptides.2008.09.002. PMID:18838093.

Gaertner, R.F., Wyss-Coray, T., Von Euw, D., Lesné, S., Vivien, D., and Lacombe, P. 2005. Reduced brain tissue perfusion in TGF-β1 transgenic mice showing Alzheimer's disease-like cerebrovascular abnormalities. Neurobiol. Dis. **19**(1-2): 38–46. doi:10.1016/j.nbd.2004.11.008. PMID:15837559.

Galea, E., Feinstein, D.L., and Lacombe, P. 2006. Pioglitazone does not increase cerebral glucose utilisation in a murine model of Alzheimer's disease and decreases it in wild-type mice. Diabetologia, **49**(9): 2153–2161. doi:10.1007/s00125-006-0326-0. PMID:16830140.

Grammas, P., and Ovase, R. 2002. Cerebrovascular transforming growth factor-β contributes to inflammation in the Alzheimer's disease brain. Am. J. Pathol. **160**(5): 1583–1587. PMID:12000710.

Hamel, E. 2006. Perivascular nerves and the regulation of cerebrovascular tone. J. Appl. Physiol. **100**(3): 1059–1064. doi:10.1152/japplphysiol.00954.2005. PMID:16467392.

Harris, A.K., Elgebaly, M.M., Li, W., Sachidanandam, K., and Ergul, A. 2008. Effect of chronic endothelin receptor antagonism on cerebrovascular function in type 2 diabetes. Am. J. Physiol. Regul. Integr. Comp. Physiol. **294**(4): R1213–R1219. PMID:18287215.

Haydon, P.G., and Carmignoto, G. 2006. Astrocyte control of synaptic transmission and neurovascular coupling. Physiol. Rev. **86**(3): 1009–1031. doi:10.1152/physrev.00049.2005. PMID:16816144.

Iadecola, C. 2004. Neurovascular regulation in the normal brain and in Alzheimer's disease. Nat. Rev. Neurosci. **5**(5): 347–360. doi:10.1038/nrn1387. PMID:15100718.

Kalaria, R.N., and Pax, A.B. 1995. Increased collagen content of cerebral microvessels in Alzheimer's disease. Brain Res. **705**(1-2): 349–352. doi:10.1016/0006-8993(95)01250-8. PMID:8821769.

Kitazono, T., Heistad, D.D., and Faraci, F.M. 1993. Role of ATP-sensitive K+ channels in CGRP-induced dilatation of basilar artery in vivo. Am. J. Physiol. **265**(2 Pt 2): H581–H585. PMID:8368361.

Koehler, R.C., Roman, R.J., and Harder, D.R. 2009. Astrocytes and the regulation of cerebral blood flow. Trends Neurosci. **32**(3): 160–169. doi:10.1016/j.tins.2008.11.005. PMID:19162338.

Krupinski, J., Kumar, P., Kumar, S., and Kaluza, J. 1996. Increased expression of TGF-β1 in brain tissue after ischemic stroke in humans. Stroke, **27**(5): 852–857. PMID:8623105.

Lacombe, P., Mathews, P.M., Schmidt, S.D., Breidert, T., Heneka, M.T., Landreth, G.E., et al. 2004. Effect of anti-inflammatory agents on transforming growth factor beta over-expressing mouse brains: a model revised. J. Neuroinflammation, **1**(1): 11. doi:10.1186/1742-2094-1-11. PMID:15285804.

Leask, A., and Abraham, D.J. 2004. TGF-β signaling and the fibrotic response. FASEB J. **18**(7): 816–827. doi:10.1096/fj.03-1273rev. PMID:15117886.

Lin, A.H., Luo, J., Mondshein, L.H., ten Dijke, P., Vivien, D., Contag, C.H., and Wyss-Coray, T. 2005. Global analysis of Smad2/3-dependent TGF-β signaling in living mice reveals prominent tissue-specific responses to injury. J. Immunol. **175**(1): 547–554. PMID:15972691.

Luedecking, E.K., DeKosky, S.T., Mehdi, H., Ganguli, M., and Kamboh, M.I. 2000. Analysis of genetic polymorphisms in the transforming growth factor-β1 gene and the risk of Alzheimer's disease. Hum. Genet. **106**(5): 565–569. doi:10.1007/s004390050026. PMID:10914688.

Malaguarnera, L., Motta, M., Di Rosa, M., Anzaldi, M., and Malaguarnera, M. 2006. Interleukin-18 and transforming growth factor-β1 plasma levels in Alzheimer's disease and vascular dementia. Neuropathology, **26**(4): 307–312. doi:10.1111/j.1440-1789.2006.00701.x. PMID:16961066.

Miki, K., Ishibashi, S., Sun, L., Xu, H., Ohashi, W., Kuroiwa, T., and Mizusawa, H. 2009. Intensity of chronic cerebral hypoperfusion determines white/gray matter injury and cognitive/motor dysfunction in mice. J. Neurosci. Res. **87**(5): 1270–1281. doi:10.1002/jnr.21925. PMID:18951530.

Nakazato, F., Tada, T., Sekiguchi, Y., Murakami, K., Yanagisawa, S., Tanaka, Y., and Hongo, K. 2002. Disturbed spatial learning of rats after intraventricular administration of transforming growth factor-β1. Neurol. Med. Chir. (Tokyo), **42**(4): 151–157. doi:10.2176/nmc.42.151. PMID:12013666.

Nicolakakis, N., Aboulkassim, T., Ongali, B., Lecrux, C., Fernandes, P., Rosa-Neto, P., et al. 2008. Complete rescue of cerebrovascular function in aged Alzheimer's disease transgenic mice by antioxidants and pioglitazone, a peroxisome proliferator-activated receptor γ agonist. J. Neurosci. **28**(37): 9287–9296. doi:10.1523/jneurosci.3348-08.2008. PMID:18784309.

Nilsson, T., Cantera, L., Adner, M., and Edvinsson, L. 1997. Presence of contractile endothelin-A and dilatory endothelin-B receptors in human cerebral arteries. Neurosurgery, **40**(2): 346–353. doi:10.1097/00006123-199702000-00023. PMID:9007869.

Niwa, K., Araki, E., Morham, S.G., Ross, M.E., and Iadecola, C. 2000. Cyclooxygenase-2 contributes to functional hyperemia in whisker-barrel cortex. J. Neurosci. **20**(2): 763–770. PMID:10632605.

Pierre, L.N., and Davenport, A.P. 1998. Relative contribution of endothelin A and endothelin B receptors to vasoconstriction in small arteries from human heart and brain. J. Cardiovasc. Pharmacol. **31**(Supplement 1 Suppl 1): S74–S76. doi:10.1097/00005344-199800001-00024. PMID:9595405.

Rosenblum, W.I., Shimizu, T., and Nelson, G.H. 1993. Endothelium-dependent effects of substance P and calcitonin gene-related peptide on mouse pial arterioles. Stroke, **24**(7): 1043–1047, discussion 1047–1048. PMID:7686695.

Ruitenberg, A., den Heijer, T., Bakker, S.L., van Swieten, J.C., Koudstaal, P.J., Hofman, A., and Breteler, M.M. 2005. Cerebral hypoperfusion and clinical onset of dementia: the Rotterdam Study. Ann. Neurol. **57**(6): 789–794. doi:10.1002/ana.20493. PMID:15929050.

Sun, X., He, G., Qing, H., Zhou, W., Dobie, F., Cai, F., et al. 2006. Hypoxia facilitates Alzheimer's disease pathogenesis by up-regulating BACE1 gene expression. Proc. Natl. Acad. Sci. U.S.A. **103**(49): 18727–18732. doi:10.1073/pnas.0606298103. PMID:17121991.

Szok, D., Hansen-Schwartz, J., and Edvinsson, L. 2001. In depth pharmacological characterization of endothelin B receptors in the rat middle cerebral artery. Neurosci. Lett. **314**(1-2): 69–72. doi:10.1016/S0304-3940(01)02293-5. PMID:11698149.

Tong, X.K., and Hamel, E. 2007. Transforming growth factor-β 1 impairs endothelin-1-mediated contraction of brain vessels by inducing mitogen-activated protein (MAP) kinase phosphatase-1 and inhibiting p38 MAP kinase. Mol. Pharmacol. **72**(6): 1476–1483. doi:10.1124/mol.107.039602. PMID:17848599.

Tong, X.K., Nicolakakis, N., Kocharyan, A., and Hamel, E. 2005. Vascular remodeling versus amyloid β-induced oxidative stress in the cerebrovascular dysfunctions associated with Alzheimer's disease. J. Neurosci. **25**(48): 11165–11174. doi:10.1523/jneurosci.4031-05.2005. PMID:16319316.

Tong, X.K., Nicolakakis, N., Fernandes, P., Ongali, B., Brouillette, J., Quirion, R., and Hamel, E. 2009. Simvastatin improves cerebrovascular function and counters soluble amyloid-β, inflammation and oxidative stress in aged APP mice. Neurobiol. Dis. **35**(3): 406–414. doi:10.1016/j.nbd.2009.06.003. PMID:19524673.

van der Wal, E.A., Gómez-Pinilla, F., and Cotman, C.W. 1993. Transforming growth factor-β1 is in plaques in Alzheimer and Down pathologies. Neuroreport, **4**(1): 69–72. doi:10.1097/00001756-199301000-00018. PMID:8453039.

Wessale, J.L., Adler, A.L., Novosad, E.I., Calzadilla, S.V., Dayton, B.D., Marsh, K.C., et al. 2002. Pharmacology of endothelin receptor antagonists ABT-627, ABT-546, A-182086 and A-192621: ex vivo and in vivo studies. Clin. Sci. (Lond.), **103**(Suppl 48): 112S–117S. PMID:12193067.

Widder, J., Bauersachs, J., Fraccarollo, D., Ertl, G., and Schilling, L. 2000. Endothelium-dependent and -independent vasoreactivity of rat basilar artery in chronic heart failure. J. Cardiovasc. Pharmacol. **35**(4): 515–522. doi:10.1097/00005344-200004000-00001. PMID:10774779.

Wyss-Coray, T., Feng, L., Masliah, E., Ruppe, M.D., Lee, H.S., Toggas, S.M., et al. 1995. Increased central nervous system production of extracellular matrix components and development of hydrocephalus in transgenic mice overexpressing transforming growth factor-β1. Am. J. Pathol. **147**(1): 53–67. PMID:7604885.

Wyss-Coray, T., Masliah, E., Mallory, M., McConlogue, L., Johnson-Wood, K., Lin, C., and Mucke, L. 1997. Amyloidogenic role of cytokine TGF-β1 in transgenic mice and in Alzheimer's disease. Nature, **389**(6651): 603–606. doi:10.1038/39321. PMID:9335500.

Wyss-Coray, T., Lin, C., Sanan, D.A., Mucke, L., and Masliah, E. 2000. Chronic overproduction of transforming growth factor-β1 by astrocytes promotes Alzheimer's disease-like microvascular degeneration in transgenic mice. Am. J. Pathol. **156**(1): 139–150. PMID:10623661.

Yamada, M., Lamping, K.G., Duttaroy, A., Zhang, W., Cui, Y., Bymaster, F.P., et al. 2001. Cholinergic dilation of cerebral blood vessels is abolished in M(5) muscarinic acetylcholine receptor knockout mice. Proc. Natl. Acad. Sci. U.S.A. **98**(24): 14096–14101. doi:10.1073/pnas.251542998. PMID:11707605.

Zarow, C., Barron, E., Chui, H.C., and Perlmutter, L.S. 1997. Vascular basement membrane pathology and Alzheimer's disease. Ann. N. Y. Acad. Sci. **826**(1 Cerebrovascul): 147–160. doi:10.1111/j.1749-6632.1997.tb48467.x. PMID:9329687.

The American Journal of Pathology, Vol. 177, No. 6, December 2010

DOI: 10.2353/ajpath.2010.100339

Neurobiology

Transgenic Mice Overexpressing APP and Transforming Growth Factor-β1 Feature Cognitive and Vascular Hallmarks of Alzheimer's Disease

Brice Ongali,* Nektaria Nicolakakis,* Clotilde Lecrux,* Tahar Aboulkassim,* Pedro Rosa-Neto,[†‡] Panayiota Papadopoulos,* Xin-Kang Tong,* and Edith Hamel*

From the Laboratory of Cerebrovascular Research, and the Brain Imaging Centre,[†] Montreal Neurological Institute, and Douglas Hospital Research Centre,[‡] McGill University, Montréal, Québec, Canada*

High brain levels of amyloid-β (Aβ) and transforming growth factor-β1 (TGF-β1) have been implicated in the cognitive and cerebrovascular alterations of Alzheimer's disease (AD). We sought to investigate the impact of combined increases in Aβ and TGF-β1 on cerebrovascular, neuronal, and mnemonic function using transgenic mice overproducing these peptides (A/T mice). In particular, we measured cerebrovascular reactivity, evoked cerebral blood flow and glucose uptake during brain activation, cholinergic status, and spatial memory, along with cerebrovascular fibrosis, amyloidosis, and astrogliosis, and their evolution with age. An assessment of perfusion and metabolic responses was considered timely, given ongoing efforts for their validation as AD biomarkers. Relative to wild-type littermates, A/T mice displayed an early progressive decline in cerebrovascular dilatory ability, preserved contractility, and reduction in constitutive nitric oxide synthesis that establishes resting vessel tone. Altered levels of vasodilator-synthesizing enzymes and fibrotic proteins, resistance to antioxidant treatment, and unchanged levels of the antioxidant enzyme, superoxide dismutase-2, accompanied these impairments. A/T mice featured deficient neurovascular and neurometabolic coupling to whisker stimulation, cholinergic denervation, cerebral and cerebrovascular Aβ deposition, astrocyte activation, and impaired Morris water maze performance, which gained severity with age. The combined Aβ- and TGF-β1-driven pathology recapitulates salient cerebrovascular, neuronal, and cognitive AD landmarks and yields a versatile model toward highly anticipated diagnostic and therapeutic tools for patients featuring Aβ and TGF-β1 increments. ***(Am J Pathol 2010, 177:3071–3080; DOI: 10.2353/ajpath.2010.100339)***

Alzheimer's disease (AD) features neuronal and synaptic dysfunction, abnormal cerebral protein deposits, activated glia and progressive cognitive decline.[1–3] AD patients also exhibit structural cerebrovascular alterations,[4,5] and early deficits in resting and evoked cerebral glucose uptake and cerebral blood flow responses, which can undermine optimal brain function, and aggravate an ongoing pathogenic process.[6–8] These changes have been linked to increased levels and deposition of amyloid-β (Aβ) in brain parenchyma (senile plaques) and blood vessel walls (cerebral amyloid angiopathy; CAA),[9,10] and to up-regulation of the profibrotic transforming growth factor-β1 (TGF-β1), perhaps a key molecular mediator of the AD cerebrovascular pathology.[11–15]

Transgenic mice overproducing Aβ and TGF-β1 (A/T mice) were originally developed to study the possible modulatory role of TGF-β1 on amyloid deposition.[11,16] These early studies reported decreased plaque burden and accelerated vascular Aβ accumulation in young and adult A/T animals.[11,16] More recently, reduced parenchymal and vascular Aβ deposition was demonstrated when TGF-β signaling was genetically blocked in old transgenic AD mice.[17] Though contradictory, these studies collectively suggest that TGF-β1 may regulate amyloid pathology in the AD brain, an idea supported by the correlation between

Supported by grant MOP-84275 from the Canadian Institutes of Health Research (E.H.); a grant from the Alzheimer Society of Canada (E.H.); a CIHR studentship (N.N.); fellowships from les Fonds de la Recherche en Santé du Québec and Jeanne Timmins Costello (B.O.); and a Heart and Stroke Foundation of Canada/Canadian Stroke Network fellowship (C.L.).

B.O. and N.N. contributed equally to this work.

Accepted for publication August 26, 2010.

Supplemental material for this article can be found on *http://ajp.amjpathol.org.*

Address reprint requests to Edith Hamel, Ph.D., Department of Neurology and Neurosurgery, Montreal Neurological Institute, McGill University, Montréal, QC, Canada H3A 2B4. E-mail: edith.hamel@mcgill.ca.

TGF-β1 mRNA levels and CAA scores in patients.[11] Although the amyloid pathology has been partially characterized in A/T animals, data are completely lacking on their cognitive and cholinergic status, functional cerebrovascular integrity, and evoked perfusion and metabolic responses to neuronal activation. Such results would aid in the validation of A/T mice for the study of AD. It is therefore all the more surprising that this information is unavailable given the known detrimental cerebrovascular effects of Aβ and TGF-β1,[15,18–20] and the current interest in activity-driven brain hemodynamics and metabolism as clinical predictors or markers for AD therapeutic efficacy.

We sought to characterize the progression of cerebrovascular and cognitive markers with age in A/T mice. Particularly, we studied arterial reactivity and responsiveness to antioxidants *in vitro*, and investigated vascular proteins related to vasomotor function, oxidative stress and fibrosis. Additionally, we examined glial activation, amyloidosis, and indicators of neuronal/cognitive integrity, ie, the cholinergic innervation, the neuronally-driven cerebral blood flow and glucose uptake responses during whisker stimulation, and performance in the Morris water maze. Our novel findings highlight A/T mice as a most suitable model in which to explore therapeutic strategies against cerebrovascular and neuronal alterations of AD pathophysiology.

Materials and Methods

A/T Transgenic Mice

All experiments were in compliance with the Animal Ethics Committee of the Montreal Neurological Institute and the guidelines of the Canadian Council on Animal Care. A/T animals were generated from the crossing of mice overexpressing mutated human amyloid precursor protein (APPSwe,Ind) driven by the platelet-derived growth factor β promoter (APP mice, line J20)[21] and mice overexpressing constitutively active TGF-β1 under the control of the glial fibrillary acidic protein (GFAP) promoter (TGF mice, line T64)[22] on a C57BL/6J background. Approximately equal numbers of female and male heterozygous transgenic A/T mice and age-matched wild-type (WT) littermates were used at 6–8 (young), ~12 (adult), and ~18 (old) months of age. Singly transgenic APP or TGF mice of the same ages, either littermates of the A/T mice or from different cohorts, were used for comparisons with A/T mice in some experiments, and were similarly prepared. Transgenes were detected with touchdown PCR on tail-extracted DNA.[15] Mice were housed under a 12-hour light-dark cycle, in a room with controlled temperature (23°C) and humidity (50%), with food and tap water available ad libitum.

Vascular and Brain Tissue Collection

Mice were killed by cervical dislocation. Middle cerebral arteries were immediately tested in reactivity studies, while vessels of the circle of Willis and their branches, along with cortex and hippocampus were collected, snap-frozen and stored (−80°C) for subsequent Western blot and enzyme-linked immunosorbent assay studies. Separate mouse cohorts were perfused intracardially (4% paraformaldehyde in 0.1 mol/L phosphate-buffered saline, pH = 7.4) under deep anesthesia (65 mg/kg sodium pentobarbital, intraperitoneally), and brains post-fixed overnight. Some hemibrains were cryoprotected, frozen in isopentane and stored (−80°C) until cutting into 25-μm-thick free-floating coronal sections on a freezing microtome. Others were embedded in paraffin and cut 5 μm thick for use in immunohistochemistry.

Vascular Reactivity

Isolated, pressurized and submaximally preconstricted (serotonin, 2×10^{-7} mol/L) middle cerebral artery segments were tested for dilatation to acetylcholine (ACh; 10^{-10} to 10^{-5} mol/L) or calcitonin gene-related peptide (10^{-10} to 10^{-6} mol/L) using on-line videomicroscopy.[15] Constriction to endothelin-1 (10^{-10} to 10^{-6} mol/L) or diameter decrease during nitric oxide (NO) synthase (NOS) inhibition with N$^{\omega}$-nitro-L-arginine (10^{-5} mol/L; 35 minutes) were tested on vessels at basal tone. In some vessels, dilatation to ACh was tested before and after incubation (30–60 minutes) with the free radical scavenger superoxide dismutase (SOD; 120U/ml; Sigma, Oakville ON, Canada) or an inhibitor of NADPH oxidase (apocynin; 1 mmol/L; Sigma), the main enzymatic source of superoxide ($O_2^{\cdot-}$) in brain vessels of APP mice.[20] Percent changes in vessel diameter from basal or preconstricted tone were plotted as a function of agonist concentration or time course of NOS inhibition. The maximal response and the concentration eliciting half of the maximal response (EC_{50} value or $pD_2 = -[\log EC_{50}]$) generated by GraphPad Prism software (version 4, San Diego, CA) were used to evaluate agonist efficacy and potency, respectively.

Western Blot

Vessels were sonicated in Laemmli buffer for protein extraction, as described.[15] Proteins (12–15 μg) were separated by SDS-polyacrylamide gel electrophoresis and transferred to nitrocellulose membranes, which were incubated (1 hour) in TBST blocking buffer (50 mmol/L Tris-HCl, pH = 7.5, 150 mmol/L NaCl, 0.1% Tween 20) containing 5% skim milk, then incubated overnight with either rabbit anti-SOD2 (1:2000; Stressgen, Ann Arbor, MI), -connective tissue growth factor (1:300; Abcam, Cambridge, MA), -vascular endothelial growth factor (1:500; Santa Cruz Biotechnology, Santa Cruz, CA), -matrix metalloproteinase 9 (1:1000; Millipore, Temecula, CA) or mouse anti-endothelial NOS (1:500; BD Transduction Laboratories, San Jose, CA), -cyclooxygenase-2 (1:200; Santa Cruz Biotechnology), or -β-actin (1:10000; Sigma). Membranes were further incubated (2 hours) with horseradish peroxidase-conjugated secondary antibodies (1:2000; Jackson ImmunoResearch, West Grove, PA), and proteins visualized with enhanced chemiluminescence (ECL Plus kit; Amersham, ON, Mississauga, Canada) using a phosphor Imager (Scanner STORM 860; GE Health Care, Piscataway,

NJ), followed by densitometric quantification with ImageQuant 5.0 (Molecular Dynamics, Sunnyvale, CA).

Enzyme-Linked Immunosorbent Assay Measurement of Aβ

Levels of soluble and insoluble $A\beta_{1\text{-}40}$ and $A\beta_{1\text{-}42}$ were measured in hemicortices using an enzyme-linked immunosorbent assay (BioSource International, Camarillo, CA), as previously described in full,[23] and results expressed as nanomoles per gram of protein in the supernatant or formic acid-soluble fraction.

Histochemistry and Immunohistochemistry

Dewaxed thin sections (5 μm) were stained with 1% Sirius red (~30 minutes) to reveal total collagen in the pia and intracortical microvessels (MVs) or were pretreated with 1% H_2O_2 (10 minutes) and incubated overnight at room temperature with goat anti-collagen I (1:300; Millipore), -choline acetyltransferase (ChAT; 1:250; Millipore) or mouse anti-Aβ (6E10 targeting total Aβ; 1:3000; Covance, Emeryville, CA) followed by species-specific biotinylated IgG, the avidin-biotin complex, and the reaction visualized with 0.05% 3,3′-diaminobenzidine-nickel (Vector Laboratories, Burlingame, CA). ChAT immunostaining was tested only in adult and old A/T mice when cholinergic innervation is preserved in TGF mice,[24] but significantly reduced in singly transgenic APP mice.[23,25] Free-floating thick sections were stained with 1% Thioflavin S (8 minutes) to reveal mature, dense core amyloid plaques or incubated with rabbit anti-GFAP (1:1000; DAKO, Mississauga, ON, Canada), followed by donkey anti-rabbit cyanin 2 (Cy2)-conjugated secondary antibody (1:400; Jackson ImmunoResearch) for the detection of activated astrocytes. Sections were observed under light microscopy or epifluorescence (Leitz Aristoplan microscope, Leica, Montréal, QC), and digital pictures acquired (Coolpix 4500; Nikon, Tokyo, Japan). Double immunodetection of activated astrocytes and Aβ plaques was performed with simultaneous incubation of rabbit anti-GFAP and mouse 6E10, followed by donkey anti-rabbit Cy2- and anti-mouse Cy3-conjugated secondary antibodies.

Staining Quantification

Digital images (two or three sections/mouse, three to five mice/group) taken under the same conditions were analyzed with MetaMorph (6.1r3, Universal Imaging, Downingtown, PA). Collagen I and Sirius red staining intensities of the pia and intracortical MVs (four to 13 vessels/mouse) were quantified in magnified images and expressed as an optical density ratio against the intensity of the adjacent parenchyma. The areas of interest (somatosensory/cingulate cortex, hippocampus) containing Thioflavin S- and GFAP-positive elements were manually outlined in low-power images, while high-power microscope images of layers II to IV of the somatosensory cortex were used for quantification of ChAT-immunoreactive fibers (cell bodies were excluded). The number and/or area occupied by Thioflavin S-positive plaques, GFAP-positive astrocytes, and ChAT-positive cholinergic fibers was quantified and expressed as number or surface area occupied in the delineated areas of interest.

Morris Water Maze

The ability of mice to learn and remember the location of a hidden platform located in a predefined (target) quadrant using visuospatial cues was tested for 5 consecutive days in a circular pool filled with water (25°C, clouded with powdered skim milk), as previously described.[23] At least 2 hours after the last hidden platform trial on day 5, mice were submitted to a 60-second probe trial (platform removed), followed by a cue trial (30 seconds) testing visual acuity and motivation, which required escape to a visible platform in at least one of two trials. Mice that failed to reach the visible platform were excluded from the analysis. Daily escape latencies to the hidden platform, as well as percent time spent and distance traveled in the target quadrant during the probe trial, along with swim speed, were measured with the 2020 Plus tracking system and Water 2020 software (Ganz FC62D video camera; HVS Image, Buckingham, UK). Animals were dried under a heating lamp after each trial, and all experiments were started at the same time every day.

Laser Doppler Flowmetry

In all age groups, laser Doppler flowmetry measurements of evoked cerebral blood flow (Transonic Systems Inc., Ithaca, NY) in response to sensory stimulation were carried out one week following the Morris water maze in anesthetized mice (ketamine, 80 mg/kg intraperitoneally; Wyeth, St-Laurent QC, Canada) fixed in a stereotaxic frame.[23] Cerebral blood flow was recorded before, during and after whisker stimulation (20 seconds at 8–10 Hz), with four or five recordings acquired every 30 to 40 seconds and averaged per mouse. Cortical cerebral blood flow change was expressed as percent increase relative to baseline. The entire procedure was performed blind to the identity of the mouse.

[^{18}F]Fluoro-2-Deoxy-D-Glucose-PET

Eighteen-month-old A/T mice and WT littermates were fasted overnight and scanned for cerebral uptake of [^{18}F]fluoro-2-deoxy-D-glucose induced by whisker stimulation (8–10 Hz, electric toothbrush, 45 minutes) under isoflurane sedation (1 to 2% in medical air) in a CTI Concorde R4 microPET scanner (Siemens Preclinical Solutions, Knoxville, TN), as previously described.[23] Animals were kept warm with a heating lamp, while cardiac and respiration rate were maintained stable through online monitoring (Biopac Inc., Goleta, CA). Glycemia levels were measured before and after scans, and were similar in both WT and A/T groups (not shown). Functional metabolic images were reconstructed using a maximum *a posteriori* probability algorithm, and coregistered to re-

spective high-resolution WT or A/T mouse structural MRI templates. MR images were acquired in separate groups of mice (WT, $n = 5$ and A/T, $n = 4$) with a 7 T Bruker Pharmascan system (Bruker Biospin, Ettlingen, Germany) using a 28-mm inner diameter quadrature volume resonator, and a 3D True FISP sequence with the following parameters: matrix size = 128 × 128 × 64, field of view = 1.8 cm × 1.8 cm × 0.9 cm, spatial resolution = 140 μm × 140 μm × 140 μm, excitation flip angle = 30°, repetition time = 5.2 ms, echo time = 2.6 ms, number of excitations = 4, number of phase cycles = 4, total scan time = 35 minutes. The images were reconstructed using a maximum intensity algorithm and the population averages generated using the approach described elsewhere.[26] Regions of interest were drawn on the somatosensory cortices and the magnitude of activation expressed as the ratio of [^{18}F]fluoro-2-deoxy-D-glucose standard uptake value in the activated contralateral relative to the ipsilateral cortex.[27] Final images represent the standard uptake value obtained by correcting individually for animal body weight and injected radioactivity dose.

Statistical Analysis

Data are means ± SEM, and were compared by Student's *t*-test or one-way analysis of variance followed by Newman-Keuls posthoc tests. Morris water maze latency curves were analyzed by two-way analysis of variance followed by Bonferroni posthoc test, with day and genotype as factors. All statistical analyses were performed with GraphPad and $P < 0.05$ was considered significant.

Results

A/T Mice Develop an Early Progressive Decline of Cerebral Arterial Function

Isolated middle cerebral arteries from young and adult A/T mice displayed ~50% loss of their ability to dilate to ACh and calcitonin gene-related peptide relative to vessels of age-matched WT littermates (Figure 1; Supplemental Table 1 at *http://ajp.amjpathol.org*). By 18 months of age, A/T mice further exhibited significantly impaired maximal diameter decrease during NOS inhibition with N^{ω}-nitro-L-arginine, indicating a decline in constitutive endothelial NO synthesis that is crucial for establishing resting vessel tone. There was no contractile deficit to endothelin-1 in A/T arteries at any age (Figure 1; Supplemental Table 1 at *http://ajp.amjpathol.org*). The progressive deficits in arterial responsiveness could not be attributed to desensitization of cerebrovascular receptors, as agonist potencies (pD_2 values) were comparable between WT and A/T mice at all ages (Supplemental Table 1 at *http://ajp.amjpathol.org*). Cerebrovascular impairments of similar magnitude have been consistently measured in singly transgenic APP and TGF mice. Noteworthy was the lack of a synergistic Aβ and TGF-β1 effect in A/T arteries, as evidenced in the qualitative comparison with reactivity data from APP and TGF arteries. (Supplemental Figure 1; Supplemental Table 1 at *http://ajp.amjpathol.org*).[15,23,24,28,29] This was particularly well illustrated in A/T mice by their preserved contractile response to endothelin-1, in contrast to the deficit in TGF arteries; milder calcitonin gene-related peptide deficit relative to that in aged TGF animals; and later decline in N^{ω}-

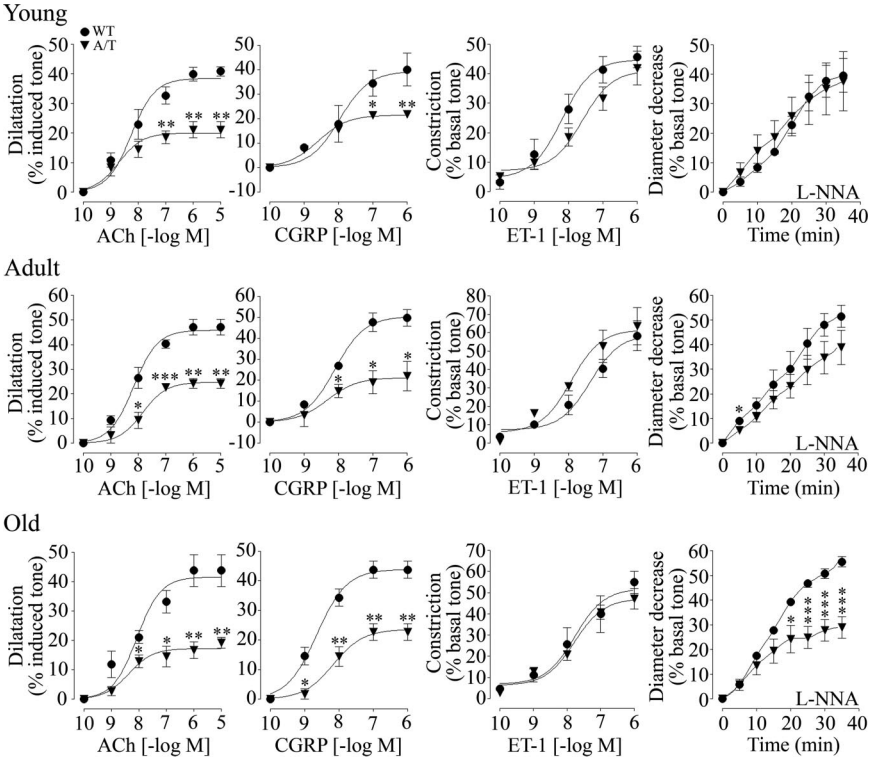

Figure 1. Age-related impairment in cerebrovascular reactivity in young (6–8 months), adult (~12 months), and old (~18 months) A/T mice (inverted triangles) relative to age-matched WT littermates (circles). Early dilatory deficits to ACh and calcitonin gene-related peptide (CGRP) in young and adult A/T mice were accompanied by a late decline in constitutive NO synthesis in old A/T animals, as seen with N^{ω}-nitro-L-arginine-mediated inhibition of NOS (L-NNA, 10^{-5} mol/L). Constriction to endothelin-1 (ET-1) was preserved at all ages. Error bars represent SEM. Number of animals are indicated in Supplemental Table 1 at *http://ajp.amjpatbol.org*. Comparison to WT using Student's *t*-test. $^{*}P < 0.05$, $^{**}P < 0.01$, $^{***}P < 0.001$.

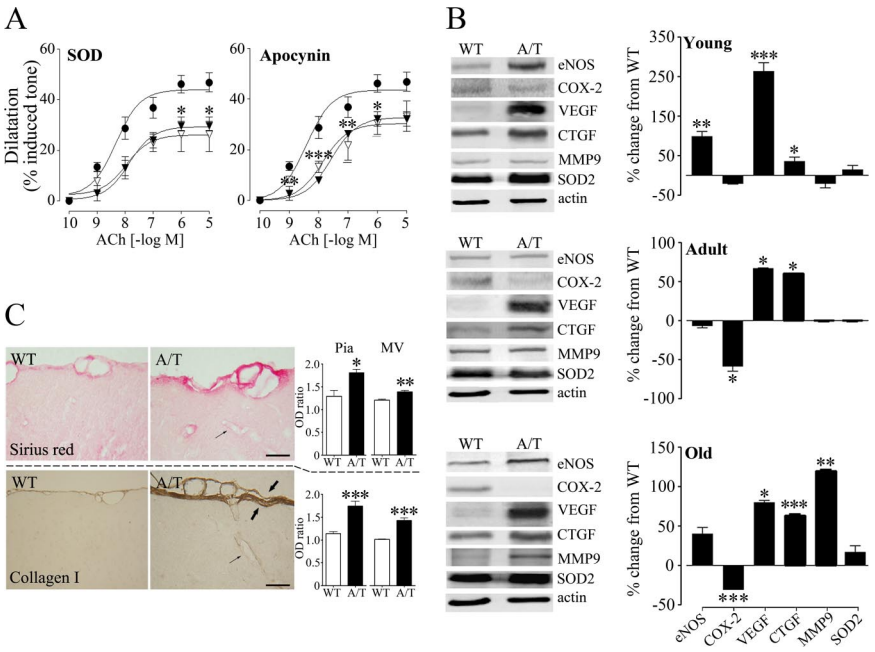

Figure 2. A/T mouse vessels were characterized by resistance to antioxidants, alterations in vascular signaling molecules and cerebrovascular fibrosis. **A:** The impaired ACh-mediated dilatation of aged A/T (inverted filled triangles) relative to WT mice (circles) was not improved in A/T arteries after *in vitro* incubation (inverted open triangles) with the $O_2^{\cdot-}$ scavenger SOD or a blocker of its synthesis, apocynin (n = 3–4 mice/group). **B:** Disturbed levels of vasodilator-synthesizing enzymes, endothelial NOS eNOS and cyclooxygenase-2 (COX-2) and of markers related to vascular remodeling, vascular endothelial growth factor (VEGF), connective tissue growth factor (CTGF), matrix metalloproteinase 9 (MMP-9) but not of the oxidative stress marker SOD2, as measured by Western blot in pial vessels of A/T relative to WT mice. Actin was used to normalize loading variation (n = 3–6 mice/group). **C:** Collagen accumulation in the pia (**thick arrows**) and intraparenchymal microvessels (MVs, **thin arrows**) of 18-month-old A/T relative to WT mice, measured as an optical density (OD) ratio of the vessel intensity to that of adjacent parenchyma in Sirius red-stained (**top**) and collagen I-immunoreactive (**bottom**) 5-μm-thick paraffin sections (n = 3–9 mice/group). Scale bar = 20 μm. Error bars represent SEM. $^{*}P < 0.05$, $^{**}P < 0.01$, $^{***}P < 0.001$ when compared with WT using Student's t-test or one-way analysis of variance followed by Newman-Keuls posthoc test.

nitro-L-arginine response versus its early onset in the singly transgenic lines.

A/T Mice Display Arterial Dysfunction Not Related to Oxidative Stress

We sought to elucidate the mechanism of cerebrovascular impairment in aged A/T mice by treating arteries with SOD or apocynin, which respectively scavenges $O_2^{\cdot-}$ and abrogates its production. Antioxidants have been shown to normalize cerebrovascular responses of APP,[15,18,23,30] but not TGF mice,[24] and we wished to determine whether free radicals accounted for the cerebrovascular dysfunction in the A/T model. These *in vitro* antioxidant approaches were ineffective as they were unable to restore ACh-mediated dilatations (Figure 2A). Furthermore, no significant change was detected in A/T vessels at any age in the levels of the antioxidant enzyme SOD2, which is induced by $O_2^{\cdot-}$ and can be used as an indicator of enhanced oxidative stress (Figure 2B). Instead, pial vessels from A/T mice exhibited changes in enzymes synthesizing vasodilators, ie, reduced levels of cyclooxygenase-2 beginning as a trend in young, and becoming significant in adult and old mice, as well as significant up-regulation of endothelial NOS in young mice. A/T arteries also featured robust increases in levels of growth factors (vascular endothelial growth factor, connective tissue growth factor) involved in vascular fibrosis, starting in young and persisting in old mice. Arteries also exhibited late up-regulation of matrix metalloproteinase 9, an enzyme involved in the breakdown of the extracellular matrix during vascular remodeling (Figure 2B). Furthermore, A/T mice featured significant collagen accumulation in penetrating MVs and in the surface pial membrane, resulting in its greater thickness (Figure 2C). Sirius red staining intensity was markedly augmented in the pia (81%) and MVs (39%) compared to the adjacent parenchyma of 18 month-old A/T mice, with substantially smaller increments in WT animals in these respective vascular beds (pia: 29%, MVs: 21%). Analogous collagen I increases were seen in the pia (74%) and MVs (42%) of A/T mice (Figure 2C), which likely accounted for the increased rigidity of their vessels perceived during dissection, handling, and cannulation. In contrast, collagen I immunostaining was very weak in WT mice, being increased by 14% in the pia but barely detectable in MVs (1%) relative to the parenchyma (Figure 2C), confirming our previous report of collagen I up-regulation in the context of vascular pathology.[15] Collectively, these data argue against oxidative stress as the main pathogenic mechanism of vascular dysfunction, and point to disturbances in enzymes and proteins underlying vascular structure and signaling. We cannot rule out that chronic *in vivo* antioxidant treatment might be effective. However, based on the recent failure of this approach in TGF mice featuring similar cerebrovascular fibrosis, vascular protein alterations, and *in vitro* resistance to antioxidants,[24] we are inclined to consider alternate mechanisms of vascular dysfunction in A/T mice, ones most likely shared with the TGF model.

A/T Mice Exhibit AD-Like Neuropathological Changes

A/T mice exhibited an increase in levels of soluble and insoluble $A\beta_{1\text{-}40}$ and $A\beta_{1\text{-}42}$ between 6–8 and 12 months, with further increases in levels of $A\beta_{1\text{-}40}$, but not of $A\beta_{1\text{-}42}$ at 18 months of age, as measured in the cortex by enzyme-linked immunosorbent assay (Figure 3A). They also displayed age-dependent Aβ plaque deposition in the cortex and hippocampus, shown by a gradual increase in the number and surface area (plaque load) occupied by Thioflavin S-positive dense core plaques from young to adult animals (Figure 3B). Between 12 and 18 months,

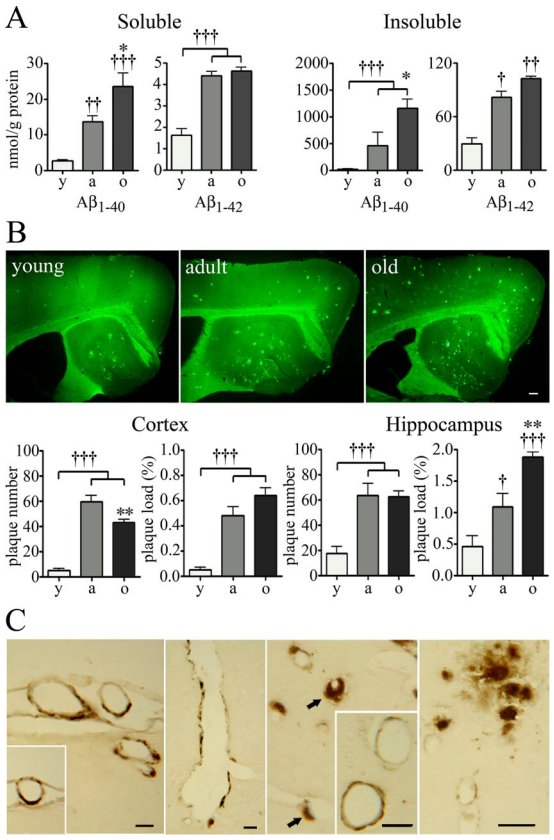

Figure 3. Progressive amyloidosis in A/T mice. **A:** Levels of soluble and insoluble $A\beta_{1\text{-}40}$ and $A\beta_{1\text{-}42}$ increased as a function of age in A/T mice, as assayed in hemicortices by enzyme-linked immunosorbent assay. **B:** Gradual increase in the number and load (percentage of surface area) of Thioflavin S-positive amyloid plaques in the cortex and hippocampus of A/T mice. No such deposits were seen in WT animals (not shown). y, young; a, adult; o, old. **C:** Extensive CAA in the vasculature of aged A/T mice, as respectively seen from left to right, in surface pial vessels, a penetrating cortical artery, arterioles with associated extraluminal deposits (**arrows**) and hippocampal arteries (**inset**), and in hippocampal arterioles and capillaries, next to which parenchymal $A\beta$ plaques can be seen. Scale bars = 20 μm. Error bars represent SEM (n = 4 mice/group). $^{\dagger}P < 0.05$, $^{\dagger\dagger}P < 0.01$, $^{\dagger\dagger\dagger}P < 0.001$ for comparison to young mice or $^{*}P < 0.05$, $^{**}P < 0.01$ for comparison to adult mice using one-way analysis of variance followed by Newman-Keuls posthoc test.

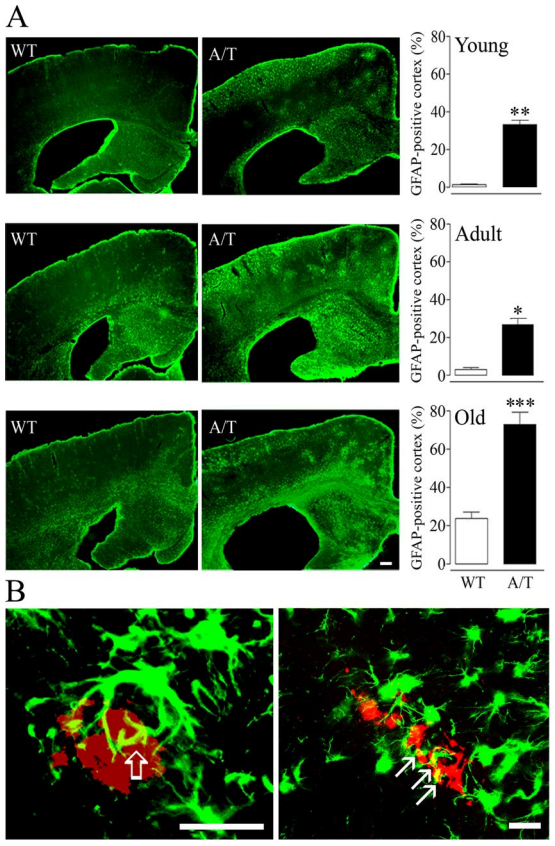

Figure 4. **A:** Enhanced astrocyte activation seen as clusters and diffuse GFAP-positive material in the brains of A/T mice with a smaller age-related activation also detectable in WT littermates. Astrocyte activation was expressed as the percent cortical area occupied by GFAP-positive cells. Scale bar = 20 μm. **B:** Activated astrocytes (green) were found associated with $A\beta$ deposits (red) in the parenchyma (**left**) and with cerebral vessels (**right**). Note, in yellow, the contact points between astrocytic processes and an $A\beta$ plaque (**thick open arrow**) or an amyloid-laden vessel (CAA) (**thin arrows**) (n = 3–7 mice/group). Scale bars: **left**, 40 μm; **right**, 20 μm. Error bars represent SEM. $^{*}P < 0.05$, $^{**}P < 0.01$, $^{***}P < 0.001$ when compared with WT using Student's t-test.

plaque number reached a plateau in the hippocampus, or slightly decreased in the cortex, while plaque load continued to expand or stayed the same in these respective areas, indicating an increase in the size of certain plaques during this period. Together with the significant increments in soluble and insoluble $A\beta_{1\text{-}40}$ from 12 to 18 months, this finding suggests that existing $A\beta$ plaques may have acted as seeds for additional $A\beta_{1\text{-}40}$ deposition. In comparative experiments, we found a trend for diminished plaque load in young A/T relative to APP mice, which became significant in adult and aged animals (Supplemental Figure 2 at *http://ajp.amjpathol.org*). This would support the argued modulatory effect of TGF-β1 on amyloid deposition, and suggest a clearance phenomenon, as previously observed in young and old A/T mice.[11,16] Its occurrence later in our model may reflect the higher $A\beta$ levels of the J20 APP line[21] used to generate A/T mice, instead of the previously used J9.[11,16] Finally, inspection of $A\beta$ immunoreactivity in thin sections from 18-month-old A/T mice revealed parenchymal $A\beta$ senile plaques and widespread CAA in pial, intracortical, and hippocampal brain vessels (Figure 3C), confirming previous reports in young and adult A/T animals.[11,16]

In addition, A/T mice displayed an inflammatory response characterized by activated GFAP-positive astrocytes. The GFAP-positive area in the cortex increased from young to old A/T mice, with a smaller age-dependent activation in WT animals. Activated astrocytes in A/T mice distributed in clusters as well as diffusely throughout the cortex (Figure 4A), and surrounded $A\beta$ plaques and amyloid-laden vessels (Figure 4B). Interestingly, this pattern was reminiscent of both the cluster-like activation of APP mice[23] and diffuse, perivascular astrocytosis of TGF mice.[11,22,24]

Neuronal and Cognitive Impairments in A/T Mice

Adult and aged A/T mice featured a ~22 to 23% reduction ($P < 0.05$ for both ages) in the number of cortical cholinergic fibers (Figure 5A). Further, [^{18}F]fluoro-2-de-

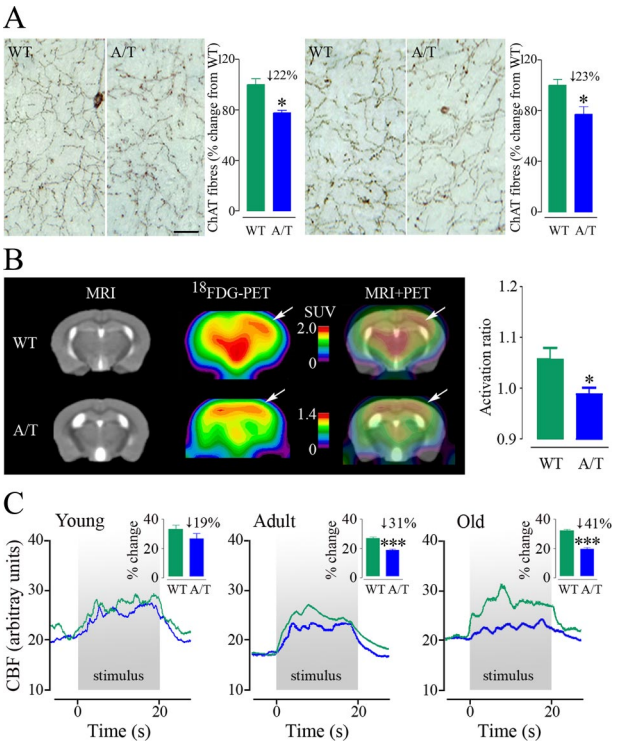

Figure 5. Neuronal dysfunction in A/T mice. **A:** Decline in the number of cortical cholinergic fibers in paraffin sections from adult (**left**) and old (**right**) A/T mice, relative to WT littermates, as detected with ChAT immunohistochemistry. Scale bar = 20 μm. Values above histograms indicate the percentage of fiber loss compared to control animals. **B:** Decrease in the cerebral glucose uptake response to whisker stimulation in the somatosensory cortex (**arrows**) of 18-month-old A/T relative to WT mice (n = 3–5 mice/group). Standard uptake value (SUV) scales were adjusted to match the local activation spots in the two groups rather than the global brain uptake. The activation ratio is the corrected SUV in the activated contralateral relative to the ipsilateral somatosensory cortex. **C:** Gradual decline in the activity-driven hemodynamic response to whisker stimulation in A/T mice (blue) compared to age-matched WT controls (green), as measured by laser Doppler flowmetry (n = 4–5 mice/group). Values above histograms indicate the percent loss of the response compared to control animals. Error bars represent SEM. Comparisons to WT, $^{*}P < 0.05$, $^{***}P < 0.001$ using Student's t-test.

oxy-D-glucose-PET scans following whisker stimulation revealed a significant impairment of glucose uptake in the activated somatosensory cortex of aged A/T animals (activation ratio A/T: 0.99 ± 0.01 versus WT: 1.06 ± 0.02, $P < 0.05$) (Figure 5B) that may have derived from the observed alterations in vascular, astroglial and neuronal compartments.[31] Moreover, there was a gradual loss of the neuronally-driven hemodynamic response to sensory stimulation, which was significant in adult (−31%, $P < 0.001$) and progressively more severe in aged animals (−41%, $P < 0.001$) (Figure 5C). The extent of the deficit compared well to that seen in APP mice, although it was more progressive (Supplemental Table 2 at *http://ajp.amjpathol.org*). Finally, A/T mice showed increased latencies to locate the hidden platform in the Morris water maze at 6–8 months of age, whereas performance in the probe trial was lower but not significantly different from that of control mice, indicating a learning deficit but no clear memory impairment at this age. A significant deficit in probe trial performance emerged in 12-month-old and continued in 18-month-old A/T animals (Figure 6), which was not due to differences in swim speed, visual acuity,

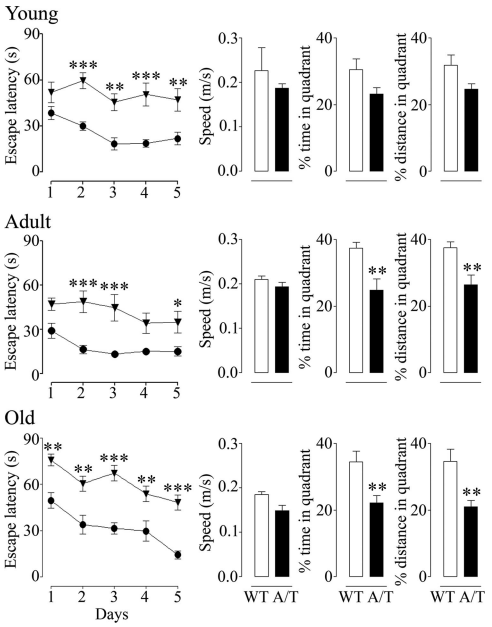

Figure 6. Progressive decline in Morris water maze performance in A/T mice (inverted triangles) compared to aged-matched WT counterparts (circles). Young mice featured impaired acquisition during hidden-platform testing, but only a trend toward decline in memory retention during the probe trial. Significant probe trial deficits appeared in adult and old A/T mice. Error bars represent SEM (n = 8–16 mice/group). Comparisons to WT, $^{*}P < 0.05$, $^{**}P < 0.01$, $^{***}P < 0.001$ using two-way analysis of variance followed by Bonferroni posthoc test (latency curves) or using Student's t-test (probe trial histograms).

locomotor defects or lack of motivation, as demonstrated by successful escape onto the visible platform. Comparatively, APP mice showed deficits in both the learning and memory components of the test at all ages, as shown at 6 months, whereas TGF mice performed as well as WT mice in this task up to 18 months of age (Supplemental Figure 3 at *http://ajp.amjpathol.org*).

Discussion

Since the original development of transgenic mice overproducing both Aβ and TGF-β1,[11,16] this is the first characterization of their cerebrovascular, neuronal and mnemonic integrity. More importantly, our study provides novel functional data on activity-induced changes in cerebral glucose uptake and cerebrovascular status that are in line with current research initiatives to develop markers for early diagnosis and treatment efficacy. As a result, the A/T model may be used to better assess interactions between Aβ and TGF-β1 in AD, and to develop therapeutic strategies that can rescue both cerebrovascular and mnemonic hallmarks of AD pathophysiology.

AD-Like Cerebrovascular Pathology in A/T Mice and Therapeutic Implications

An appealing characteristic of A/T mice is the development of a functional and structural cerebrovascular pathology, simultaneously triggered by soluble Aβ, TGF-β1, CAA, and basement membrane thickening, as seen in human AD.[4,5,32,33] The interaction between vascular fi-

brosis and CAA is of interest, as matrix proteins such as collagen and perlecan accumulating in AD basement membranes[33] have the ability to bind Aβ and enhance its fibrillogenesis.[34] CAA may thus result from the enhanced capacity of thickened vessels to amass Aβ. This would agree with the ability of TGF-β1 to prompt vascular Aβ deposition when overexpressed in the brains of young APP mice (2 to 3 months), as CAA was not seen in singly transgenic APP animals of equivalent age.[11] It is also in line with the reported correlation between TGF-β1 mRNA levels and CAA scores in AD brains.[11] CAA may additionally result from vascular wall alterations that hinder vessel pulsations believed to drive Aβ clearance along the perivascular drainage route within arterial and arteriolar basement membranes.[35] Such a scenario is supported by the perivascular accumulation of Aβ seen here in concentric circles around some A/T brain vessels (Figure 3C). A/T mice thus offer the opportunity to test whether strategies that can reverse or attenuate excessive matrix protein accumulation and vascular stiffness will diminish CAA. Used in conjunction with Aβ immunotherapy, these could help counter the transient increase in CAA and risk of cerebral microhemorrhages reported with vaccination in AD models[36] and human trials.[37] In addition, attenuating CAA could improve the function of astrocytes, key intermediaries in neurovascular coupling.[38] CAA can induce loss of the water channel aquaporin 4 and of various potassium channel subtypes in astrocytic end-feet[39] that, combined with the progressive astrocyte activation measured here, could have contributed to the age-related impairment of perfusion responses. Normalizing CAA could thus ameliorate glial function and perfusion.

Therapies against the deleterious vasoactive properties of soluble Aβ would be most useful.[40] Indeed, the peptide potently deregulates vascular function, even in young APP mice devoid of CAA, by activating vascular NADPH oxidase and $O_2^{\cdot-}$ synthesis, which results in the sequestration of vasodilators and free radical damage to vascular enzymes and receptors.[15,18,20,30] These dysfunctions are promptly reversed by antioxidants *in vitro* and *in vivo*, even in arteries from aged APP mice.[15,23,41] A caveat to pure antioxidant therapy is warranted by its inefficacy when applied to fibrotic TGF arteries,[15] and here, to A/T arteries. Both the $O_2^{\cdot-}$ scavenger SOD, and NADPH oxidase inhibitor, apocynin, were unable to restore ACh-mediated dilatations. Though chronic *in vivo* antioxidant treatment would be ultimately conclusive, it was ineffective in TGF mice,[24] suggesting that a combined approach with compounds targeting structural alterations or vasodilatory signaling pathways should be favored.

The relevance of the A/T model for the study of altered brain hemodynamics in AD is strengthened not only by reports of TGF-β1 up-regulation in the brain and vasculature of AD patients,[11–14,42] but also in elderly individuals who have suffered a stroke[43] and in subjects with hypertension and diabetes,[44] conditions that acutely or chronically limit cerebral blood flow and increase the risk for developing AD,[6,45] especially if they co-occur in the same individual.[46] In at-risk patients, TGF-β1 could conceivably regulate Aβ production directly. This is suggested by the presence of a TGF-β1-responsive element in the APP promoter and TGF-β1-stimulated release of endogenous A$\beta_{1\text{-}40/42}$ peptides by cultured human astrocytes.[47] Alternatively, TGF-β1 production may be triggered by Aβ,[48] or both peptides may be up-regulated concomitantly in neurons, glia, and vascular cells by acute ischemic events or chronic cerebrovascular insufficiency.[49,50] In A/T mice, Aβ and TGF-β1 are overproduced from birth and throughout the lifespan, and it seems that their interaction is responsible for the progressive hemodynamic deficit of A/T animals. This deficit appears later than in APP or TGF mice, and surpasses that of TGF animals but reaches that of APP mice (Supplemental Table 2 at *http://ajp.amjpathol.org*[24,29]). In all, this emphasizes the usefulness of the A/T model as a platform for pursuing strategies aimed at counteracting impaired brain hemodynamics that could promote or result from Aβ and TGF-β1 elevations.

Contribution of Aβ versus TGF-β1 to the Neuronal and Cognitive Status of A/T Mice

The cholinergic, metabolic and cognitive deficits of A/T mice reflect mainly an Aβ-driven process, as they are not exhibited by singly transgenic TGF mice,[24] and the deficit severity matches that of APP mice.[23,25,28] Namely, the loss of cortical ChAT-positive fibers, a landmark of AD[51] reproduced in APP mouse models[25,52–54] but not in TGF mice,[24] has been attributed to the cholinotoxic effects of soluble Aβ.[55] It seems unrelated to Aβ deposition, since no relationship could be established between the presence and location of Aβ plaques and denervation severity.[25] However, despite the increase in soluble Aβ oligomers from adult to old A/T mice, the cholinergic denervation did not gain in severity with aging. This stabilization could result from a TGF-β1 protective effect on neurons. In support of such a role is the delayed probe trial deficit in 12-month-old A/T mice relative to its earlier onset in 6-month-old APP animals, known for their early synaptic and cognitive dysfunction.[56,57] TGF-β1-mediated neuroprotection has been suggested during ischemic and Aβ injuries[48,50,58] through the regulation of pro- and antiapoptotic proteins or factors that counter the effects of Aβ, such as collagen VI.[48,58,59] However, evidence for a TGF-β1 neurodegenerative action has also been presented.[17,60] Further, neuronal malfunction was apparent in A/T mice, in the form of impaired stimulus-evoked cerebral glucose uptake and eventual spatial memory decline. Moreover, given the detrimental cerebrovascular effects of TGF-β1,[15,19,24,29,61] alternative neuroprotective approaches should be considered. For example, therapies aimed at the cellular and molecular underpinnings of the impaired metabolic response may hold promise. These include key glycolytic enzymes or neuronal (GLUT3) and vascular/astrocytic (GLUT1) glucose transporters that are reduced in AD.[62]

Conclusion

The present study highlighted the progressive circulatory and neuronal deficits resulting from Aβ and TGF-β1 co-overproduction. As both elements coexist and interact in the AD brain, and altered brain hemodynamics are receiving renewed attention in AD pathogenesis, the current study provides new data on a unique mouse model with which to test strategies aimed at rescuing disrupted neuronal, glial, and vascular networks.

Acknowledgments

We thank Dr. Lennart Mucke (Gladstone Institute of Neurological Disease and Department of Neurology, UCSF, CA) and the J. David Gladstone Institutes for the $hAPP_{Swe,Ind}$ and TGF-β1 transgenic mouse breeders, Ms. Priscilla Fernandes for the laser Doppler flowmetry experiments, Mr. Antonio Aliaga for performing the PET scans, and Mr. Jason Cakiroglu and Dr. Barry Bedell (Small Animal Imaging Laboratory, SAIL, Montreal Neurological Institute) for the MRI templates.

References

1. de la Torre JC: Is Alzheimer's disease a neurodegenerative or a vascular disorder? Data, dogma, and dialectics. Lancet Neurol 2004, 3:184–190
2. Zlokovic BV: Neurovascular mechanisms of Alzheimer's neurodegeneration. Trends Neurosci 2005, 28:202–208
3. Kalaria RN, Maestre GE, Arizaga R, Friedland RP, Galasko D, Hall K, Luchsinger JA, Ogunniyi A, Perry EK, Potocnik F, Prince M, Stewart R, Wimo A, Zhang ZX, Antuono P: Alzheimer's disease and vascular dementia in developing countries: prevalence, management, and risk factors. Lancet Neurol 2008, 7:812–826
4. Mancardi GL, Perdelli F, Rivano C, Leonardi A, Bugiani O: Thickening of the basement membrane of cortical capillaries in Alzheimer's disease. Acta Neuropathol 1980, 49:79–83
5. Perlmutter LS, Chui HC: Microangiopathy, the vascular basement membrane and Alzheimer's disease: a review. Brain Res Bull 1990, 24:677–686
6. Iadecola C: Neurovascular regulation in the normal brain and in Alzheimer's disease. Nat Neurosci Rev 2004, 5:347–360
7. Sun X, He G, Qing H, Zhou W, Dobie F, Cai F, Staufenbiel M, Huang LE, Song W: Hypoxia facilitates Alzheimer's disease pathogenesis by up-regulating BACE1 gene expression. Proc Natl Acad Sci USA 2006, 103:18727–18732
8. Langbaum JB, Chen K, Lee W, Reschke C, Bandy D, Fleisher AS, Alexander GE, Foster NL, Weiner MW, Koeppe RA, Jagust WJ, Reiman EM: Alzheimer's Disease Neuroimaging Initiative. Categorical and correlational analyses of baseline fluorodeoxyglucose positron emission tomography images from the Alzheimer's Disease Neuroimaging Initiative (ADNI) Neuroimage 2009, 45:1107–1116
9. Vinters HV, Wang ZZ, Secor DL: Brain parenchymal and microvascular amyloid in Alzheimer's disease. Brain Pathol 1996, 6:179–195
10. Roher AE, Kuo YM, Esh C, Knebel C, Weiss N, Kalback W, Luehrs DC, Childress JL, Beach TG, Weller RO, Kokjohn TA: Cortical and leptomeningeal cerebrovascular amyloid and white matter pathology in Alzheimer's disease. Mol Med 2003, 9:112–122
11. Wyss-Coray T, Masliah E, Mallory M, McConlogue L, Johnson-Wood K, Lin C, Mucke L: Amyloidogenic role of cytokine TGF-β1 in transgenic mice and in Alzheimer's disease. Nature 1997, 389:603–606
12. Wyss-Coray T, Lin C, Sanan DA, Mucke L, Masliah E: Chronic overproduction of transforming growth factor-beta1 by astrocytes promotes Alzheimer's disease-like microvascular degeneration in transgenic mice. Am J Pathol 2000, 156:139–150
13. Grammas P, Ovase R: Cerebrovascular transforming growth factor-β contributes to inflammation in the Alzheimer's disease brain. Am J Pathol 2002, 160:1583–1587
14. Tarkowski E, Issa R, Sjögren M, Wallin A, Blennow K, Tarkowski A, Kumar P: Increased intrathecal levels of the angiogenic factors VEGF and TGF-beta in Alzheimer's disease and vascular dementia. Neurobiol Aging 2002, 23:237–243
15. Tong XK, Nicolakakis N, Kocharyan A, Hamel E: Vascular remodeling versus amyloid β-induced oxidative stress in the cerebrovascular dysfunctions associated with Alzheimer's disease. J Neurosci 2005, 25:11165–11174
16. Wyss-Coray T, Lin C, Yan F, Yu GQ, Rohde M, McConlogue L, Masliah E, Mucke L: TGF-beta1 promotes microglial amyloid-beta clearance and reduces plaque burden in transgenic mice. Nat Med 2001, 7:612–618
17. Town T, Laouar Y, Pittenger C, Mori T, Szekely CA, Tan J, Duman RS, Flavell RA: Blocking TGF-β-Smad2/3 innate immune signaling mitigates Alzheimer-like pathology. Nat Med 2008, 14:681–687
18. Iadecola C, Zhang F, Niwa K, Eckman C, Turner SK, Fischer E, Younkin S, Borchelt DR, Hsiao KK, Carlson GA: SOD1 rescues cerebral endothelial dysfunction in mice overexpressing amyloid precursor protein. Nat Neurosci 1999, 2:157–161
19. Gaertner RF, Wyss-Coray T, Von Euw D, Lesné S, Vivien D, Lacombe P: Reduced brain tissue perfusion in TGF-β1 transgenic mice showing Alzheimer's disease-like cerebrovascular abnormalities. Neurobiol Dis 2005, 19:38–46
20. Park L, Anrather J, Zhou P, Frys K, Pitstick R, Younkin S, Carlson GA, Iadecola C: NADPH-oxidase-derived reactive oxygen species mediate the cerebrovascular dysfunction induced by the amyloid beta peptide. J Neurosci 2005, 25:1769–1777
21. Mucke L, Masliah E, Yu GQ, Mallory M, Rockenstein EM, Tatsuno G, Hu K, Kholodenko D, Johnson-Wood K, McConlogue L: High-level neuronal expression of Aβ1-42 in wild-type human amyloid protein precursor transgenic mice: synaptotoxicity without plaque formation. J Neurosci 2000, 20:4050–4058
22. Wyss-Coray T, Feng L, Masliah E, Ruppe MD, Lee HS, Toggas SM, Rockenstein EM, Mucke L: Increased central nervous system production of extracellular matrix components and development of hydrocephalus in transgenic mice overexpressing transforming growth factor-beta 1. Am J Pathol 1995, 147:53–67
23. Nicolakakis N, Aboulkassim T, Ongali B, Lecrux C, Fernandes P, Rosa-Neto P, Tong XK, Hamel E: Complete rescue of cerebrovascular function in aged Alzheimer's disease transgenic mice by antioxidants and pioglitazone, a peroxisome proliferator-activated receptor gamma agonist. J Neurosci 2008, 28:9287–9296
24. Nicolakakis N, Aboulkassim T, Aliaga A, Tong XK, Rosa-Neto P, Hamel E: Intact memory in TGF-β1 transgenic mice featuring chronic cerebrovascular deficit: recovery with pioglitazone. J Cereb Blood Flow Metab doi: 10.1038/jcbfm.2010.78
25. Aucoin JS, Jiang P, Aznavour N, Tong XK, Buttini M, Descarries L, Hamel E: Selective cholinergic denervation, independent from oxidative stress, in a mouse model of Alzheimer's disease. Neurosci 2005, 132:73–86
26. Lau JC, Lerch JP, Sled JG, Henkelman RM, Evans AC, Bedell BJ: Longitudinal neuroanatomical changes determined by deformation-based morphometry in a mouse model of Alzheimer's disease. NeuroImage 2008, 42:19–27
27. Kornblum HI, Araujo DM, Annala AJ, Tatsukawa KJ, Phelps ME, Cherry SR: In vivo imaging of neuronal activation and plasticity in the rat brain by high resolution positron emission tomography (microPET). Nature Biotechnol 2000, 18:655–660
28. Tong XK, Nicolakakis N, Fernandes P, Ongali B, Brouillette J, Quirion R, Hamel E: Simvastatin improves cerebrovascular function and counters soluble amyloid-beta, inflammation and oxidative stress in aged APP mice. Neurobiol Dis 2009, 35:406–414
29. Papadopoulos P, Ongali B, Hamel E: Selective in vivo antagonism of endothelin receptors in transforming growth factor-β1 transgenic mice that mimic the vascular pathology of Alzheimer's disease. Can J Physiol Pharmacol 2010, 88:652–660
30. Park L, Zhou P, Pitstick R, Capone C, Anrather J, Norris EH, Younkin L, Younkin S, Carlson G, McEwen BS, Iadecola C: Nox2-derived radicals contribute to neurovascular and behavioral dysfunction in mice overexpressing the amyloid precursor protein. Proc Natl Acad Sci USA 2008, 105:1347–1352
31. Pellerin L, Bouzier-Sore AK, Aubert A, Serres S, Merle M, Costalat R,

Magistretti PJ: Activity-dependent regulation of energy metabolism by astrocytes: an update. Glia 2007, 55:1251–1262
32. Roher AE, Lowenson JD, Clarke S, Woods AS, Cotter RJ, Gowing E, Ball MJ: β-Amyloid-(1-42) is a major component of cerebrovascular amyloid deposits: implications for the pathology of Alzheimer disease. Proc Natl Acad Sci USA 1993, 90:10836–10840
33. Kalaria RN, Pax AB: Increased collagen content of cerebral microvessels in Alzheimer's disease. Brain Res 1995, 705:349–352
34. Castillo GM, Ngo C, Cummings J, Wight TN, Snow AD: Perlecan binds to the β-amyloid proteins (Aβ) of Alzheimer's disease, accelerates Aβ fibril formation, and maintains Aβ fibril stability. J Neurochem 1997, 69:2452–2465
35. Weller RO, Subash M, Preston SD, Mazanti I, Carare RO: Perivascular drainage of amyloid-β peptides from the brain and its failure in cerebral amyloid angiopathy and Alzheimer's disease. Brain Pathol 2008, 18:253–266
36. Wilcock DM, Gharkholonarehe N, Van Nostrand WE, Davis J, Vitek MP, Colton CA: Amyloid reduction by amyloid-β vaccination also reduces mouse tau pathology and protects from neuron loss in two mouse models of Alzheimer's disease. J Neurosci 2009, 29: 7957–7965 Erratum in. J Neurosci 2010, 30:1197–1198
37. Boche D, Zotova E, Weller RO, Love S, Neal JW, Pickering RM, Wilkinson D, Holmes C, Nicoll JA: Consequence of Aβ immunization on the vasculature of human Alzheimer's disease brain. Brain 2008, 131:3299–3310
38. Haydon PG, Carmignoto G: Astrocyte control of synaptic transmission and neurovascular coupling. Physiol Rev 2006, 86:1009–1031
39. Wilcock DM, Vitek MP, Colton CA: Vascular amyloid alters astrocytic water and potassium channels in mouse models and humans with Alzheimer's disease. Neuroscience 2009, 159:1055–1069
40. Han BH, Zhou ML, Abousaleh F, Brendza RP, Dietrich HH, Koenigsknecht-Talboo J, Cirrito JR, Milner E, Holtzman DM, Zipfel GJ: Cerebrovascular dysfunction in amyloid precursor protein transgenic mice: contribution of soluble and insoluble amyloid-β peptide, partial restoration via γ-secretase inhibition. J Neurosci 2008, 28:13542–13550
41. Hamel E, Nicolakakis N, Aboulkassim T, Ongali B, Tong XK: Oxidative stress and cerebrovascular dysfunction in mouse models of Alzheimer's disease. Exp Physiol 2008, 93:116–120
42. Luterman JD, Haroutunian V, Yemul S, Ho L, Purohit D, Aisen PS, Mohs R, Pasinetti GM: Cytokine gene expression as a function of the clinical progression of Alzheimer disease dementia. Arch Neurol 2000, 57:1153–1160
43. Krupinski J, Kumar P, Kumar S, Kaluza J: Increased expression of TGF-β1 in brain tissue after ischemic stroke in humans. Stroke 1996, 27:852–857
44. Peterson MC: Circulating transforming growth factor β-1: a partial molecular explanation for associations between hypertension, diabetes, obesity, smoking and human disease involving fibrosis. Med Sci Monit 2005, 11:RA229–RA232
45. Kalaria RN: The role of cerebral ischemia in Alzheimer's disease. Neurobiol Aging 2000, 21:321–330
46. Luchsinger JA, Reitz C, Honig LS, Tang M-X, Shea S, Mayeux R: Aggregation of vascular risk factors and risk of incident Alzheimer disease. Neurology 2005, 65:545–551
47. Lesné S, Docagne F, Gabriel C, Liot G, Lahiri DK, Buée L, Plawinski L, Delacourte A, MacKenzie ET, Buisson A, Vivien D: Transforming growth factor-β1 potentiates amyloid-β generation in astrocytes and in transgenic mice. J Biol Chem 2003, 278:18408–18418
48. Cheng JS, Dubal DB, Kim DH, Legleiter J, Cheng IH, Yu GQ, Tesseur I, Wyss-Coray T, Bonaldo P, Mucke L: Collagen VI protects neurons against Aβ toxicity. Nat Neurosci 2009, 12:119–121
49. Bennett SAL, Pappas BA, Stevens WD, Davidson CM, Fortin T, Chen J: Cleavage of amyloid precursor protein elicited by chronic cerebral hypoperfusion. Neurobiol Aging 2000, 21:207–214
50. Dhandapani KM, Brann DW: Transforming growth factor-β: a neuroprotective factor in cerebral ischemia. Cell Biochem Biophys 2003, 39:13–22
51. Geula C, Mesulam MM: Cortical cholinergic fibers in aging and Alzheimer's disease: a morphometric study. Neuroscience 1989, 33:469–481
52. Wong TP, Debeir T, Duff K, Cuello AC: Reorganization of cholinergic terminals in the cerebral cortex and hippocampus in transgenic mice carrying mutated presenilin-1 and amyloid precursor protein transgenes. J Neurosci 1999, 19:2706–2716
53. Jaffar S, Counts SE, Ma SY, Dadko E, Gordon MN, Morgan D, Mufson EJ: Neuropathology of mice carrying mutant APP(swe) and/or PS1 (M146L) transgenes: alterations in the p75(NTR) cholinergic basal forebrain septohippocampal pathway. Exp Neurol 2001, 170:227–243
54. Klingner M, Apelt J, Kumar A, Sorger D, Sabri O, Steinbach J, Scheunemann M, Schliebs R: Alterations in cholinergic and noncholinergic neurotransmitter receptor densities in transgenic Tg2576 mouse brain with beta-amyloid plaque pathology. Int J Dev Neurosci 2003, 21:357–369
55. Auld DS, Kornecook TJ, Bastianetto S, Quirion R: Alzheimer's disease and the basal forebrain cholinergic system: relations to beta-amyloid peptides, cognition, and treatment strategies. Prog Neurobiol 2002, 68:209–245
56. Hsia AY, Masliah E, McConlogue L, Yu GQ, Tatsuno G, Hu K, Kholodenko D, Malenka RC, Nicoll RA, Mucke L: Plaque-independent disruption of neural circuits in Alzheimer's disease mouse models. Proc Natl Acad Sci USA 1999, 96:3228–3233
57. Palop JJ, Jones B, Kekonius L, Chin J, Yu GQ, Raber J, Masliah E, Mucke L: Neuronal depletion of calcium-dependent proteins in the dentate gyrus is tightly linked to Alzheimer's disease-related cognitive deficits. Proc Natl Acad Sci USA 2003, 100:9572–9577
58. Caraci F, Battaglia G, Busceti C, Biagioni F, Mastroiacovo F, Bosco P, Drago F, Nicoletti F, Sortino MA, Copani A: TGF-β1 protects against Aβ-neurotoxicity via the phosphatidylinositol-3-kinase pathway. Neurobiol Dis 2008, 30:234–242
59. Tesseur I, Zou K, Esposito L, Bard F, Berber E, Can JV, Lin AH, Crews L, Tremblay P, Mathews P, Mucke L, Masliah E, Wyss-Coray T: Deficiency in neuronal TGF-beta signaling promotes neurodegeneration and Alzheimer's pathology. J Clin Invest 2006, 116:3060–3069
60. Salins P, He Y, Olson K, Glazner G, Kashour T, Amara F: TGF-beta1 is increased in a transgenic mouse model of familial Alzheimer's disease and causes neuronal apoptosis. Neurosci Lett 2008, 430:81–86
61. Tong XK, Hamel E: Transforming growth factor-beta 1 impairs endothelin-1-mediated contraction of brain vessels by inducing mitogen-activated protein (MAP) kinase phosphatase-1 and inhibiting p38 MAP kinase. Mol Pharmacol 2007, 72:1476–1483
62. Simpson IA, Chundu KR, Davies-Hill T, Honer WG, Davies P: Decreased concentrations of GLUT1 and GLUT3 glucose transporters in the brains of patients with Alzheimer's disease. Ann Neurol 1994, 35:546–551